Manganese and Nickel Complexes as Catalysts for Aromatic Oxidation

Novel Methodologies for Non-Noble Metal Catalysis

Mangaan- en nikkelcomplexen als katalysatoren voor aromatische oxidatie

Nieuwe methoden voor katalyse met niet-edelmetalen

(met een samenvatting in het Nederlands)

Proefschrift

ter verkrijging van de graad van doctor aan de Universiteit Utrecht op gezag van de rector magnificus, prof.dr. H.R.B.M. Kummeling, ingevolge het besluit van het college voor promoties in het openbaar te verdedigen op

te uur

door

Eduard Masferrer Rius

geboren op 20 augustus 1993 te Arbúcies (Girona), Spanje

Promotor: Prof. dr. R. J. M. Klein Gebbink

This thesis was accomplished with financial support through the NoNoMeCat project (675020-MSCA-ITN-2015-ETN).

Manganese and Nickel Complexes as Catalysts for Aromatic Oxidation

Novel Methodologies for Non-Noble Metal Catalysis

Masferrer Rius, Eduard

Manganese and Nickel Complexes as Catalysts for Aromatic Oxidation
Novel Methodologies for Non-Noble Metal Catalysis

ISBN:

The work described in this PhD thesis was carried out at the Organic Chemistry and Catalysis group, Debye Institute for Nanomaterials Science, Faculty of Science, Utrecht University, Utrecht, The Netherlands

Front Cover:
Cover Design:

Table of Contents

Chapter 1

Non-Noble Metal Aromatic Oxidation Catalysis: from Metalloenzymes to Synthetic Complexes

Abstract

The development of selective aromatic oxidation catalysts based on non-noble metals has emerged over the last decades, mainly due to the importance of phenol products as intermediates for the generation of pharmaceuticals or functional polymers. In nature, metalloenzymes can perform a wide variety of oxidative processes using molecular oxygen, including arene oxidations, however, the implementation of such enzymes in the chemical industry remains challenging. In this context, chemists have tried to mimic nature and design synthetic non-noble metal catalysts inspired by these enzymes. This introduction chapter aims at providing a general overview on aromatic oxidation reactions catalyzed by metalloenzymes as well as synthetic first-row transition-metal complexes as homogeneous catalysts. The enzymes and complexes discussed in this chapter have been classified on the basis of the transition-metal ion present in their active site, *i.e.*, iron, copper, nickel, and manganese. The main points of discussion focus on enzyme structure and function, catalyst design, mechanism of operation in terms of oxidant activation and substrate oxidation, and substrate scope. At the end of the chapter, the aim and scope of this thesis is outlined.

1.1 Overview of Arene Oxidations

1.1.1 Relevance and Challenges

Oxidations of organic compounds are essential reactions that are widely studied in academia as well as in the chemical industry.[1, 2] The interest in these reactions is based on the fact that oxygenated organic molecules can be used as intermediates to produce different classes of chemicals, as well as end products. Since the last decades, improvements have been made in the development of different catalytic oxidation systems, however, in most cases the selective oxidation of the organic substrate represents a critical challenge. Of more recent interest are C–H oxidations that can be applied for late-stage functionalization and in which C–H bonds are basically considered as functional groups.[3-7]

A particular area of interest has been the direct oxygenation of aromatic compounds to the corresponding phenol products (Figure 1), which has been a challenging class of reactions for decades. Indeed, the direct hydroxylation of benzene to phenol using molecular oxygen as a benign oxidant has been known as one of the "10 challenges for catalysis".[8, 9] Phenols are essential intermediates in the generation of a broad range of products, like pharmaceuticals or functional polymers, which make them highly desired.[6, 10-12] However, the direct transformation of an aromatic C–H bond into a hydroxyl functionality, such as in benzene oxidation, is difficult because of poor substrate reactivity (an aromatic C–H bond has a high bond dissociation energy of about 112 kcal·mol^{-1}).[13] To overcome this challenge, the generation of highly reactive and selective oxygen species is necessary. However, often phenol products are more easily oxidized than non-oxidized aromatic compounds, causing a chemoselectivity issue. Generally, the oxidation of phenols to the corresponding catechols, hydroquinones or benzoquinones is well documented, particularly in oxidations catalyzed by metalloporphyrins (Figure 1).[14-18] Besides, a lack of discrimination between different oxidation sites produces a regioselectivity issue, especially when alkylbenzenes are used, where oxidation at the weaker and activated (benzylic) aliphatic C(sp^3)–H bonds is thermodynamically preferred over oxidation at the aromatic ring.

Generally, the field of homogeneous catalysis has been dominated by noble metal complexes, which are based on elements that are generally considered toxic for humans and the environment, and are associated with high costs due to their low availability in the earth crust.[19] In this context, non-noble metal complexes have appeared as attractive catalysts, particularly in oxidation catalysis. Within this field, chemists have typically looked at nature for inspiration. A widely applied approach has been the development of synthetic catalytic systems that can mimic the active site and functionality of metalloenzymes to carry out oxidative processes. A well-known inspiration example are iron-containing metalloenzymes that are able to activate molecular oxygen.[20-26] However, other kinds of metalloenzymes containing copper, nickel or

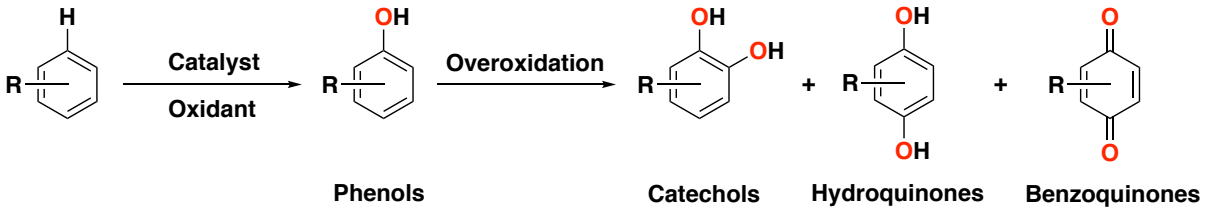

Figure 1. Direct hydroxylation of aromatic substrates to the corresponding phenol products, and overoxidation to catechols, hydroquinones or benzoquinones products.

manganese have also been investigated in this field.[22, 25, 27-32] Generally, the active site is the only area of the enzyme that is being mimicked in such bioinspired complexes. A downside of this design strategy is that these synthetic complexes generally display poor selectivities, whereas the natural counterparts show outstanding selectivities due to their highly elaborated structure, including the second coordination sphere around the active site.[22, 33] Thus, a lot of efforts have been devoted to the understanding of the geometric and electronic structure/function correlations between the synthetic and their enzyme 'molds'.[34, 35]

In the current chapter, we provide an overview on homogeneous, non-noble metal catalysis for aromatic oxidation reactions. Several reviews can be found in literature regarding heterogeneous catalytic systems for oxidation chemistry, also detailing arene oxidation reactivity.[36-38] Of note, a review on heterogeneous catalysts for the direct hydroxylation of benzene to phenol, with a special focus on mesoporous transition metal-based catalysts, was very recently published.[39] The present overview on homogeneous catalysts systems specifically targets catalytic systems capable of performing the direct hydroxylation of an aromatic substrate using a metal-based oxidant and avoiding the use of unselective hydroxyl radicals generated via Fenton-type processes. We have classified this chapter on basis of the transition-metal that is used in catalysis, *i.e.*, iron, copper, nickel, and manganese. First, we introduce the most important families of metalloenzymes capable of catalyzing aromatic oxidation reactions, followed by a description of the development of synthetic bioinspired transition-metal complexes for arene oxidation. Special attention is given to complexes based on aminopyridine ligands, which have been extensively used and investigated in general in the field of homogeneous oxidation chemistry.[40] Initially, we will review enzymes and complexes based on iron and copper, since these are the two metals that chemists have employed most in the field of oxidation chemistry, in particular for aromatic oxidation. In the second part, nickel- and manganese-based complexes will be covered. Although less examples for arene oxidation are known using these metals, the experimental chapters in this thesis will focus on the development of arene oxidation catalysts based on these metals. At this point, it is important to mention that complexes containing other first-row transition metals, such as cobalt or vanadium, have also been proven to be active for aromatic oxidation. For further information

on these complexes and their catalytic activity, the reader is referred to a number of selected examples.[41-46]

1.1.2 Hydroxyl Radicals *vs* Metal-based Oxidants

Fenton-type chemistry has been known and studied in detail for quite some time.[47-49] Overall, this chemistry consists of the reaction between an iron(II) salt and H_2O_2 to generate an oxidized iron(III) species and hydroxyl radicals.[50-52] The oxidation of aromatic substrates, such as benzene and benzene derivatives, by Fenton-type chemistry using H_2O_2 as oxidant has been investigated and is well-understood, and studies have shown that hydroxyl radicals are added rapidly to the aromatic ring.[53-56] After addition of the hydroxyl radical to the benzene ring, the reaction can proceed either by dimerization of the hydroxycyclohexadienyl radical and dehydration to form biphenyl, or alternatively by oxidation to generate phenol (Figure 2). Other oxidants, such as *tert*-butylhydroperoxide (TBHP), can also engage in a Fenton-type process, generating free-diffusing *tert*-butoxy and *tert*-butylperoxy radicals that can engage in hydrogen abstraction reactions with aliphatic C–H bonds.[57-59] However, TBHP activation does not produce hydroxyl radicals, and *tert*-butoxy radicals, unlike hydroxyl radicals, do not add to aromatic rings.[60] For this reason, the effectiveness of using TBHP in arene hydroxylation reactions has been used as an evidence against the involvement of hydroxyl radicals, and consequently in favor of the involvement of metal-based oxidants.[61]

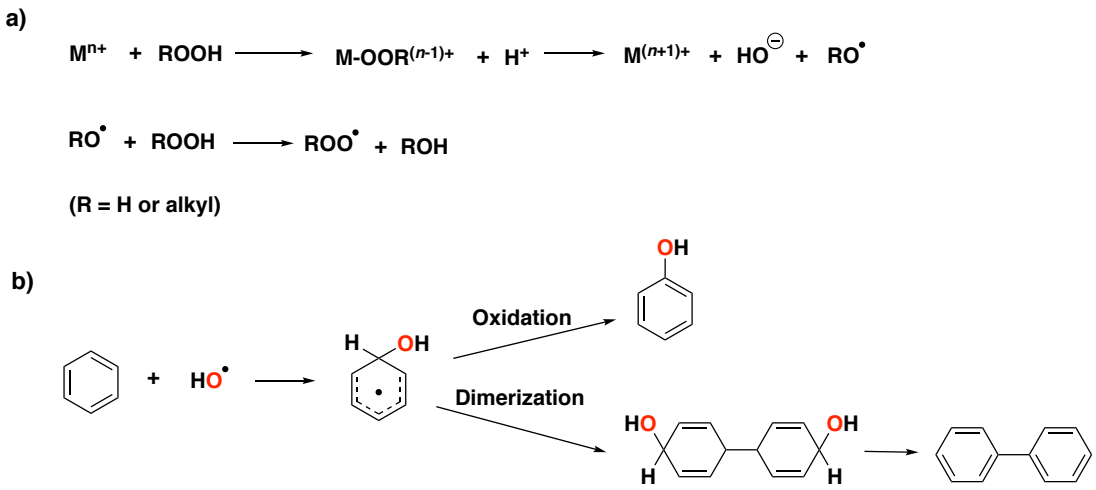

Figure 2. a) Generation of free diffusing oxygen-centered radicals via initial Fenton reaction. **b)** Hydroxylation of benzene by addition of hydroxyl radicals to generate phenol and biphenyl.

In 1954, another process involving hydroxyl radicals was reported, known as the Udenfriend system.[62-64] This consists of a mixture of an iron(II) salt with EDTA (EDTA = ethylenediaminetetraacetic acid) and ascorbic acid under an oxygen atmosphere, which is able

to generate hydroxyl radicals that can attack aromatic substrates in the same way as described for Fenton-type chemistry. A system using iron(II) salts and tetrahydropterins as reducing agents has also been reported to be efficient for the hydroxylation of aromatic compounds using dioxygen as oxidant. In this particular case, hydroxylation of electron-rich arenes, such as anisole, phenetole, toluene and ethylbenzene is possible, favoring *meta*-hydroxylation in all cases.[65] Overall, free-diffusing oxygen-centered radicals are known to provide low catalytic efficiencies and selectivities, leading to side products through lateral site chain oxidation for alkylbenzene substrates.[55, 56, 66, 67] For this reason, over the past years research efforts have focused on the development of catalytic systems that make use of metal-based oxidants rather than hydroxyl radicals, so that higher selectivities and efficiencies for aromatic oxidations can be achieved.

1.2 Iron in Biological and Synthetic Systems

1.2.1 Iron-containing Metalloenzymes

Iron is one of most often found transition-metals in the active sites of metalloenzymes. Numerous iron-containing enzymes are known to be able to activate oxygen to perform oxidative processes. Among these enzymes, we can distinguish two groups based on the active site structure: heme and non-heme containing enzymes (Figure 3). The first group has been well investigated and their chemistry is well understood.

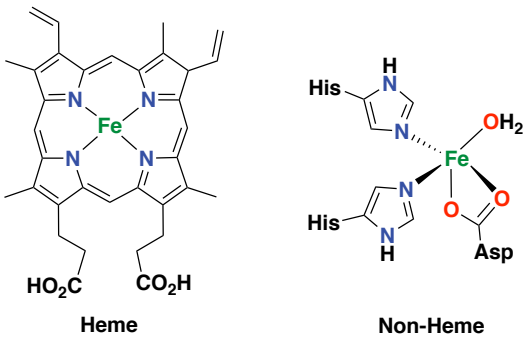

Figure 3. Schematic diagram of the typical heme prosthetic group (iron protoporphyrin IX) found in the active site of heme enzymes (left),[69, 70] and of the 2-His-1-carboxylate facial triad active site found in the mononuclear non-heme enzyme naphthalene dioxygenase (NDO; right).[26, 34, 76, 82]

The main feature of this group of enzymes is the prosthetic heme group that bears the iron center in their active site.[26, 68-72] Within this group we can distinguish heme-containing enzymes like cytochrome P450's, peroxidases, nitric oxide synthases, chloroperoxidases, heme oxygenases, or indoleamine 2,3-dioxygenase and tryptophan 2,3-dioxygenase. Non-heme enzymes, on the other hand, can be classified in mononuclear and dinuclear depending on the

number of iron atoms in their active site. [23, 34, 73] Within the former type, different types of mononuclear active sites have been identified. One very common active site features an iron center bound to two histidine ligands and one carboxylate ligand in a facial manner; this structural feature is known as the "2-His-1-carboxylate facial triad".[23, 24, 35, 74-79] One remarkable example of this last family of enzymes are Rieske oxygenases, which can perform the *syn*-dihydroxylation of aromatic substrates, among other substrate oxidations, with high levels of regio- and stereospecificity.[24, 80, 81] In the following sections, some of the most important iron-containing metalloenzymes able to perform aromatic oxidation reactions are discussed, in terms of the structure of their active site and their catalytic oxidation capabilities.

1.2.1.1 Cytochrome P450

Cytochromes (CYP) are ubiquitous in all life forms, going from bacteria to humans. Within this family, cytochrome P450 is one of the most important classes of iron enzymes found in nature that metabolize atmospheric dioxygen in an oxygenase catalytic cycle, and a lot of details on the mechanism of dioxygen activation for this enzyme family are known. Overall, this class of iron enzymes takes part in several processes, ranging from the detoxification of xenobiotic compounds to drug metabolism and the biosynthesis of steroids.[69, 83-86]

Among the different oxidative processes, cytochrome P450 is best known for its monooxygenation capability, *i.e.*, the insertion of an oxygen atom from molecular oxygen into an organic compound. Among these reactions are aromatic oxidations, as well as arene and alkene epoxidations, and the oxygenation of heteroatoms. Because of the catalytic capabilities of cytochrome P450 enzymes, a lot of research efforts have been devoted to the investigation of cytochrome P450 variants as catalysts for site-selective and enantioselective C–H hydroxylation reactions in the past decades.[87-90] Several studies have shown the coordination chemistry of the active site of cytochrome P450's in detail, which nowadays has been well established based on several X-ray crystal structures.[69, 91-96] It is based on a ferric iron center coordinated to four nitrogen atoms (protoporphyrin IX) and a cysteinate sulfur atom; this last residue occupies an axial position at the metal center, whereas the other axial position contains a hydroxide ligand or a water molecule.[68, 97, 98] The mechanism of operation of cytochrome P450's starts with the ferric compound accepting an electron to form the respective ferrous state of the enzyme. Next, reaction with molecular oxygen produces an Fe(III)-OOH species that undergoes O–O bond cleavage to generate the real active oxidant, which is a high-valent Fe(IV)-oxo porphyrin π radical cation complex, also known as Compound I (CpdI) (Figure 4a).[14, 84, 99-102] For the oxidation of aliphatic C–H bonds, this last species transfers the oxo group to the substrate following a two-step process, known as the "oxygen rebound" mechanism.[86, 103, 104] First, a hydrogen atom abstraction takes place from the substrate to the oxo group, and secondly, a fast rebound to the substrate carbon radical by the hydroxyl group occurs.

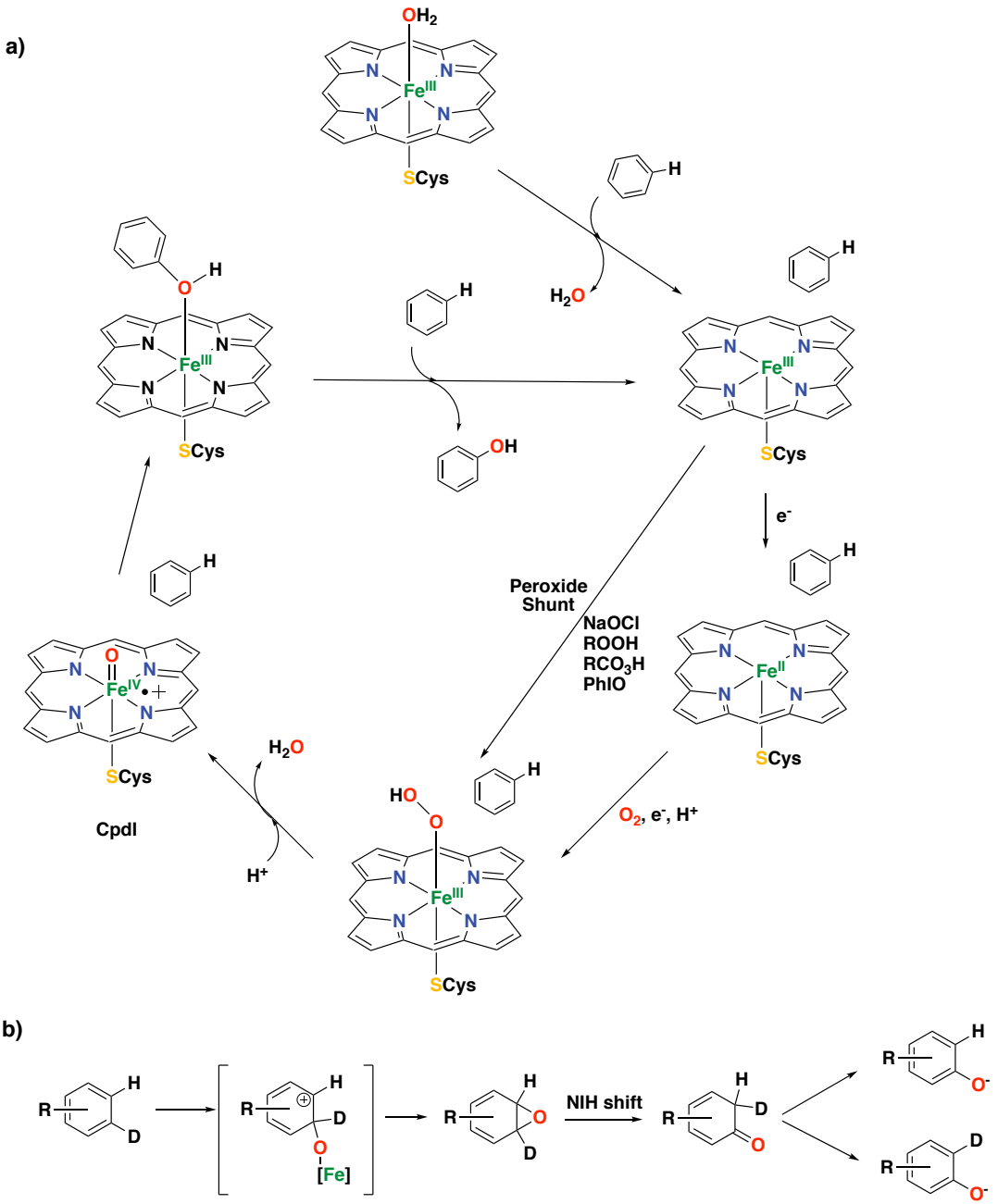

Figure 4. a) Established catalytic cycle for arene oxidation catalyzed by cytochrome P450.[68, 93, 107-109] **b)** Oxidation of deuterated aromatic compounds catalyzed by cytochrome P450, illustrating the "NIH shift" process.[106, 107]

In contrast, oxidation of aromatic substrates with CpdI proceeds via the oxidation of a π-bond, generating arene oxides, that transform to an unstable ketone intermediate via heterolytic cleavage of the epoxide followed by migration of a hydride ion (known as "NIH shift"). [105-107] The last step is the tautomerization of the ketone compound to generate the final phenol product (Figure 4b).[107, 108] Worth mentioning is the use of hydro- and alkylperoxides, sodium hypochlorite, iodosobenzene or peracids, which allow the conversion of the resting state directly to the high-valent iron-oxo species; this cycle is known as the "peroxide shunt".[68]

1.2.1.2 Rieske Oxygenases

Rieske oxygenases are a family of bacterial enzymes based on a non-heme iron center, with the metal facially coordinated to two histidine residues and one carboxylate residue (Figure 5b).[77] This class of enzymes have been well-studied, and they have been found to be effective in several oxidative reactions, such as selective C–H hydroxylations and stereoselective *syn*-dihydroxylations of arenes and alkenes.[80, 110, 111] Basically, the reactions performed by this class of enzymes are involved in the biodegradation of aromatic compounds.[24, 76, 80, 81] Rieske oxygenases are based on a reductase and an oxygenase component.[112] The first one is a Rieske-type dinucelar iron cluster that mediates the electron transfer from NAD(P)H to the oxygenase component. The latter is characterized by an octahedral mononuclear non-heme iron(II) that can perform the activation of dioxygen to oxidize a hydrocarbon substrate.[113, 114]

One particular member of this family of enzymes is naphthalene-1,2-dioxygenase (NDO), which was crystallographically characterized in 1998.[110-112] The proposed catalytic cycle for the *syn*-dihydroxylation of naphthalene consists of the reaction of dioxygen and an electron with the iron center to generate an Fe(III)-peroxo intermediate.[77, 111, 115, 116]

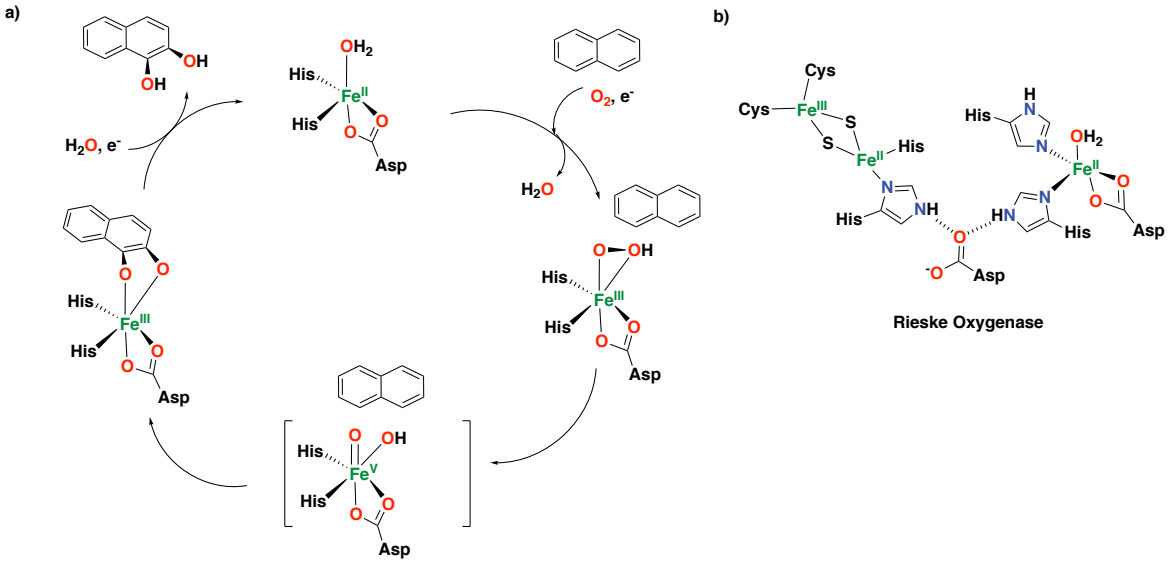

Figure 5. a) Proposed catalytic cycle for the oxidation of naphthalene catalyzed by Rieske dioxygenases, involving the generation of an Fe(V)(O)(OH) species. **b)** Active site of Naphthalene 1,2-dioxygenase (NDO), showing the Rieske [2Fe:2S] cluster (reductase component) and the catalytic iron center (oxygenase component).[112]

The cycle follows with the heterolytic cleavage of the O–O bond of the peroxo intermediate to generate what is proposed to be an Fe(V)(O)(OH) species, responsible for the oxidation of the substrate to form the syn-diol product (Figure 5a).[23, 76, 117, 118] Overall, the mechanism proposed for Rieske oxygenases resembles that of cytochrome P450 regarding the activation of dioxygen

via a heterolytic O–O bond cleavage step. Besides, NDO can also perform the reaction in the presence of hydrogen peroxide via a "peroxide shunt".[119]

1.2.1.3 Bacterial Multicomponent Monooxygenases

Bacterial multicomponent monooxygenases (BMMs) are a family of non-heme iron enzymes that comprize a carboxylate-bridged diiron core in the active site.[120-122] Such enzymes catalyze the oxidation of various hydrocarbons, such as alkanes, alkenes and aromatic compounds.[123-126] Within this family we can distinguish several classes of multicomponent monooxygenases, such as soluble methane monooxygenases (sMMOs), toluene/*o*-xylene monooxygenases (ToMOs) and phenol hydroxylases (PHs).[127-129] Among these, sMMO is the only enzyme that can catalyze the difficult conversion of methane to methanol, which is one of the most challenging reactions found in nature[123], whereas ToMO performs the hydroxylation of aromatics and alkenes[125, 130], and PH hydroxylates aromatic compounds (Figure 6, left).[129] The hydroxylation of toluene by ToMO occurs through the generation of an epoxide and a subsequent NIH shift that forms *p*-cresol in 95% yield (*o*- and *m*-cresols are formed in ~4% yield).[107, 120, 131]

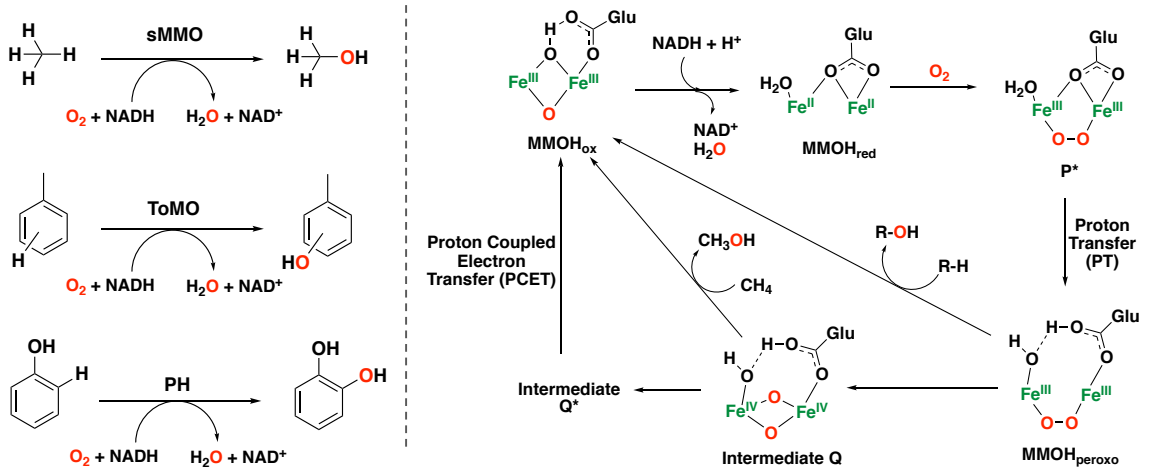

Figure 6. Left: Hydroxylation reactions catalyzed by some of the most representative bacterial multicomponent monooxygenases.[14, 120] Right: Catalytic mechanism of sMMO for dioxygen activation and substrate oxidation, involving the $MMOH_{ox}$, $MMOH_{red}$, intermediate **P***, $MMOH_{peroxo}$ and intermediate **Q** species.[14, 120, 133]

One of the most studied catalytic cycles is the one of sMMO for methane hydroxylation (Figure 6, right). In addition, sMMO has been shown to be capable of oxidizing benzene to phenol.[132] Initially, the oxidized diiron(III) species ($MMOH_{ox}$) is activated by two-electron reduction to a diiron(II) species ($MMOH_{red}$). Then, the reaction with dioxygen forms peroxo intermediate **P*** (via a superoxo species). Intermediate **P*** then converts into $MMOH_{peroxo}$ through a proton

transfer, which can decay to $MMOH_{ox}$ via oxidation of electrophilic substrates, or convert to diiron(IV) intermediate **Q** by homolytic cleavage of the O–O bond, which is able to hydroxylate methane. In the absence of methane, intermediate **Q** decays to intermediate **Q*** and then to $MMOH_{ox}$.[14, 120, 123, 133-137]

The mechanism of ToMO and PH has also been investigated in detail, but it is less well understood compared to that of sMMO. Overall, these classes of bacterial multicomponent monooxygenases show a very similar diiron active site, which may imply a similar mechanism regarding the activation of dioxygen generating peroxodiiron(III) and **Q**-type species.[128, 138] Nevertheless, an unprecedented peroxodiiron(III) species has been elucidated for ToMO and no evidences of **Q**-type intermediates are known yet, suggesting that the mechanism may differ from that described for sMMO. The general mechanism for dioxygen activation and substrate oxidation has been proposed to proceed through an electrophilic attack by a peroxodiiron(III) intermediate on the arene, to form an arene epoxide that ultimately leads to the aromatic oxidized product bound to the diiron(III) core (see Figure 7 for representative scheme of phenol oxidation).[139]

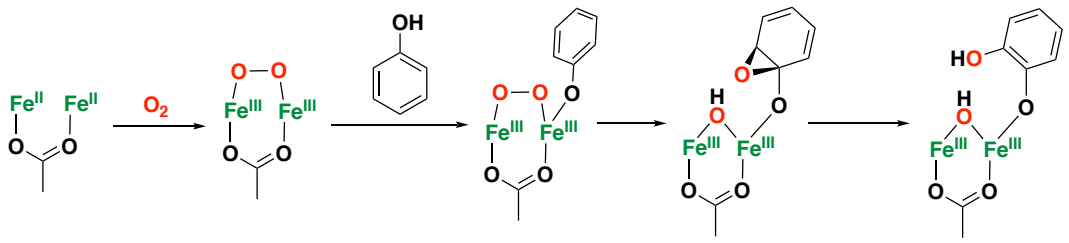

Figure 7. Schematic representation of the mechanism of PH for dioxygen activation and phenol hydroxylation. A similar mechanism is postulated for toluene hydroxylation, however, substrate orientation is controlled by residues of the active site rather than by coordination to the diiron core.[139]

1.2.1.4 Pterin-Dependent Aromatic Amino Acid Hydroxylases

Aryl amino acid hydroxylases, or also known as pterin-dependent oxygenases, are a class of enzymes that utilize tetrahydrobiopterin (BH_4) as a two-electron cofactor. Within this family, we can distinguish phenylalanine (PheOH), tyrosine (TyrOH) and tryptophan hydroxylases (TrpOH), which perform the hydroxylation of phenylalanine, tyrosine and tryptophan, respectively (Figure 8).[23, 34, 140-144] In addition, pterin-dependent hydroxylases can also perform epoxidations and benzylic hydroxylation reactions, in a similar way as the reactivity observed for cytochrome P450 enzymes.[68, 142]

A general mechanism has been proposed regarding of oxygen activation and substrate oxidation by these enzymes (Figure 9). Initially, tetrahydrobiopterin (BH_4) reacts with dioxygen to form a hydroperoxydihydropterin intermediate that reacts with the iron(II) center of the

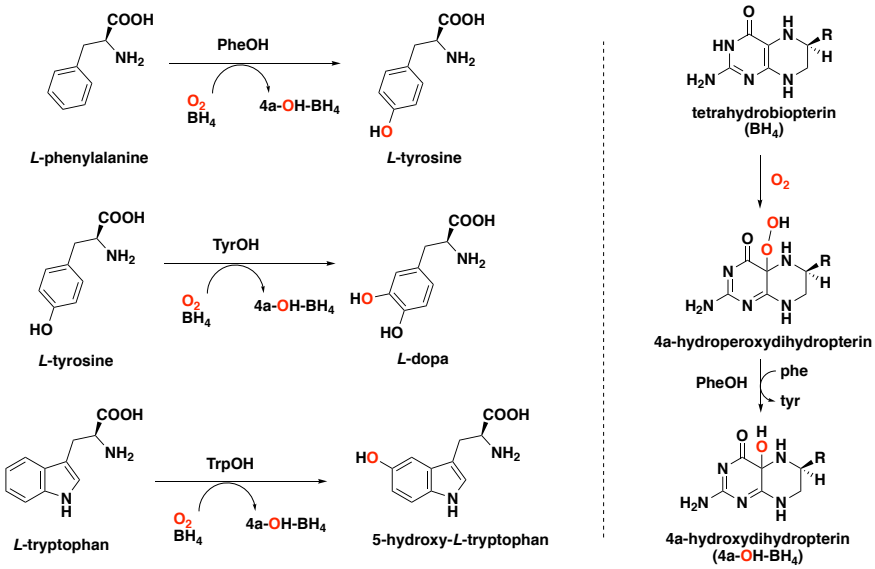

Figure 8. Left: Arene hydroxylation reactions catalyzed by pterin-dependent amino acid hydroxylases. Right: Reaction of the tetrahydropterin cofactor with dioxygen in the presence of aryl amino acid hydroxylases.

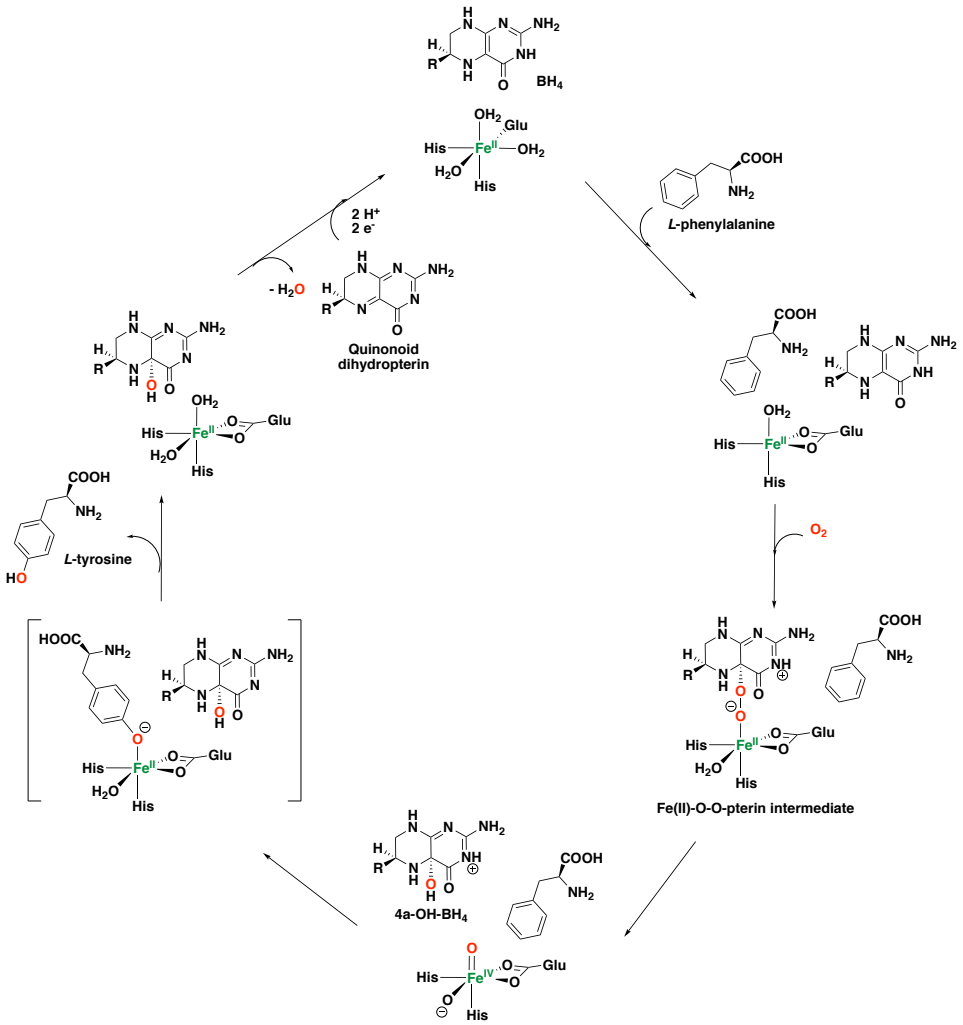

Figure 9. Proposed catalytic mechanism for phenylalanine hydroxylases (PheOH).[23, 34]

active site of the enzyme to generate an Fe(II)–O–O–pterin intermediate.[34, 140, 142, 145] Alternatively, the direct reaction of dioxygen with the iron center to form an Fe(III)–peroxo complex may take place, which then reacts with the tetrahydrobiopterin compound.[143, 146-148] Subsequently, heterolytic cleavage of the O–O bond takes place to form a hydroxydihydropterin compound and an Fe(IV) oxo species responsible for the arene hydroxylation reaction. Several studies using labelled dioxygen have corroborate this last step because of the incorporation of labelled oxygen into both the amino acid and the hydroxydihydropterin product.[149-151] Once the hydroxylated amino acid is formed, the resting state of the enzyme is restored, and the oxidized tetrahydrobiopterin undergoes dehydration to generate a quinonoid dihydropterin. This latter compound is reduced by an external reductase to regenerate the tetrahydrobiopterin and start a new catalytic turnover.[145] Computational studies have also been performed to investigate the mechanism of pterin-dependent aromatic amino acid hydroxylases.[152, 153]

1.2.2 Synthetic Iron Systems

Most of the synthetic iron complexes reported for aromatic oxidation are supported by polydentate N-based donor ligands and make use of the environmentally benign $2e^-$ oxidant H_2O_2. Overall, these systems have been extensively studied for the oxidation of inert C(sp^3)–H and C=C bonds, whereas aromatic oxidations using these complexes has mostly been studied in recent years. The mechanism of action of these bioinspired non-heme iron complexes has been extensively studied and is proposed to proceed through the involvement of highly stereoselective, high oxidation-state metal-based oxidants.[26, 154-159]

1.2.2.1 Iron-Based Systems and Oxidation Mechanism

The first example of a stereospecific hydrocarbon hydroxylation reaction catalyzed by a bioinspired non-heme iron complex was reported by Que and co-workers in 1997 using Fe(II) complex **8** supported by the tpa ligand (tpa = tris(2-pyridylmethyl)amine) with H_2O_2 as the oxidant (see Figure 14b for the structure of complex **8**).[160] The results shown in this study, based on the ratio of alcohol/ketone (A/K) products in the oxidation of cylcohexane (A/K > 5), retention of configuration in specific oxidation reactions (such as the oxidation of *cis*-1,2-dimethylcyclohexane), regioselectivity in the oxidation of tertiary C–H bonds over secondary C–H bonds (adamantane oxidation), and kinetic isotope effect (KIE) experiments, pointed towards a metal-based species as the active oxidant. Besides, the idea of a metal-based oxidant was also proposed in other studies using different aminopyridine ligands based on the tpa ligand scaffold.[161]

Generally, this type of iron catalysts is supported by tetradentate aminopyridine ligands, with the ligands being either tripodal or linear. Different geometries around the metal center can be

adopted in the case of linear tetradentate aminopyridine ligands, such as for the bpmcn ligand (bpmcn = *N,N'*-dimethyl-*N,N'*-bis(2-picolyl)cyclohexane-*trans*-1,2-diamine). On the one hand, complexes with two *cis* positions open for coordination can form, whereas on the other hand, the two open coordination sites can be *trans* to each other. For the *cis* topologies, two configurations are possible, namely *cis*-α and *cis*-β, and different reactivities have been found depending on the specific geometry that the complex may adopt (Figure 10).[82, 157, 162-166]

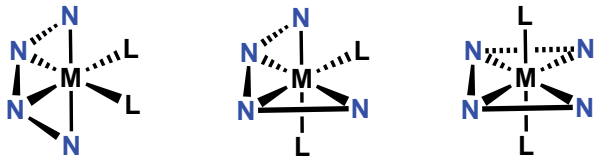

Figure 10. Different topologies for complexes with linear tetradentate aminopyridine ligands. L is an open coordination site.

A lot of debate has emerged regarding the mechanism of activation of H_2O_2 by non-heme iron complexes that are able to perform hydroxylation reaction. Nonetheless, a general mechanistic pathway has been elucidated for iron complexes supported by strong-field tetradentate aminopyridine ligands with two *cis* open sites. This pathway proposes the generation of an Fe(V)(O)(OH) species generated via the O–O bond cleavage of an Fe(III)(OOH) intermediate with the help of a proton provided by a water molecule, reminiscent of the mechanism of Rieske dioxygenases (Figure 11).[26, 156-158, 167, 168]

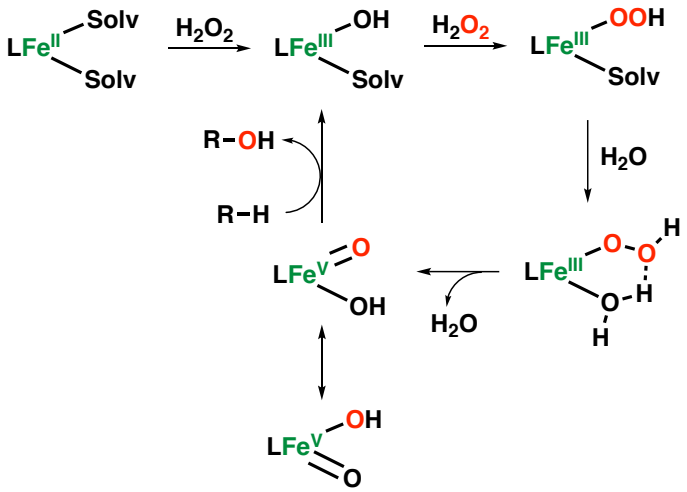

Figure 11. Water-assisted mechanism proposed for the generation of an Fe(V)(O)(OH) species in hydroxylation reactions catalyzed by non-heme iron complexes supported by strong-field tetradentate aminopyridine ligands with two cis open sites.

This pathway has been called the "water assisted mechanism", and several studies on olefin epoxidation and *syn*-dihydroxylation reactions have pointed out the involvement of Fe(V)(O)(OH) species as the electrophilic oxidant responsible for the oxidation reactions by

these kind of complexes.[169-171] Indeed, several pieces of evidence that demonstrate the existence of these high-valent iron oxo-hydroxo species have been reported in recent years.[172-175]

Another very important aspect of this chemistry was the introduction of carboxylic acid additives, which act as co-ligands binding to the metal center and modulating the reactivity of the complexes towards H_2O_2. For the first time in 2001, Jacobsen and co-workers introduced the use of acetic acid in combination with an iron complex supported by the bpmen ligand (bpmen = *N*,*N*'-dimethyl-*N*,*N*'-bis(2-picolyl)ethylenediamine) and H_2O_2, which enhanced the catalytic activity of the iron system in the epoxidation of olefins.[176] Later, White and co-workers demonstrated the same beneficial effect of carboxylic acids in aliphatic C–H bond oxidations.[177]

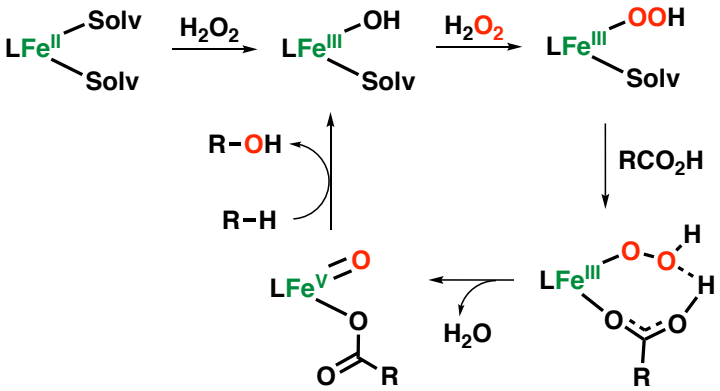

Figure 12. Carboxylic acid-assisted mechanism proposed for the generation of an Fe(V)(O)(OCOR) species in the hydroxylation reaction catalyzed by non-heme iron complexes supported by strong-field tetradentate aminopyridine ligands with two cis open sites.

This remarkable study showed for the first time that an iron complex supported by the robust bpbp ligand (bpbp = *N*,*N*'-bis(2-pyridylmethyl)-2,2'-bipyrrolidine) can perform C–H oxidations in synthetically useful yields and, in addition, is able to discriminate between different C–H bonds within a complex substrate molecule.[178, 179] Various mechanistic studies have been carried out to elucidate the effect of the carboxylic acid in the activation of H_2O_2, and have lead a proposed mechanistic pathway now known as the "carboxylic acid assisted mechanism" (Figure 12).[26, 57, 82, 156-158, 167, 168, 180] In this pathway, an Fe(V)(O)(OCOR) intermediate is postulated as the active species, which forms through the heterolytic cleavage of the O–O bond of an Fe(III)(OOH) intermediate with the help of the carboxylic acid instead of a water molecule. Overall, the use of a carboxylic acid as additive and co-ligand in aliphatic and aromatic oxidations, as well as epoxidation reactions, has been found to generate catalytic systems with higher activities in most of the cases.

1.2.2.2 Iron-catalyzed Arene Oxidation

As discussed previously, bioinspired non-heme iron complexes have been widely investigated in the field of aliphatic C(sp^3)–H oxidation and alkene epoxidation reactions, whereas catalytic arene oxidations with such complexes have remained challenging until recently.[181] Initial reports on aromatic oxidation reactions using iron are based on the incorporation of an aromatic ring into the ligand structure of the complex and therefore represent examples of intramolecular arene hydroxylation reactions. Even though these examples do not represent catalytic systems, their study has allowed for further insight into the mechanism of these reactions. In 1993, Moro-oka and co-workers described the hydroxylation of a series of trispyrazolylborate-based ferric bis-phenoxo complexes (**1**, **2** and **3**) to form catecholato complexes using *m*CPBA as the oxidant, resulting in a system that acts as a functional model for tyrosine hydroxylase.[182] Reaction of the Fe(III) complexes with 1 equiv. of *m*CPBA resulted in the formation of the corresponding catechol in quantitative yields, and a proposed reaction mechanism includes the formation of an acylperoxo intermediate (Figure 13a). However, attempts to detect the (acylperoxo)-phenoxo intermediate were unsuccessful. Later, Fontecave and co-workers reported on diiron complexes that act as models for methane monooxygenase, based on an ethylenediamine tetraacetic acid (EDTA) derived ligand bearing two electron-rich phenyl groups.[183, 184] Complex **4** is able to react with aqueous H_2O_2, which leads to the *ortho*-hydroxylation of one of the phenyl groups of the ligand, generating a monomeric iron species (Figure 13b). This intramolecular reaction also proceeds in the presence of dioxygen and excess ascorbate as a reductant, while alkylhydroperoxides, sodium hypochlorite and *m*CPBA do not oxidize the diiron complex. Similar iron complexes supported by the *N,N'*-bis(pyridin-2-ylmethyl)-*N,N'*-bis(3,4,5-trimethoxybenzyl)ethane-1,2-diamine ligand ([Fe(II)(L)X_2], **5** and **6**) were reported to react with aqueous H_2O_2 leading to *ortho*-hydroxylation of one of the substituted phenyl moieties of the ligand as well (Figure 13c).[185] However, for complex **6**, in which the chloride ligands have been exchanged by acetonitrile solvent molecules, the organic ligand does not undergo aromatic hydroxylation, but instead N-dealkylation of the ligand was observed. In addition, this complex showed activity for epoxidation reactions and hydroxylation of alkanes.[185] For complex **5** it was proposed that the hydroxylation reaction proceeds through the reaction with H_2O_2 via an outer-sphere electron transfer to generate hydroxyl radicals that add to the aromatic ring of the ligand. In contrast, complex **6** is proposed to generate iron peroxo and oxo complexes because of the more labile sites of this complex, which allows for an inner-sphere reaction of H_2O_2 with the metal center.[185]

In 1999, Que and co-workers reported on iron complex **7** based on a modified tpa ligand containing a pendant phenyl group, Fe(6-Ph-tpa)$(NCCH_3)_2](ClO_4)_2$ (6-Ph-tpa = bis(2-pyridylmethyl)-6-phenyl-2-pyridylmethylamine), that is capable of performing an

intramolecular hydroxylation of the phenyl group of the ligand to form an Fe(III)-phenolate species (Figure 14a).[186] Reaction of complex **7** with TBHP at low temperature afforded a transient blue species formulated as Fe(III)(OOtBu)(6-Ph-tpa) that decays over 4 h at –60 °C to give the final iron complex bearing the hydroxylated ligand.[186]

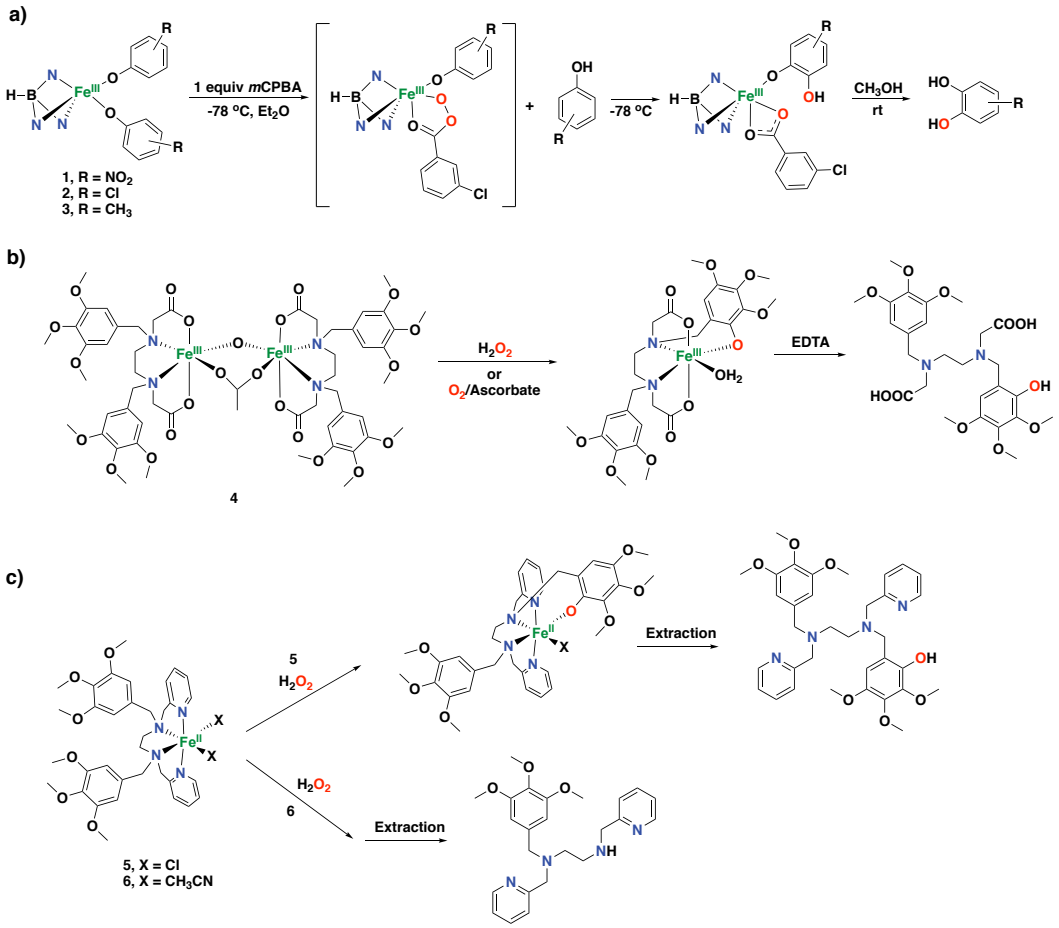

Figure 13. Early examples of iron complexes capable of intramolecular aromatic hydroxylation of the organic ligand.

Indirect evidence suggested the involvement of an Fe(IV) oxo species as the active oxidant in this reaction. Complex **7** also performs the *ortho*-hydroxylation of the ligand phenyl ring efficiently and selectively by reaction with iodosobenzene.[187] The same reactivity with TBHP was also demonstrated for other iron complexes with modified versions of the 6-Ph-tpa ligand.[188] In 2005, it was shown that the parent iron complex **8** supported by the tpa ligand is capable of oxidizing ligated perbenzoic acids through the self-hydroxylation of the aromatic ring forming iron(III)-salicylate complexes (Figure 14b).[189]

Iron complex **9** supported by the linear tetradentate bpmen ligand was also found to perform the *ortho*- and *ipso*-hydroxylation of benzoic acids to afford salicylates and phenolates, respectively (Figure 14c).[190, 191] Later on, hydroxylation of externally added aromatic substrates

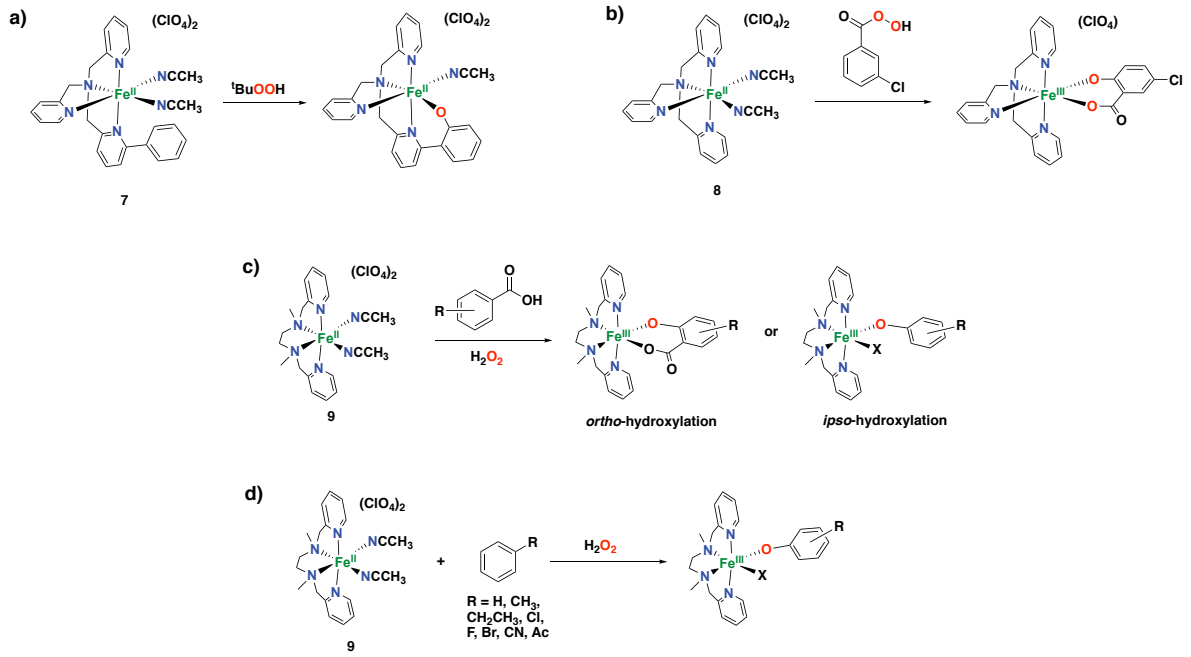

Figure 14. Iron(II) complexes capable of performing arene hydroxylation reactions with different oxidants, generating phenolate or salicylate species.

without directing groups was found to be effective using iron complex **9** in combination with H_2O_2 as oxidant, although strong coordination of the generated phenolates to the resulting iron(III) center prevented efficient catalysis, *i.e.* **9** performs up to 1.4 turn-overs (Figure 14d).[192]

A lot of efforts have been devoted to the investigation of the active oxidant responsible of the arene hydroxylation reaction using these iron complexes. Whereas for some an Fe(IV)-oxo species generated via the homolysis of the O–O bond has been postulated as the oxidant responsible for the oxidation reaction,[186, 188] an Fe(V)-oxo species has been proposed as an alternative active species in other cases.[154, 159, 189, 191-193]

Computational studies have also been performed to provide mechanistic insight in the *ortho*-hydroxylation of aromatic compounds by non-heme iron complexes. Particularly, DFT calculations have clearly shown that Fe(III)-hydroperoxo species are sluggish oxidants, whereas the heterolytic cleavage of the former species to generate a transient Fe(V)-oxo oxidant has been postulated as a plausible reaction mechanism on arene oxidations.[194] Moreover, some studies have demonstrated that Fe(IV)-oxo species are inactive in the hydroxylation of externally added aromatic substrates.[192, 195-197]

Nam and co-workers provided further insight in the capabilities and reaction mechanisms of the oxidation of aromatic substrates by non-heme iron(IV)-oxo complexes.[198] Iron complexes containing Bn-tpen and N4Py ligands (Bn-tpen = *N*-benzyl-*N*,*N*',*N*'-tris(2-pyridylmethyl)ethane-1,2-diamine and N4Py = *N*,*N*-bis(2-pyridylmethyl)-*N*-bis(2-

pyridyl)methylamine) were considered in these studies. Experimental data, such as a large and negative Hammett *p* value and an inverse C–H/C–D KIE effect, together with computational investigations indicated that arene hydroxylation by these iron(IV)-oxo complex does not occur via a hydrogen atom abstraction, but instead proceeds through an electrophilic aromatic substitution pathway. Oxidation of anthracene as the substrate produced the anthraquinone as the product, which is generated via the reaction of two metal oxo complexes as has been described previously for the generation of quinone compounds.[15-17] Worth mentioning is that these non-heme iron(IV)-oxo complexes do not perform the hydroxylation of benzene or naphthalene, which highlights the low reactivity of bioinspired iron(IV)-oxo species in arene hydroxylation reactions.[198]

In 2002, Mansuy and co-workers described a non-heme iron complex supported by the TPAA ligand (TPAA = tris-[*N*-2-pyridylmethyl)-2-aminoethyl]amine), which is effective in the hydroxylation of aromatic compounds using H_2O_2 as oxidant, whereas this complex shows poor catalytic activity for olefin epoxidation and alkane hydroxylation (see Figure 15a for the structure of the TPAA ligand).[199] Overall, this complex shows up to 10 turnovers for the oxidation of anisole (53% yield based on the oxidant), but shows poor activities for the oxidation of less electron-rich substrates, such as benzene or chlorobenzene.[199] Non-heme iron complexes with tetradentate and pentadentate aminopyridine ligands, namely L_4^3, L_5^2 and L_5^3 (Figure 15a), have shown comparable arene hydroxylation capabilities in combination with H_2O_2. In addition, for most of these iron complexes it has been demonstrated that the addition of an appropriate reducing agent, such as hydroquinones, thiophenol or tetrahydropterins, dramatically enhances the yields of the hydroxylation aromatic products (up to 69% yield for anisole oxidation based on the oxidant catalyzed by iron complex based on the L_5^2 ligand, *i.e.* TON = 13.8).[200]

A more recent study on the non-heme iron complexes containing the TPEN (TPEN = *N,N,N',N'*-tetrakis-(2-pyridylmethyl)ethane-1,2-diamine) and $L_6^2$4E ligands has shown activity for the hydroxylation of electron-rich anisole, as well as for benzene and chlorobenzene. In particular, the former complex performed best in the presence of 1-naphthol as reducing agent, with a yield up to 86% for anisole oxidation (TON = 17.2), whereas the latter complex performed best employing thiophenol as reducing agent, with a yield up to 38% for anisole oxidation (TON = 7.6).[201] Worth mentioning is that these systems make use of substrate-excess conditions, providing high product selectivities, however, with low substrate conversions.

Bianchi and co-workers described a method for the selective hydroxylation of benzene to phenol catalyzed by an iron complex using H_2O_2 as benign oxidant and trifluoroacetic acid as co-catalyst in a biphasic system.[202] The study investigated a series of bidentate N,N-, N,O- and

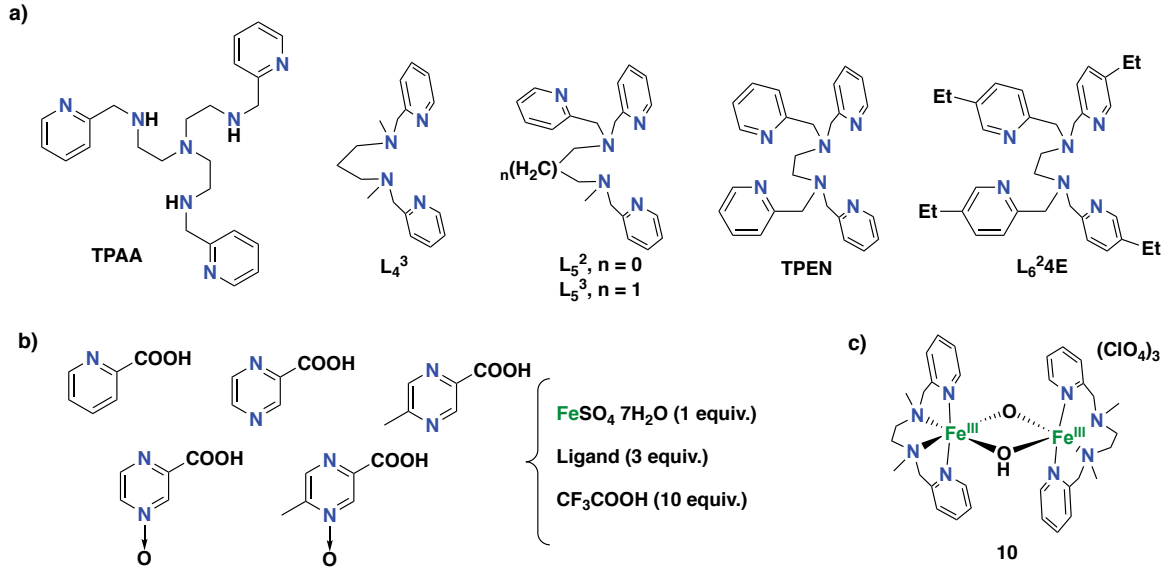

Figure 15. a) Aminopyridine ligands studied in iron-mediated arene hydroxylation reactions under substrate-excess conditions in the presence of a reductant.[199-201] **b)** Three-component system for the hydroxylation of aromatics using a biphasic reaction medium under substrate-excess conditions.[202-204] **c)** Example of a diiron complex that mimics the reactivity of toluene monooxygenases.[205]

O,O-based ligands, finding that the most efficient catalyst system was obtained by using 5-carboxy-2-methylpyrazine-*N*-oxide as ligand (see Figure 15b for ligand structures). The system was used under substrate-excess conditions, providing poor benzene conversions, while H_2O_2 conversion was 94%. Selectivity for the phenol product was 85% based on benzene conversion. Remarkably, the use of a biphasic system (mixture of water, acetonitrile, and aromatic substrate) allowed easy recovery and recycling of the catalyst. Later, the same authors reported on the use of a similar system, using pyrazine-3-carboxylic acid *N*-oxide as the ligand (Figure 15b), for the direct hydroxylation of a series of aromatic substrates to the corresponding phenol products.[203] The authors highlight the low selectivity obtained for the oxidation of electron-rich arenes, as well as possible competition for hydroxylation of the lateral alkyl chain in the case of alkylbenzenes. Finally, another study showed how small modifications in the structure of the ligand used in this biphasic system can produce significant differences in activities for the oxidation of benzene and toluene; the system using pyrazine-3-carboxylic acid *N*-oxide as the ligand being the most efficient for the synthesis of phenols.[204]

Biswas and co-workers have also described an iron system for the hydroxylation of aromatic C–H bonds under substrate-excess conditions.[205] This system consists of diiron(III) complex **10** supported by the bpmen ligand (Figure 15c), that is able to carry out the hydroxylation of benzene and alkylbenzenes with high selectivities, albeit with very low turnover numbers. The addition of acetic acid was found to produce a small increase in phenol yields. For alkylbenzene oxidations, products deriving from the hydroxylation of the lateral alkyl chain were also

observed. On the basis of its dinuclear nature, this system mimics the activity of toluene monooxygenase and methane monooxygenase.

In 2014, Kühn and co-workers reported iron complex **11** capable of hydroxylating aromatic substrates to the corresponding phenol products under catalytic conditions, with equimolar amounts of substrate/oxidant or excess of the oxidant.[206] This particular catalyst is based on a chelating di-pyridyl-di-NHC ligand (NHC = N-heterocyclic carbene; Figure 16).

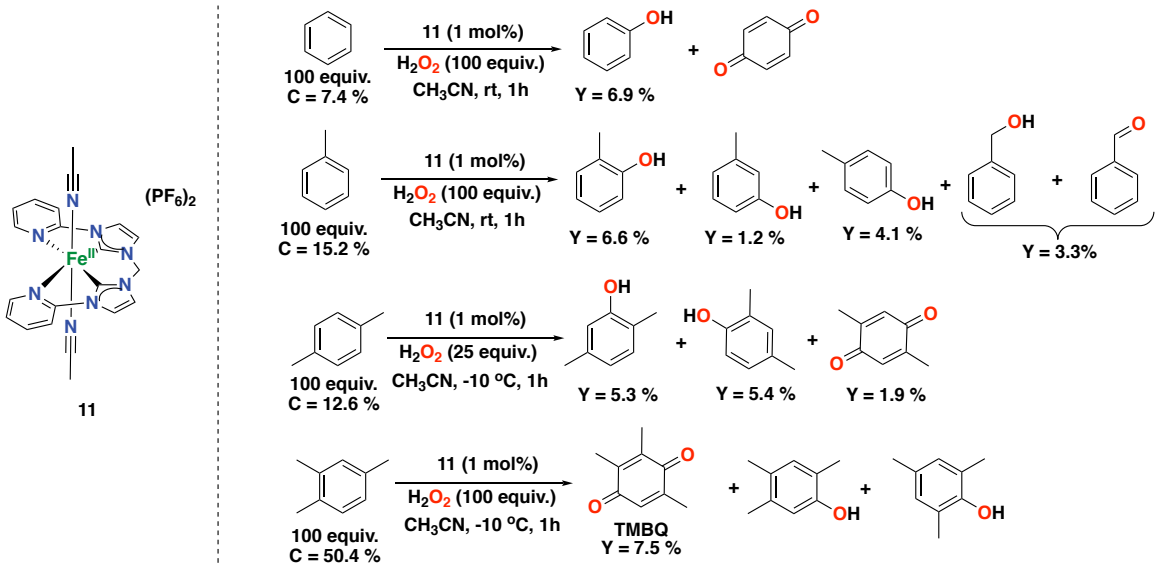

Figure 16. Reaction products of the catalytic oxidation of benzene and benzene derivatives catalyzed by NHC-based iron complex **11** with H_2O_2 as the oxidant.[206, 210] C: substrate conversion. Y: product yield.

The difference of this complex compared to other complexes typically used in oxidation chemistry is that the iron center in coordinated in part by NHC-based carbon donors.[207] NHCs are considered as good σ-donors and, therefore, the authors anticipated that the corresponding complex would exhibit high kinetic stability towards oxidation conditions.[208, 209] Complex **11** is able to oxidize benzene to phenol using equimolar amounts of H_2O_2 and substrate, albeit in low conversion (7.4%) and phenol yield (6.9%, *i.e.* TON = 6.9), but with high selectivity (94%). The major by-product in this reaction is *para*-benzoquinone. The involvement of hydroxyl radicals in this catalytic system was discarded since no formation of biphenyl was observed. Based on an experimental inverse C–H/C–D KIE of 0.9, the authors have postulated a mechanism that involves an sp^2-to-sp^3 hybridization change during the attack of a putative high-valent iron-oxo to the aromatic ring forming a σ-complex. Complex **11** is capable of hydroxylating methyl substituted arene substrates as well, such as toluene, *p*-xylene and pseudocumene (Figure 16). Mixtures of phenol products were observed together with some alkyl side chain oxidation products in some cases, overall showing a high selectivity for arene oxidation over benzylic oxidation reactions (up to 11.9% total yield for aromatic oxidation of toluene, and up to 12.6% total yield for *p*-xylene oxidation). A so-called NIH-shift for a methyl

group was observed for the current system in the oxidation of *p*-xylene, which resembles the same process observed for arene oxidations catalyzed by cytochrome P450 or pterin-dependent aromatic amino acid hydroxylases. The system was also tested for the oxidation of pseudocumene, affording trimethylbenzoquinone (TMBQ) in 7.5% yield (a valuable chemical for vitamin E synthesis).[206, 210]

In 2016, Silva and co-workers reported on the reactivity of a series of iron complexes (**12-17**) based on acetylacetonate and Schiff base ligands in the direct hydroxylation of benzene to phenol with H_2O_2 (Figure 17a).[42] Within this study it was found that the complex based on a N_4-donor Schiff base ligand shows the highest activity and selectivity for the hydroxylation of benzene under substrate-limiting conditions, with 65% conversion and 98% phenol selectivity, generating *para*-benzoquinone as overoxidized side-product.[42] This system has shown some of the highest conversions and phenol selectivities ever reported for arene hydroxylation using iron catalysts with H_2O_2 as oxidant.

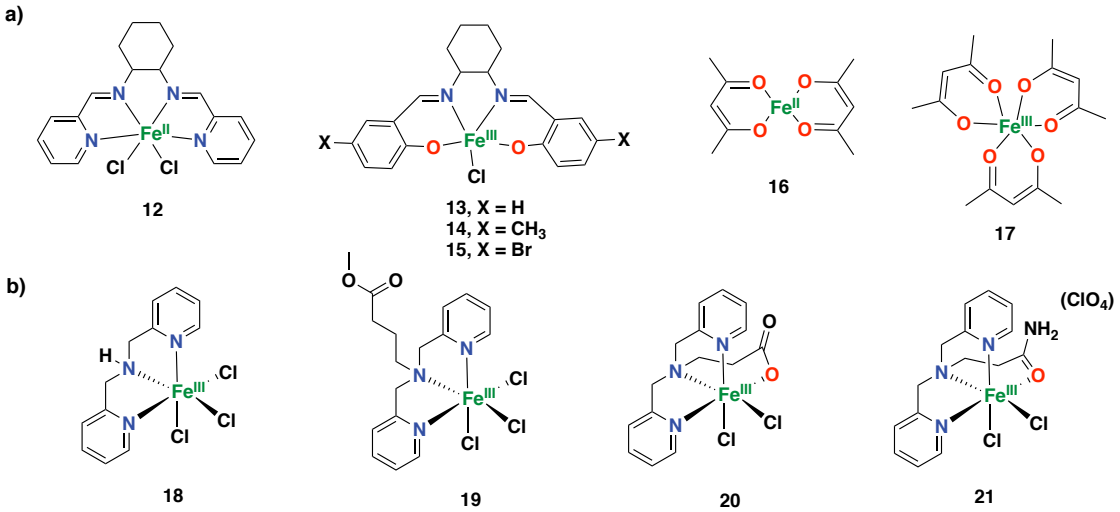

Figure 17. a) Iron complexes supported by acetylacetonate and Schiff base ligands tested for the direct aromatic hydroxylation of benzene to phenol with H_2O_2.[42] **b)** Iron(III) complexes tested for the hydroxylation of toluene with H_2O_2 as oxidant.[211]

A later study by Antunes et al. describes the reactivity of a series of iron(III) complexes (**18-21**) based on the BMPA and similar ligands as catalysts for the hydroxylation of toluene with H_2O_2 as oxidant (BMPA = bis-(2-pyridylmethyl)amine; Figure 17b).[211] All complexes tested in this study showed reactivity for the oxidation of toluene, generating mixtures of phenol products (*ortho*-, *meta*- and *para*-isomers), as well as products deriving from lateral alkyl chain oxidation (benzaldehyde and benzyl alcohol). Complex **18** based on the BMPA ligand showed the higher yields of all catalysts tested in this study, with a 30% total product yield for the oxidation of toluene at 50 °C after 24 h.[211]

Despite the extensively investigation of non-heme iron complexes based on aminopyridine ligands, studies have also shown the effectiveness of imine-based non-heme iron complexes for different oxidative processes.[212] A remarkable example in the field of arene oxidations catalyzed by imine-based iron complexes was recently reported by Di Stefano and co-workers using iminopyridine iron(II) complex **22**, prepared in situ by self-assembly of commercial starting materials (iron(II) triflate, 2-picolylamine and 2-picolylaldehyde), and H_2O_2 as oxidant under mild reaction conditions (Figure 18).[213]

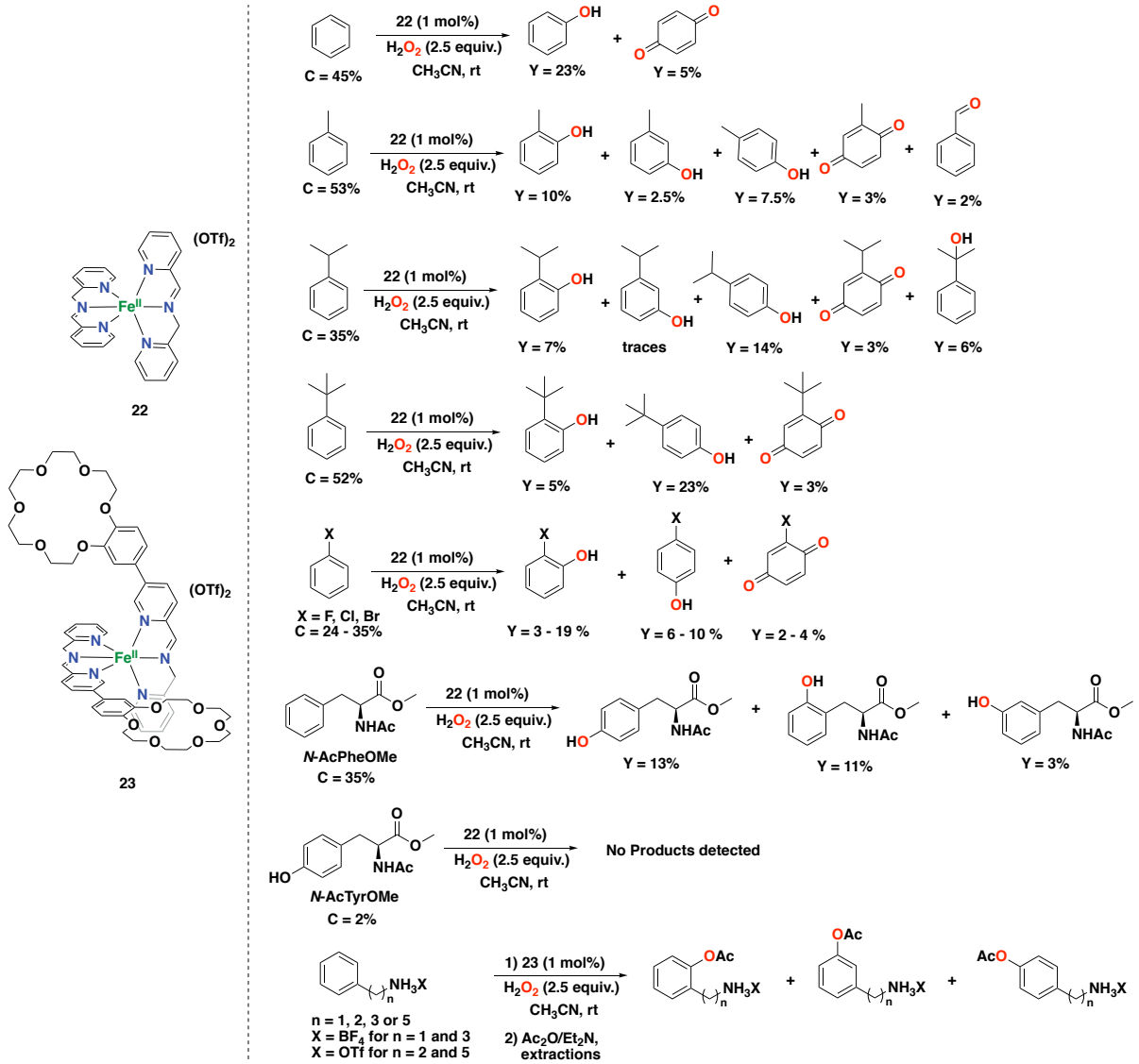

Figure 18. Reaction products of the catalytic oxidation of benzene, benzene derivatives and aromatic amino acids catalyzed by iminopyridine iron(II) complexes **22** and **23** with H_2O_2 as oxidant.[213-215] C: substrate conversion. Y: product yield.

The authors found that complex **22** is capable of oxidizing benzene in 23% phenol yield after 90 min of reaction time, generating benzoquinone as overoxidized by-product in only 5% yield. The oxidation of benzene was also effective on a 0.5 g scale, generating phenol in 26% yield.

A metal-based reaction was postulated as a plausible mechanism for this system since no biphenyl product was detected, suggesting that oxygen-centered radicals are likely not involved. Besides, oxidation of benzene derivatives was also performed with this iminopyridine iron system. Oxidation of phenol afforded *para*-benzoquinone in 13% yield exclusively. Oxidation of toluene afforded the corresponding cresol products (mixture of *ortho*-, *meta*- and *para*-isomers) in a total yield of 20%, as well as overoxidized methyl-p-benzoquinone in 3% yield and alkyl chain oxidation product benzaldehyde in 2% yield. Oxidation of ethylbenzene provided products deriving from hydroxylation at the aromatic ring as well as from alkyl side chain oxidation, albeit in smaller amounts. However, when cumene was considered, which bears a more encumbered isopropyl substituent with a weak tertiary benzylic C–H bond, the yield for the alkyl side chain oxidation alcohol product increased (6% yield). Hydroxylation of *tert*-butylbenzene was also proven to be effective, generating phenols in a total yield of 28%, with *tert*-butyl-p-benzoquinone by-product in only 3% yield. For all alkylbenzenes tested, mixtures of *ortho* and *para*-phenols were obtained, whereas *meta*-phenols formed in small amounts, suggesting that an electrophilic aromatic substitution-type of mechanism is operative for this catalytic system. Oxidation of halobenzenes was also effective, exclusively generating *ortho*- and *para*-phenols, together with quinone by-products. The electron-rich substrate anisole was oxidized in 21% total yield, providing a mixture of *ortho*-phenol, *para*-phenol and benzoquinone. This product profile agrees with the fact that electron-donating groups favor the oxidation by electrophilic oxidants. On the contrary, electron-withdrawing substituents suppress the reactivity of the catalyst towards the aromatic ring.

Iron complex **22** has also been found to be effective for the oxidation of several aliphatic C–H bonds,[216] as well as alcohol oxidation to ketones.[217] Noteworthy is that benzylic alcohols are oxidized in low yields due to competitive arene hydroxylation, showing that the **22**/H_2O_2 catalytic system has a preference for oxidizing aromatic over aliphatic sites. Moreover, the oxidation of monocyclic and polycyclic aromatic systems showed a clear chemoselectivity for aromatic over aliphatic side chain oxidation. However, for more activated polycyclic substrates with lower BDEs of the benzylic C–H bond, the chemoselectivity decreased.[218]

A mechanism for H_2O_2 activation and substrate oxidation by complex **22** has been proposed to include decoordination of one of the pyridine donor arms.[213, 219] Initially, the starting Fe(II) complex is oxidized to an Fe(III) intermediate, after which detachment of one of the pyridine arms of the ligand allows the complex to react with H_2O_2 to generate an Fe(III) hydroperoxo species (Figure 19). Further generation of the active species is still a matter of debate, but generation of a high-valent Fe(V) oxo species is proposed to be unlikely since imine-based ligands usually favor low oxidation states of the metal center.[219]

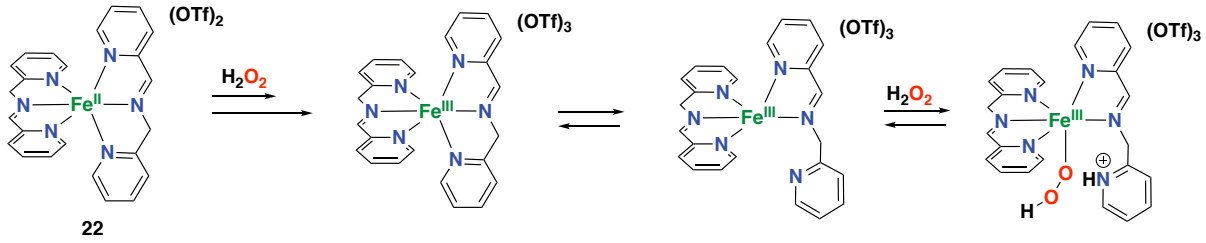

Figure 19. Proposed mechanism for H_2O_2 activation with iminopyridine iron(II) complex **22**.[219]

Complex **22** was also shown to be capable of oxidizing an aromatic amino acid derivative with H_2O_2. Particularly, the oxidation of a protected phenylalanine (*N*-AcPheOMe) yields the corresponding tyrosine (*N*-AcTyrOMe) as the main product (13% yield), together with the two isomeric phenolic derivatives in 14% total yield (Figure 18).[214] Interestingly, no formation of products deriving from benzylic hydroxylation were observed. An important point to highlight is that **22** does not seem to suffer from irreversible phenolate binding to the iron center, which generally avoids catalytic turnover by catalyst inhibition, as found for several examples presented in this review.

More recently, Di Stefano and co-workers designed a modified version of iminopyridine iron(II) complex **22**, by decorating the ligand with crown-ether moieties. Complex **23** catalyzes the oxidation of aromatic compounds endowed with an alkylammonium anchoring group with H_2O_2 with a moderate activity (up to 31% total yield) and selectivity for hydroxylation of the *meta* over the *ortho* site (up to 1.5 for *meta*/*ortho* ratio; Figure 18).[215] The selectivity observed was proposed to be guided by the steric bulk provided by the crown-ether moieties of the ligand, with minor contribution from substrate recognition.

In 2018, Talsi and co-workers described iron complex **24** based on a bpbp type ligand as catalyst for the hydroxylation of aromatics with H_2O_2 or peracetic acid as oxidants and a carboxylic acid as co-ligand (Figure 20).[220] Particularly, iron complex **24** is based on a diferric core, which was previously found to be effective in other oxidative processes, such as alkane hydroxylations and alkene epoxidation reactions.[221-223] Complex **24** was found to be also effective in the oxidation of different aromatic substrates, such as benzene and mono- and dialkylbenzenes (Figure 21). With 0.62 mol% of catalyst loading, 4 equiv. aqueous H_2O_2 and 10 equiv. acetic acid, a total TON of 12.6 in benzene oxidation was achieved, forming hydroquinone (TON = 11.4) as the major, overoxidized product, next to phenol as a minor product (TON = 1.2). For the oxidation of toluene, cresols were obtained in only 1.9 turnovers as a mixture of *ortho*- and *para*-phenols, whereas the major products were the corresponding methylhydroquinone (TON = 8.2) and 4-(hydroxymethyl)phenol (TON = 4.9). Products deriving exclusively from the oxidation of the alkyl side chain were also obtained. Oxidation of other alkylbenzene derivatives provided similar results, with the corresponding

hydroquinones as the major product (Figure 21). Overall, overoxidized products and poor selectivities for the oxidation of the aromatic ring were obtained, resulting in mixtures of products in which oxidation has taken place on aromatic as well as aliphatic positions.[220]

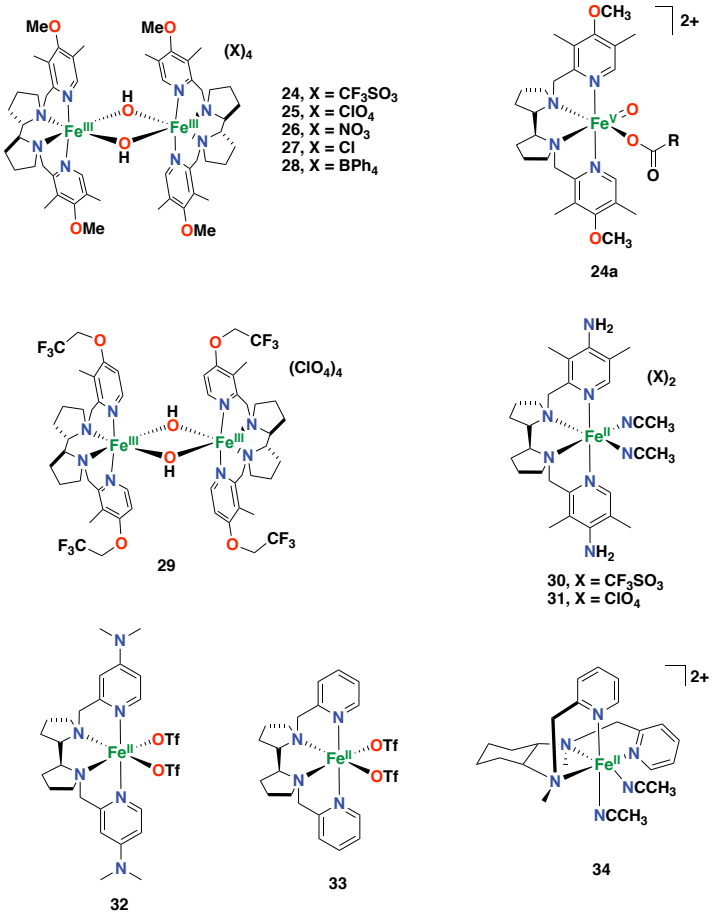

Figure 20. Structures of iron complexes supported by tetradentate aminopyridine ligands that catalyze aromatic oxidation using H_2O_2.

Regarding the active oxidant responsible for the arene hydroxylation reaction, the mechanism was proposed to proceed through Fe(V)-oxo species **24a**, which is formed as a monomeric species upon the reaction of differic complex **24** with H_2O_2 and the carboxylic acid additive at low temperatures.[221, 222, 224] This assignment was based on characteristic EPR parameters, which were similar to those for previously reported non-heme Fe(V)-oxo species.[225, 226]

Subsequently, Bryliakov and co-workers explored a series of related iron complexes **24**-**33** based on (substituted) bpbp ligands and containing different counter anions for the oxidation of alkylbenzenes.[227] Among the different counter anions tested, it was found that complex **24**, containing triflate ions, performed the best, with the highest efficiency and selectivity for the oxidation of *o*-xylene. Complex **25**, with perchlorate counter anions, showed a slightly lower catalytic activity, whereas complexes **26-28**, with other counteranions, performed less

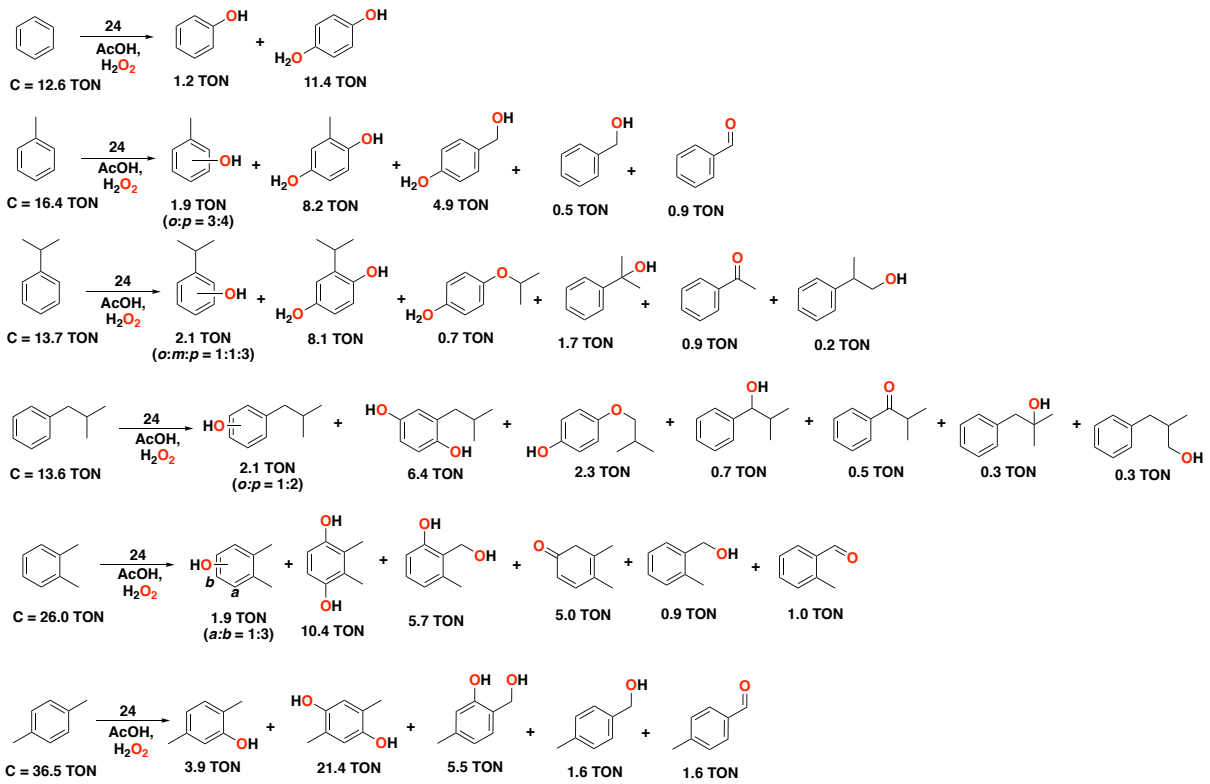

Figure 21. Reaction products of the catalytic oxidation of benzene and benzene derivatives catalyzed by diferric complex **24** as catalyst with H_2O_2 as oxidant and AcOH as carboxylic acid additive. Reaction conditions: complex **24** (0.62 mol% cat. / 1.24 μmol Fe), substrate (100 μmol), H_2O_2 (400 μmol), AcOH (1000 μmol) in CH_3CN at 0 °C for 1.5 h. See the corresponding reference for further details on the oxidation of other alkylbenzene substrates.[220]

efficiently for arene oxidation. Importantly, all these iron complexes are active in aromatic oxidation, but show low selectivities, as shown by the formation of considerable amounts of mixed aromatic/aliphatic double oxygenation products.

Among the series of iron complexes tested in this study, it was found that the mononuclear, non-substituted bpbp complex **33** (1.24 mol%) performed best for the oxidation of several aromatic substrates with H_2O_2 (4 equiv.), employing acetic acid (10 equiv.) as additive (Figure 22).[227] Complex **33** is capable of oxidizing benzene, providing hydroquinone as the major product (TON = 9.6), together with small amounts of phenol (TON = 2.2). For toluene oxidation, the hydroquinone was again generated as the main product (TON = 11.1), together with small amounts of cresol products (TON = 2.9). Products in which oxidation has taken place at the benzylic position were also observed in considerable amounts. Oxidation of other alkylbenzene substrates, including mono and dialkylbenzenes, was also performed. Of interest is the oxidation of *p*-xylene, in which a high conversion (TON = 51.5) and yield for the hydroquinone product (TON = 30.3) was observed. Overall, hydroquinone products were

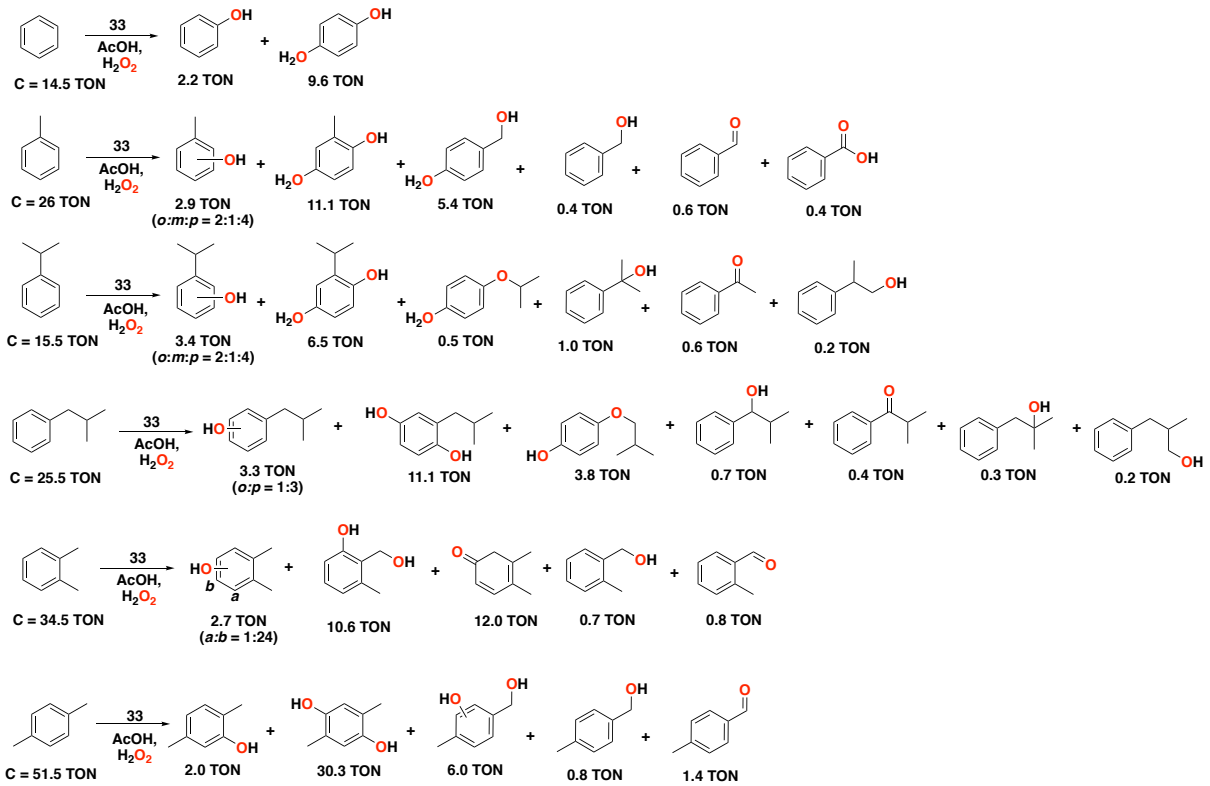

Figure 22. Reaction products of the catalytic oxidation of benzene and benzene derivatives catalyzed by complex **33** as catalyst with H_2O_2 as oxidant and AcOH as carboxylic acid additive. Reaction conditions: complex **33** (1.24 μmol Fe), substrate (100 μmol), H_2O_2 (400 μmol), AcOH (1000 μmol) in CH_3CN at 0 °C for 1.5 h. See the corresponding reference for further details on the oxidation of other alkylbenzene substrates.[227]

obtained as the main product, with small amounts of phenol products and benzylic oxidation products, in a similar way as observed for complex **24** (compare Figure 21 and Figure 22).

The authors also tested other mononuclear iron complexes based on the parent bpbp ligand and comprising differently substituted pyridine rings, but these were found to perform less efficiently compared to parent complex **33**. For instance, the use of mononuclear complexes **30** and **31**, containing an amino group at the pyridine ring instead of a methoxy group, did not improve the reactivity in the oxidation of *o*-xylene with respect to that of complex **24** or **33**. A similar reactivity was also found when the diferric trifluoroethoxy iron complex **29** was employed, whereas complex **32**, bearing dimethylamino substituents, was less efficient. Finally, complex **8**, containing the parent tripodal tpa ligand, was also tested in this same study, also showing poor catalytic activity.

An exploration of different carboxylic acid additives in the aromatic oxidation of *m*-xylene catalyzed by complex **33** revealed that 2-ethylhexanoic acid provided the best results among a series of different linear and branched carboxylic acids tested.[228] Using optimized conditions,

i.e. complex **33** (1.24 mol%), with 2-ethylhexanoic acid additive (10 equiv.) and H_2O_2 (4 equiv.), the oxidation of a series of aromatic substrates was performed (Figure 23).

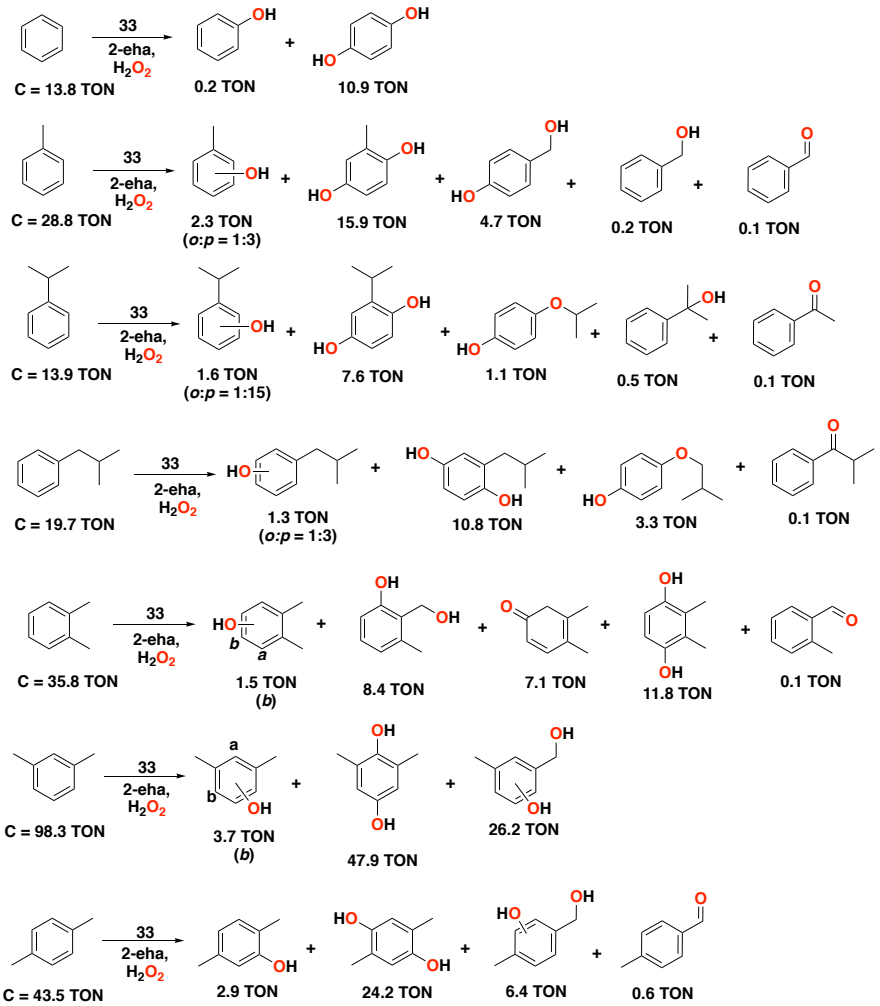

Figure 23. Reaction products of the catalytic oxidation of benzene and benzene derivatives catalyzed by complex **33** with H_2O_2 as oxidant and 2-eha as carboxylic acid additive. Reaction conditions: complex **33** (1.24 μmol Fe), substrate (100 μmol), H_2O_2 (400 μmol), 2-eha (1000 μmol) in CH_3CN at 0 °C for 1.5 h. See the corresponding reference for further details on the oxidation of other alkylbenzene substrates.[228] 2-eha = 2-ethylhexanoic acid.

Benzene was oxidized to hydroquinone (TON = 10.9), with small amounts of phenol product being formed (TON = 0.2). For the oxidation of toluene, the corresponding hydroquinone was formed in 15.9 turnovers, with small amounts of phenol products and products deriving from oxidation at the aliphatic side chain. Catalytic oxidation of a series of mono and dialkylbenzene substrates gave similar results to those obtained when acetic acid was employed, however, yields for the oxidized products were slightly higher when 2-ethylhexanoic acid was used (compare Figure 22 and Figure 23). Interestingly, *m*-xylene was oxidized with a conversion of 98.3 turnovers using these conditions, providing the corresponding hydroquinone in up to 47.9 turnovers.

In an independent study, Que and co-workers tested the reactivity of iron complex **34** ([Fe(*β*-bpmcn)$(CH_3CN)_2]^{2+}$) in the oxidation of benzene (Figure 20), which was found to perform several catalytic turnovers to generate phenol in the presence of $Sc(OTf)_3$ or $HClO_4$ additives.[229] Generally, it has been established that iron complex **34** is a sluggish oxidation catalyst with H_2O_2 as the oxidant.[165] Nevertheless, it was found that by adding a strong Lewis acid like $Sc(OTf)_3$ or a Brønsted acid like $HClO_4$, a highly electrophilic oxidant is formed that is able to carry out 4 catalytic turnovers in the hydroxylation of benzene to phenol at –40 °C. The authors have proposed that an interaction between Sc^{3+} and the iron-oxo oxidant or its iron-hydroperoxo precursor occurs, in a similar way as it has been proposed in other studies for related iron complexes.[230-234] In another study, Que and co-workers showed that activation of the non-heme iron-hydroperoxo species generated with the **34**/H_2O_2 system can also be accomplished using $Fe^{III}(OTf)_3$ as a Lewis acid, leading to the formation of the iron(V)-oxo oxidant.[235] This system was found to be slightly more active in the hydroxylation of benzene to phenol, affording up to 5.4 turnovers. This finding is of interest since it provided insight into the role of a second iron center, which can be related to the activity of diiron active sites found in metalloenzymes, such as in sMMOs.

Finally in 2021, Han and co-workers reported on an iron complex supported by the *L*-cystine-derived BCPOM ligand and its activity in the arene hydroxylation reaction with H_2O_2 as oxidant (Figure 24).[236]

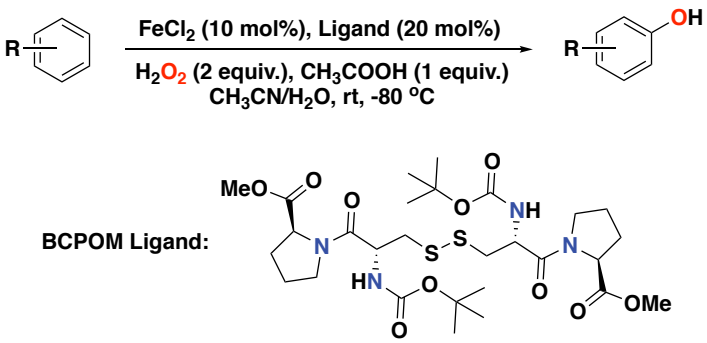

Figure 24. Arene oxidation reaction catalyzed by $FeCl_2$, the L-cystine-derived BCPOM ligand and H_2O_2 as oxidant.

The selectivity of this system is excellent, with good yields, and a compatibility with a broad number of substrates. For instance, for the oxidation of protected anilines, oxidation takes place at the *para*-position with respect to the amide substituent with up to 68% isolated product yield. Oxidation of arenes containing methyl, dimethyl or isopropyl substituents were also tested and afforded the phenol products in up to 70% isolated yield. The BCPOM-based system is also active in the oxidation of strongly electron-deficient arene substrates, including aryl ketones

and aldehydes. Of note, the system makes use of 10 mol% of $FeCl_2$ as the metal salt precursor and 20 mol% of ligand.

1.3 Copper in Biological and Synthetic Systems

1.3.1 Copper-containing Metalloenzymes

Copper-containing enzymes also play an important role in biological oxidation chemistry and, accordingly, are a big source of inspiration in the area of homogeneous oxidation catalysis.[22, 25, 27] Copper enzymes can be classified by the number of copper centers in their active site; either one copper center (mononuclear)[237] or two or more copper centers (di- or polynuclear).[27, 238] Examples that stand out among this class of copper-containing metalloenzymes are galactose oxidase (*i.e.* radical copper oxidases that use copper(II)-tyrosyl radical intermediates), amine oxidase, dopamine β-monooxygenase and peptidylglycine α-hydroxylating monooxygenase (*i.e.* enzymes that involve monocopper-oxygen species as intermediates during catalysis), and tyrosinase and catechol oxidases (*i.e.* enzymes that contain dicopper(I) active sites).

1.3.1.1 Tyrosinase and Catechol Oxidases

In this section we briefly discuss copper-containing metalloenzymes capable of performing the oxidation of aromatic substrates. Tyrosinase and catechol oxidases are well-known copper-containing metalloenzymes that catalyze the two-electron oxidation of catechols to *o*-quinones.[239] The difference is that tyrosinase oxidases can also perform the *o*-hydroxylation of phenols to catechols, along with the further oxidation to *o*-quinones.[240, 241] This reactivity is of importance in melanin biosynthesis.

The active site of tyrosinase comprises a dinuclear copper(I) center in which each metal center is coordinated to three histidine residues (catechol oxidases and haemocyanin share a similar active site).[242] Reaction with O_2 forms a (peroxo)dicopper(II) species in which oxygen is bound in a side-on bridging (μ-η^2:η^2) binding mode.[243] The overall catalytic cycle for phenol oxidation by tyrosinase (phenolase cycle) to generate a quinone product is depicted in Figure 25.[14, 107, 238, 240, 241] The *deoxy* species can bind O_2 to form the *oxy* intermediate, as stated above. Then, the phenol substrate (in its phenolate form) coordinates to the *oxy* intermediate to only one of the copper centers and *ortho*-hydroxylation occurs to generate an *o*-catecholate dianion that binds in single bridging mode to both copper centers and in a bidentate fashion to only one of the copper centers. Subsequently, a two-electron oxidation yields the final *o*-quinone, thereby restoring the *deoxy* species. An additional catalytic cycle involves the oxidation of external catechol substrates to form *o*-quinones (diphenolase activity; not shown).

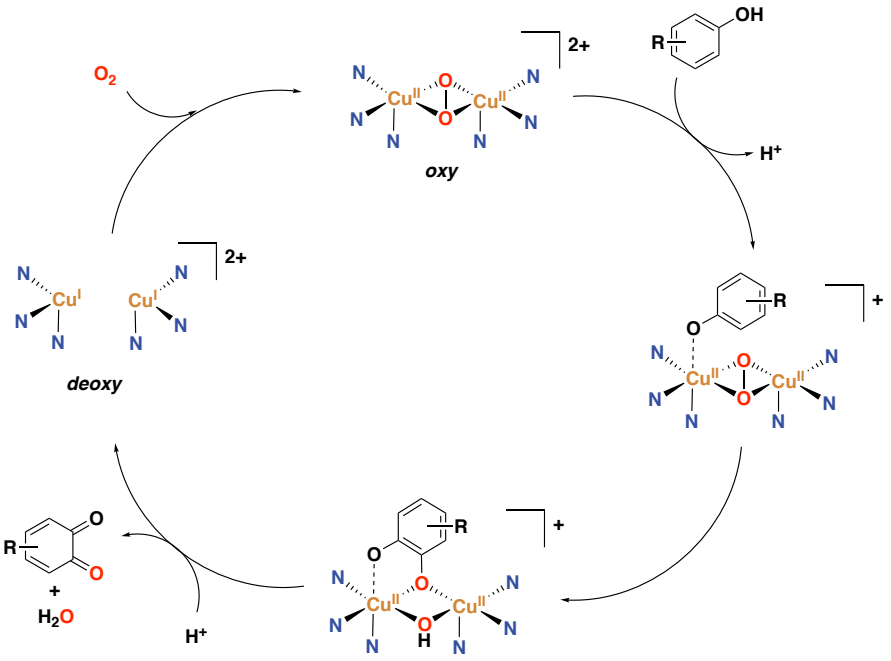

Figure 25. Oxidation of monophenols to o-quinones catalyzed by tyrosinase oxidase.[14, 107, 240, 241, 244]

1.3.2 Synthetic Copper Systems

Inspired by copper-containing metalloenzymes, chemists have tried to copy their interesting activity and selectivity by mimicking their active sites. Accordingly, various studies have reported on the synthesis of bioinspired model complexes for these copper-containing metalloenzymes. In general, the ligands used in these models contain nitrogen atom donors to reproduce the histidine environment around the catalytic active site of the metalloenzyme. Within this context, these studies have mainly employed pyridines, secondary and tertiary amines, and benzimidazole donor groups.

Within this field, Karlin with co-workers have published numerous examples of copper complexes capable of performing oxidation processes related to the reactions catalyzed by tyrosinase oxidase.[245-253] Generally, the ligands used in their studies contain a *meta*-xylyl linker, which allows for the proper orientation of the two copper centers to react with external reagents in a cooperative manner. Earlier examples are based on dinuclear copper(I) complexes of the general structure presented in Figure 26 for complex **35**, bearing two aminopyridine moieties bridged by a *m*-xylyl linker, which react with O_2 to form intermediate species **36** that contains a side-on (μ-η^2:η^2) coordinated peroxo ligand. Intermediate **36** is responsible for the intramolecular hydroxylation of the aromatic ring in the *m*-xylyl linker of the ligand to afford compound **37**.[245-247, 251]

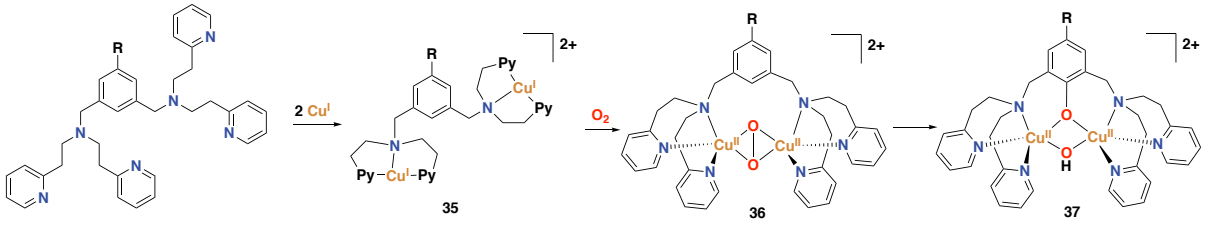

Figure 26. Representative synthetic copper complex **35** inspired by tyrosinase oxidase, reported by Karlin et al. [245-247] Upon complexation of copper to the dinucleating aminopyridine ligand, reaction with dioxygen leads to a side-on (μ-η^2:η^2) peroxo copper intermediate that can perform an intramolecular aromatic hydroxylation. Py = pyridine; R = H, MeO, ^{t}Bu, F, CN, NO_2.

Other dicopper model complexes have also been found to react with dioxygen, to subsequently display arene hydroxylation reactivity (Figure 27). For instance, a dicopper complex supported by triazacyclononan-based ligands bridged by *m*-xylyl groups reacts with dioxygen at –80 °C to from species **38** with a (μ-η^2:η^2) peroxo moiety that could be spectroscopically traced by means of UV-Vis and resonance Raman. Such species are subsequently able to hydroxylate the bridging arene group of the ligand.[254] A dicopper complex supported by the 1,3-bis{[3-(*N*,*N*-dimethyl)propyl]iminomethyl}benzene ligand also reacts with dioxygen to afford a Cu_2O_2 species that performs arene hydroxylation of the ligand to afford compound **39**, which was isolated and characterized by X-ray crystalography.[255] In a similar way, a dicopper complex ligated to a dinucleating hexaaza macrocycle is capable of performing intramolecular arene hydroxylation of the ligand to yield compound **40**.[256] Casella and co-workers reported a synthetic dicopper complex derived from ligand L-66 (L-66 = α,α'-bis{bis[2-(1'-methyl-2'-benzimidazolyl)ethyl]amino}-*m*-xylene), which for the first time, performed the intermolecular hydroxylation of phenols, therefore displaying similar reactivity as found for tyrosinase oxidase.[257] Reaction of the dicopper(I) complex with dioxygen was shown by low temperature UV-Vis and resonance Raman to generate intermediate **41** with a highly reminiscent structure to that of prototypical intermediate **36**. Species **41** is able to hydroxylate external phenol substrates, such as the *o*-hydroxylation of 4-carbomethoxyphenolate to the catecholate product (about 40% yield with respect to intermediate **41**) and the oxidation of 3,5-di-*tert*-butyl-catechol to the corresponding quinone (the formation of the product was demonstrated by low temperature UV-Vis).[257] Later, related benzimidazole-based copper-oxygen intermediates, such as **42**, were also found to react with external phenols to form quinones at different temperatures.[258]

Mononuclear copper complexes have also been used to generate Cu_2O_2 intermediates that can mimic the activity of tyrosinase.[259-262] For instance, Itoh and co-workers reported the synthesis of a side-on (μ-η^2:η^2) peroxo complex **43**, supported by the *N*,*N*-bis[2-(2-pyridyl)-ethyl]-α,α-dideuteriobenzylamine ligand. This complex is able to perform the intermolecular

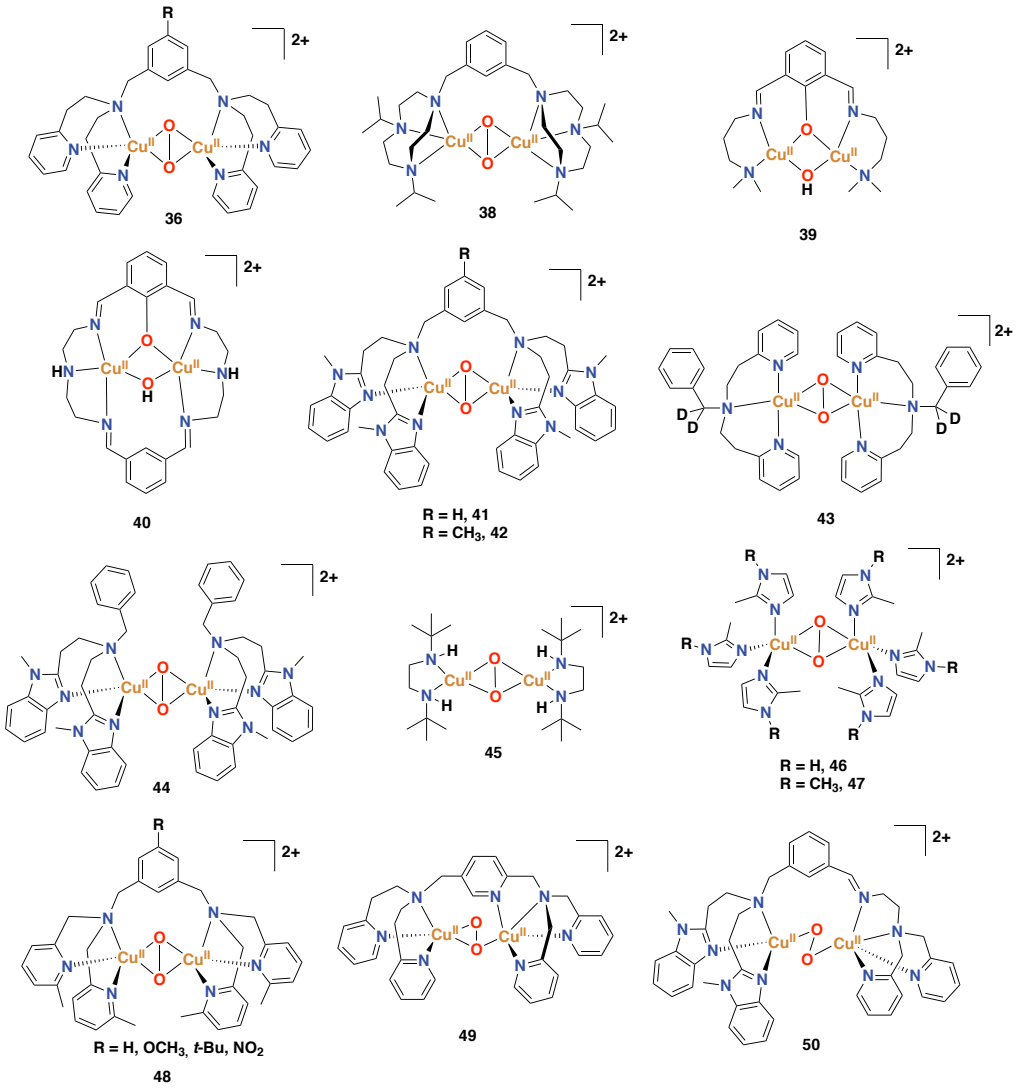

Figure 27. Selected examples of dicopper(II) dioxygen complexes (supported by mono- and dinucleating ligands, as well as non-symmetrical dinucleating ligands) that mimic the activity of tyrosinase.[254-262, 264, 266-269]

hydroxylation of lithium salts of phenols (*p*-X-C_6H_4-OLi; X = Cl, Me and CO_2Me) to generate the corresponding catechols with up to 90% isolated yield in a stoichiometric reaction.[259]Another mononuclear copper complex supported by *N*,*N*-bis(2-(*N*-methylbenzimidazol-2-yl)ethyl)benzylamine has also been found to react with dioxygen to generate a binuclear (μ-η^2:η^2) peroxo complex **44**, that can perform the *o*-hydroxylation of externally added phenols.[260] Next, (μ-η^2:η^2) peroxo dicopper complexes supported by bidentate ligands have also been reported. For instance, complex **45** (supported by a bidentate secondary diamine ligand) was synthesized from the reaction of its corresponding mononuclear copper(I) complex with dioxygen, and its reactivity with phenolates to yield catechols and quinone products was described.[261, 262] The mechanism through which complex **45** reacts with phenolate substrates works in the presence of dioxygen has been shown to involve the formation of a

bis(μ-oxo)dicopper(III) intermediate prior to the aromatic hydroxylation step (vide infra; Figure 28b).[263] (μ-η^2:η^2) Peroxo dicopper(II) complexes **46** and **47** supported by monodentate imidazole ligands have also been reported and their reactivity has been explored towards the hydroxylation of exogenous phenolic substrates to afford catechols in good stoichiometric yields at –125 °C, representing more recent examples of bioinspired copper complexes based on the active site of tyrosinase enzyme.[264] Along the same line, mononuclear copper complex supported by imine-based ligand containing pyrazole groups have been reported, and their reaction with dioxygen has been proposed to generate a side-on (μ-η^2:η^2) bound dicopper species that can react with 2,4-di-*tert*-butyl-phenolate (DTBP-H) to generate 3,5-di-*tert*-butyl-*o*-quinone (DTBQ).[265] Suzuki and co-workers have reported on side-on (μ-η^2:η^2)-peroxo dicopper(II) complex **48** supported by H-L-H-type ligands (H-L-H = 1,3-bis-[bis(6-methyl-2-pyridylmethyl)aminomethyl]benzene). This species is very similar to species **36** previously reported by Karlin and co-workers, and not only performs the aromatic ligand hydroxylation of the *m*-xylyl linker but also performs the intermolecular epoxidation of styrene and hydroxylation of THF.[269]

Unsymmetrical dinucleating ligands have also been employed in the field of synthetic copper-oxygen chemistry. For instance, Itoh and co-workers reported on a dicopper complex supported by an asymmetric pentapyridine dinucleating ligand.[267] Upon reaction with dioxygen, they postulated that dicopper(II) species **49** with an unprecedented (μ-η^1:η^2) binding mode is formed, by comparison of its UV-Vis spectra and resonance Raman features with that of well-characterized (μ-η^1:η^1)-peroxo dicopper(II) and (μ-η^2:η^2)-peroxo dicopper(II) complexes. Later, Costas and co-workers reported on a non-symmetrical dicopper(I) complex supported by an non-symmetric dinucleating ligand, which upon reaction with dioxygen generates (μ-η^1:η^1) peroxo dicopper(II) complex **50**.[268] The reactivity of this species was studied by means of experimental and computational methods, and it was found to perform the *ortho* hydroxylation of externally added sodium *p*-chlorophenolate to form *p*-chlorocatechol in 39% yield with respect to **50**.

Generally, a side-on (μ-η^2:η^2) coordination mode of the O_2-ligand in these kind of Cu:O_2 complexes has been proposed to be the responsible for the hydroxylation reaction. However, an equilibrium has been demonstrated to exist between the side-on (μ-η^2:η^2) peroxo dicopper species and a bis(μ-oxo)dicopper(III) species, in which the later can be formed upon cleavage of the O–O bond.[270-273] Accordingly, the capability of bis(μ-oxo)dicopper(III) species to perform aromatic hydroxylation reactions was scrutinized, and indeed, for some cases this reactivity has been demonstrated.[241, 256, 263, 266, 270, 271, 274, 275] For example, Tolman and co-workers made use of a mononuclear copper(I) complex containing a bidentate pyridine/amine ligand with a pendant phenyl group, which upon reaction with dioxygen formed bis(μ-oxo)

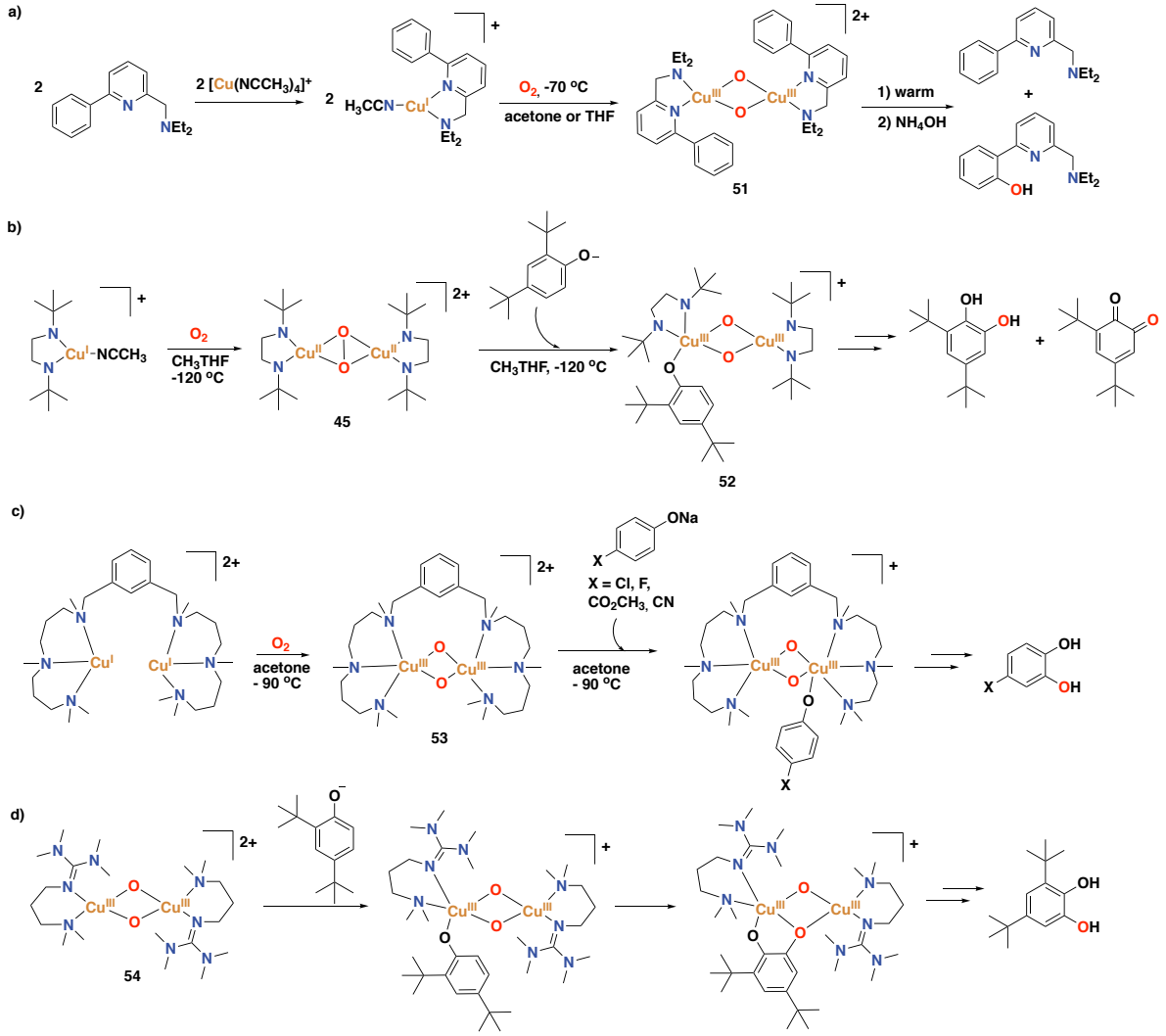

Figure 28. a) Synthesis of a copper(I) complex that performs the hydroxylation of an arene of the ligand upon reaction with dioxygen through bis(μ-oxo)dicopper(III) intermediate **51**.[275] **b)** Mechanism of phenolate oxidation by a mononuclear copper(I) complex, involving formation of intermediates **45** and **52**.[263] **c)** Mechanism of phenolate oxidation by a dinuclear copper(I) complex, involving bis(μ-oxo)dicopper(III) intermediate **53**.[266] **d)** Reaction of bis(μ-oxo)dicopper(III) complex **54** with phenolates to afford catechol products.[276]

dicopper(III) species **51** that can perform the intramolecular aromatic hydroxylation of a phenyl group (Figure 28a).[275] Stack and co-workers have studied the reactivity of (μ-η^2:η^2)-peroxo dicopper(II) complex **45** towards phenols, and they could demonstrate that upon addition of the substrate at –120 ºC a bis(μ-oxo)dicopper(III)-phenolate complex **52** formed prior to the hydroxylation step (Figure 28b).[263] This intermediate was characterized by UV-Vis, resonance Raman, and Cu K-edge X-ray absorption spectroscopy. Later, Costas and co-workers reported a dicopper(I) complex containing a tertiary N-methylated hexaaza ligand with a bridging *m*-xylyl linker, which generates bis(μ-oxo)dicopper(III) species **53** upon reaction with dioxygen at –90 ºC. Intermediate **53** is able to bind and hydroxylate phenolates, and indeed the authors

were able to trap and spectroscopically characterize the species that results from the reaction of sodium *p*-chlorophenolate with species **53** and that precedes phenolate hydroxylation. The 4-chlorocatechol product was formed in 67% yield with respect to the initial dicopper(I) complex.[266] Stack and co-workers reported another bis(μ-oxo)dicopper(III) species (**54**) supported by a permethylated-amine-guanidine ligand based on the 1,3-propanediamine backbone that is able to perform the *ortho*-hydroxylation of phenolates to afford catechol products.[276]

Mononuclear oxygenated copper complexes, such as end-on bound superoxo copper(II) species or copper(II)-alkylperoxide complexes, have also been shown to perform aromatic oxidation reactivity (Figure 29a and b).[277] For instance, copper(II) complexes **55** supported by tridentate bis[(pyridin-2-yl)methyl]benzylamine ligands containing *m*-substituted phenyl substituents at the 6th position of each pyridine group were reported to react with H_2O_2 in acetone to form 2-hydroxy-2-hydroperoxypropane species **56**. The latter intermediate undergoes an aromatic ligand hydroxylation reaction to afford copper(II)-phenolate complex **57** (Figure 29a).[278] This reaction pathway has been studied by means of spectroscopic and kinetic analysis and an electrophilic aromatic substitution mechanism has been proposed.[279] A carbonyl copper complex, supported by an electron-rich tripodal tetradentate aminopyridine ligand based on the tpa scaffold, was reported to react with dioxygen to generate end-on bound superoxo copper(II) compound **58**. The reactivity of the latter complex was tested for the oxidation of phenol substrates, leading to decomposition of complex **58** to generate a phenoxyl radical in 40% yield, together with the generation of 1,4-benzoquinone (24% yield) and arylhydroperoxide (Figure 29c).[249] Thus, the reactivity of complex **58** was not exclusively towards aromatic oxidation. Another study reported on the reactivity of a similar end-on superoxo copper(II) complex (**59**), supported by the TMG_3tren ligand (TMG_3tren = tris(2-(N-tetramethylguanidyl)ethyl)amine), towards external phenol substrates (Figure 29d).[250] Complex **59** could be characterized by means of X-ray crystallography, providing structural evidence for the existence of an end-on superoxo copper(II) species.[280] Reaction with phenol substrates showed products in which aromatic oxidation had occurred, in a similar way as the reactivity previously found for complex **58**. Upon reaction of complex **59** with 4-MeO-2,6-*t*Bu_2-phenol, 1,4-benzoquinone was formed in 22% yield, together with the stabilized phenoxyl radical (37% yield) and the arylhydroperoxide product. Interestingly, for the generation of the 1,4-benzoquinone product the displacement of a methoxy group has taken place. Reaction with 2,6-*t*Bu_2-phenol and 2,4,6-*t*Bu_3-phenol lead to formation of the benzoquinone product in 33% and 35% yield, respectively. Finally, reaction with 3,5-*t*Bu_2-catechol lead to the corresponding benzoquinone product in 20% yield (Figure 29d). From all reactions of complex **59** with phenols, a hydroxylated copper(II) alkoxide complex in which a methyl group on the ligand has been hydroxylated was detected.[250] Later on, a new end-on bound superoxo copper(II)

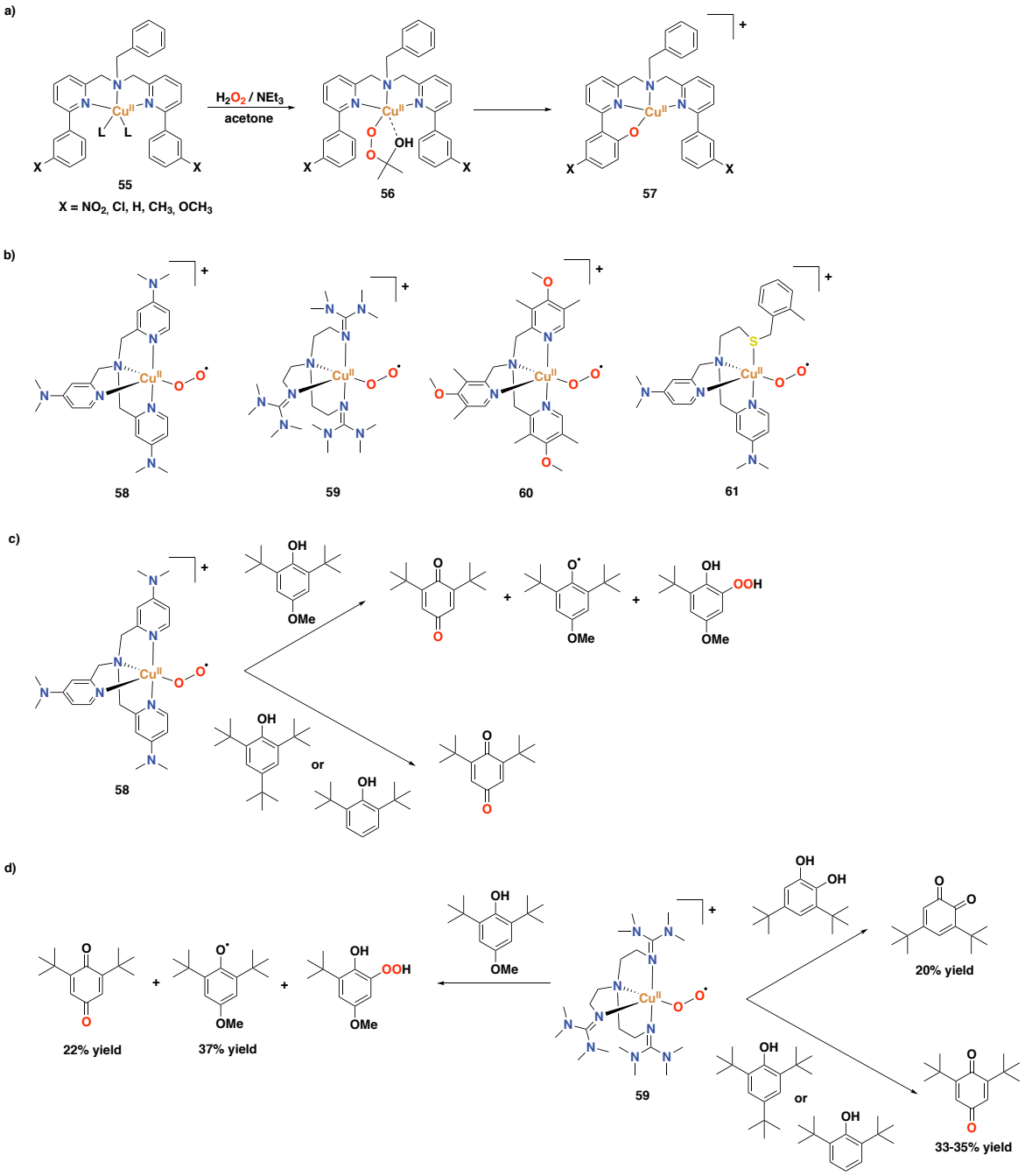

Figure 29. a) Aromatic hydroxylation reactivity of a mononuclear copper(II)-alkylperoxo complex.[278, 279] **b)** Selected end-on bound superoxo copper(II) complexes.[249, 250, 252, 253] **c)** Reactivity of complex **58** towards phenol substrates.[249] **d)** Reactivity of complex **59** towards phenol substrates.[250]

complex (**60**) supported by another electron-rich aminopyridine ligand containing dimethylmethoxy substituents on each pyridine ring was reported, and its reactivity towards *para*-substituted 2,6-di-*tert*-butyl-phenols was shown to afford 2,6-di-*tert*-butyl-1,4-benxoquinone in up to 50% yield.[252] Much more recently, copper(II)-superoxo species **61** in which the metal center is coordinated to two pyridyl groups, one tertiary amine and one

thioether donor was also described to perform the oxidation of 2,6-di-*tert*-butyl-4-methoxyphenol to 2,6-di-*tert*-butyl-1,4-benzoquinone.[253]

All the examples reported until that point were based on stoichiometric reactions. However, in recent years, examples of catalytic copper systems have been developed, and their catalytic activity has been demonstrated towards the oxidation of aromatic substrates.[281-285] Generally, chemists have tried to developed systems that generate metal-based oxidants to perform aromatic hydroxylation reactions, whereas systems that generate hydroxyl radicals through Fenton-type processes were aimed to be avoided because of their non-selective oxidation chemistry (vide supra). However, some examples have shown that hydroperoxyl radicals generated through Fenton-type processes can perform the aromatic oxidation of benzene to phenol in high activities and selectivites. For instance, Karlin, Fukuzumi and co-workers reported on a system based on a mononuclear copper complex supported by the tpa ligand, which reacts with H_2O_2 to generate hydroperoxyl radicals and performs the oxidation of benzene to phenol.[286] Particularly, they demonstrated that by incorporating the copper complex into mesoporous silica-alumina (Al-MCM-41), they could enhance the activity of the system, reaching up to 4320 turnovers for phenol formation.[286]

A study reported by Pérez and co-workers showed that catalytic amounts of copper complexes supported by trispyrazolylborate type ligands can perform the direct oxidation of aromatic C–H bonds with H_2O_2 under acid-free conditions (Figure 30, complex **62** for general structure).[281] Particularly, they tested the system for the oxidation of benzene to phenol (and 1,4-benzoquinone as a overoxidized product), showing conversions within the range of 14 - 30%, and selectivities towards phenol of 67 - 85%. In addition, oxidation of anthracene to 9,10-anthraquinone (98% isolated yield), and 2-ethylanthracene to 2-ethyl-9,10-anthraquinone (98% isolated yield) occurred successfully. In a follow-up study, the same authors reported on a mechanistic investigation, combining experimental and DFT studies, in which they demonstrated that these copper systems perform the aromatic hydroxylation through a copper-oxyl species.[282] Moreover, they proposed that hydroxylation occurs through two competing pathways, either via an electrophilic aromatic substitution pathway in which the copper-oxyl species acts as the electrophile, or via a rebound mechanism in which the hydrogen on the substrate is abstracted by the copper-oxyl species prior to C–O bond formation.[282]

Liu and co-workers reported a catalyst based on dicopper(II) complex **63** supported by two 2-((((1- methyl-1H-imidazol-2-yl)methyl)(pyridin-2-ylmethyl)amino)methyl)phenol ligands (Figure 30), that can perform the direct hydroxylation of benzene to phenol using H_2O_2 as oxidant, with up to 11.9% phenol yield and 79.3 turnovers.[283]

Later on, Kodera and co-workers developed dicopper(II) complex **64** based on the bis(tpa) ligand (6-hpa). This complex was reported to catalyze the selective hydroxylation of benzene to phenol using H_2O_2 reaching a turnover number higher than 12,000 after 40 h for phenol formation in CH_3CN at 50 °C, and with a turnover frequency [mol phenol·(mol catalyst)$^{-1}$·h^{-1}] of 1010.[284] Noteworthy, these are the highest values reported until now for benzene hydroxylation with H_2O_2 catalyzed by a homogeneous catalyst.

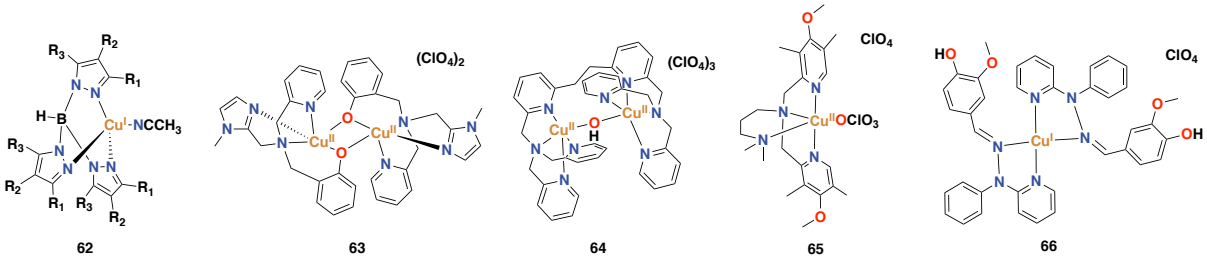

Figure 30. Synthetic copper complexes that display catalytic activity for the hydroxylation of aromatic substrates through a metal-based mechanism.[281, 283-285, 287]

With regard to the mechanism for H_2O_2 activation and benzene hydroxylation, the authors proposed that upon addition of 1 equiv. of H_2O_2 in the presence of Et_3N at –40 °C, an end-on *trans*-peroxodicopper(II) (**Cu_2O_2**) complex is formed (Figure 31). Then, in the presence of excess amounts of H_2O_2, **Cu_2O_2** decomposes to form hydroperoxocopper(II) complex **$(CuO_2H)_2$**. This latter complex is proposed to release H_2O reversibly with the assistance of H_2O to give a copper-bound oxyl and peroxyl radical, which is stabilized by hydrogen-bonding interactions with H_2O. Then, the copper-oxyl radical is proposed to react with benzene in the rate-limiting step through an electrophilic aromatic oxidation mechanism to form phenol.[284]

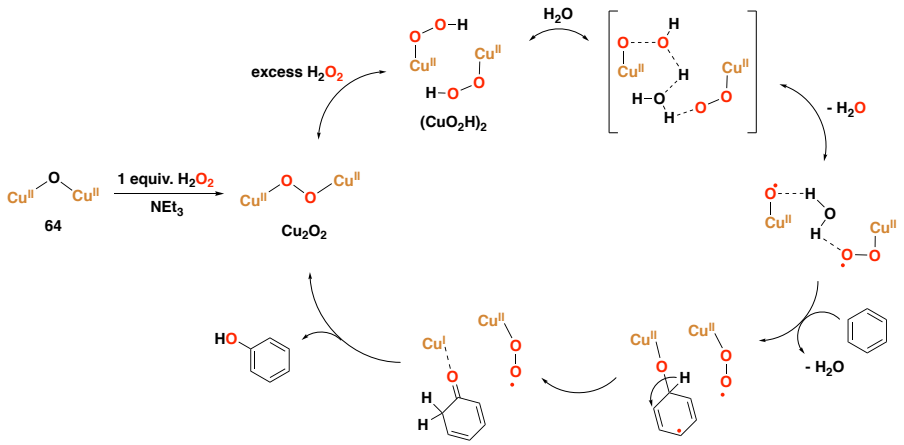

Figure 31. Proposed mechanism for the activation of H_2O_2 and hydroxylation of benzene to phenol catalyzed by complex **64** supported by the 6-hpa ligand.[284]

Recently, Mayilmurugan and co-workers have described a set of copper(II) complexes based on tripodal tetradentate aminopyridine ligands, and have reported that complex **65** containing

an electron-rich pyridine is the best for the aromatic hydroxylation of benzene with H_2O_2, affording phenol in 37% yield and with 98% selectivity.[285] The authors proposed that oxidation of benzene occurs, most likely, through the generation of a copper(II) hydroperoxo intermediate (Figure 32), and evidence for such species has been obtained using vibrational and electronic spectra, as well as ESI mass spectrometry.

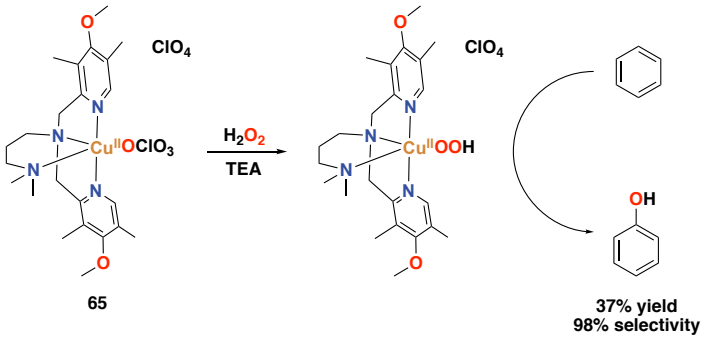

Figure 32. Proposed mechanism for benzene hydroxylation catalyzed by complex **61** through a copper(II) hydroperoxo species.[285] TEA = triethylamine.

Mayilmurugan, Ghosh and co-workers also reported on catalyst **66**, in which copper(I) is supported by bidentate nitrogen ligands (Figure 30), that can perform the direct hydroxylation of benzene to phenol in 29% yield, with the benzoquinone by-product being generated in <1% yield.[287] The authors also reported on the effectiveness of using this catalyst for the oxidation of toluene, which afforded *p*-cresol and *o*-cresol in 37% yield and benzaldehyde in 21% yield, showing a selectivity for aromatic oxidation of 42%.

1.4 Nickel in Biological and Synthetic Systems

1.4.1 Nickel-containing Metalloenzymes

Despite being less studied in the literature compared to iron and copper-containing metalloenzymes, several nickel enzymes are known to be involved in a number of different oxidation processes. Examples include glyoxalase I, quercetin 2,4-dioxygenase, acireductone dioxygenase, urease, superoxide dismutase, [NiFe]-hydrogenase, carbon monoxide dehydrogenase, acetyl-coenzyme A synthase/decarbonylase, methyl-coenzyme M reductase, and lactate racemase.[288] Among these nickel-based metalloenzymes, none of them is capable of performing arene hydroxylation, in contrast to what is known for iron- or copper-based Rieske oxygenases, pterin-dependent oxygenases, tyrosinase oxidases, and others. Despite this fact, several synthetic nickel-oxygen species have been identified and reported to be capable of performing aromatic and alkane oxidation, as well as epoxidation reactions.[289] Because of that, chemists have also studied biological oxidation reactions proceeding in nickel-containing

metalloenzymes, with a special interest in (putative) reactive nickel-superoxo, -peroxo and -oxo intermediates involved in these enzymatic oxidations. As an example, we briefly discuss nickel superoxide dismutases in this section, in terms of their catalytic active site, their mechanism of action, and the nickel-oxygen intermediates involved.

1.4.1.1 Nickel Superoxide Dismutase

Superoxide dismutases (SOD) are a class of metalloenzymes that protect cells from toxic products of aerobic metabolism. These nickel-containing metalloenzymes regulate the formation of superoxide by converting superoxide into hydrogen peroxide and molecular oxygen.[31] It was in 1996 that this class of NiSOD was found in Streptomyces and cyanobacteria.[30]

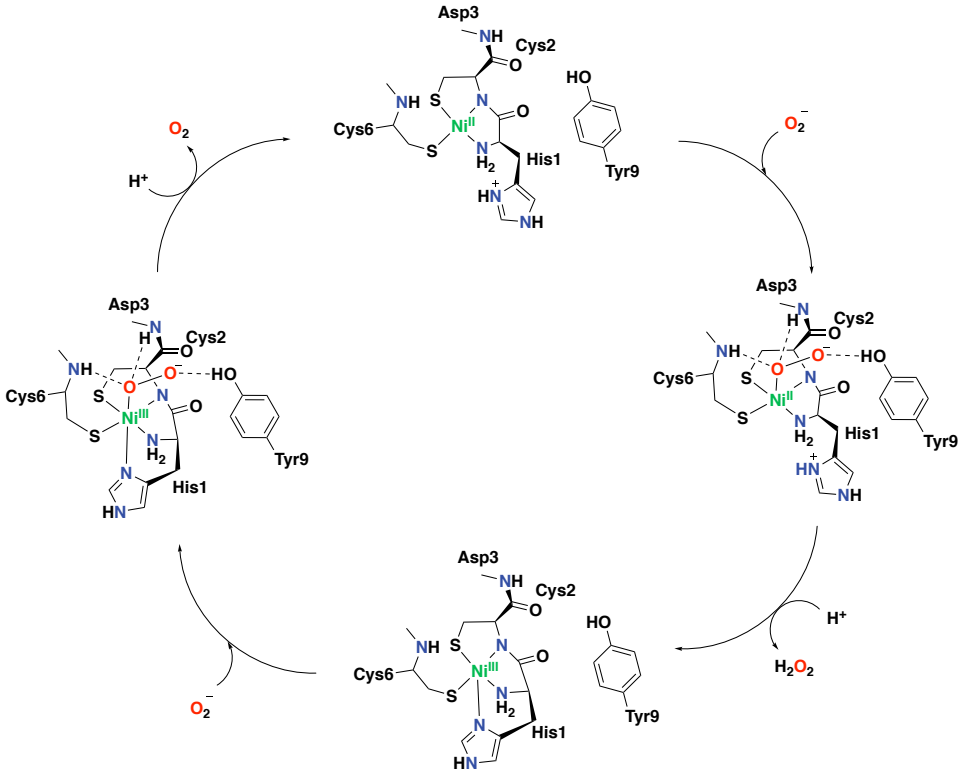

Figure 33. Catalytic cycle of nickel superoxide dismutase (NiSOD).[31]

The active site of NiSOD comprizes a Ni(II) atom bound to two sulphide donors (from Cys2 and Cys6) and two nitrogen donors (the N-terminal amine of His1 and the backbone amide of Cys2) in an undistorted square planar geometry (Figure 33).[31] In the first step of the catalytic cycle, a superoxide anion binds to the nickel center, forming a superoxo-nickel(II) intermediate. The ligated oxygen atom in this intermediate is stabilized by hydrogen bonding with two backbone amide moieties (Asp3 and Cys6). Additional stabilization is caused by hydrogen bonding of the non-ligated oxygen atom with the oxygen atom of Tyr9. Electron transfer from

Ni(II) to the superoxide, coupled with a proton transfer from Asp3, Cys6 or Tyr9 (and not from His1 since it is located on the wrong side of the nickel ion), forms hydrogen peroxide as product and generates a Ni(III) species. The Ni(III) intermediate has a five-coordinate square pyramidal geometry due to a second binding with His1. Then, a second superoxide molecule binds to Ni(III), forming a superoxo-nickel(III) species, followed by electron transfer from superoxide to Ni(III), to form molecular oxygen and regenerate the original Ni(II) four-coordinated intermediate.

1.4.2 Synthetic Aromatic Oxidation Systems based on Nickel

An early study reported by Kimura and co-workers in 1984 described a nickel(II) compound supported by a macrocyclic polyamine that is able to activate dioxygen and oxidize aromatic substrates to generate hydroxylated products.[290] This study represents an early example of nickel-based systems that model biological monooxygenases in the selective hydroxylation of aromatic substrates.

More recently, Suzuki and co-workers reported on the development of bis(μ-oxo)dinickel(III) complexes supported by H-L-H-type ligands (H-L-H = 1,3-bis-[bis(6-methyl-2-pyridylmethyl)aminomethyl]benzene), in which different substituents were introduced onto the xylyl linker of the ligand.[291] This study was a follow-up on the exploration of copper complexes based on the same type of ligands performed by the same authors (Figure 27, complex **48** for general structure).[269] Whereas the nickel complexes reacted with H_2O_2 to generate a bis(μ-oxo)dinickel(III) species, the copper counterparts reacted with dioxygen to formed a (μ-η^2:η^2)-peroxo dicopper(II) complex. Both species have been demonstrated to undergo arene hydroxylation of the xylyl linker.[269, 291]

As a follow-up of the study on copper(II) complexes containing tridentate bis[(pyridin-2-yl)methyl]benzylamine ligands carrying *m*-substituted 6-phenyl rings on each pyridine group, in which intramolecular aromatic ligand hydroxylation occurred (see Figure 29a), Itoh and co-workers extended their investigation to the corresponding nickel complexes.[292] In this particular study, the authors synthesized and characterized a series of nickel(II) complexes supported by tridentate ligands that contain different substituents at the *meta* position of the phenyl substituents (OCH_3, CH_3, H, Cl, NO_2) (Figure 34, complex **63** for general structure). These complexes were found to react with H_2O_2 in acetone to from bis(μ-oxo)dinickel(III) intermediate **64**. This species decomposes to form (μ-phenoxo)(μ-hydroxo)dinickel(II) species **65** in which one of the phenyl groups on the ligand has been hydroxylated. This aromatic hydroxylation reaction was proposed to proceed through an electrophilic aromatic substitution mechanism. Finally, mononuclear nickel(II) complex **66** is formed, containing the hydroxylated ligand, together with a (μ-hydroxo)dinickel(II) species. Complex **66** was characterized by ESI-

MS and X-ray crystallographic analysis (see Figure 34).[292] Worthy of note is that the mechanism of action proposed for these nickel(II) complexes differs from the one proposed for the analogues copper(II) complexes. For the former complexes a bis(μ-oxo)dinickel(III) species seems to be involved, whereas for the latter complexes a 2-hydroxy-2-hydroperoxypropane adduct is generated (see Figure 29a and Figure 34 for comparison).[278, 279, 292]

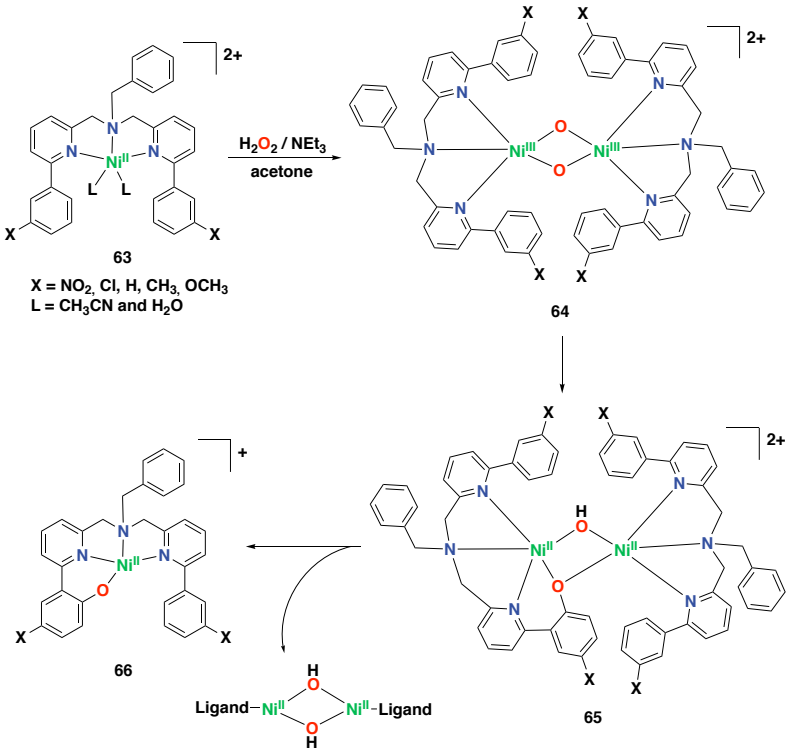

Figure 34. Reaction of nickel(II) complex **63** with H_2O_2 and triethylamine at low temperature to yield bis(μ-oxo)dinickel(III) intermediate **64** that can hydroxylate a phenyl ring of one of the ligands through the formation of intermediate **65**.[292]

Itoh and co-workers have also investigated nickel complexes derived from tpa ligands bearing with one, two or three aryl substituents.[293] Particularly, they found that nickel complexes with two (**67**) or three aryl substituents react with H_2O_2 to afford bis(μ-oxo)dinickel(III) species (like complex **68**) at low temperatures (Figure 35), in contrast to what was observed for the nickel complexes derived from tpa ligands bearing fewer aryl rings, which hardly react with the oxidant. Bis(μ-oxo)dinickel(III) species (like complex **68**) were detected using UV-Vis and resonance Raman, and its features compared with other known bis(μ-oxo)dinickel(III) intermediates.[294-299] Interestingly, it was reported that the former complexes can undergo intramolecular aromatic hydroxylation of the aminopyridine ligand to afford mononuclear nickel species **69** in which one aryl ring on the ligand has been hydroxylated and binds to the metal center.[293] Remarkably, complex **67** was found to be capable of hydroxylating externally added benzene substrates at 60 °C, although phenol was only obtained in 3% yield. The authors

described that the extremely low yield can be attributed to the competition between intermolecular and intramolecular reactions.

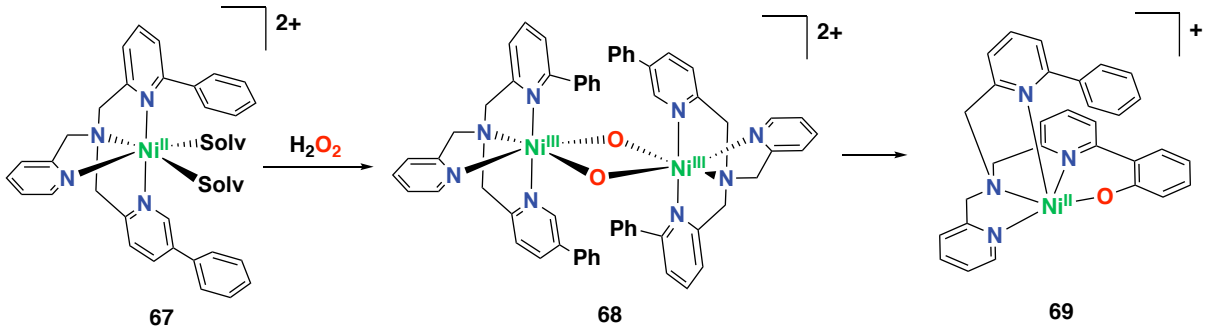

Figure 35. Formation of a bis(μ-oxo)dinickel(III) intermediate and intramolecular arene hydroxylation of the ligand.[293, 300]

In 2015, the same group reported an interesting study in which they described the catalytic ability of nickel(II) complexes as homogeneous catalysts for the direct hydroxylation of benzene to phenol employing H_2O_2 as oxidant.[300] In these catalytic reactions the substrate is mixed with H_2O_2 in the presence of a catalytic amount of the nickel complex (10 mol% catalyst loading) and triethylamine. The best catalyst in this study proved to be nickel complex **70**, supported by the tepa ligand (tepa = tris[2-(pyridine-2-yl)ethyl]amine), which provided 21% phenol yield based on the amount of substrate and small amounts of overoxidized products. The same complex was also used for the oxidation of the alkylbenzene substrates toluene, ethylbenzene, and cumene. Interestingly, the selectivity for aromatic oxidation was up to 90% for these substrates. Nevertheless, reactions do not exceed two turnovers per nickel. In an independent experiment, the authors reported high turnover numbers using extremely low concentrations of the nickel complex and very long reaction times (TON = 749 after 216 h). Based on an experimental kinetic isotope effect, the authors excluded the involvement of hydroxyl radicals in these reactions and postulated a metal-based mechanism. In addition, it was proposed that the aromatic hydroxylation occurs via an electrophilic aromatic substitution mechanism and through the formation of a bis(μ-oxo)dinickel(III) intermediate.[300] However, no experimental evidence was provided for the involvement of such an active oxidant. Recently, Itoh and co-workers reported on the synthesis and characterization of a bis(μ-oxo)dinickel(III) complex bearing a similar ligand, exhibiting hydrogen abstraction and oxygenation reactivity towards external substrates, but no aromatic oxidation reactivity was described.[301]

Recently, Mayilmurugan and co-workers reported on related nickel(II) complexes supported by tetradentate aminopyridine ligands for the direct hydroxylation of benzene and toluene to the corresponding phenol products with H_2O_2 as oxidant (Figure 37).[302] Interestingly, oxidation

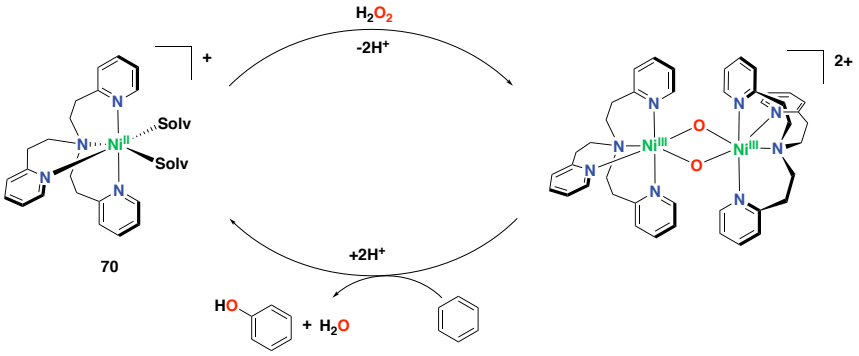

Figure 36. Proposed catalytic mechanism for the direct hydroxylation of benzene to phenol catalyzed by nickel(II) complex **70** supported by a tripodal tetradentate aminopyridine ligand, and involving a bis(*μ*-oxo)dinickel(III) intermediate.[300]

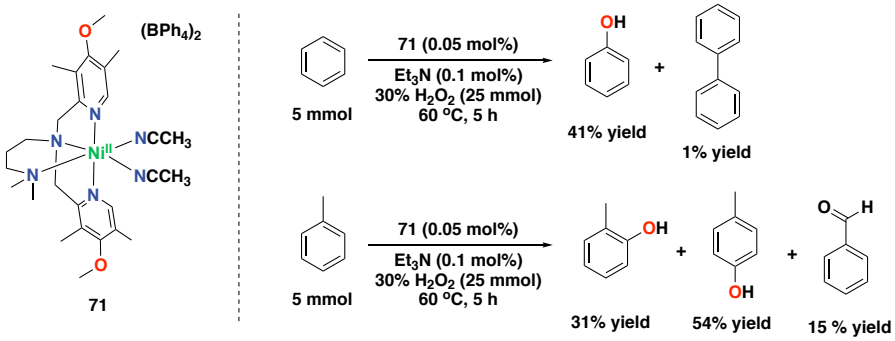

Figure 37. Reaction products of the catalytic oxidation of benzene and toluene catalyzed by nickel(II) complex **71** with H_2O_2 as oxidant and triethylamine as additive.

did not occur when phenol was used as substrate, thus preventing overoxidation to hydroquinone or benzoquinone products. By employing nickel(II) complex **71** bearing an electron-rich ligand (0.05 mol% catalyst loading), the authors reported up to 41% phenol yield and 820 turnovers. Aromatic hydroxylation was proposed to occur through the formation of a bis(*μ*-oxo)dinickel(III) intermediate, in a similar way as in the mechanism proposed by Itoh and co-workers (Figure 36).[302]

1.5 Manganese in Biological and Synthetic Systems

1.5.1 Manganese-containing Metalloenzymes

Manganese, in a similar way as iron, is a non-toxic, inexpensive and earth abundant first-row transition metal. So far, no manganese-containing enzymes are known to perform aromatic oxidation in nature. Nevertheless, manganese plays an important role in the oxygen-evolving complex (OEC) in photosystem II (PS II). PS II is an enzyme present in the thylakoid membranes of oxygenic photosynthetic organisms. Particularly, it is in the oxygen-evolving

complex (OEC) where the oxidation of water to dioxygen occurs.[303, 304] Several X-ray crystal structure determinations have been successfully achieved for PS II, thus allowing for a better understanding of the structure geometry and components involved in the oxidation reaction.[305] The OEC consists of an oxo-bridged structure containing four Mn atoms and one Ca atom, linked via three di-μ-oxo and one mono-μ-oxo-bridged Mn–Mn interactions and the Ca cofactor is linked by single-O bridging to two Mn centers.[306]

1.5.2 Synthetic Manganese Systems

Due to the advantages of manganese (*i.e.* earth abundant, non-toxic and cheap), in the last years researchers have focused on the exploration of the reactivity of synthetic manganese-based complexes. This element has several available oxidation states (–3 to +7), consequently resulting in a great variety of reactivities for manganese-containing coordination complexes.[307, 308] For instance, complexes in which the manganese center has a low oxidation state can perform chemistry similar to main group elements, whereas high oxidation manganese complexes can perform oxidation chemistry. Along this vein, manganese complexes have been widely studied in various catalytic oxidation reactions, such as (asymmetric) epoxidation reactions[309] and (enantioselective) aliphatic C–H oxidation[310, 311], whereas only few examples are known for aromatic oxidation reactions.

Nam and co-workers reported on manganese(II) complex **72** (Figure 38) bearing the Bn-TPEN ligand (Bn-TPEN = *N*-benzyl-*N*,*N'N'*-tris(2-pyridylmethyl)-1,2-diaminoethane), which upon reaction with iodosylbenzene forms a manganese(IV)-oxo complex that is active in the oxidation of naphthalene, among other types of oxidation reactions.[312] Nonetheless, no efficient catalytic turnover numbers were achieved.

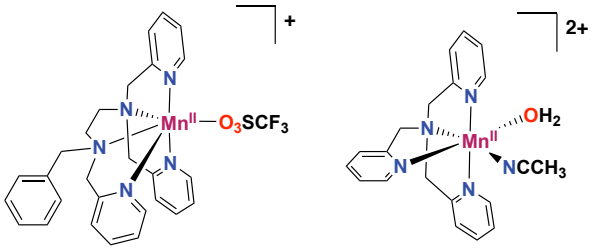

72 73

Figure 38. Synthetic manganese complexes that display aromatic oxidation reactivity. Complex **73** is incorporated into a mesoporous silica-alumina (Al-MCM-41).[312, 313]

In 2015 Fukuzumi and co-workers described the remarkably selective hydroxylation of benzene derivatives to phenols with H_2O_2 employing manganese-tpa complex **73** incorporated into mesoporous silica-alumina (Al-MCM-41).[313] The selectivity obtained for phenol formation was excellent and the authors showed the importance of the incorporation of the complex into the

solid support, which prevents the formation of bis(μ-oxo)dimanganese(III,IV) species that are catalytically much less active.

1.6 Aim and Scope of this Thesis

The general aim of the research described in this thesis is focused on the direct conversion of aryl, and to lesser extent alkyl, C–H bonds into the corresponding C–OH functionality, which represents a highly important transformation in both academia and industry. The strategy used in this thesis to accomplish such transformations relies on the development of transition metal complexes as homogeneous catalysts. In addition, the focal point of the current thesis aims at the transition from the use of noble metal catalysts to catalysts based on first-row transition metals, which is of special interest since the latter ones are more abundant and affordable, and usually less toxic. Particularly, in this thesis we have explored complexes based on nickel and manganese as the metal center, since these elements have been less explored in the field of arene oxidation compared to iron and copper. Moreover, the thesis focusses on the use of the environmentally benign oxidant hydrogen peroxide, which only generates water and dioxygen as by-products.

As the first experimental chapter in this thesis, **Chapter 2** investigates molecular nickel(II) complexes supported by tripodal tetradentate aminopyridine ligands as catalysts for the direct hydroxylation of benzene to phenol with H_2O_2 as oxidant. Particularly, the reactivity of several nickel complexes bearing modified aminopyridine ligands is presented, and their activities have been compared to the work reported by Itoh and co-workers.[300] In addition, the effectiveness of several commercially available nickel(II) salts in the oxidation of aromatic substrates with a fluorinated alcohol solvent and H_2O_2 is explored.

Chapter 3 and **Chapter 4** of this thesis focus on the exploration of bioinspired manganese(II) complexes bearing linear tetradentate aminopyridine ligands as catalysts for the direct hydroxylation of aromatic substrates to the corresponding phenol products employing H_2O_2 as oxidant. In **Chapter 3** we envisioned that the introduction of bulky *tris*-(isopropyl)silyl groups into the ligand of the complex might prevent catalyst inhibition through phenolate-binding to the manganese center, and might consequently enhance catalytic turnover. The exploration of such bulky complexes towards arene oxidation is presented in this chapter, along with a mechanistic study to better understand how aromatic oxidation is brought about by these complexes.

Next, **Chapter 4** describes a follow-up investigation on the exploration of manganese(II) complexes for arene oxidation, and an evaluation of the sensitivity of the reactions described in

Chapter 3 to electronic and steric effects is presented. A set of complexes bearing different pyridine donors are presented, and their reactivity towards alkylbenzenes is explored. In addition, we show a comparison between the reactivity of C_2-symmetric and C_1-symmetric manganese complexes, as well as the design of new manganese complexes that combine electron-rich and bulky pyridines. In addition, particular attention is focused on the product profile of these oxidation reactions (aromatic *vs*. benzylic oxidation).

Inspired by the findings on chemoselectivity described in Chapter 4, enantioselective benzylic oxidation reactions catalyzed by manganese complexes with H_2O_2 as oxidant are explored in **Chapter 5**. New highly electron-rich manganese(II) complexes bearing 4-pyrrolidinopyridine moieties are presented, and their reactivity towards oxidation of alkylbenzenes is shown and compared with the state-of-the-art homogeneous catalysts. This chapter also describes the use of some of newly developed Mn-complexes in asymmetric epoxidation reactions.

Finally, **Chapter 6** of this thesis describes a novel family of tetradentate amino-imidazole ligands that comprise bulky diphenylimidazole donor moieties. This study mainly focuses on experimental attempts to complex this new family of ligands to manganese, and is complemented with a computational study. In doing so, C_2-symmetric complexes bearing the new ligands are compared with C_1-symmetric complexes. At the end, exploration of the imidazole-based complexes towards oxidation of aromatic substrates is presented.

1.7 References

1. Arakawa, H.; Aresta, M.; Armor, J. N.; Barteau, M. A.; Beckman, E. J.; Bell, A. T.; Bercaw, J. E.; Creutz, C.; Dinjus, E.; Dixon, D. A.; Domen, K.; DuBois, D. L.; Eckert, J.; Fujita, E.; Gibson, D. H.; Goddard, W. A.; Goodman, D. W.; Keller, J.; Kubas, G. J.; Kung, H. H.; Lyons, J. E.; Manzer, L. E.; Marks, T. J.; Morokuma, K.; Nicholas, K. M.; Periana, R.; Que, L.; Rostrup-Nielson, J.; Sachtler, W. M. H.; Schmidt, L. D.; Sen, A.; Somorjai, G. A.; Stair, P. C.; Stults, B. R.; Tumas, W., Catalysis Research of Relevance to Carbon Management: Progress, Challenges, and Opportunities. *Chem. Rev.* **2001,** *101* (4), 953-996.

2. Punniyamurthy, T.; Velusamy, S.; Iqbal, J., Recent Advances in Transition Metal Catalyzed Oxidation of Organic Substrates with Molecular Oxygen. *Chem. Rev.* **2005,** *105* (6), 2329-2363.

3. White, M. C.; Zhao, J., Aliphatic C–H Oxidations for Late-Stage Functionalization. *J. Am. Chem. Soc.* **2018,** *140* (43), 13988-14009.

4. Hong, B.; Luo, T.; Lei, X., Late-Stage Diversification of Natural Products. *ACS Cent. Sci.* **2020,** *6* (5), 622-635.

5. Feng, K.; Quevedo, R. E.; Kohrt, J. T.; Oderinde, M. S.; Reilly, U.; White, M. C., Late-stage oxidative C(sp^3)–H methylation. *Nature* **2020,** *580* (7805), 621-627.

6. Genovino, J.; Sames, D.; Hamann, L. G.; Touré, B. B., Accessing Drug Metabolites via Transition-Metal Catalyzed C–H Oxidation: The Liver as Synthetic Inspiration. *Angew. Chem. Int. Ed.* **2016,** *55* (46), 14218-14238.

7. Börgel, J.; Tanwar, L.; Berger, F.; Ritter, T., Late-stage aromatic C–H oxygenation. *J. Am. Chem. Soc.* **2018,** *140* (47), 16026-16031.

8. Haggin, J., Chemists seek greater recognition for catalysis. *Chem. Eng. News,* **1993,** *71* (22).

9. Cornils, B.; Herrmann, W. A., Concepts in homogeneous catalysis: the industrial view. *J. Catal.* **2003,** *216* (1-2), 23-31.

10. Weber, M.; Weber, M.; Kleine-Boymann, M., In *Ullmann's Encyclopedia of Industrial Chemistry*, Wiley-VCH: Weinheim, Germany, 2004; pp 503-519.

11. Fukuzumi, S.; Ohkubo, K., One-Step Selective Hydroxylation of Benzene to Phenol. *Asian J. Org. Chem.* **2015,** *4* (9), 836-845.

12. Sheldon, R. A.; Kochi, J. K., In *Metal-Catalyzed Oxidations of Organic Compounds*, Academic Press, New York, 1981; pp 315-339.

13. Luo, Y.-R., *Comprehensive Handbook of Chemical Bond Energies*. CRC Press: Boca Raton, FL, 2007.

14. Lewis, J. C.; Coelho, P. S.; Arnold, F. H., Enzymatic functionalization of carbon–hydrogen bonds. *Chem. Soc. Rev.* **2011,** *40* (4), 2003-2021.

15. Song, R.; Sorokin, A.; Bernadou, J.; Meunier, B., Metalloporphyrin-catalyzed oxidation of 2-methylnaphthalene to vitamin K3 and 6-methyl-1,4-naphthoquinone by potassium monopersulfate in aqueous solution. *J. Org. Chem.* **1997,** *62* (3), 673-678.

16. Sorokin, A.; Meunier, B., Oxidation of polycyclic aromatic hydrocarbons catalyzed by iron tetrasulfophthalocyanine FePcS: inverse isotope effects and oxygen labeling studies. *Eur. J. Inorg. Chem.* **1998,** *1998* (9), 1269-1281.

17. Higuchi, T.; Satake, C.; Hirobe, M., Selective quinone formation by oxidation of aromatics with heteroaromatic N-oxides catalyzed by ruthenium porphyrins. *J. Am. Chem. Soc.* **1995,** *117* (34), 8879-8880.

18. Khavasi, H. R.; Davarani, S. S. H.; Safari, N., Remarkable solvent effect on the yield and specificity of oxidation of naphthalene catalyzed by iron(III) porphyrins. *J. Mol. Catal. A: Chem.* **2002,** *188* (1-2), 115-122.

19. Klein Gebbink, R. J. M.; Moret, M.-E., *Non-Noble Metal Catalysis: Molecular Approaches and Reactions*. John Wiley & Sons: 2019.

20. Wallar, B. J.; Lipscomb, J. D., Dioxygen activation by enzymes containing binuclear non-heme iron clusters. *Chem. Rev.* **1996,** *96* (7), 2625-2658.

21. Que Jr, L.; Ho, R. Y., Dioxygen activation by enzymes with mononuclear non-heme iron active sites. *Chem. Rev.* **1996,** *96* (7), 2607-2624.

22. Holm, R. H.; Kennepohl, P.; Solomon, E. I., Structural and functional aspects of metal sites in biology. *Chem. Rev.* **1996,** *96* (7), 2239-2314.

23. Costas, M.; Mehn, M. P.; Jensen, M. P.; Que, L., Dioxygen activation at mononuclear nonheme iron active sites: enzymes, models, and intermediates. *Chem. Rev.* **2004,** *104* (2), 939-986.

24. Bruijnincx, P. C.; van Koten, G.; Klein Gebbink, R. J. M., Mononuclear non-heme iron enzymes with the 2-His-1-carboxylate facial triad: recent developments in enzymology and modeling studies. *Chem. Soc. Rev.* **2008,** *37* (12), 2716-2744.

25. Que, L.; Tolman, W. B., Biologically inspired oxidation catalysis. *Nature* **2008,** *455* (7211), 333-340.

26. Guo, M.; Corona, T.; Ray, K.; Nam, W., Heme and nonheme high-valent iron and manganese oxo cores in biological and abiological oxidation reactions. *ACS Cent. Sci.* **2019,** *5* (1), 13-28.

27. Solomon, E. I.; Chen, P.; Metz, M.; Lee, S. K.; Palmer, A. E., Oxygen binding, activation, and reduction to water by copper proteins. *Angew. Chem. Int. Ed.* **2001,** *40* (24), 4570-4590.

28. Pecoraro, V. L.; Baldwin, M. J.; Gelasco, A., Interaction of manganese with dioxygen and its reduced derivatives. *Chem. Rev.* **1994,** *94* (3), 807-826.

29. Law, N. A.; Caudle, M. T.; Pecoraro, V. L., Manganese redox enzymes and model systems: properties, structures, and reactivity. In *Adv. Inorg. Chem.*, Elsevier: 1998; Vol. 46, pp 305-440.

30. Youn, H.-D.; Kim, E.-J.; Roe, J.-H.; HAH, Y. C.; KANG, S.-O., A novel nickel-containing superoxide dismutase from Streptomyces spp. *Biochem. J.* **1996,** *318* (3), 889-896.

31. Barondeau, D. P.; Kassmann, C. J.; Bruns, C. K.; Tainer, J. A.; Getzoff, E. D., Nickel superoxide dismutase structure and mechanism. *Biochemistry* **2004,** *43* (25), 8038-8047.

32. Ragsdale, S. W., Nickel-based enzyme systems. *J. Biol. Chem.* **2009,** *284* (28), 18571-18575.

33. Kirby, A. J.; Hollfelder, F., *From enzyme models to model enzymes*. Royal Society of Chemistry: 2009.

34. Solomon, E. I.; Brunold, T. C.; Davis, M. I.; Kemsley, J. N.; Lee, S.-K.; Lehnert, N.; Neese, F.; Skulan, A. J.; Yang, Y.-S.; Zhou, J., Geometric and electronic structure/function correlations in non-heme iron enzymes. *Chem. Rev.* **2000,** *100* (1), 235-350.

35. Neidig, M. L.; Solomon, E. I., Structure–function correlations in oxygen activating non-heme iron enzymes. *Chem. Commun.* **2005,** (47), 5843-5863.

36. Matsumoto, K.; Tachikawa, S.; Hashimoto, N.; Nakano, R.; Yoshida, M.; Shindo, M., Aerobic C–H Oxidation of Arenes Using a Recyclable, Heterogeneous Rhodium Catalyst. *J. Org. Chem.* **2017,** *82* (8), 4305-4316.

37. Santoro, S.; Kozhushkov, S. I.; Ackermann, L.; Vaccaro, L., Heterogeneous catalytic approaches in C–H activation reactions. *Green Chem.* **2016,** *18* (12), 3471-3493.

38. Reay, A. J.; Fairlamb, I. J., Catalytic C–H bond functionalisation chemistry: the case for quasi-heterogeneous catalysis. *Chem. Commun.* **2015,** *51* (91), 16289-16307.

39. Rahmani, N.; Amiri, A.; Ziarani, G. M.; Badiei, A., Review of some transition metal-based mesoporous catalysts for the direct hydroxylation of benzene to phenol (DHBP). *Mol. Catal.* **2021,** *515*, 111873.

40. Vicens, L.; Olivo, G.; Costas, M., Rational Design of Bioinspired Catalysts for Selective Oxidations. *ACS Catal.* **2020,** *10* (15), 8611-8631.

41. Bailey, C. L.; Drago, R. S., Utilization of O_2 for the specific oxidation of organic substrates with cobalt(II) catalysts. *Coord. Chem. Rev.* **1987,** *79* (3), 321-332.

42. Carneiro, L.; Silva, A. R., Selective direct hydroxylation of benzene to phenol with hydrogen peroxide by iron and vanadyl based homogeneous and heterogeneous catalysts. *Catal. Sci. Technol.* **2016,** *6* (22), 8166-8176.

43. Han, J. W.; Jung, J.; Lee, Y.-M.; Nam, W.; Fukuzumi, S., Photocatalytic oxidation of benzene to phenol using dioxygen as an oxygen source and water as an electron source in the presence of a cobalt catalyst. *Chem. Sci.* **2017,** *8* (10), 7119-7125.

44. Anandababu, K.; Muthuramalingam, S.; Velusamy, M.; Mayilmurugan, R., Single-step benzene hydroxylation by cobalt(II) catalysts via a cobalt(III)-hydroperoxo intermediate. *Catal. Sci. Technol.* **2020,** *10* (8), 2540-2548.

45. Lemke, K.; Ehrich, H.; Lohse, U.; Berndt, H.; Jähnisch, K., Selective hydroxylation of benzene to phenol over supported vanadium oxide catalysts. *Appl. Catal. A: Gen.* **2003,** *243* (1), 41-51.

46. Zhang, J.; Tang, Y.; Li, G.; Hu, C., Room temperature direct oxidation of benzene to phenol using hydrogen peroxide in the presence of vanadium-substituted heteropolymolybdates. *Appl. Catal. A: Gen.* **2005,** *278* (2), 251-261.

47. Fenton, H., LXXIII.—Oxidation of tartaric acid in presence of iron. *J. Chem. Soc., Trans.* **1894,** *65*, 899-910.

48. Haber, F.; Weiss, J., Üeber die Katalyse des Hydroperoxydes. *Naturwissenschaften* **1932,** *20* (51), 948-950.

49. Haber, F.; Weiss, J., The catalytic decomposition of hydrogen peroxide by iron salts. *Proc. R. Soc. London A Math. Phys. Sci.* **1934,** *147* (861), 332-351.

50. Walling, C., Intermediates in the reactions of Fenton type reagents. *Acc. Chem. Res.* **1998,** *31* (4), 155-157.

51. MacFaul, P. A.; Wayner, D.; Ingold, K., A radical account of "oxygenated Fenton chemistry". *Acc. Chem. Res.* **1998,** *31* (4), 159-162.

52. Goldstein, S.; Meyerstein, D., Comments on the mechanism of the "Fenton-like" reaction. *Acc. Chem. Res.* **1999,** *32* (7), 547-550.

53. Merz, J.; Waters, W., 511. The oxidation of aromatic compounds by means of the free hydroxyl radical. *J. Chem. Soc.* **1949**, 2427-2433.

54. Smith, J. L.; Norman, R., 539. Hydroxylation. Part I. The oxidation of benzene and toluene by Fenton's reagent. *J. Chem. Soc.* **1963**, 2897-2905.

55. Walling, C.; Johnson, R. A., Fenton's reagent. V. Hydroxylation and side-chain cleavage of aromatics. *J. Am. Chem. Soc.* **1975,** *97* (2), 363-367.

56. Kurata, T.; Watanabe, Y.; Katoh, M.; Sawaki, Y., Mechanism of aromatic hydroxylation in the Fenton and related reactions. One-electron oxidation and the NIH shift. *J. Am. Chem. Soc.* **1988,** *110* (22), 7472-7478.

57. Cussó, O.; Garcia-Bosch, I.; Ribas, X.; Lloret-Fillol, J.; Costas, M., Asymmetric epoxidation with H_2O_2 by manipulating the electronic properties of non-heme iron catalysts. *J. Am. Chem. Soc.* **2013,** *135* (39), 14871-14878.

58. MacFaul, P. A.; Ingold, K.; Wayner, D.; Que, L., A Putative Monooxygenase Mimic Which Functions via Well-Disguised Free Radical Chemistry1. *J. Am. Chem. Soc.* **1997,** *119* (44), 10594-10598.

59. Ingold, K. U.; MacFaul, P. A., *Biomimetic oxidations catalyzed by transition metal complexes*. Meunier, B., Ed.; Imperial College Press: London, 2000; p 45.

60. Hiatt, R.; Clipsham, J.; Visser, T., The induced decomposition of tert-butyl hydroperoxide. *Can. J. Chem.* **1964,** *42* (12), 2754-2757.

61. Masferrer-Rius, E.; Borrell, M.; Lutz, M.; Costas, M.; Klein Gebbink, R. J. M., Aromatic C–H Hydroxylation Reactions with Hydrogen Peroxide Catalyzed by Bulky Manganese Complexes. *Adv. Synth. Catal.* **2021**.

62. Udenfriend, S.; Clark, C. T.; Axelrod, J.; Brodie, B. B., Ascorbic acid in aromatic hydroxylation. *J. Biol. Chem.* **1954,** *208*, 731-738.

63. Brodie, B. B.; Axelrod, J.; Shore, P. A.; Udenfriend, S., Ascorbic acid in aromatic hydroxylation II. Products formed by reaction of substrates with ascorbic acid, ferrous ion, and oxygen. *J. Biol. Chem.* **1954,** *208* (2), 741-750.

64. Slavik, R.; Peters, J.-U.; Giger, R.; Bürkler, M.; Bald, E., Synthesis of potential drug metabolites by a modified Udenfriend reaction. *Tetrahedron Lett.* **2011,** *52* (7), 749-752.

65. Mathieu, D.; Bartoli, J. F.; Battioni, P.; Mansuy, D., Monooxygenation of aromatic compounds by dioxygen with bioinspired systems using non-heme iron catalysts and tetrahydropterins: comparison with other reducing agents and interesting regioselectivity favouring meta-hydroxylation. *Tetrahedron* **2004,** *60* (17), 3855-3862.

66. Metelitsa, D. I., Mechanisms of the hydroxylation of aromatic compounds. *Russ. Chem. Rev.* **1971,** *40* (7), 563.

67. Kunai, A.; Hata, S.; Ito, S.; Sasaki, K., The role of oxygen in the hydroxylation reaction of benzene with Fenton's reagent. Oxygen 18 tracer study. *J. Am. Chem. Soc.* **1986,** *108* (19), 6012-6016.

68. Sono, M.; Roach, M. P.; Coulter, E. D.; Dawson, J. H., Heme-containing oxygenases. *Chem. Rev.* **1996,** *96* (7), 2841-2888.

69. Meunier, B.; De Visser, S. P.; Shaik, S., Mechanism of oxidation reactions catalyzed by cytochrome P450 enzymes. *Chem. Rev.* **2004,** *104* (9), 3947-3980.

70. Poulos, T. L., Heme enzyme structure and function. *Chem. Rev.* **2014,** *114* (7), 3919-3962.

71. De Montellano, P. R. O., *Cytochrome P450: Structure, Mechanism, and Biochemistry*. 3rd ed.; Kluwer Academic/Plenum Publishers: New York, 2005.

72. Meunier, B., Biomimetic Oxidations Catalyzed by Transition Metal Complexes. Imperial College Press: London: 2000; pp 171-214.

73. Tshuva, E. Y.; Lippard, S. J., Synthetic models for non-heme carboxylate-bridged diiron metalloproteins: strategies and tactics. *Chem. Rev.* **2004,** *104* (2), 987-1012.

74. Hegg, E. L.; Jr, L. Q., The 2-His-1-carboxylate facial triad—an emerging structural motif in mononuclear non-heme iron(II) enzymes. *Eur. J. Biochem.* **1997,** *250* (3), 625-629.

75. Que, L., One motif—many different reactions. *Nat. Struct. Biol.* **2000,** *7* (3), 182-184.

76. Abu-Omar, M. M.; Loaiza, A.; Hontzeas, N., Reaction mechanisms of mononuclear non-heme iron oxygenases. *Chem. Rev.* **2005,** *105* (6), 2227-2252.

77. Koehntop, K. D.; Emerson, J. P.; Que, L., The 2-His-1-carboxylate facial triad: a versatile platform for dioxygen activation by mononuclear non-heme iron(II) enzymes. *J. Biol. Inorg. Chem.* **2005,** *10* (2), 87-93.

78. Kryatov, S. V.; Rybak-Akimova, E. V.; Schindler, S., Kinetics and mechanisms of formation and reactivity of non-heme iron oxygen intermediates. *Chem. Rev.* **2005,** *105* (6), 2175-2226.

79. Kovaleva, E. G.; Lipscomb, J. D., Versatility of biological non-heme Fe(II) centers in oxygen activation reactions. *Nat. Chem. Biol.* **2008,** *4* (3), 186.

80. Gibson, D.; Resnick, S.; Lee, K.; Brand, J.; Torok, D.; Wackett, L.; Schocken, M.; Haigler, B., Desaturation, dioxygenation, and monooxygenation reactions catalyzed by naphthalene dioxygenase from Pseudomonas sp. strain 9816-4. *J. Bacteriol.* **1995,** *177* (10), 2615-2621.

81. Wolfe, M. D.; Parales, J. V.; Gibson, D. T.; Lipscomb, J. D., Single Turnover Chemistry and Regulation of O_2 Activation by the Oxygenase Component of Naphthalene 1,2-Dioxygenase. *J. Biol. Chem.* **2001,** *276* (3), 1945-1953.

82. Cussó, O.; Ribas, X.; Costas, M., Biologically inspired non-heme iron-catalysts for asymmetric epoxidation; design principles and perspectives. *Chem. Commun.* **2015,** *51* (76), 14285-14298.

83. Denisov, I. G.; Makris, T. M.; Sligar, S. G.; Schlichting, I., Structure and chemistry of cytochrome P450. *Chem. Rev.* **2005,** *105* (6), 2253-2278.

84. Ortiz de Montellano, P. R., Hydrocarbon hydroxylation by cytochrome P450 enzymes. *Chem. Rev.* **2010,** *110* (2), 932-948.

85. Meunier, B.; Bernadou, J., Active iron-oxo and iron-peroxo species in cytochromes P450 and peroxidases; oxo-hydroxo tautomerism with water-soluble metalloporphyrins. In *Metal-Oxo and Metal-Peroxo Species in Catalytic Oxidations*, Springer: 2000; pp 1-35.

86. De Montellano, P. R. O., Cytochrome P450: Structure, Mechanism, and Biochemistry. 3rd ed.; Springler ed.: New York: 2005; pp 1-42.

87. Kille, S.; Zilly, F. E.; Acevedo, J. P.; Reetz, M. T., Regio-and stereoselectivity of P450-catalysed hydroxylation of steroids controlled by laboratory evolution. *Nat. Chem.* **2011,** *3* (9), 738.

88. Narayan, A. R.; Jiménez-Osés, G.; Liu, P.; Negretti, S.; Zhao, W.; Gilbert, M. M.; Ramabhadran, R. O.; Yang, Y.-F.; Furan, L. R.; Li, Z.; Podust, L. M.; Montgomery, J.; Houk, K. N.; Sherman, D. H., Enzymatic hydroxylation of an unactivated methylene C–H bond guided by molecular dynamics simulations. *Nat. Chem.* **2015,** *7* (8), 653.

89. Roiban, G. D.; Agudo, R.; Reetz, M. T., Cytochrome P450 Catalyzed Oxidative Hydroxylation of Achiral Organic Compounds with Simultaneous Creation of Two Chirality Centers in a Single C-H Activation Step. *Angew. Chem. Int. Ed.* **2014,** *53* (33), 8659-8663.

90. Zhang, K.; Shafer, B. M.; Demars, M. D.; Stern, H. A.; Fasan, R., Controlled oxidation of remote sp^3 C–H bonds in artemisinin via P450 catalysts with fine-tuned regio-and stereoselectivity. *J. Am. Chem. Soc.* **2012,** *134* (45), 18695-18704.

91. Poulos, T. L.; Finzel, B.; Gunsalus, I.; Wagner, G. C.; Kraut, J., The 2.6-Å crystal structure of Pseudomonas putida cytochrome P-450. *J. Biol. Chem.* **1985,** *260* (30), 16122-16130.

92. Li, H.; Narasimhulu, S.; Havran, L. M.; Winkler, J. D.; Poulos, T. L., Crystal structure of cytochrome P450cam complexed with its catalytic product, 5-exo-hydroxycamphor. *J. Am. Chem. Soc.* **1995,** *117* (23), 6297-6299.

93. Schlichting, I.; Berendzen, J.; Chu, K.; Stock, A. M.; Maves, S. A.; Benson, D. E.; Sweet, R. M.; Ringe, D.; Petsko, G. A.; Sligar, S. G., The catalytic pathway of cytochrome P450cam at atomic resolution. *Science* **2000,** *287* (5458), 1615-1622.

94. Yano, J. K.; Wester, M. R.; Schoch, G. A.; Griffin, K. J.; Stout, C. D.; Johnson, E. F., The structure of human microsomal cytochrome P450 3A4 determined by X-ray crystallography to 2.05-Å resolution. *J. Biol. Chem.* **2004,** *279* (37), 38091-38094.

95. Kells, P. M.; Ouellet, H.; Santos-Aberturas, J.; Aparicio, J. F.; Podust, L. M., Structure of cytochrome P450 PimD suggests epoxidation of the polyene macrolide pimaricin occurs via a hydroperoxoferric intermediate. *Chem. Biol.* **2010,** *17* (8), 841-851.

96. Shah, M. B.; Jang, H.-H.; Zhang, Q.; Stout, C. D.; Halpert, J. R., X-ray crystal structure of the cytochrome P450 2B4 active site mutant F297A in complex with clopidogrel: insights into compensatory rearrangements of the binding pocket. *Arch. Biochem. Biophys.* **2013,** *530* (2), 64-72.

97. Dawson, J. H.; Sono, M., Cytochrome P-450 and chloroperoxidase: thiolate-ligated heme enzymes. Spectroscopic determination of their active-site structures and mechanistic implications of thiolate ligation. *Chem. Rev.* **1987,** *87* (5), 1255-1276.

98. Mueller, E. J.; Loida, P. J.; Sligar, S. G., Twenty-five Years of P450 cam Research. In *Cytochrome P450*, Springer: 1995; pp 83-124.

99. King, N. K.; Winfield, M., Oxygen uptake and evolution by iron porphyrin enzymes. *Aust. J. Chem.* **1959,** *12* (1), 47-64.

100. Dunford, H.; Stillman, J., Structure and functional properties of peroxidases and catalases. *Coord. Chem. Rev.* **1976,** *19*, 187-251.

101. Meunier, B.; Bernadou, J., Metal-oxo species in P450 enzymes and biomimetic models. Oxo-hydroxo tautomerism with water-soluble metalloporphyrins. *Top. Catal.* **2002,** *21* (1-3), 47-54.

102. Rittle, J.; Green, M. T., Cytochrome P450 compound I: capture, characterization, and C–H bond activation kinetics. *Science* **2010,** *330* (6006), 933-937.

103. Groves, J. T.; McClusky, G. A., Aliphatic hydroxylation via oxygen rebound. Oxygen transfer catalyzed by iron. *J. Am. Chem. Soc.* **1976,** *98* (3), 859-861.

104. Groves, J. T.; McClusky, G. A.; White, R. E.; Coon, M. J., Aliphatic hydroxylation by highly purified liver microsomal cytochrome P-450. Evidence for a carbon radical intermediate. *Biochem. Biophys. Res. Commun.* **1978,** *81*, 154.

105. Daly, J.; Jerina, D.; Witkop, B., Arene oxides and the NIH shift: the metabolism, toxicity and carcinogenicity of aromatic compounds. *Experientia* **1972,** *28* (10), 1129-1149.

106. Guroff, G.; Daly, J. W.; Jerina, D. M.; Renson, J.; Witkop, B.; Udenfriend, S., Hydroxylation-induced migration: the NIH shift. *Science* **1967,** *157* (3796), 1524-1530.

107. Ullrich, R.; Hofrichter, M., Enzymatic hydroxylation of aromatic compounds. *Cell. Mol. Life Sci.* **2007,** *64* (3), 271-293.

108. de Montellano, P. R. O.; de Voss, J. J., Substrate oxidation by cytochrome P450 enzymes. In *Cytochrome P450 - Structure, Mechanism and Biochemistry*, 3rd ed. Kluwer Academic/Plenum Publishers, New York: 2005; pp 183-245.

109. Groves, J. T., High-valent iron in chemical and biological oxidations. *J. Inorg. Biochem.* **2006,** *100* (4), 434-447.

110. Barry, S. M.; Challis, G. L., Mechanism and catalytic diversity of Rieske non-heme iron-dependent oxygenases. *ACS Catal.* **2013,** *3* (10), 2362-2370.

111. Karlsson, A.; Parales, J. V.; Parales, R. E.; Gibson, D. T.; Eklund, H.; Ramaswamy, S., Crystal structure of naphthalene dioxygenase: side-on binding of dioxygen to iron. *Science* **2003,** *299* (5609), 1039-1042.

112. Kauppi, B.; Lee, K.; Carredano, E.; Parales, R. E.; Gibson, D. T.; Eklund, H.; Ramaswamy, S., Structure of an aromatic-ring-hydroxylating dioxygenase–naphthalene 1,2-dioxygenase. *Structure* **1998,** *6* (5), 571-586.

113. Parales, R. E.; Parales, J. V.; Gibson, D. T., Aspartate 205 in the catalytic domain of naphthalene dioxygenase is essential for activity. *J. Bacteriol.* **1999,** *181* (6), 1831-1837.

114. Perry, C.; De Los Santos, E. L.; Alkhalaf, L. M.; Challis, G. L., Rieske non-heme iron-dependent oxygenases catalyse diverse reactions in natural product biosynthesis. *Nat. Prod. Rep.* **2018,** *35* (7), 622-632.

115. Martins, B. M.; Svetlitchnaia, T.; Dobbek, H., 2-Oxoquinoline 8-monooxygenase oxygenase component: active site modulation by Rieske-[2Fe-2S] center oxidation/reduction. *Structure* **2005,** *13* (5), 817-824.

116. Hsueh, K.-L.; Westler, W. M.; Markley, J. L., NMR investigations of the Rieske protein from Thermus thermophilus support a coupled proton and electron transfer mechanism. *J. Am. Chem. Soc.* **2010,** *132* (23), 7908-7918.

117. Wolfe, M. D.; Altier, D. J.; Stubna, A.; Popescu, C. V.; Münck, E.; Lipscomb, J. D., Benzoate 1,2-dioxygenase from Pseudomonas putida: single turnover kinetics and regulation of a two-component Rieske dioxygenase. *Biochemistry* **2002,** *41* (30), 9611-9626.

118. Bugg, T. D.; Ramaswamy, S., Non-heme iron-dependent dioxygenases: unravelling catalytic mechanisms for complex enzymatic oxidations. *Curr. Op. Chem. Biol.* **2008,** *12* (2), 134-140.

119. Wolfe, M. D.; Lipscomb, J. D., Hydrogen peroxide-coupled *cis*-diol formation catalyzed by naphthalene 1,2-dioxygenase. *J. Biol. Chem.* **2003,** *278* (2), 829-835.

120. Lippard, S. J., Hydroxylation of C–H bonds at carboxylate-bridged diiron centres. *Philos. Trans. R. Soc. London, Ser. A,* **2005,** *363* (1829), 861-877.

121. Rosenzweig, A. C.; Frederick, C. A.; Lippard, S. J., Crystal structure of a bacterial non-haem iron hydroxylase that catalyses the biological oxidation of methane. *Nature* **1993,** *366* (6455), 537-543.

122. Que Jr, L.; True, A. E., Dinuclear iron-and manganese-oxo sites in biology. *Prog. Inorg. Chem.* **1990**, 97-200.

123. Merkx, M.; Kopp, D. A.; Sazinsky, M. H.; Blazyk, J. L.; Müller, J.; Lippard, S. J., Dioxygen activation and methane hydroxylation by soluble methane monooxygenase: a tale of two irons and three proteins. *Angew. Chem. Int. Ed.* **2001,** *40* (15), 2782-2807.

124. Notomista, E.; Lahm, A.; Di Donato, A.; Tramontano, A., Evolution of bacterial and archaeal multicomponent monooxygenases. *J. Mol. Evol.* **2003,** *56* (4), 435-445.

125. Leahy, J. G.; Batchelor, P. J.; Morcomb, S. M., Evolution of the soluble diiron monooxygenases. *FEMS Microbiol. Rev.* **2003,** *27* (4), 449-479.

126. Green, J.; Dalton, H., Substrate specificity of soluble methane monooxygenase. Mechanistic implications. *J. Biol. Chem.* **1989,** *264* (30), 17698-17703.

127. Siewert, I.; Limberg, C., Low-Molecular-Weight Analogues of the Soluble Methane Monooxygenase (sMMO): From the Structural Mimicking of Resting States and Intermediates to Functional Models. *Chem. Eur. J.* **2009,** *15* (40), 10316-10328.

128. Sazinsky, M. H.; Bard, J.; Di Donato, A.; Lippard, S. J., Crystal Structure of the Toluene/o-Xylene Monooxygenase Hydroxylase from *Pseudomonas stutzeri* OX1. *J. Biol. Chem.* **2004,** *279* (29), 30600-30610.

129. Sazinsky, M. H.; Dunten, P. W.; McCormick, M. S.; DiDonato, A.; Lippard, S. J., X-ray Structure of a Hydroxylase Regulatory Protein Complex from a Hydrocarbon-Oxidizing Multicomponent Monooxygenase, *Pseudomonas* sp. OX1 Phenol Hydroxylase. *Biochemistry* **2006,** *45* (51), 15392-15404.

130. Chauhan, S.; Barbieri, P.; Wood, T. K., Oxidation of trichloroethylene, 1,1-dichloroethylene, and chloroform by toluene/o-xylene monooxygenase from *Pseudomonas stutzeri* OX1. *Appl. Environ. Microbiol.* **1998,** *64* (8), 3023-3024.

131. Mitchell, K. H.; Rogge, C. E.; Gierahn, T.; Fox, B. G., Insight into the mechanism of aromatic hydroxylation by toluene 4-monooxygenase by use of specifically deuterated toluene and p-xylene. *Proc. Natl. Acad. Sci.* **2003,** *100* (7), 3784-3789.

132. Colby, J.; Stirling, D. I.; Dalton, H., The soluble methane mono-oxygenase of Methylococcus capsulatus (Bath). Its ability to oxygenate n-alkanes, n-alkenes, ethers, and alicyclic, aromatic and heterocyclic compounds. *Biochem. J.* **1977,** *165* (2), 395-402.

133. Friedle, S.; Reisner, E.; Lippard, S. J., Current challenges of modeling diiron enzyme active sites for dioxygen activation by biomimetic synthetic complexes. *Chem. Soc. Rev.* **2010,** *39* (8), 2768-2779.

134. Kovaleva, E.; Neibergall, M.; Chakrabarty, S.; Lipscomb, J. D., Finding intermediates in the O2 activation pathways of non-heme iron oxygenases. *Acc. Chem. Res.* **2007,** *40* (7), 475-483.

135. Tinberg, C. E.; Lippard, S. J., Revisiting the mechanism of dioxygen activation in soluble methane monooxygenase from M. capsulatus (Bath): evidence for a multi-step, proton-dependent reaction pathway. *Biochemistry* **2009,** *48* (51), 12145-12158.

136. Valentine, A. M.; Stahl, S. S.; Lippard, S. J., Mechanistic studies of the reaction of reduced methane monooxygenase hydroxylase with dioxygen and substrates. *J. Am. Chem. Soc.* **1999,** *121* (16), 3876-3887.

137. Beauvais, L. G.; Lippard, S. J., Reactions of the peroxo intermediate of soluble methane monooxygenase hydroxylase with ethers. *J. Am. Chem. Soc.* **2005,** *127* (20), 7370-7378.

138. Song, W. J.; Lippard, S. J., Mechanistic studies of reactions of peroxodiiron(III) intermediates in T201 variants of toluene/o-xylene monooxygenase hydroxylase. *Biochemistry* **2011,** *50* (23), 5391-5399.

139. Murray, L. J.; Naik, S. G.; Ortillo, D. O.; García-Serres, R.; Lee, J. K.; Huynh, B. H.; Lippard, S. J., Characterization of the arene-oxidizing intermediate in ToMOH as a diiron(III) species. *J. Am. Chem. Soc.* **2007,** *129* (46), 14500-14510.

140. Kappock, T. J.; Caradonna, J. P., Pterin-dependent amino acid hydroxylases. *Chem. Rev.* **1996,** *96* (7), 2659-2756.

141. Flatmark, T.; Stevens, R. C., Structural insight into the aromatic amino acid hydroxylases and their disease-related mutant forms. *Chem. Rev.* **1999,** *99* (8), 2137-2160.

142. Fitzpatrick, P. F., Tetrahydropterin-dependent amino acid hydroxylases. *Annu. Rev. Biochem.* **1999,** *68* (1), 355-381.

143. Klinman, J. P., Life as aerobes: are there simple rules for activation of dioxygen by enzymes? *J. Biol. Inorg. Chem.* **2001,** *6* (1), 1-13.

144. Nagatsu, T.; Levitt, M.; Udenfriend, S., Tyrosine hydroxylase the initial step in norepinephrine biosynthesis. *J. Biol. Chem.* **1964,** *239* (9), 2910-2917.

145. Davis, M. D.; Kaufman, S., Evidence for the formation of the 4a-carbinolamine during the tyrosine-dependent oxidation of tetrahydrobiopterin by rat liver phenylalanine hydroxylase. *J. Biol. Chem.* **1989,** *264* (15), 8585-8596.

146. Francisco, W. A.; Tian, G.; Fitzpatrick, P. F.; Klinman, J. P., Oxygen-18 kinetic isotope effect studies of the tyrosine hydroxylase reaction: Evidence of rate limiting oxygen activation. *J. Am. Chem. Soc.* **1998,** *120* (17), 4057-4062.

147. Bassan, A.; Blomberg, M. R.; Siegbahn, P. E., Mechanism of Dioxygen Cleavage in Tetrahydrobiopterin-Dependent Amino Acid Hydroxylases. *Chem. Eur. J.* **2003,** *9* (1), 106-115.

148. Kemsley, J. N.; Wasinger, E. C.; Datta, S.; Mitić, N.; Acharya, T.; Hedman, B.; Caradonna, J. P.; Hodgson, K. O.; Solomon, E. I., Spectroscopic and Kinetic Studies of PKU Inducing Mutants of Phenylalanine Hydroxylase: Arg158Gln and Glu280Lys. *J. Am. Chem. Soc.* **2003,** *125* (19), 5677-5686.

149. Dix, T. A.; Bollag, G. E.; Domanico, P.; Benkovic, S. J., Phenylalanine hydroxylase: absolute configuration and source of oxygen of the 4a-hydroxytetrahydropterin species. *Biochemistry* **1985,** *24* (12), 2955-2958.

150. Daly, J.; Levitt, M.; Guroff, G.; Udenfriend, S., Isotope studies on the mechanism of action of adrenal tyrosine hydroxylase. *Arch. Biochem. Biophys.* **1968,** *126* (2), 593-598.

151. Siegmund, H.-U.; Kaufman, S., Hydroxylation of 4-methylphenylalanine by rat liver phenylalanine hydroxylase. *J. Biol. Chem.* **1991,** *266* (5), 2903-2910.

152. Olsson, E.; Martinez, A.; Teigen, K.; Jensen, V. R., Formation of the Iron–Oxo Hydroxylating Species in the Catalytic Cycle of Aromatic Amino Acid Hydroxylases. *Chem. Eur. J.* **2011,** *17* (13), 3746-3758.

153. Olsson, E.; Martinez, A.; Teigen, K.; Jensen, V. R., Substrate Hydroxylation by the Oxido–Iron Intermediate in Aromatic Amino Acid Hydroxylases: A DFT Mechanistic Study. *Eur. J. Inorg. Chem.* **2011,** *2011* (17), 2720-2732.

154. Kal, S.; Xu, S.; Que Jr, L., Bio-inspired Nonheme Iron Oxidation Catalysis: Involvement of Oxoiron(V) Oxidants in Cleaving Strong C–H Bonds. *Angew. Chem. Int. Ed.* **2020,** *59* (19), 7332-7349.

155. Bryliakov, K. P.; Talsi, E. P., Active sites and mechanisms of bioinspired oxidation with H_2O_2, catalyzed by non-heme Fe and related Mn complexes. *Coord. Chem. Rev.* **2014,** *276*, 73-96.

156. Oloo, W. N.; Que Jr, L., Bioinspired Nonheme Iron Catalysts for C–H and C=C Bond Oxidation: Insights into the Nature of the Metal-Based Oxidants. *Acc. Chem. Res.* **2015,** *48* (9), 2612-2621.

157. Olivo, G.; Cussó, O.; Costas, M., Biologically inspired C–H and C=C oxidations with hydrogen peroxide catalyzed by iron coordination complexes. *Chem. Asian J.* **2016,** *11* (22), 3148-3158.

158. Olivo, G.; Cussó, O.; Borrell, M.; Costas, M., Oxidation of alkane and alkene moieties with biologically inspired nonheme iron catalysts and hydrogen peroxide: from free radicals to stereoselective transformations. *J. Biol. Inorg. Chem.* **2017,** *22* (2-3), 425-452.

159. Lyakin, O. Y.; Bryliakov, K. P.; Talsi, E. P., Non-heme oxoiron(V) intermediates in chemo-, regio- and stereoselective oxidation of organic substrates. *Coord. Chem. Rev.* **2019,** *384*, 126-139.

160. Kim, C.; Chen, K.; Kim, J.; Que, L., Stereospecific alkane hydroxylation with H_2O_2 catalyzed by an iron(II) –tris(2-pyridylmethyl)amine complex. *J. Am. Chem. Soc.* **1997,** *119* (25), 5964-5965.

161. Chen, K.; Que, L., Stereospecific alkane hydroxylation by non-heme iron catalysts: mechanistic evidence for an $Fe^{V}O$ active species. *J. Am. Chem. Soc.* **2001,** *123* (26), 6327-6337.

162. Aldrich-Wright, J. R.; Vagg, R. S.; Williams, P. A., Design of chiral picen-based metal complexes for molecular recognition of α-aminoacids and nucleic acids. *Coord. Chem. Rev.* **1997,** *166*, 361-389.

163. Knof, U.; von Zelewsky, A., Predetermined chirality at metal centers. *Angew. Chem. Int. Ed.* **1999,** *38* (3), 302-322.

164. Ng, C.; Sabat, M.; Fraser, C. L., Metal complexes with cis α topology from stereoselective quadridentate ligands with amine, pyridine, and quinoline donor groups. *Inorg. Chem.* **1999,** *38* (24), 5545-5556.

165. Costas, M.; Que, J., Lawrence, Ligand topology tuning of iron-catalyzed hydrocarbon oxidations. *Angew. Chem. Int. Ed.* **2002,** *41* (12), 2179-2181.

166. Lee, D.; Park, H., Ligand Taxonomy for Bioinorganic Modeling of Dioxygen-Activating Non-Heme Iron Enzymes. *Chem. Eur. J.* **2020**, *26* (27), 5916-5926.

167. Gamba, I.; Codolà, Z.; Lloret-Fillol, J.; Costas, M., Making and breaking of the O–O bond at iron complexes. *Coord. Chem. Rev.* **2017,** *334*, 2-24.

168. Dantignana, V.; Company, A.; Costas, M., Oxoiron(V) Complexes of Relevance in Oxidation Catalysis of Organic Substrates. *Isr. J. Chem.* **2020**, *60* (10-11), 1004-1018.

169. Borrell, M.; Costas, M., Mechanistically driven development of an iron catalyst for selective *syn*-dihydroxylation of alkenes with aqueous hydrogen peroxide. *J. Am. Chem. Soc.* **2017,** *139* (36), 12821-12829.

170. Chen, K.; Costas, M.; Kim, J.; Tipton, A. K.; Que, L., Olefin cis-dihydroxylation versus epoxidation by non-heme iron catalysts: two faces of an Fe^{III}–OOH coin. *J. Am. Chem. Soc.* **2002,** *124* (12), 3026-3035.

171. Borrell, M.; Costas, M., Greening oxidation catalysis: iron catalyzed alkene syn-dihydroxylation with aqueous hydrogen peroxide in green solvents. *ACS Sustainable Chem. Eng.* **2018,** *6* (7), 8410-8416.

172. Prat, I.; Mathieson, J. S.; Güell, M.; Ribas, X.; Luis, J. M.; Cronin, L.; Costas, M., Observation of Fe(V)=O using variable-temperature mass spectrometry and its enzyme-like C–H and C=C oxidation reactions. *Nat. Chem.* **2011,** *3* (10), 788.

173. Hitomi, Y.; Arakawa, K.; Funabiki, T.; Kodera, M., An Iron(III)–Monoamidate Complex Catalyst for Selective Hydroxylation of Alkane C–H Bonds with Hydrogen Peroxide. *Angew. Chem. Int. Ed.* **2012,** *51* (14), 3448-3452.

174. Xu, S.; Veach, J. J.; Oloo, W. N.; Peters, K. C.; Wang, J.; Perry, R. H.; Que, L., Detection of a transient $Fe^{V}(O)(OH)$ species involved in olefin oxidation by a bio-inspired non-haem iron catalyst. *Chem. Commun.* **2018,** *54* (63), 8701-8704.

175. Borrell, M.; Andris, E.; Navrátil, R.; Roithová, J.; Costas, M., Characterized *cis*-$Fe^{V}(O)(OH)$ intermediate mimics enzymatic oxidations in the gas phase. *Nat. Commun.* **2019,** *10* (1), 1-9.

176. White, M. C.; Doyle, A. G.; Jacobsen, E. N., A synthetically useful, self-assembling MMO mimic system for catalytic alkene epoxidation with aqueous H_2O_2. *J. Am. Chem. Soc.* **2001,** *123* (29), 7194-7195.

177. Chen, M. S.; White, M. C., A predictably selective aliphatic C–H oxidation reaction for complex molecule synthesis. *Science* **2007,** *318* (5851), 783-787.

178. Chen, M. S.; White, M. C., Combined effects on selectivity in Fe-catalyzed methylene oxidation. *Science* **2010,** *327* (5965), 566-571.

179. White, M. C., Adding aliphatic C–H bond oxidations to synthesis. *Science* **2012,** *335* (6070), 807-809.

180. Mas-Ballesté, R.; Que, L., Iron-catalyzed olefin epoxidation in the presence of acetic acid: insights into the nature of the metal-based oxidant. *J. Am. Chem. Soc.* **2007,** *129* (51), 15964-15972.

181. Lyakin, O. Y.; Talsi, E. P., Direct C–H Oxidation of Aromatic Substrates in the Presence of Biomimetic Iron Complexes. In *Frontiers of Green Catalytic Selective Oxidations*, Springer: 2019; pp 253-276.

182. Kitajima, N.; Ito, M.; Fukui, H.; Morooka, Y., A reaction mimic of tyrosine hydroxylase: hydroxylation of a phenoxo ferric complex to a catecholato complex with *m*CPBA. *J. Am. Chem. Soc.* **1993,** *115* (20), 9335-9336.

183. Ménage, S.; Galey, J. B.; Hussler, G.; Seité, M.; Fontecave, M., Aromatic Hydroxylation by H_2O_2 and O_2 Catalyzed by a μ-Oxo Diiron(III) Complex. *Angew. Chem. Int. Ed.* **1996,** *35* (20), 2353-2355.

184. Ménage, S.; Galey, J.-B.; Dumats, J.; Hussler, G.; Seité, M.; Luneau, I. G.; Chottard, G.; Fontecave, M., O_2 activation and aromatic hydroxylation performed by diiron complexes. *J. Am. Chem. Soc.* **1998,** *120* (51), 13370-13382.

185. Mekmouche, Y.; Ménage, S.; Toia-Duboc, C.; Fontecave, M.; Galey, J. B.; Lebrun, C.; Pécaut, J., H_2O_2-Dependent Fe-Catalyzed Oxidations: Control of the Active Species. *Angew. Chem. Int. Ed.* **2001,** *40* (5), 949-952.

186. Lange, S. J.; Miyake, H.; Que, L., Evidence for a nonheme Fe(IV)=O species in the intramolecular hydroxylation of a phenyl moiety. *J. Am. Chem. Soc.* **1999,** *121* (26), 6330-6331.

187. Jensen, M. P.; Mehn, M. P.; Que Jr, L., Intramolecular Aromatic Amination through Iron-Mediated Nitrene Transfer. *Angew. Chem. Int. Ed.* **2003,** *42* (36), 4357-4360.

188. Jensen, M. P.; Lange, S. J.; Mehn, M. P.; Que, E. L.; Que, L., Biomimetic Aryl Hydroxylation Derived from Alkyl Hydroperoxide at a Nonheme Iron Center. Evidence for an Fe^{IV}=O Oxidant. *J. Am. Chem. Soc.* **2003,** *125* (8), 2113-2128.

189. Oh, N. Y.; Seo, M. S.; Lim, M. H.; Consugar, M. B.; Park, M. J.; Rohde, J.-U.; Han, J.; Kim, K. M.; Kim, J.; Que Jr, L., Self-hydroxylation of perbenzoic acids at a nonheme iron(II) center. *Chem. Commun.* **2005,** (45), 5644-5646.

190. Taktak, S.; Flook, M.; Foxman, B. M.; Que Jr, L.; Rybak-Akimova, E. V., *ortho*-Hydroxylation of benzoic acids with hydrogen peroxide at a non-heme iron center. *Chem. Commun.* **2005,** (42), 5301-5303.

191. Makhlynets, O. V.; Das, P.; Taktak, S.; Flook, M.; Mas-Ballesté, R.; Rybak-Akimova, E. V.; Que Jr, L., Iron-Promoted ortho-and/or ipso-Hydroxylation of Benzoic Acids with H_2O_2. *Chem. Eur. J.* **2009,** *15* (47), 13171-13180.

192. Makhlynets, O. V.; Rybak-Akimova, E. V., Aromatic Hydroxylation at a Non-Heme Iron Center: Observed Intermediates and Insights into the Nature of the Active Species. *Chem. Eur. J.* **2010,** *16* (47), 13995-14006.

193. Makhlynets, O. V.; Oloo, W. N.; Moroz, Y. S.; Belaya, I. G.; Palluccio, T. D.; Filatov, A. S.; Müller, P.; Cranswick, M. A.; Que, L.; Rybak-Akimova, E. V., H_2O_2 activation with biomimetic non-haem iron complexes and AcOH: connecting the g= 2.7 EPR signal with a visible chromophore. *Chem. Commun.* **2014,** *50* (6), 645-648.

194. Ansari, A.; Kaushik, A.; Rajaraman, G., Mechanistic Insights on the ortho-Hydroxylation of Aromatic Compounds by Non-heme Iron Complex: A Computational Case Study on the Comparative Oxidative Ability of Ferric-Hydroperoxo and High-Valent Fe^{IV}=O and Fe^{V}=O Intermediates. *J. Am. Chem. Soc.* **2013,** *135* (11), 4235-4249.

195. Ségaud, N.; Rebilly, J.-N.; Sénéchal-David, K.; Guillot, R.; Billon, L.; Baltaze, J.-P.; Farjon, J.; Reinaud, O.; Banse, F. d. r., Iron Coordination Chemistry with New Ligands Containing Triazole and Pyridine Moieties. Comparison of the Coordination Ability of the N-Donors. *Inorg. Chem.* **2013,** *52* (2), 691-700.

196. Martinho, M.; Banse, F.; Bartoli, J.-F.; Mattioli, T. A.; Battioni, P.; Horner, O.; Bourcier, S.; Girerd, J.-J., New example of a non-heme mononuclear iron(IV) oxo complex. Spectroscopic data and oxidation activity. *Inorg. Chem.* **2005,** *44* (25), 9592-9596.

197. Rebilly, J. N.; Zhang, W.; Herrero, C.; Dridi, H.; Sénéchal-David, K.; Guillot, R.; Banse, F., Hydroxylation of aromatics by H_2O_2 catalyzed by mononuclear non-heme iron complexes: Role of triazole hemilability in substrate-induced bifurcation of the H_2O_2 activation mechanism. *Chem. Eur. J.* **2020,** *26*, 659-668.

198. de Visser, S. P.; Oh, K.; Han, A.-R.; Nam, W., Combined Experimental and Theoretical Study on Aromatic Hydroxylation by Mononuclear Nonheme Iron(IV)–Oxo Complexes. *Inorg. Chem.* **2007,** *46* (11), 4632-4641.

199. Bartoli, J.-F.; Lambert, F.; Morgenstern-Badarau, I.; Battioni, P.; Mansuy, D., Unusual efficiency of a non-heme iron complex as catalyst for the hydroxylation of aromatic compounds by hydrogen peroxide: comparison with iron porphyrins. *C. R. Chimie* **2002,** *5* (4), 263-266.

200. Balland, V.; Mathieu, D.; Pons-Y-Moll, N.; Bartoli, J. F.; Banse, F.; Battioni, P.; Girerd, J.-J.; Mansuy, D., Non-heme iron polyazadentate complexes as catalysts for oxidations by H_2O_2: particular efficiency in aromatic hydroxylations and beneficial effects of a reducing agent. *J. Mol. Catal. A: Chem.* **2004,** *215* (1-2), 81-87.

201. Thibon, A.; Bartoli, J.-F.; Guillot, R.; Sainton, J.; Martinho, M.; Mansuy, D.; Banse, F., Non-heme iron polyazadentate complexes as catalysts for aromatic hydroxylation by H_2O_2: Particular efficiency of tetrakis(2-pyridylmethyl)ethylenediamine–iron(II) complexes. *J. Mol. Catal. A* **2008,** *287* (1-2), 115-120.

202. Bianchi, D.; Bortolo, R.; Tassinari, R.; Ricci, M.; Vignola, R., A novel iron-based catalyst for the biphasic oxidation of benzene to phenol with hydrogen peroxide. *Angew. Chem. Int. Ed.* **2000,** *39* (23), 4321-4323.

203. Bianchi, D.; Bertoli, M.; Tassinari, R.; Ricci, M.; Vignola, R., Direct synthesis of phenols by iron-catalyzed biphasic oxidation of aromatic hydrocarbons with hydrogen peroxide. *J. Mol. Catal. A: Chem.* **2003,** *200* (1-2), 111-116.

204. Bianchi, D.; Bertoli, M.; Tassinari, R.; Ricci, M.; Vignola, R., Ligand effect on the iron-catalysed biphasic oxidation of aromatic hydrocarbons by hydrogen peroxide. *J. Mol. Catal. A: Chem.* **2003,** *204*, 419-424.

205. Kejriwal, A.; Bandyopadhyay, P.; Biswas, A. N., Aromatic hydroxylation using an oxo-bridged diiron(III) complex: a bio-inspired functional model of toluene monooxygenases. *Dalton Trans.* **2015,** *44* (39), 17261-17267.

206. Raba, A.; Cokoja, M.; Herrmann, W. A.; Kühn, F. E., Catalytic hydroxylation of benzene and toluene by an iron complex bearing a chelating di-pyridyl-di-NHC ligand. *Chem. Commun.* **2014,** *50* (78), 11454-11457.

207. Raba, A.; Cokoja, M.; Ewald, S.; Riener, K.; Herdtweck, E.; Pöthig, A.; Herrmann, W. A.; Kühn, F. E., Synthesis and Characterization of Novel Iron(II) Complexes with Tetradentate Bis(N-heterocyclic carbene)–Bis (pyridine)(NCCN) Ligands. *Organometallics* **2012,** *31* (7), 2793-2800.

208. Rogers, M. M.; Stahl, S. S., N-Heterocyclic carbenes as ligands for high-oxidation-state metal complexes and oxidation catalysis. In *N-Heterocyclic Carbenes in Transition Metal Catalysis*, Springer: 2006; pp 21-46.

209. Strassner, T., The role of NHC ligands in oxidation catalysis. In *Organometallic Oxidation Catalysis*, Springer: 2006; pp 125-148.

210. Lindhorst, A. C.; Schütz, J.; Netscher, T.; Bonrath, W.; Kühn, F. E., Catalytic oxidation of aromatic hydrocarbons by a molecular iron–NHC complex. *Catal. Sci. Technol.* **2017,** *7* (9), 1902-1911.

211. Silva, G. C.; Carvalho, N. M.; Horn Jr, A.; Lachter, E. R.; Antunes, O. A., Oxidation of aromatic compounds by hydrogen peroxide catalyzed by mononuclear iron(III) complexes. *J. Mol. Catal. A: Chem.* **2017,** *426*, 564-571.

212. Olivo, G.; Lanzalunga, O.; Di Stefano, S., Non-Heme Imine-Based Iron Complexes as Catalysts for Oxidative Processes. *Adv. Synth. Catal.* **2016,** *358* (6), 843-863.

213. Capocasa, G.; Olivo, G.; Barbieri, A.; Lanzalunga, O.; Di Stefano, S., Direct hydroxylation of benzene and aromatics with H_2O_2 catalyzed by a self-assembled iron complex: evidence for a metal-based mechanism. *Catal. Sci. Technol.* **2017,** *7* (23), 5677-5686.

214. Ticconi, B.; Colcerasa, A.; Di Stefano, S.; Lanzalunga, O.; Lapi, A.; Mazzonna, M.; Olivo, G., Oxidative functionalization of aliphatic and aromatic amino acid derivatives with H_2O_2 catalyzed by a nonheme imine based iron complex. *RSC Adv.* **2018,** *8* (34), 19144-19151.

215. Capocasa, G.; Di Berto Mancini, M.; Frateloreto, F.; Lanzalunga, O.; Olivo, G.; Di Stefano, S., Easy Synthesis of a Self-Assembled Imine-Based Iron(II) Complex Endowed with Crown-Ether Receptors. *Eur. J. Org. Chem.* **2020,** *23*, 3390-3397.

216. Olivo, G.; Arancio, G.; Mandolini, L.; Lanzalunga, O.; Di Stefano, S., Hydrocarbon oxidation catalyzed by a cheap nonheme imine-based iron(II) complex. *Catal. Sci. Technol.* **2014,** *4* (9), 2900-2903.

217. Olivo, G.; Giosia, S.; Barbieri, A.; Lanzalunga, O.; Di Stefano, S., Alcohol oxidation with H2O2 catalyzed by a cheap and promptly available imine based iron complex. *Org. Biomol. Chem.* **2016,** *14* (45), 10630-10635.

218. Ticconi, B.; Capocasa, G.; Cerrato, A.; Di Stefano, S.; Lapi, A.; Marincioni, B.; Olivo, G.; Lanzalunga, O., Insight into the chemoselective aromatic vs. side-chain hydroxylation of alkylaromatics with H_2O_2 catalyzed by a non-heme imine-based iron complex. *Catal. Sci. Technol.* **2021,** *11* (1), 171-178.

219. Olivo, G.; Nardi, M.; Vìdal, D.; Barbieri, A.; Lapi, A.; Gómez, L.; Lanzalunga, O.; Costas, M.; Di Stefano, S., C–H Bond Oxidation Catalyzed by an Imine-Based Iron Complex: A Mechanistic Insight. *Inorg. Chem.* **2015,** *54* (21), 10141-10152.

220. Lyakin, O. Y.; Zima, A. M.; Tkachenko, N. V.; Bryliakov, K. P.; Talsi, E. P., Direct Evaluation of the Reactivity of Nonheme Iron(V)–Oxo Intermediates toward Arenes. *ACS Catal.* **2018,** *8* (6), 5255-5260.

221. Lyakin, O. Y.; Zima, A. M.; Samsonenko, D. G.; Bryliakov, K. P.; Talsi, E. P., EPR Spectroscopic Detection of the Elusive Fe^{V}=O Intermediates in Selective Catalytic Oxofunctionalizations of Hydrocarbons Mediated by Biomimetic Ferric Complexes. *ACS Catal*. **2015,** *5* (5), 2702-2707.

222. Zima, A. M.; Lyakin, O. Y.; Ottenbacher, R. V.; Bryliakov, K. P.; Talsi, E. P., Dramatic effect of carboxylic acid on the electronic structure of the active species in Fe(PDP)-catalyzed asymmetric epoxidation. *ACS Catal*. **2016,** *6* (8), 5399-5404.

223. Zima, A. M.; Lyakin, O. Y.; Ottenbacher, R. V.; Bryliakov, K. P.; Talsi, E. P., Iron-catalyzed enantioselective epoxidations with various oxidants: Evidence for different active species and epoxidation mechanisms. *ACS Catal*. **2017,** *7* (1), 60-69.

224. Zima, A. M.; Lyakin, O. Y.; Lubov, D. P.; Bryliakov, K. P.; Talsi, E. P., Aromatic C–H oxidation by non-heme iron(V)-oxo intermediates bearing aminopyridine ligands. *J. Mol. Catal*. **2020,** *483*, 110708.

225. Van Heuvelen, K. M.; Fiedler, A. T.; Shan, X.; De Hont, R. F.; Meier, K. K.; Bominaar, E. L.; Münck, E.; Que, L., One-electron oxidation of an oxoiron(IV) complex to form an $[O=Fe^{V}=NR]^{+}$ center. *Proc. Natl. Acad. Sci. U.S.A*. **2012,** *109* (30), 11933-11938.

226. Serrano-Plana, J.; Oloo, W. N.; Acosta-Rueda, L.; Meier, K. K.; Verdejo, B.; García-España, E.; Basallote, M. G.; Münck, E.; Que Jr, L.; Company, A.; Costas, M., Trapping a Highly Reactive Nonheme Iron Intermediate That Oxygenates Strong C–H Bonds with Stereoretention. *J. Am. Chem. Soc*. **2015,** *137* (50), 15833-15842.

227. Tkachenko, N. V.; Ottenbacher, R. V.; Lyakin, O. Y.; Zima, A. M.; Samsonenko, D. G.; Talsi, E. P.; Bryliakov, K. P., Highly Efficient Aromatic C–H Oxidation with H_2O_2 in the Presence of Iron Complexes of the PDP Family. *ChemCatChem* **2018,** *10* (18), 4052-4057.

228. Tkachenko, N. V.; Lyakin, O. Y.; Zima, A. M.; Talsi, E. P.; Bryliakov, K. P., Effect of different carboxylic acids on the aromatic hydroxylation with H_2O_2 in the presence of an iron aminopyridine complex. *J. Organomet. Chem*. **2018,** *871*, 130-134.

229. Kal, S.; Draksharapu, A.; Que Jr, L., Sc^{3+} (or $HClO_4$) Activation of a Nonheme Fe^{III}–OOH Intermediate for the Rapid Hydroxylation of Cyclohexane and Benzene. *J. Am. Chem. Soc*. **2018,** *140* (17), 5798-5804.

230. Li, F.; Van Heuvelen, K. M.; Meier, K. K.; Münck, E.; Que Jr, L., Sc^{3+}-triggered oxoiron(IV) formation from O_2 and its non-heme iron(II) precursor via a Sc^{3+}–peroxo–Fe^{3+} intermediate. *J. Am. Chem. Soc*. **2013,** *135* (28), 10198-10201.

231. Lee, Y.-M.; Bang, S.; Kim, Y. M.; Cho, J.; Hong, S.; Nomura, T.; Ogura, T.; Troeppner, O.; Ivanović-Burmazović, I.; Sarangi, R., A mononuclear nonheme iron(III)–peroxo complex binding redox-inactive metal ions. *Chem. Sci*. **2013,** *4* (10), 3917-3923.

232. Zhang, J.; Wei, W.-J.; Lu, X.; Yang, H.; Chen, Z.; Liao, R.-Z.; Yin, G., Nonredox metal ions promoted olefin epoxidation by iron(II) complexes with H_2O_2: DFT calculations reveal multiple channels for oxygen transfer. *Inorg. Chem*. **2017,** *56* (24), 15138-15149.

233. Nodzewska, A.; Watkinson, M., Remarkable increase in the rate of the catalytic epoxidation of electron deficient styrenes through the addition of $Sc(OTf)_3$ to the MnTMTACN catalyst. *Chem. Commun*. **2018,** *54* (12), 1461-1464.

234. Chatterjee, S.; Paine, T. K., Olefin *cis*-Dihydroxylation and Aliphatic C–H Bond Oxygenation by a Dioxygen-Derived Electrophilic Iron–Oxygen Oxidant. *Angew. Chem. Int. Ed*. **2015,** *54*, 9338-9342.

235. Kal, S.; Que Jr, L., Activation of a Non-Heme Fe^{III}-OOH by a Second Fe^{III} to Hydroxylate Strong C–H Bonds: Possible Implications for Soluble Methane Monooxygenase. *Angew. Chem. Int. Ed.* **2019,** *58* (25), 8484-8488.

236. Cheng, L.; Wang, H.; Cai, H.; Zhang, J.; Gong, X.; Han, W., Iron-catalyzed arene C–H hydroxylation. *Science* **2021,** *374* (6563), 77-81.

237. Klinman, J. P., Mechanisms whereby mononuclear copper proteins functionalize organic substrates. *Chem. Rev.* **1996,** *96* (7), 2541-2562.

238. Fontecave, M.; Pierre, J.-L., Oxidations by copper metalloenzymes and some biomimetic approaches. *Coord. Chem. Rev.* **1998,** *170* (1), 125-140.

239. Klabunde, T.; Eicken, C.; Sacchettini, J. C.; Krebs, B., Crystal structure of a plant catechol oxidase containing a dicopper center. *Nat. Struct. Mol. Biol.* **1998,** *5* (12), 1084-1090.

240. Solomon, E. I.; Sundaram, U. M.; Machonkin, T. E., Multicopper oxidases and oxygenases. *Chem. Rev.* **1996,** *96* (7), 2563-2606.

241. Rolff, M.; Schottenheim, J.; Decker, H.; Tuczek, F., Copper–O_2 reactivity of tyrosinase models towards external monophenolic substrates: molecular mechanism and comparison with the enzyme. *Chem. Soc. Rev.* **2011,** *40* (7), 4077-4098.

242. Decker, H.; Schweikardt, T.; Tuczek, F., The first crystal structure of tyrosinase: all questions answered? *Angew. Chem. Int. Ed.* **2006,** *45* (28), 4546-4550.

243. Matoba, Y.; Kumagai, T.; Yamamoto, A.; Yoshitsu, H.; Sugiyama, M., Crystallographic evidence that the dinuclear copper center of tyrosinase is flexible during catalysis. *J. Biol. Chem.* **2006,** *281* (13), 8981-8990.

244. Serrano-Plana, J.; Garcia-Bosch, I.; Company, A.; Costas, M., Structural and reactivity models for copper oxygenases: cooperative effects and novel reactivities. *Acc. Chem. Res.* **2015,** *48* (8), 2397-2406.

245. Karlin, K. D.; Hayes, J. C.; Gultneh, Y.; Cruse, R. W.; McKown, J. W.; Hutchinson, J. P.; Zubieta, J., Copper-mediated hydroxylation of an arene: model system for the action of copper monooxygenases. Structures of a binuclear copper(I) complex and its oxygenated product. *J. Am. Chem. Soc.* **1984,** *106* (7), 2121-2128.

246. Karlin, K. D.; Nasir, M. S.; Cohen, B. I.; Cruse, R. W.; Kaderli, S.; Zuberbuehler, A. D., Reversible dioxygen binding and aromatic hydroxylation in O_2-reactions with substituted xylyl dinuclear copper(I) complexes: syntheses and low-temperature kinetic/thermodynamic and spectroscopic investigations of a copper monooxygenase model system. *J. Am. Chem. Soc.* **1994,** *116* (4), 1324-1336.

247. Pidcock, E.; Obias, H. V.; Zhang, C. X.; Karlin, K. D.; Solomon, E. I., Investigation of the reactive oxygen intermediate in an arene hydroxylation reaction performed by xylyl-bridged binuclear copper complexes. *J. Am. Chem. Soc.* **1998,** *120* (31), 7841-7847.

248. Becker, M.; Schindler, S.; Karlin, K. D.; Kaden, T. A.; Kaderli, S.; Palanché, T.; Zuberbühler, A. D., Intramolecular ligand hydroxylation: Mechanistic high-pressure studies on the reaction of a dinuclear copper(I) complex with dioxygen. *Inorg. Chem.* **1999,** *38* (9), 1989-1995.

249. Maiti, D.; Fry, H. C.; Woertink, J. S.; Vance, M. A.; Solomon, E. I.; Karlin, K. D., A 1: 1 copper–dioxygen adduct is an end-on bound superoxo copper(II) complex which undergoes oxygenation reactions with phenols. *J. Am. Chem. Soc.* **2007,** *129* (2), 264-265.

250. Maiti, D.; Lee, D. H.; Gaoutchenova, K.; Würtele, C.; Holthausen, M. C.; Narducci Sarjeant, A. A.; Sundermeyer, J.; Schindler, S.; Karlin, K. D., Reactions of a Copper(II) Superoxo Complex Lead to C–H and O–H Substrate Oxygenation: Modeling Copper-Monooxygenase C–H Hydroxylation. *Angew. Chem. Int. Ed.* **2008,** *47*, 82-85.

251. Karlin, K. D.; Zhang, C. X.; Rheingold, A. L.; Galliker, B.; Kaderli, S.; Zuberbühler, A. D., Reversible dioxygen binding and arene hydroxylation reactions: Kinetic and thermodynamic studies involving ligand electronic and structural variations. *Inorganica Chim. Acta* **2012,** *389*, 138-150.

252. Lee, J. Y.; Peterson, R. L.; Ohkubo, K.; Garcia-Bosch, I.; Himes, R. A.; Woertink, J.; Moore, C. D.; Solomon, E. I.; Fukuzumi, S.; Karlin, K. D., Mechanistic insights into the oxidation of substituted phenols via hydrogen atom abstraction by a cupric–superoxo complex. *J. Am. Chem. Soc.* **2014,** *136* (28), 9925-9937.

253. Kim, S.; Lee, J. Y.; Cowley, R. E.; Ginsbach, J. W.; Siegler, M. A.; Solomon, E. I.; Karlin, K. D., A N_3S(thioether)-ligated Cu^{II}-superoxo with enhanced reactivity. *J. Am. Chem. Soc.* **2015,** *137* (8), 2796-2799.

254. Mahapatra, S.; Kaderli, S.; Llobet, A.; Neuhold, Y.-M.; Palanché, T.; Halfen, J. A.; Young, V. G.; Kaden, T. A.; Que, L.; Zuberbühler, A. D.; Tolman, W. B., Binucleating ligand structural effects on (μ-peroxo)-and bis(μ-oxo) dicopper complex formation and decay: Competition between arene hydroxylation and aliphatic C–H bond activation. *Inorg. Chem.* **1997,** *36* (27), 6343-6356.

255. Sander, O.; Henß, A.; Näther, C.; Würtele, C.; Holthausen, M. C.; Schindler, S.; Tuczek, F., Aromatic Hydroxylation in a Copper Bis(imine) Complex Mediated by a μ-η^2:η^2 Peroxo Dicopper Core: A Mechanistic Scenario. *Chem. Eur. J.* **2008,** *14* (31), 9714-9729.

256. Menif, R.; Martell, A. E.; Squattrito, P. J.; Clearfield, A., New hexaaza macrocyclic binucleating ligands. Oxygen insertion with a dicopper(I) Schiff base macrocyclic complex. *Inorg. Chem.* **1990,** *29* (23), 4723-4729.

257. Santagostini, L.; Gullotti, M.; Monzani, E.; Casella, L.; Dillinger, R.; Tuczek, F., Reversible dioxygen binding and phenol oxygenation in a tyrosinase model system. *Chem. Eur. J.* **2000,** *6* (3), 519-522.

258. Palavicini, S.; Granata, A.; Monzani, E.; Casella, L., Hydroxylation of phenolic compounds by a peroxodicopper(II) complex: Further insight into the mechanism of tyrosinase. *J. Am. Chem. Soc.* **2005,** *127* (51), 18031-18036.

259. Itoh, S.; Kumei, H.; Taki, M.; Nagatomo, S.; Kitagawa, T.; Fukuzumi, S., Oxygenation of phenols to catechols by a (μ-η^2:η^2-peroxo) dicopper(II) complex: mechanistic insight into the phenolase activity of tyrosinase. *J. Am. Chem. Soc.* **2001,** *123* (27), 6708-6709.

260. Battaini, G.; De Carolis, M.; Monzani, E.; Tuczek, F.; Casella, L., The phenol *ortho*-oxygenation by mononuclear copper(I) complexes requires a dinuclear μ-η^2:η^2-peroxodicopper(II) complex rather than mononuclear CuO_2 species. *Chem. Commun.* **2003,** (6), 726-727.

261. Mirica, L. M.; Vance, M.; Rudd, D. J.; Hedman, B.; Hodgson, K. O.; Solomon, E. I.; Stack, T., A Stabilized μ-η^2:η^2 Peroxodicopper(II) Complex with a Secondary Diamine Ligand and Its Tyrosinase-like Reactivity. *J. Am. Chem. Soc.* **2002,** *124* (32), 9332-9333.

262. Mirica, L. M.; Rudd, D. J.; Vance, M. A.; Solomon, E. I.; Hodgson, K. O.; Hedman, B.; Stack, T. D. P., μ-η^2:η^2-Peroxodicopper(II) complex with a secondary diamine ligand: a functional model of tyrosinase. *J. Am. Chem. Soc.* **2006,** *128* (8), 2654-2665.

263. Mirica, L. M.; Vance, M.; Rudd, D. J.; Hedman, B.; Hodgson, K. O.; Solomon, E. I.; Stack, T. D. P., Tyrosinase reactivity in a model complex: an alternative hydroxylation mechanism. *Science* **2005,** *308* (5730), 1890-1892.

264. Citek, C.; Lyons, C. T.; Wasinger, E. C.; Stack, T. D. P., Self-assembly of the oxy-tyrosinase core and the fundamental components of phenolic hydroxylation. *Nat. Chem.* **2012,** *4* (4), 317-322.

265. Hamann, J. N.; Tuczek, F., New catalytic model systems of tyrosinase: fine tuning of the reactivity with pyrazole-based N-donor ligands. *Chem. Commun.* **2014,** *50* (18), 2298-2300.

266. Company, A.; Palavicini, S.; Garcia-Bosch, I.; Mas-Ballesté, R.; Que Jr, L.; Rybak-Akimova, E. V.; Casella, L.; Ribas, X.; Costas, M., Tyrosinase-Like Reactivity in a $Cu^{III}_2(\mu\text{-}O)_2$ Species. *Chem. Eur. J.* **2008,** *14* (12), 3535-3538.

267. Tachi, Y.; Aita, K.; Teramae, S.; Tani, F.; Naruta, Y.; Fukuzumi, S.; Itoh, S., Dicopper–Dioxygen Complex Supported by Asymmetric Pentapyridine Dinucleating Ligand. *Inorg. Chem.* **2004,** *43* (15), 4558-4560.

268. Garcia-Bosch, I.; Company, A.; Frisch, J. R.; Torrent-Sucarrat, M.; Cardellach, M.; Gamba, I.; Güell, M.; Casella, L.; Que Jr, L.; Ribas, X.; Luis, J. M.; Costas, M., O_2 Activation and Selective Phenolate ortho Hydroxylation by an Unsymmetric Dicopper $\mu\text{-}\eta^1\text{:}\eta^1$-Peroxido Complex. *Angew. Chem. Int. Ed.* **2010,** *49*, 2406 –2409.

269. Matsumoto, T.; Furutachi, H.; Kobino, M.; Tomii, M.; Nagatomo, S.; Tosha, T.; Osako, T.; Fujinami, S.; Itoh, S.; Kitagawa, T.; Suzuki, M., Intramolecular arene hydroxylation versus intermolecular olefin epoxidation by $(\mu\text{-}\eta^2\text{:}\eta^2$-peroxo)dicopper(II) complex supported by dinucleating ligand. *J. Am. Chem. Soc.* **2006,** *128* (12), 3874-3875.

270. Mirica, L. M.; Ottenwaelder, X.; Stack, T. D. P., Structure and spectroscopy of copper–dioxygen complexes. *Chem. Rev.* **2004,** *104* (2), 1013-1046.

271. Lewis, E. A.; Tolman, W. B., Reactivity of dioxygen–copper systems. *Chem. Rev.* **2004,** *104* (2), 1047-1076.

272. Halfen, J. A.; Mahapatra, S.; Wilkinson, E. C.; Kaderli, S.; Young Jr, V. G.; Que Jr, L.; Zuberbühler, A. D.; Tolman, W. B., Reversible cleavage and formation of the dioxygen O–O bond within a dicopper complex. *Science* **1996**, 1397-1400.

273. Tolman, W. B., Making and breaking the dioxygen O–O bond: New insights from studies of synthetic copper complexes. *Acc. Chem. Res.* **1997,** *30* (6), 227-237.

274. Op't Holt, B. T.; Vance, M. A.; Mirica, L. M.; Heppner, D. E.; Stack, T. D. P.; Solomon, E. I., Reaction coordinate of a functional model of tyrosinase: spectroscopic and computational characterization. *J. Am. Chem. Soc.* **2009,** *131* (18), 6421-6438.

275. Holland, P. L.; Rodgers, K. R.; Tolman, W. B., Is the Bis(μ-oxo)dicopper Core Capable of Hydroxylating an Arene? *Angew. Chem. Int. Ed.* **1999,** *38* (8), 1139-1142.

276. Herres-Pawlis, S.; Verma, P.; Haase, R.; Kang, P.; Lyons, C. T.; Wasinger, E. C.; Flörke, U.; Henkel, G.; Stack, T. D. P., Phenolate hydroxylation in a bis(μ-oxo)dicopper(III) complex: lessons from the guanidine/amine series. *J. Am. Chem. Soc.* **2009,** *131* (3), 1154-1169.

277. Itoh, S., Developing mononuclear copper–active-oxygen complexes relevant to reactive intermediates of biological oxidation reactions. *Acc. Chem. Res.* **2015,** *48* (7), 2066-2074.

278. Kunishita, A.; Teraoka, J.; Scanlon, J. D.; Matsumoto, T.; Suzuki, M.; Cramer, C. J.; Itoh, S., Aromatic Hydroxylation Reactivity of a Mononuclear Cu(II) –Alkylperoxo Complex. *J. Am. Chem. Soc.* **2007,** *129* (23), 7248-7249.

279. Kunishita, A.; Scanlon, J. D.; Ishimaru, H.; Honda, K.; Ogura, T.; Suzuki, M.; Cramer, C. J.; Itoh, S., Reactions of copper(II)-H_2O_2 adducts supported by tridentate bis(2-pyridylmethyl)amine ligands: Sensitivity to solvent and variations in ligand substitution. *Inorg. Chem.* **2008,** *47* (18), 8222-8232.

280. Würtele, C.; Gaoutchenova, E.; Harms, K.; Holthausen, M. C.; Sundermeyer, J.; Schindler, S., Crystallographic characterization of a synthetic 1:1 end-on copper dioxygen adduct complex. *Angew. Chem. Int. Ed.* **2006,** *45* (23), 3867-3869.

281. Conde, A.; Diaz-Requejo, M. M.; Pérez, P. J., Direct, copper-catalyzed oxidation of aromatic C–H bonds with hydrogen peroxide under acid-free conditions. *Chem. Commun.* **2011,** *47* (28), 8154-8156.

282. Vilella, L.; Conde, A.; Balcells, D.; Díaz-Requejo, M. M.; Lledós, A.; Pérez, P. J., A competing, dual mechanism for catalytic direct benzene hydroxylation from combined experimental-DFT studies. *Chem. Sci.* **2017,** *8* (12), 8373-8383.

283. Wu, L.; Zhong, W.; Xu, B.; Wei, Z.; Liu, X., Synthesis and characterization of copper(II) complexes with multidentate ligands as catalysts for the direct hydroxylation of benzene to phenol. *Dalton Trans.* **2015,** *44* (17), 8013-8020.

284. Tsuji, T.; Zaoputra, A. A.; Hitomi, Y.; Mieda, K.; Ogura, T.; Shiota, Y.; Yoshizawa, K.; Sato, H.; Kodera, M., Specific enhancement of catalytic activity by a dicopper core: selective hydroxylation of benzene to phenol with hydrogen peroxide. *Angew. Chem. Int. Ed.* **2017,** *56* (27), 7779-7782.

285. Muthuramalingam, S.; Anandababu, K.; Velusamy, M.; Mayilmurugan, R., Benzene Hydroxylation by Bioinspired Copper(II) Complexes: Coordination Geometry versus Reactivity. *Inorg. Chem.* **2020,** *59* (9), 5918-5928.

286. Yamada, M.; Karlin, K. D.; Fukuzumi, S., One-step selective hydroxylation of benzene to phenol with hydrogen peroxide catalysed by copper complexes incorporated into mesoporous silica–alumina. *Chem. Sci.* **2016,** *7* (4), 2856-2863.

287. Kumari, S.; Muthuramalingam, S.; Dhara, A. K.; Singh, U.; Mayilmurugan, R.; Ghosh, K., Cu(I) complexes obtained via spontaneous reduction of Cu(II) complexes supported by designed bidentate ligands: bioinspired Cu(I) based catalysts for aromatic hydroxylation. *Dalton Trans.* **2020,** *49* (39), 13829-13839.

288. Boer, J. L.; Mulrooney, S. B.; Hausinger, R. P., Nickel-dependent metalloenzymes. *Arch. Biochem. Biophys.* **2014,** *544*, 142-152.

289. Corona, T.; Company, A., Spectroscopically characterized synthetic mononuclear nickel–oxygen species. *Chem. Eur. J.* **2016,** *22* (38), 13422-13429.

290. Kimura, E.; Machida, R., A mono-ozygenase model for selective aromatic hydroxylation with nickel(II)-macrocyclic polyamines. *J. Chem. Soc. Chem. Commun.* **1984,** (8), 499-500.

291. Honda, K.; Cho, J.; Matsumoto, T.; Roh, J.; Furutachi, H.; Tosha, T.; Kubo, M.; Fujinami, S.; Ogura, T.; Kitagawa, T.; Suzuki, M., Oxidation Reactivity of Bis(μ-oxo) Dinickel(III) Complexes: Arene Hydroxylation of the Supporting Ligand. *Angew. Chem. Int. Ed.* **2009,** *48* (18), 3304-3307.

292. Kunishita, A.; Doi, Y.; Kubo, M.; Ogura, T.; Sugimoto, H.; Itoh, S., Ni(II)/H_2O_2 reactivity in bis[(pyridin-2-yl)methyl]amine tridentate ligand system. Aromatic hydroxylation reaction by bis(μ-oxo)dinickel(III) complex. *Inorg. Chem.* **2009,** *48* (11), 4997-5004.

293. Tano, T.; Doi, Y.; Inosako, M.; Kunishita, A.; Kubo, M.; Ishimaru, H.; Ogura, T.; Sugimoto, H.; Itoh, S., Nickel(II) Complexes of tpa Ligands with 6-Phenyl Substituents (Phntpa). Structure and H_2O_2-Reactivity. *Bull. Chem. Soc. Jpn.* **2010,** *83* (5), 530-538.

294. Hikichi, S.; Yoshizawa, M.; Sasakura, Y.; Akita, M.; Moro-oka, Y., First Synthesis and Structural Characterization of Dinuclear M(III) Bis(μ-oxo) Complexes of Nickel and Cobalt with Hydrotris(pyrazolyl)borate Ligand. *J. Am. Chem. Soc.* **1998,** *120* (40), 10567-10568.

295. Itoh, S.; Bandoh, H.; Nagatomo, S.; Kitagawa, T.; Fukuzumi, S., Aliphatic hydroxylation by a bis(μ-oxo)dinickel(III) complex. *J. Am. Chem. Soc.* **1999,** *121* (38), 8945-8946.

296. Shiren, K.; Ogo, S.; Fujinami, S.; Hayashi, H.; Suzuki, M.; Uehara, A.; Watanabe, Y.; Moro-oka, Y., Synthesis, Structures, and Properties of Bis(μ-oxo)nickel(III) and Bis(μ-superoxo)nickel(II) Complexes: An Unusual Conversion of a $Ni^{III}_2(\mu\text{-}O)_2$ Core into a $Ni^{II}_2(\mu\text{-}OO)_2$ Core by H_2O_2 and Oxygenation of Ligand. *J. Am. Chem. Soc.* **2000,** *122* (2), 254-262.

297. Mandimutsira, B. S.; Yamarik, J. L.; Brunold, T. C.; Gu, W.; Cramer, S. P.; Riordan, C. G., Dioxygen activation by a nickel thioether complex: Characterization of a $Ni^{III}_2(\mu\text{-}O)_2$ Core. *J. Am. Chem. Soc.* **2001,** *123* (37), 9194-9195.

298. Itoh, S.; Bandoh, H.; Nakagawa, M.; Nagatomo, S.; Kitagawa, T.; Karlin, K. D.; Fukuzumi, S., Formation, Characterization, and Reactivity of Bis(μ-oxo)dinickel(III) Complexes Supported by A Series of Bis[2-(2-pyridyl)ethyl]amine Ligands. *J. Am. Chem. Soc.* **2001,** *123* (45), 11168-11178.

299. Schenker, R.; Mandimutsira, B. S.; Riordan, C. G.; Brunold, T. C., Spectroscopic and Computational Studies on $[(PhTttBu)_2Ni_2(\mu\text{-}O)_2]$: Nature of the Bis-μ-oxo $(Ni^{3+})_2$ "Diamond" Core. *J. Am. Chem. Soc.* **2002,** *124* (46), 13842-13855.

300. Morimoto, Y.; Bunno, S.; Fujieda, N.; Sugimoto, H.; Itoh, S., Direct hydroxylation of benzene to phenol using hydrogen peroxide catalyzed by nickel complexes supported by pyridylalkylamine ligands. *J. Am. Chem. Soc.* **2015,** *137* (18), 5867-5870.

301. Morimoto, Y.; Takagi, Y.; Saito, T.; Ohta, T.; Ogura, T.; Tohnai, N.; Nakano, M.; Itoh, S., A Bis(μ-oxido)dinickel(III) Complex with a Triplet Ground State. *Angew. Chem. Int. Ed.* **2018,** *57* (26), 7640-7643.

302. Muthuramalingam, S.; Anandababu, K.; Velusamy, M.; Mayilmurugan, R., One step phenol synthesis from benzene catalysed by nickel(II) complexes. *Catal. Sci. Technol.* **2019,** *9* (21), 5991-6001.

303. McEvoy, J. P.; Brudvig, G. W., Water-splitting chemistry of photosystem II. *Chem. Rev.* **2006,** *106* (11), 4455-4483.

304. Cady, C. W.; Crabtree, R. H.; Brudvig, G. W., Functional models for the oxygen-evolving complex of photosystem II. *Coord. Chem. Rev.* **2008,** *252* (3-4), 444-455.

305. Umena, Y.; Kawakami, K.; Shen, J.-R.; Kamiya, N., Crystal structure of oxygen-evolving photosystem II at a resolution of 1.9 Å. *Nature* **2011,** *473* (7345), 55-60.

306. Cinco, R. M.; McFarlane Holman, K. L.; Robblee, J. H.; Yano, J.; Pizarro, S. A.; Bellacchio, E.; Sauer, K.; Yachandra, V. K., Calcium EXAFS establishes the Mn-Ca cluster in the oxygen-evolving complex of photosystem II. *Biochemistry* **2002,** *41* (43), 12928-12933.

307. Cahiez, G.; Duplais, C.; Buendia, J., Chemistry of organomanganese(II) compounds. *Chem. Rev.* **2009,** *109* (3), 1434-1476.

308. Carney, J. R.; Dillon, B. R.; Thomas, S. P., Recent advances of manganese catalysis for organic synthesis. *Eur. J. Org. Chem.* **2016,** *2016* (23), 3912-3929.

309. Philip, R. M.; Radhika, S.; Abdulla, C. A.; Anilkumar, G., Recent Trends and Prospects in Homogeneous Manganese-Catalysed Epoxidation. *Adv. Synth. Catal.* **2021,** *363* (5), 1272-1289.

310. Chen, J.; Jiang, Z.; Fukuzumi, S.; Nam, W.; Wang, B., Artificial nonheme iron and manganese oxygenases for enantioselective olefin epoxidation and alkane hydroxylation reactions. *Coord. Chem. Rev.* **2020,** *421*, 213443.

311. Sun, W.; Sun, Q., Bioinspired manganese and iron complexes for enantioselective oxidation reactions: ligand design, catalytic activity, and beyond. *Acc. Chem. Res.* **2019,** *52* (8), 2370-2381.

312. Wu, X.; Seo, M. S.; Davis, K. M.; Lee, Y.-M.; Chen, J.; Cho, K.-B.; Pushkar, Y. N.; Nam, W., A highly reactive mononuclear non-heme manganese(IV)–Oxo complex that can activate the strong C–H bonds of alkanes. *J. Am. Chem. Soc.* **2011,** *133* (50), 20088-20091.

313. Aratani, Y.; Yamada, Y.; Fukuzumi, S., Selective hydroxylation of benzene derivatives and alkanes with hydrogen peroxide catalysed by a manganese complex incorporated into mesoporous silica–alumina. *Chem. Commun.* **2015,** *51* (22), 4662-4665.

Chapter 2

On the Ability of Nickel Complexes Derived from Tripodal Aminopyridine Ligands to Catalyze Arene Hydroxylations

Abstract

The development of catalysts for the selective hydroxylation of aromatic C–H bonds is an essential challenge in current chemical research. The accomplishment of this goal requires the discovery of powerful metal-based oxidizing species capable of hydroxylating inert aromatic bonds in a selective manner, avoiding the generation of non-selective oxygen-centered radicals. Herein we show an investigation on the ability of nickel(II) complexes supported by tripodal tetradentate aminopyridine ligands to catalyze the direct hydroxylation of benzene to phenol with H_2O_2 as oxidant. We have found that modifications on the ligand structure of the nickel complex do not translate into different reactivity, which differs from previous findings for nickel-based arene hydroxylations. Besides, several nickel(II) salts have been found to be effective in the oxidation of aromatic C–H bonds. The use of fluorinated alcohols as solvent has been found to result in an increase in phenol yield; however, showing no more than two turn-overs per nickel. These findings raise questions on the nature of the oxidizing species responsible for the arene hydroxylation reaction.

This chapter is based on:

Masferrer-Rius, E.; Hopman, R. M.; van der Kleij, J.; Lutz, M.; Klein Gebbink, R. J. M. *CHIMIA*, **2020**, *74*, 489-494

2.1 Introduction

Oxidations of organic compounds are essential reactions and have been intensively studied in academia as well as in the chemical industry.[1, 2] Interest is born from the fact that oxygenated organic molecules can further be used to produce different classes of chemicals. Nowadays, many improvements have been made in the development of different oxidation catalysts; however, the selective oxidation of organic substrates, such as aromatic compounds, still represents a critical challenge in modern chemical research.

Phenols are essential intermediates in the generation of a broad range of products, like pharmaceuticals and polymers.[3-6] Currently, the industrial production of phenol from benzene is carried out via the cumene process, which overall suffers from low efficiencies in product yield.[7] The direct introduction of a hydroxyl functionality through activation of an aromatic C–H bond is difficult because of the high stability of aromatic compounds and the high bond dissociation energy of an aromatic C–H bond (112 kcal mol^{-1}).[8] To overcome this challenge, the generation of highly reactive and selective metal-oxygen species is necessary. However, often phenol products are more easily to be oxidized than non-oxidized aromatic compounds, causing a chemoselectivity issue. Besides, a lack of discrimination between different oxidation sites results in a regioselectivity issue, especially when substituted benzenes are used in which the oxidation of benzylic C–H bonds is preferred over oxidation at the aromatic ring.

On the one hand, hydroxyl radicals, as well as hydroperoxyl radicals, are well known to oxidize aromatic compounds; however, poor selectivity is usually observed due to the non-discriminative reactivity of oxygen-centered radicals.[9, 10] On the other hand, metal-based oxidants are known to lead to more selective hydroxylation reactions.[11] Along this line, some progress has been made for the direct hydroxylation of benzene to phenol using H_2O_2 as the benign oxidant catalyzed by homogeneous catalysts (Figure 1), also providing some mechanistic insights.[12-19]

Over the last years, much interest has been devoted to the study of bioinspired iron complexes, which are minimalistic models of natural oxygenase enzymes.[20] These systems have been extensively studied for the oxidation of aliphatic C–H groups and epoxidation reactions with H_2O_2,[21] whereas hydroxylation of aromatic compounds has remained challenging since the last years. The main problem is that the phenol products bind irreversibly to the iron center, which prevents catalytic turnover.[22-24] For instance, several studies on the use of iron complexes supported by the tpa and bpmen aminopyridine ligands (tpa = tris(2-pyridylmethyl)amine) and bpmen = *N,N'*-dimethyl-*N,N'*-bis(2-picolyl)ethylenediamine) showed that these complexes were capable of oxidizing aromatic C–H bonds, but do not allow for catalytic turnover.[22-24]

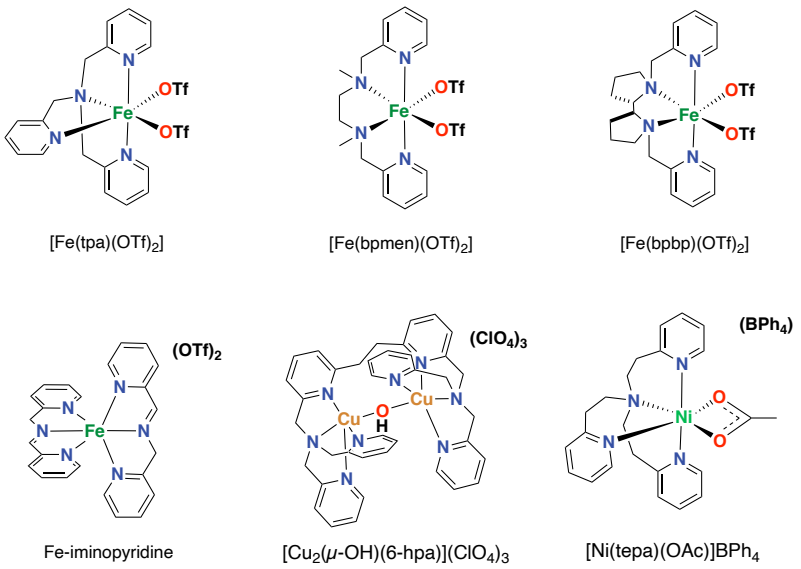

Figure 1. Examples of metal complexes previously used in catalytic arene hydroxylation reactions with H_2O_2.

Recently, a series of iron complexes supported by the bpbp type ligands (bpbp = *N*,*N*'-bis(2-pyridylmethyl)-2,2'-bipyrrolidine) were found to be active for the hydroxylation of aromatic substrates with H_2O_2, but with poor selectivities due to the generation of overoxidation products.[12-14] Non-heme imine-based iron complexes have also been investigated in the field of hydroxylation reactions.[25] For instance, an iminopyridine iron(II) complex prepared in situ by self-assembly of commercially starting materials was found to be active for the hydroxylation of aromatic rings using H_2O_2 as the oxidant, likely through a metal-based electrophilic aromatic substitution mechanism.[15]

Other first-row transition metals have also been shown to be capable of performing arene hydroxylation reactions with H_2O_2 as benign oxidant. Kodera and co-workers reported a dinuclear copper complex stabilized by the 6-hpa ligand (6-hpa = 1,2-bis{2-[bis(2-pyridylmethyl)aminomethyl]-6-pyridyl}ethane) for the selective hydroxylation of benzene to phenol with H_2O_2, showing high activity for phenol formation.[16] Another remarkable example is the selective hydroxylation of benzene catalyzed by a [Ni(tepa)(OAc)]BPh_4 (tepa = tris(2-pyridylethyl)amine) / H_2O_2 system, which was reported to work through a metal-based mechanism, affording a maximum of 749 turnover numbers in 216 h at 60 ºC for phenol production when using an 10000-fold excess of benzene with respect to the catalyst.[18] The authors found that among a series of nickel complexes supported by tripodal tetradentate aminopyridine ligands, the one supported by the tepa ligand is able to chemoselectively catalyze the hydroxylation of benzene and alkylbenzenes at high H_2O_2 loadings, without the formation of substantial amounts of over-oxidized products.[18] Remarkably though, when this complex was used in catalysis in 10 mol% loading with respect to the benzene substrate only 21% phenol

(2.1 turnovers per nickel) was formed in 5 h reaction time at 60 ºC. Based on the previous work from Itoh and co-workers, another recently reported study shows improved nickel-based catalysts for the selection oxidation of benzene to phenol through modifications of aminopyridine ligands by introduction of electron-rich pyridines, affording phenol with up to 820 turnover numbers in 5 h at 60 ºC using 0.05 mol% loading of catalyst.[19]

Many efforts have focused on the development of highly selective catalyst system for phenol formation. These studies parallel the development of catalysts for the selective hydroxylation of aliphatic C–H bonds to the corresponding alcohols, avoiding the generation of overoxidized ketone products. In an effort to get more selective catalysts, several of the latter studies have described the use of fluorinated alcohol solvents, *i.e.* 2,2,2-trifluoroethanol (TFE) or 1,1,1,3,3,3-hexafluoro-2-propanol (HFIP), in hydroxylation reactions; showing improved selectivities for the first-formed hydroxylation product and avoiding overoxidation reactions.[26-30]

Inspired by previous studies on arene hydroxylation catalyzed by nickel complexes,[18, 19] we studied the effect of different tripodal aminopyridine ligands for the direct hydroxylation of benzene to phenol with H_2O_2 by nickel under mild reaction conditions. Our findings show that the use of different tripodal tetradentate aminopyridine ligand designs in the nickel complexes does not lead to a different reactivity in arene hydroxylation reactions, showing that this type of ligands does not play an important role in catalysis. Besides, we show that the oxidation of benzene can be achieved using simple nickel salts with high chemoselectivity. The effect of solvents, such as fluorinated alcohols, is found to produce and enhance activity for phenol formation, highlighting the use of this kind of solvents on oxidation processes. On basis of these results, we discuss some mechanistic considerations for arene hydroxylations using molecular nickel complexes derived from aminopyridine ligands.

2.2 Results and Discussion

2.2.1 Aminopyridine Ligands and Nickel Complexes

For our study, we have investigated several nickel complexes supported by aminopyridine ligands as arene hydroxylation catalysts with H_2O_2 as the benign oxidant under mild reaction conditions (Figure 2). Our aim was to investigate if small modifications in the structure of the aminopyridine ligand would influence the reactivity of the complexes in arene hydroxylation reactions.

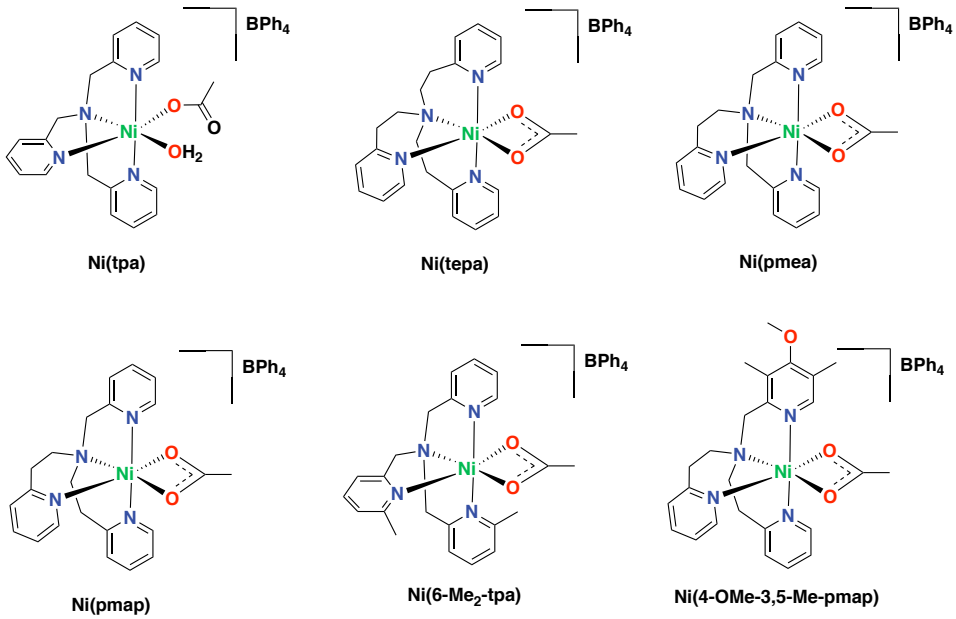

Figure 2. Nickel(II) complexes supported by tripodal tetradentate aminopyridine ligands employed in this Chapter.

Based on the work of Itoh and co-workers,[18] we focused on the use of tripodal tetradentate aminopyridine ligands, playing with the length of the arms. First, we synthesized the parent tpa ligand, containing three methylene arms, and the tepa ligand, which contains three ethylene arms. Of interest was also the pmea ligand (pmea = (2-(2-pyridylethyl))bis(2-pyridylmethyl)amine), and the pmap ligand (pmap = bis(2-(2-pyridylethyl))-2-pyridylmethylamine). Finally, we envisioned an enhancement on efficiency towards aromatic C–H oxidations by introducing electron-donating substituents into some of the pyridines, such as the 6-Me_2-tpa and 4-OMe-3,5-Me-pmap ligands (6-Me_2-tpa = bis(6-methyl-2-pyridylmethyl)(2-pyridylmethyl)amine, and 4-OMe-3,5-Me-pmap = bis(2-(2-pyridylethyl))-(4-methoxy-3,5-dimethyl)-2-pyridylmethylamine). The benefit of such electron-rich pyridine donors has been shown for several C–H and C=C oxidation reactions with non-heme iron and manganese complexes,[31-34] as well as for arene hydroxylation reactions with nickel complexes.[19]

The corresponding nickel complexes were synthesized by mixing the nickel acetate tetrahydrate and the different aminopyridine ligands; subsequent addition of sodium tetraphenylborate lead to precipitate of the final complex. Several of the complexes were analyzed by X-ray crystal structure, showing a mononuclear nickel(II) species exhibiting a distorted octahedral geometry. Details of the synthesis and characterization of the ligands and complexes can be found in the experimental section.

2.2.2 Screening of Complexes

Next, we have focused on the oxidation of benzene as model substrate to selectively screen for aromatic oxidation (Scheme 1). Catalytic experiments were carried out using 40 μmol of benzene, 40 μmol of triethylamine as a base, and 5.7 mmol of H_2O_2 (142 equiv.) in acetonitrile as solvent, with 10 mol% of catalyst; following the initial conditions described by Itoh.[18]

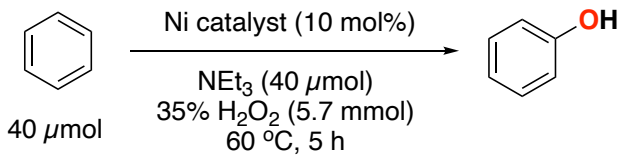

Scheme 1. Catalytic hydroxylation of benzene to phenol catalyzed by nickel(II) complexes with H_2O_2 under mild reaction conditions.

Reactions were run under air, at 60 °C, for 5 h using a closed reaction vessel. Crude mixtures were analyzed by GC, detecting mainly phenol as oxidized product, whereas formation of *para*-benzoquinone as an over-oxidized by-product was not observed. Thus, all complexes tested show chemoselectivity for phenol formation, as was reported previously for similar Ni/H_2O_2 systems.[18, 19] Furthermore, biphenyl was detected after analysis of the crude mixtures. The formation of biphenyl seems to originates from the tetraphenylborate counterion of the complex, since it is known that biphenyl can form through radical decomposition of tetraphenylborate.[35,36] Similar oxidation experiments without benzene substrate afford biphenyl as well, corroborating that benzene is not the source for biphenyl formation. Interestingly, acetamide was detected as the main product in the crude reaction mixtures. Acetamide may from through the oxidation of triethylamine, which can be oxidized in the presence of H_2O_2.[37, 38] However, the amounts of acetamide obtained were higher than the amount of triethylamine used, suggesting that the acetonitrile solvent is hydrated to acetamide under our experimental conditions.

Overall, these first catalytic experiments using acetonitrile as solvent provided poor phenol yields, ranging from 9.0 to 10.5 % (Table 1). These findings compare quite well with the initial experiments performed by Itoh and co-workers, for which they reported 2 turnover numbers for the oxidation of benzene catalyzed by **Ni(tepa)** under the same experimental conditions.[18] Not only do our results represent a single turn-over per nickel, the differences in phenol yields between the different complexes lie within the experimental error of our GC analysis. Accordingly, these results indicate no particular complex in the series of complexes tested catalyzes benzene hydroxylation more effectively than another complex. Our results might even indicate that the aminopyridine ligand plays no important role in performing the oxidation reaction. A control experiment without any complex as catalyst showed that no phenol product

formation occurs in the absence of a nickel complex. Thus, we can confidently conclude that a nickel complex is involved in the oxidation reaction.

Table 1. Direct hydroxylation of benzene to phenol employing Ni(II) complexes in acetonitrile.

Entry	Catalyst	Phenol Yield [%]
1	**Ni(tpa)**	9.6
2	**Ni(tepa)**	9.9
3	**Ni(pmea)**	9.7
4	**Ni(pmap)**	9.0
5	**Ni(6-Me$_2$-tpa)**	10.5
6	-	n.d.

n.d. = non-detected. [a]Reaction conditions: benzene (40 μmol), H_2O_2 (5.7 mmol), Ni complex (4 μmol), and NEt_3 (40 μmol) at 60 °C for 5 h in CH_3CN.

2.2.3 Different Reaction Solvents

Since the phenol yields were low, we decided to screen different solvents for the hydroxylation of benzene with the **Ni(tepa)** catalyst (Table 2). With acetonitrile, we could detect 4.7% phenol yield after 2.5 h, which increased to 9.9 % when the reaction was run for 5 h (Table 2, entries 1 and 2). Next, fluorinated alcohols were tested, which have been reported to be suitable solvents in different hydroxylation reactions.[26-30] TFE provided 7.6% phenol formation after 2.5 h, which slightly increase to 8% when the reaction was run for 5 h (Table 2, entries 3 and 4). Another fluorinated alcohol, HFIP, was also tested as solvent providing an enhanced activity, with 11.8 and 15.3% phenol yield after 2.5 and 5 h of reaction time, respectively. Methanol afforded poor phenol formation (3.8% yield), whereas acetone did not provide any phenol product (Table 2, entries 7 and 8); showing that these two solvents are not suitable to perform arene hydroxylation reactions with nickel complexes.

From these results, we concluded that the fluorinated alcohol HFIP is the best solvent to perform the oxidation of benzene to phenol catalyzed by the **Ni(tepa)** complex. Next, we tried higher amounts of H_2O_2, which did not afford an increase in phenol formation (Table 2, entry 9). We also envisioned an increase on catalytic activity by delivering the H_2O_2 slowly during the catalysis, as it has been shown for other C–H hydroxylation reactions using that oxidant.[39, 40] However, no improvement was observed, and phenol was formed in a much lower yield, highlighting that the disproportionation of H_2O_2 is not product-limiting, probably due to the high-excess conditions (Table 2, entry 10).

Table 2. Screening of solvents for the direct hydroxylation of benzene to phenol catalyzed by **Ni(tepa)**.[a]

Entry	Solvent	Reaction Time [h]	Phenol Yield [%]
1	CH_3CN	2.5	4.7
2	CH_3CN	5	9.9
3	TFE	2.5	7.6
4	TFE	5	8.0
5	HFIP	2.5	11.8
6	HFIP	5	15.3
7	CH_3OH	5	3.8
8	$(CH_3)_2CO$	5	n.d.
9[b]	HFIP	5	14.8
10[c]	HFIP	2.5	7.2

[a]Reaction conditions: benzene (40 μmol), H_2O_2 (5.7 mmol), Ni complex (4 μmol), and NEt_3 (40 μmol) at 60 °C. [b]500 equivalents of H_2O_2 were used. [c]H_2O_2 was added slowly within 1 h with the use of a syringe pump. n.d. = non-detected.

As it is shown in Table 3, we also screened all nickel complexes for catalysis in the HFIP solvent. Overall, we observed that for all complexes phenol yields increase when HFIP is used as the solvent compared to the use of acetonitrile, as was initially shown for the **Ni(tepa)** complex. While this observation highlights the use of a fluorinated alcohol solvent in arene hydroxylation catalysis by nickel(II) complexes, the overall yields still represent an average 1.5 turn-over number per nickel. In addition, no distinctive differences in catalytic efficiencies are observed between the different complexes. Even the nickel complexes **Ni(6-Me$_2$-tpa)** and **Ni(4-OMe-3,5-Me-pmap)** supported by electron-rich tripodal ligands did not afford substantial changes in reactivity (Table 3, entries 5 and 6). Control experiment with HFIP as solvent show us that reaction does not work without the presence of any catalyst (Table 3, entry 7). Even though a solvent screening did result in some increase in catalytic efficiency, small differences in product yields attainable with the current, yet limited, set of tripodal tetradentate aminopyridine ligands in our view does not allow for a rationalized ligand modification toward improve catalyst efficiency.

Interestingly, the simple salts nickel nitrate hexahydrate and nickel chloride hexahydrate lead to 6.7 and 3.0% phenol yield, respectively, using our current conditions (Table 3, entries 8 and 9). However, the hydroxylation reaction did not work when nickel acetate tetrahydrate was used (Table 3, entry 10). Remarkably, these results show that aromatic C–H oxidations can be done using some simple commercial nickel(II) salts with high chemoselectivity, albeit in low efficiencies.

Table 3. Direct hydroxylation of benzene to phenol employing Ni(II) complexes in HFIP.

Entry	Catalyst	Phenol Yield [%]
1	**Ni(tpa)**	14.9
2	**Ni(tepa)**	15.3
3	**Ni(pmea)**	14.6
4	**Ni(pmap)**	16.4
5	**Ni(6-Me$_2$-tpa)**	15.0
6	**Ni(4-OMe-3,5-Me-pmap)**	17.4
7	-	n.d.
8	$Ni(NO_3)_2 \cdot 6H_2O$	6.7
9	$NiCl_2 \cdot 6H_2O$	3.0
10	$Ni(CH_3CO_2)_2 \cdot 4H_2O$	n.d.

n.d. = non-detected. [a]Reaction conditions: benzene (40 μmol), H_2O_2 (5.7 mmol), Ni complex (4 μmol), and NEt_3 (40 μmol) at 60 °C for 5 h in HFIP.

2.2.4 Mechanistic Considerations

Finally, our efforts have been devoted to the understanding of the mechanism of the aromatic hydroxylation catalyzed by nickel complexes. In previous studies by Itoh and co-workers with the **Ni(tepa)** complex, it has been proposed that oxidation of benzene proceeds through a metal-based mechanism in which, after activation of H_2O_2, a dinickel(III) bis(μ-oxo) species is formed as the active oxidant (Scheme 2).[18] However, no direct evidence for the involvement of such species has been shown. A recent work by Mayilmurugan and co-workers on arene hydroxylations catalyzed by nickel complexes supported by similar tripodal tetradentate aminopyridine ligands, postulate the same dinuclear nickel species as the real oxidant responsible for the oxidation of the aromatic ring. Only recently, Itoh and co-workers have shown an example of a dinickel(III) bis(μ-oxo) species with the dpema ligand (dpema = *N*,*N*-di-[2-pyridine-2-yl]ethyl)methylamine) displaying oxygenation reactivity towards external hydrocarbon substrates, however, no reactivity of such species towards external aromatics was reported.[41]

Here, we considered the role of triethylamine as a base, and how this component could affect catalysis. In these oxidation reactions triethylamine is thought to activate H_2O_2 and facilitate its reaction with the mononuclear nickel complex. Aqueous H_2O_2 solutions are acidic (pK_a of H_2O_2 = 11.62);[42] therefore, the presence of a base in the catalytic reactions could help in the activation of H_2O_2 by deprotonating it. Indeed, we carried out some catalytic experiments using **Ni(tepa)** in acetonitrile without triethylamine, where we could observe a slight decrease in phenol

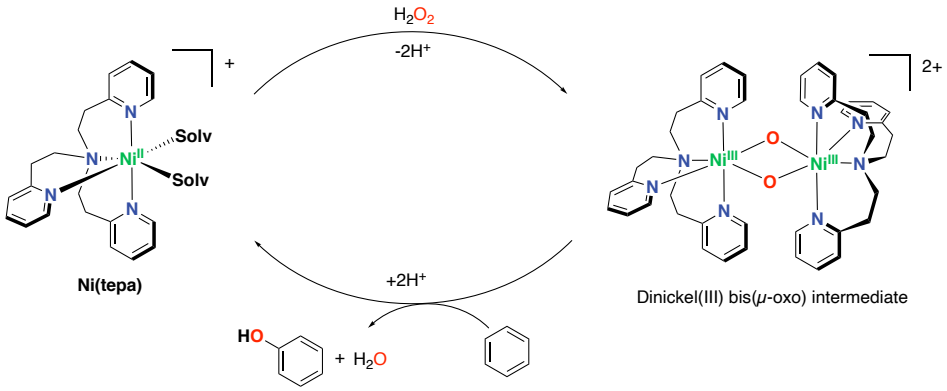

Scheme 2. Proposed catalytic mechanism for the direct hydroxylation of benzene to phenol with nickel(II) complexes based on previous studies.[18]

formation (6.9% yield) in comparison with experiments using the base (compare with Table 1, entry 2); indicating the positive role of the amine in activating the oxidant.

However, the fluorinated solvent HFIP is rather acidic (pK_a of HFIP = 9.3)[43] and could consequently affect the role of triethylamine (pK_a for the conjugate acid = 10.75)[44] in the deprotonation of H_2O_2. Carrying out a catalytic reaction with **Ni(pmea)** in HFIP and in the absence of triethylamine as a base gave a 15.4% phenol yield, which is similar to the yield obtained when triethylamine was employed (14.6%, see Table 3,). Thus, this observation made us conclude that triethylamine does not have an essential role in aromatic oxidations catalyzed by nickel complexes when HFIP is used as a solvent. Indeed, this fluorinated alcohol itself is known to activate H_2O_2, as has been showed in some selective oxidation reactions such as the epoxidation of alkenes.[45]

Overall, we believe that the reaction might proceed through a metal-based mechanism, since high chemoselectivity for the formation of phenol is observed. Generation of overoxidized products, such as hydroquinones or benzoquinones, easily occurs when oxygen-centered radicals are involved in catalysis. [46-49] However, such products have not been observed in the current and in previous studies using aminopyridine-based nickel complexes.

On the other hand, we believe that deactivation of the catalyst occurs during catalysis, which prevents efficient turnover numbers. To further investigate catalyst stability, we have studied the formation of phenol over time using the **Ni(tepa)** complex with H_2O_2, triethylamine and acetonitrile as the solvent, which showed that the phenol yield increases in the first few hours of reaction, to then come to a stop. Reaction analysis after 5 h provided us with 10% phenol yield, which remained the same for the next 24 h. Addition of an extra portion of catalyst and allowing the reaction to run for another 5 h resulted in an increase in phenol yield to 32%. Besides, attempts to obtain high turnover numbers by reproducing the same conditions described by Itoh and co-workers did not afford results that are consistent with the ones reported

in the literature.[18] Therefore, our results clearly differ from those reported by Itoh and co-workers, in which they describe up to 749 turnover numbers for phenol formation after 216 h of reaction time using the **Ni(tepa)** catalyst with H_2O_2, triethylamine and acetonitrile.[18]

2.3 Conclusions

We have presented a study on the effect of changes in the tripodal tetradentate aminopyridine ligand in nickel complexes used for the direct one-step hydroxylation of benzene to phenol in combination with H_2O_2 as benign oxidant under mild reaction conditions. Our results show that these modifications in the ligand structure do not translate into different activities in phenol formation, which differs from previous studies on nickel-based arene hydroxylations using similar tetradentate aminopyridine ligands.[18, 19] Remarkably, the oxidation of benzene could also be achieved using nickel(II) salts without the use of sophisticated ligand designs and using a fluorinated alcohol solvent, which seemed to improve phenol yields for the nickel complexes. The phenol yields obtained with the salts is significantly lower than with the complexes. The product selectivity obtained throughout our study, with no formation of catechols, hydroquinones or benzoquinones, points towards a metal-based mechanism, with no involvement of oxygen-centered radicals.

Our studies do corroborate the earlier findings of Itoh *et al*. concerning the catalytic performance of the nickel complexes at high catalyst loadings. Yet, attempts to reproduce the high-turnover numbers achieved at low catalyst loadings were not successful. Together with the findings that catalytic performance is rather insensitive towards ligand structure variation and that simple nickel salts also are able to form phenol, the molecular nature of the catalyst involved in benzene hydroxylation by the nickel complexes can be questioned. Other than the involvement of a dinickel(III) bis(μ-oxo) species proposed earlier,[18, 19] we believe that some kind of decomposition of the nickel complexes occurs under the experimental conditions, possibly leading to the formation of nickel-based nanoparticles that are involved in catalysis. Our future efforts will therefore be focused on identifying the actual nature of the hydroxylation catalyst and on the development of more active and stable catalyst systems based on nickel that allow for the high-turnover direct hydroxylation of benzene to phenol.

2.4 Experimental Section

2.4.1 General Remarks

Air- and moisture-sensitive reactions were performed under an inert nitrogen atmosphere using standard Schlenk line and glovebox techniques. All catalytic oxidation reactions were run under air with no precautions taken to exclude moisture. The solvents diethyl ether and acetonitrile were purified using

an MBraun MB SPS-800 solvent purification system. Tetrahydrofuran and methanol were dried with sodium and magnesium turnings, respectively, and distilled under nitrogen prior to use.

All other reagents and reaction products were obtained commercially from Across, Aldrich, Scharlab or Fluorochem, and used without further purification. Column chromatography was performed using Merck silica gel (60-200 mesh). ^{1}H and ^{13}C NMR spectra were recorded with a 400 MHz Varian spectrometer at 25 °C, chemical shifts (δ) are given in ppm referenced to the residual solvent peak. IR spectra were recorded with a Perkin-Elmer Spectrum One FTIR spectrometer. ESI-MS measurements were recorded with a Walters LCT Premier XE KE317 machine. GC analyses were performed on a Perkin-Elmer Clarus 500 Gas Chromatograph equipped with a PE Elite-5 column ((30m x 0.23 mm x 0.25 μm), (50% phenyl)-(50% methyl)polysiloxane) and a flame-ionization detector. X-ray diffraction analysis was carried out on a Bruker Kappa ApexII diffractometer.

CCDC 1998049-1998051 contain the supplementary crystallographic data for this chapter. These data can be obtained free of charge from The Cambridge Crystallographic Data Centre via www.ccdc.cam.ac.uk/structures.

Appendix A contains the supplementary information of this Chapter, which includes ^{1}H-NMR spectra for each ligand employed.

2.4.2 Synthesis of Ligands and Nickel Complexes

2.4.2.1 Synthesis of Pyridine Synthons

***N,N*-bis(2-(2-pyridyl)ethyl)hydroxylamine:** The compound was synthesized following a similar procedure as described in the literature.[50, 51] To a stirring suspension of hydroxylamine hydrochloride (1.02 g, 14.7 mmol) in DMF (2 mL) was added 2-vinylpyridine (3.2 mL, 3.1 g, 29.7 mmol) dropwise. The resulting clear yellow solution was left to stir for 1 day. The resulting reaction mixture was basified with saturated aqueous $NaHCO_3$, after which the organics were extracted using CH_2Cl_2 (3 x 10 mL). Organics were combined and dried over $MgSO_4$, after which the drying agent was filtered off and solvents were removed under reduced pressure. The desired product was obtained as a white solid in 48% yield (1.7 g, 7.1 mmol). ^{1}H NMR (400 MHz, $CDCl_3$) δ 8.47 (dt, 2 H), 7.54 (td, 2H), 7.12 (d, 2H), 7.08 (t, 2H), 3.09 (s, 8H).

***N,N*-bis(2-(2-pyridyl)ethylamine:** The compound was synthesized following a similar procedure as described in the literature.[50, 51] Zn-powder (2.17 g, 33.2 mmol) was added to a stirring solution of *N,N*-bis(2-(2-pyridyl)ethyl)hydroxylamine (1.72 g, 7.1 mmol) in 2N aqueous HCl (15 mL). The reaction mixture was heated to 85 °C for 22 hours. After the mixture was cooled down to rt, the pH was adjusted to 10 using an aqueous 4M K_2CO_3 solution. The resulting mixture was extracted with CH_2Cl_2 (3 x 30 mL), the organics were combined, dried over $MgSO_4$ and the drying agent was filtered off. The solvents were evaporated under reduced pressure, resulting in a yellow oil in 98% yield (1.58 g, 7.0 mmol). ^{1}H NMR (400 MHz, $CDCl_3$) δ 8.41 (d, 2H), 7.48 (td, 2H), 7.06 (d, 2H], 7.01 (td, 2H), 2.98 (t, 4H), 2.90 (t, 4H), 2.03 (s, 1H).

2.4.2.2 Synthesis of Tripodal Tetradentate Aminopyridine Ligands

Tris(2-pyridyl)methylamine (tpa) The ligand was synthesized following the same procedure as described by Wang and co-workers.[52] The desired ligand was obtained as a yellowish solid (52% yield). Spectral properties of the product agree with the literature data. ^{1}H NMR (400 MHz, CD_3CN): δ 8.47 (d, 3 H), 7.70 (t, 3 H), 7.59 (d, 3 H), 7.18 (t, 3 H), 3.81 (s, 6 H).

Tris[2-(pyridin-2-yl)ethyl]amine (tepa). The ligand was synthesized following a similar procedure as described by Réglier and co-workers.[53] 2-vinylpyridine was purified using a plug of silica before using it. A mixture of (2-pyridyl)ethylamine (0.37 g, 3 mmol) and 2-vinylpyridine (0.95 g, 9 mmol), with acetic acid (0.19 g, 3,2 mmol) in 5 mL of methanol was refluxed for 42 h. After that time, the resulting red-brown mixture was cooled and stirred with 30 mL of 15% NaOH and then extracted with CH_2Cl_2 (4 x 10 mL) to remove the product from the aqueous phase. The organic phase was dried over $MgSO_4$ and filtered through a coarse frit. The solvent was removed by rotary evaporation, leaving a brown oil that was chromatographed on alumina neutral using a 99/1 (v/v) mixture of ethyl acetate/methanol as eluent. The purified product was obtained as a slightly viscous yellow oil (50% yield). ^{1}H NMR (400 MHz, CD_3CN): δ 8.46 (d, 3 H), 7.56 (t, 3 H), 7.12 (t, 2 H), 7.07 (d, 6 H), 2.91 (m, 6 H), 2.82 (m, 6 H). ^{13}C NMR (CD_3CN): δ 161.93, 150.03, 137.00, 124.25, 121.98, 54.54, 36.64. HRMS (FAB$^+$): *m/z* 333.1995 $[M + H]^+$, calcd for $C_{21}H_{24}N_4H$ 333.2079.

(2-(2-pyridylethyl))bis(2-pyridylmethyl)amine (pmea). The ligand was synthesized following a modified procedure described by Colbran and co-workers.[54] 2-vinylpyridine was purified passing through a plug of silica before using it. 2-vinylpyridine (3.56 g, 33.75 mmol), bis(2-pyridylmethyl)amine (2.24 g, 11.25 mmol) and acetic acid (0.72 g, 12.05 mmol) in H_2O / CH_3OH (10 mL / 2.5 mL) were heated at reflux for 45 h. 20% aqueous NaOH solution (2 mL) was added to the clear dark red solution causing two layers to separate. The mixture was extracted with CH_3Cl (3 x 20 mL), the extracts dried over $MgSO_4$, filtered, and the chloroform removed under rotary evaporation. The obtained brown-orange oil was purified using column chromatography with basic alumina using CH_2Cl_2 as eluent and CH_3OH in 1-20%. The pure pmea ligand was obtained as an orange oil (1.8 g, 53% yield). ^{1}H NMR (400 MHz, $CDCl_3$): δ 8.51 (d, 2H), 8.48 (d, 1H), 7.60-7.53 (m, 3H), 7.35 (d, 2H), 7.13-7.08 (m, 4H), 3.89 (s, 4H), 3.07-2.97 (m, 4H). ^{13}C NMR (100 MHz, $CDCl_3$): δ 160.65, 159.89, 149.26, 149.05, 136.48, 136.27, 123.52, 122.93, 122.01, 121.21, 60.39, 54.59, 36.14. ATR-IR: ν [cm^{-1}]: 3052, 3008, 2928, 2818, 1588, 1568, 1473, 1432, 1362, 1148, 1123, 1048, 994, 756, 615. HRMS (FAB$^+$): *m/z* 305.1700 $[M + H]^+$, calcd for $C_{19}H_{20}N_4$ 305.1766.

Bis(2-(2-pyridylethyl))-2-pyridylmethylamine (pmap). The ligand was synthesized following a modified procedure described by Colbran and co-workers.[54] *N,N*-bis(2-(2-pyridyl)ethylamine (0.27 g, 1.5 mmol) was combined with sodium triacetoxyborohydride (0.38 g, 1.8 mmol), 2-pyridinecarbaldehyde (0.14 mL, 1.5 mmol) and 1,2-dichloroethane (6.6 mL). Under N_2-atmosphere, the reaction was stirred for 36 hours affording a yellow liquid, which over the course of a day turned green. The green solution was washed with a saturated aqueous $NaHCO_3$ solution (2 times). The organic phase was dried over $MgSO_4$, filtered, and extracted with CH_2Cl_2, which was then removed under reduced pressure affording a green/orange oil. The obtained oil was purified using column chromatography with neutral alumina using CH_2Cl_2/CH_3OH (99/1). The pure pmap ligand was obtained as a brown/orange oil (0.13 g, 28% yield). ^{1}H NMR (400 MHz, $CDCl_3$): δ 8.49 (d, 3 H), 7.55-7.47 (m, 3 H), 7.13-7.04 (m, 6 H), 3.88 (s, 2 H), 3.01-2.96 (m, 8 H). ATR-IR: ν [cm^{-1}]: 2929, 1589, 1432, 1120. HRMS (FAB$^+$): *m/z* 319.192; $[M + H]^+$, calcd for $C_{20}H_{22}N_4$ 319.189.

Bis(6-methyl-2-pyridylmethyl)(2-pyridylmethyl)amine (6-Me$_2$-tpa) The ligand was synthesized following the same procedure as described by Schindler and co-workers.[55] The desired ligand was obtained as a light-yellow solid (2.8 g, 88%). Spectral properties of the product agree with the literature data. ^{1}H NMR (400 MHz, $CDCl_3$): δ 8.50 (d, 1H,), 7.64-7.57 (m, 2H), 7.52 (t, 2H), 7.40 (d, 2H), 7.11 (t, 1H), 6.96 (d, 2H), 3.87 (s, 2H), 3.84 (s, 4H), 2.50 (s, 6H). ^{13}C NMR (100 MHz, $CDCl_3$): δ 159.78, 159.03, 157.70, 149.10, 136.73, 136.47, 122.92, 121.99, 121.51, 119.67, 60.42, 60.24, 24.50. ATR-IR:

v [cm^{-1}]: 3069, 3006, 2932, 2817, 1589, 1575, 1463, 1434, 1446, 1368, 1233, 1161, 1120, 1088, 982, 799, 793, 766, 758.

Bis(2-(2-pyridylethyl))-(4-methoxy-3,5-dimethyl)-2-pyridylmethylamine (4-OMe-3,5-Me-pmap). A solution of 2-chloromethyl-4-methoxy-3,5-dimethylpyridine hydrochloride (1 g, 4.5 mmols) in deionized water (5 mL) was cooled to 0 ºC in an ice bath. To this solution was added, with stirring, NaOH (180 mg, 4.5 mmols). To this mixture was then added a solution of *N*,*N*-bis(2-(2-pyridyl)ethylamine (1 g, 4.5 mmols) in CH_2Cl_2 (5 mL). The mixture was then allowed to warm to rt and stirred for 2 days. The crude mixture was then extracted with CH_2Cl_2, and the organic phase was dried with $MgSO_4$, filtered, and dried under reduced pressure. The resulting oil was purified by column chromatography on silica (CH_2Cl_2:CH_3OH:NEt_3 in 9:1:0.1 was used as eluent) to yield a brownish solid. (0.89 g, 54 %). ^{1}H NMR (400 MHz, $CDCl_3$): δ 8.41 (d, 2 H), 8.10 (s, 1 H), 7.47 (t, 2 H), 7.03-6.98 (m, 4 H), 3.78 (s, 2 H), 3.65 (s, 3 H), 2.97-2.90 (m, 8 H), 2.18 (s, 3 H), 1.99 (s, 3 H). ^{13}C NMR (100 MHz, $CDCl_3$): δ 164.03, 160.78, 157.16, 149.05, 149.04, 148.19, 148.16, 136.18, 136.13, 126.52, 125.13, 123.29, 120.99, 59.86, 53.70, 45.92, 35.33, 13.31, 13.27, 10.60, 10.58, 9.17, 9.14.

2.4.2.3 Synthesis of Nickel Complexes

Ni(tpa): The complex was synthesized following a reported procedure described by Itoh and co-workers.[56] The desired complex was obtained as purple crystals in 25% yield. Spectral properties of the product agree with the literature data. ATR-IR: v [cm^{-1}]: 1604.58, 1557.75, 1416.87 (COO^-), 730.89, 705.23 (BPh_4^-). HRMS (FAB^+): *m/z* 407.1003 [M-BPh_4-H_2O]$^+$, calcd for $C_{20}H_{21}N_4NiO_2$ 407.1018.

Ni(tepa): The complex was synthesized following a reported procedure described Itoh and co-workers.[57] The desired complex was obtained as a pale blue precipitate in 83% yield. Spectral properties of the product agree with the literature data. ATR-IR: v [cm^{-1}]: 1536, 1456 (OAc^-), 733, 707 (BPh_4^-). HRMS (FAB^+): *m/z* 449.1340 [M – BPh_4]$^+$, calcd for $C_{23}H_{27}N_4NiO_2$ 449.1487.

Ni(pmea): The complex was synthesized following a modified procedure described by Itoh and co-workers.[57] A solution of $Ni^{II}(OAc)_2$ $4H_2O$ (62.3 mg, 0.25 mmol) in 5 mL of methanol was added to a solution of the pmea (76.1 mg, 0.25 mmol) ligand in 5 mL methanol. The solution was stirred for 2 h at room temperature. $NaBPh_4$ (86.2 mg, 0.25 mmol) was added to the solution. The mixture was stirred for 1 h at room temperature. The purple precipitate was collected, washed with methanol, and dried (129.5 mg, 70%). Single crystals were obtained by crystallization by liquid-liquid diffusion using CH_2Cl_2 and cyclohexane. ATR-IR: v [cm^{-1}]: 3055, 3035, 2982, 1605, 1533, 1479, 1442, 1423, 1305, 1266, 1025, 766, 730, 703, 677, 612. HRMS (FAB^+): *m/z* 421.1046 [M – BPh_4]$^+$, calcd for $C_{21}H_{23}N_4NiO_2$ 421.1175.

Ni(pmap): The complex was synthesized following a modified procedure described by Itoh and co-workers.[57] A solution of $Ni^{II}(OAc)_2$ $4H_2O$ (0.1047 g, 0.42 mmol) in 5 mL methanol was added to a solution of pmap (0.13 g, 0.42 mmol) ligand in 5 mL methanol. The solution was stirred for 2 h at rt. $NaBPh_4$ (0.144 g, 0.42 mmol) was added to the solution. The mixture was stirred for 1 h at room temperature. The purple precipitate was collected, washed with methanol, and dried (120.2 mg, 64%). Single crystals were obtained by crystallization by liquid-liquid diffusion using CH_2Cl_2 and cyclohexane. ATR-IR: v [cm^{-1}]: 3571, 3054, 1880, 1606, 1540, 1444, 733, 707. HRMS (FAB^+): *m/z* 435.1158 [M – BPh_4]$^+$, calcd for $C_{22}H_{25}N_4NiO_2$ 435.1331.

Ni(6-Me_2-tpa): The complex was synthesized following a modified procedure described by Itoh and co-workers.[57]A solution of $Ni^{II}(OAc)_2$ $4H_2O$ (62.3 mg, 0.25 mmol) in 5 mL methanol was added to a solution of 6-Me_2-tpa (79.3 mg, 0.25 mmol) ligand in 5 mL methanol. The solution was stirred for 2 h

at rt. $NaBPh_4$ (86.2 mg, 0.25 mmol) was added to the solution. The mixture was stirred for 1 h at room temperature. The violet precipitate was collected, washed with methanol, and dried (120.2 mg, 64%). Single crystals were obtained by crystallization by liquid-liquid diffusion using CH_2Cl_2 and cyclohexane. ATR-IR: ν [cm^{-1}]: 3056, 3032, 3002, 1606, 1579, 1542, 1478, 1467, 1448, 1426, 1165, 1099, 788, 765, 742, 707, 675, 607. HRMS (FAB^+): m/z 435.1204 $[M - BPh_4]^+$, calcd for $C_{22}H_{24}N_4NiO_2$ 435.1331.

Ni(4-OMe-3,5-Me-pmap): The complex was synthesized following a modified procedure described by Itoh and co-workers.[57] A methanol solution (5 mL) of $Ni^{II}(OAc)_2\ 4H_2O$ (62.3 mg, 0.25 mmol) was added to a methanol solution (5 mL) of the corresponding ligand (94.13 mg, 0.25 mmol) with stirring at room temperature. Color of the solution turned to violet. After stirring for 2 h, $NaBPh_4$ (86 mg, 0.25 mmol) was added to the mixture to give a purple precipitate, which was collected by filtration, washed with methanol, and dried (120.3 mg, 54.4 %). ATR-IR: ν [cm^{-1}]: 3055, 3040, 2998, 2981, 2920, 2870, 1578, 1570, 1606, 1538, 1478, 1455, 1445, 1402, 1385, 1361, 771, 749, 733, 703.

2.4.3 X-Ray Crystal Structure Determination of Ni Complexes

2.4.3.1 X-Ray Crystal Structure Determination of Ni(pmea)

$[C_{21}H_{23}N_4NiO_2](C_{24}H_{20}B)$, Fw = 741.35, purple plate, 0.51 × 0.30 × 0.05 mm^3, monoclinic, $P2_1/n$ (no. 14), a = 13.4449(6), b = 15.3074(10), c = 18.2233(9) Å, β = 90.482(3) °, V = 3750.3(3) $Å^3$, Z = 4, D_x = 1.313 g/cm^3, μ = 0.56 mm^{-1}. The diffraction experiment was performed on a Bruker Kappa ApexII diffractometer with sealed tube and Triumph monochromator (λ = 0.71073 Å) at a temperature of 150(2) K up to a resolution of $(\sin\theta/\lambda)_{max}$ = 0.65 $Å^{-1}$. The Eval15 software[58] was used for the intensity integration. A large anisotropic mosaicity[59] about *hkl*=(1,0,1) was used for the prediction of the reflection profiles. A numerical absorption correction and scaling was performed with SADABS[60] (correction range 0.76-1.00). A total of 76642 reflections was measured, 8637 reflections were unique (R_{int} = 0.047), 6876 reflections were observed [I>2σ(I)]. The structure shown in Figure 3 was solved with Patterson superposition methods using SHELXT.[61]

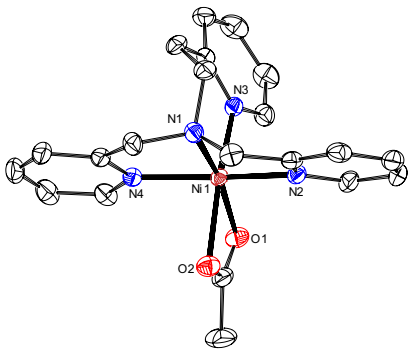

Figure 3. Displacement ellipsoid plot of the cation of **Ni(pmea)** (50% probability level). Hydrogen atoms and non-coordinated BPh_4 anion are omitted for clarity.

Structure refinement was performed with SHELXL-2016[62] on F^2 of all reflections. Non-hydrogen atoms were refined freely with anisotropic displacement parameters. Hydrogen atoms were introduced in calculated positions and refined with a riding model. 479 Parameters were refined with no restraints. R1/wR2 [I > 2σ(I)]: 0.0333 / 0.0825. R1/wR2 [all refl.]: 0.0492 / 0.0904. S = 1.041. Residual electron

density between -0.51 and 0.51 e/Å^3. Geometry calculations and checking for higher symmetry was performed with the PLATON program.[63]

2.4.3.2 X-Ray Crystal Structure Determination of Ni(pmap)

$[C_{22}H_{25}N_4NiO_2](C_{24}H_{20}B)$ + disordered solvent, Fw = 755.38[*], purple plate, 0.40 × 0.25 × 0.04 mm^3, triclinic, $P\bar{1}$ (no. 2), a = 11.1742(3), b = 12.4629(3), c = 15.8917(4) Å, α = 74.394(1), β = 88.801(1), γ = 71.060(1) °, V = 2010.78(8) Å^3, Z = 2, D_x = 1.248 g/cm$^{3[*]}$, μ = 0.53 mm$^{-1[*]}$. The diffraction experiment was performed on a Bruker Kappa ApexII diffractometer with sealed tube and Triumph monochromator (λ = 0.71073 Å) at a temperature of 150(2) K up to a resolution of $(\sin\theta/\lambda)_{max}$ = 0.65 Å^{-1}. The Eval15 software[58] was used for the intensity integration. A multiscan absorption correction and scaling was performed with SADABS[60] (correction range 0.66-0.75). A total of 46938 reflections was measured, 9240 reflections were unique (R_{int} = 0.034), 7636 reflections were observed [I>2σ(I)]. The structure shown in Figure 4 was solved with Patterson superposition methods using SHELXT.[61] Structure refinement was performed with SHELXL-2016[62] on F^2 of all reflections. The crystal structure contains large voids (146 Å^3/unit cell) filled with severely disordered cyclohexane/CH_2Cl_2 molecules. Their contribution to the structure factors was secured by the SQUEEZE algorithm[64] resulting in 46 electrons / unit cell. The *pmap* ligand was refined with a disorder model involving two coordination modes (Figure S2). The major disorder form (82.0(3) % occupancy) was refined with anisotropic displacement parameters. The nitrogen atoms of the minor disorder component (18.0(3) % occupancy) were constrained to the major form. The carbon atoms of the minor disorder component were refined with isotropic displacement parameters. Hydrogen atoms were introduced in calculated positions and refined with a riding model. 581 Parameters were refined with 88 restraints (distances, angles and molecular flatness in modelling the disorder). R1/wR2 [I > 2σ(I)]: 0.0334 / 0.0788. R1/wR2 [all refl.]: 0.0451 / 0.0831. S = 1.027. Residual electron density between -0.32 and 0.37 e/Å^3. Geometry calculations and checking for higher symmetry was performed with the PLATON program.[63]

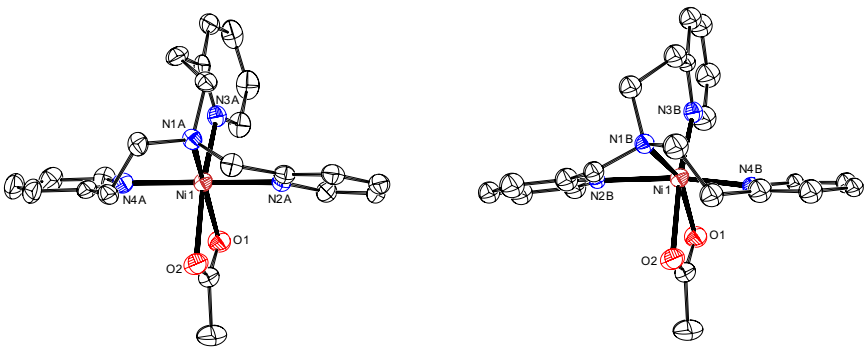

Figure 4. Displacement ellipsoid plot of the cation of **Ni(pmap)** (50% probability level). The major disorder form (82.0(3) % occupancy) is drawn on the left, the minor form (18.0(3) % occupancy) on the right. Carbon atoms of the minor disorder form were refined with isotropic displacement parameters. Hydrogen atoms,

[*] Derived values do not contain the contribution of the disordered solvent molecules.

non-coordinated BPh_4 anion and severely disordered cyclohexane/CH_2Cl_2 solvent molecules are omitted for clarity.

2.4.3.3 X-Ray Crystal Structure Determination of Ni(6-Me$_2$-tpa)

$[C_{22}H_{25}N_4NiO_2](C_{24}H_{20}B)$, Fw = 755.38, purple plate, 0.51 × 0.48 × 0.08 mm^3, monoclinic, $P2_1/n$ (no. 14), a = 18.4021(7), b = 10.0723(5), c = 21.3918(8) Å, β = 91.333(2) °, V = 3963.9(3) Å^3, Z = 4, D_x = 1.266 g/cm^3, μ = 0.53 mm^{-1}. The diffraction experiment was performed on a Bruker Kappa ApexII diffractometer with sealed tube and Triumph monochromator (λ = 0.71073 Å) at a temperature of 150(2) K up to a resolution of $(\sin \theta/\lambda)_{max}$ = 0.65 Å^{-1}. The Eval15 software[58] was used for the intensity integration. A numerical absorption correction and scaling was performed with SADABS[60] (correction range 0.82-0.97). A total of 87732 reflections was measured, 9094 reflections were unique (R_{int} = 0.047), 7865 reflections were observed [I>2σ(I)]. The structure shown in Figure 5 was solved with Patterson superposition methods using SHELXT.[61] Structure refinement was performed with SHELXL-2016[62] on F^2 of all reflections. Non-hydrogen atoms were refined freely with anisotropic displacement parameters. All hydrogen atoms were located in difference Fourier maps and refined with a riding model. 490 Parameters were refined with no restraints. R1/wR2 [I > 2σ(I)]: 0.0351 / 0.0938. R1/wR2 [all refl.]: 0.0419 / 0.0974. S = 1.028. Residual electron density between -0.31 and 0.81 e/Å^3. Geometry calculations and checking for higher symmetry was performed with the PLATON program.[63]

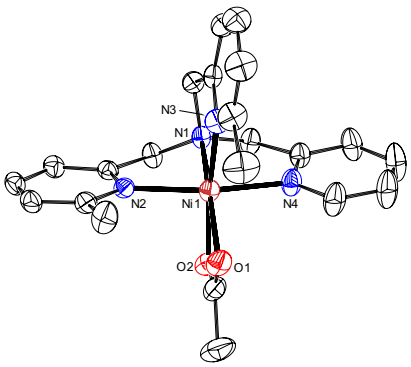

Figure 5. Displacement ellipsoid plot of the cation of **Ni(6-Me$_2$-tpa)** (50% probability level). Hydrogen atoms and non-coordinated BPh_4 anion are omitted for clarity.

2.4.4 Reaction Protocol for Catalytic Studies

2.4.4.1 General Procedure for Catalytic Hydroxylation Reaction.

In a pressurized reaction vessel, the nickel complex (4 μmol, 10 mol%) was dissolved in 1 mL of the corresponding solvent. Then, triethylamine (0.2 mL of stock solution 0.2 M, 40 μmol) and benzene (0.4 mL of stock solution 0.1 M, 40 μmol) were added. Aqueous commercial solution of hydrogen peroxide (0.5 mL of 35% aqueous H_2O_2, 5.7 mmol) was added directly under constant stirring, which was stirred for 5 h at 60 °C. After the catalytic reaction, the crude mixture was cooled to rt using an ice bath and nitrobenzene was added as internal standard (20 μmols). Then, the nickel catalyst was removed by column chromatography on silica, and then magnesium sulfate was added to remove the water from the solution. The reaction mixture was analyzed by GC analysis. Reported analysis data represent the outcome of at least two independent catalysis experiments. All peaks of interest were identified by comparison of the retention times and co-injection with the authentic samples. The products were

quantified by comparison against a known amount of internal standard using a calibration curve consisting of a plot of mole ratio (moles of organic compound/moles of internal standard) versus area ratio (area of organic compound/area of internal standard).

Author Contribution

E.M-R. and R.K.G devised the project and designed experiments. E.M-R. performed the experiments. R.M.H. and J.K. performed the synthesis of some aminopyridine ligands and nickel complexes. M.L. performed X-ray analysis. E.M-R. wrote the Chapter and R.K.G. provided comments on the experiments and Chapter content.

2.5 References

1. Arakawa, H.; Aresta, M.; Armor, J. N.; Barteau, M. A.; Beckman, E. J.; Bell, A. T.; Bercaw, J. E.; Creutz, C.; Dinjus, E.; Dixon, D. A.; Domen, K.; DuBois, D. L.; Eckert, J.; Fujita, E.; Gibson, D. H.; Goddard, W. A.; Goodman, D. W.; Keller, J.; Kubas, G. J.; Kung, H. H.; Lyons, J. E.; Manzer, L. E.; Marks, T. J.; Morokuma, K.; Nicholas, K. M.; Periana, R.; Que, L.; Rostrup-Nielson, J.; Sachtler, W. M. H.; Schmidt, L. D.; Sen, A.; Somorjai, G. A.; Stair, P. C.; Stults, B. R.; Tumas, W., Catalysis Research of Relevance to Carbon Management: Progress, Challenges, and Opportunities. *Chem. Rev.* **2001,** *101* (4), 953-996.

2. Punniyamurthy, T.; Velusamy, S.; Iqbal, J., Recent Advances in Transition Metal Catalyzed Oxidation of Organic Substrates with Molecular Oxygen. *Chem. Rev.* **2005,** *105* (6), 2329-2363.

3. Weber, M.; Weber, M.; Kleine-Boymann, M., In *Ullmann's Encyclopedia of Industrial Chemistry*, Wiley-VCH: Weinheim, Germany, 2004; pp 503-519.

4. Fukuzumi, S.; Ohkubo, K., One-Step Selective Hydroxylation of Benzene to Phenol. *Asian J. Org. Chem.* **2015,** *4* (9), 836-845.

5. Genovino, J.; Sames, D.; Hamann, L. G.; Touré, B. B., Accessing Drug Metabolites via Transition-Metal Catalyzed C–H Oxidation: The Liver as Synthetic Inspiration. *Angew. Chem. Int. Ed.* **2016,** *55* (46), 14218-14238.

6. Sheldon, R. A.; Kochi, J. K., In *Metal-Catalyzed Oxidations of Organic Compounds*, Academic Press, New York, 1981; pp 315-339.

7. Schmidt, R. J., Industrial catalytic processes–phenol production. *Appl. Catal. A.* **2005,** *280* (1), 89-103.

8. Luo, Y.-R., *Comprehensive Handbook of Chemical Bond Energies*. CRC Press: Boca Raton, FL, 2007.

9. Yuan, C.; Liang, Y.; Hernandez, T.; Berriochoa, A.; Houk, K. N.; Siegel, D., Metal-free oxidation of aromatic carbon–hydrogen bonds through a reverse-rebound mechanism. *Nature* **2013,** *499* (7457), 192-196.

10. Hage, J. P.; Llobet, A.; Sawyer, D. T., Aromatic hydroxylation by fenton reagents {Reactive intermediate [L_x^+ $Fe^{III}OOH$ (BH^+)], not free hydroxyl radical (HO•)}. *Bioorganic Med. Chem.* **1995,** *3* (10), 1383-1388.

11. Costas, M.; Chen, K.; Que Jr, L., Biomimetic nonheme iron catalysts for alkane hydroxylation. *Coord. Chem. Rev.* **2000,** *200*, 517-544.

12. Lyakin, O. Y.; Zima, A. M.; Tkachenko, N. V.; Bryliakov, K. P.; Talsi, E. P., Direct Evaluation of the Reactivity of Nonheme Iron(V)–Oxo Intermediates toward Arenes. *ACS Catal*. **2018,** *8* (6), 5255-5260.

13. Tkachenko, N. V.; Ottenbacher, R. V.; Lyakin, O. Y.; Zima, A. M.; Samsonenko, D. G.; Talsi, E. P.; Bryliakov, K. P., Highly Efficient Aromatic C–H Oxidation with H_2O_2 in the Presence of Iron Complexes of the PDP Family. *ChemCatChem* **2018,** *10* (18), 4052-4057.

14. Zima, A. M.; Lyakin, O. Y.; Lubov, D. P.; Bryliakov, K. P.; Talsi, E. P., Aromatic C–H oxidation by non-heme iron(V)-oxo intermediates bearing aminopyridine ligands. *Mol. Catal*. **2020,** *483*, 110708.

15. Capocasa, G.; Olivo, G.; Barbieri, A.; Lanzalunga, O.; Di Stefano, S., Direct hydroxylation of benzene and aromatics with H_2O_2 catalyzed by a self-assembled iron complex: evidence for a metal-based mechanism. *Catal. Sci. Technol*. **2017,** *7* (23), 5677-5686.

16. Tsuji, T.; Zaoputra, A. A.; Hitomi, Y.; Mieda, K.; Ogura, T.; Shiota, Y.; Yoshizawa, K.; Sato, H.; Kodera, M., Specific Enhancement of Catalytic Activity by a Dicopper Core: Selective Hydroxylation of Benzene to Phenol with Hydrogen Peroxide. *Angew. Chem. Int. Ed*. **2017,** *129* (27), 7887-7890.

17. Muthuramalingam, S.; Anandababu, K.; Velusamy, M.; Mayilmurugan, R., Benzene Hydroxylation by Bioinspired Copper(II) Complexes: Coordination Geometry versus Reactivity. *Inorg. Chem*. **2020,** *59* (9), 5918-5928.

18. Morimoto, Y.; Bunno, S.; Fujieda, N.; Sugimoto, H.; Itoh, S., Direct hydroxylation of benzene to phenol using hydrogen peroxide catalyzed by nickel complexes supported by pyridylalkylamine ligands. *J. Am. Chem. Soc*. **2015,** *137* (18), 5867-5870.

19. Muthuramalingam, S.; Anandababu, K.; Velusamy, M.; Mayilmurugan, R., One step phenol synthesis from benzene catalysed by nickel(II) complexes. *Catal. Sci. Technol*. **2019,** *9* (21), 5991-6001.

20. Que Jr, L.; Tolman, W. B., Biologically inspired oxidation catalysis. *Nature* **2008,** *455* (7211), 333.

21. Olivo, G.; Cussó, O.; Costas, M., Biologically Inspired C–H and C=C Oxidations with Hydrogen Peroxide Catalyzed by Iron Coordination Complexes. *Chem. Asian J*. **2016,** *11* (22), 3148-3158.

22. Oh, N. Y.; Seo, M. S.; Lim, M. H.; Consugar, M. B.; Park, M. J.; Rohde, J.-U.; Han, J.; Kim, K. M.; Kim, J.; Que Jr, L., Self-hydroxylation of perbenzoic acids at a nonheme iron(II) center. *Chem. Commun*. **2005,** (45), 5644-5646.

23. Taktak, S.; Flook, M.; Foxman, B. M.; Que Jr, L.; Rybak-Akimova, E. V., *ortho*-Hydroxylation of benzoic acids with hydrogen peroxide at a non-heme iron center. *Chem. Commun*. **2005,** (42), 5301-5303.

24. Makhlynets, O. V.; Rybak-Akimova, E. V., Aromatic Hydroxylation at a Non-Heme Iron Center: Observed Intermediates and Insights into the Nature of the Active Species. *Chem. Eur. J*. **2010,** *16* (47), 13995-14006.

25. Olivo, G.; Lanzalunga, O.; Di Stefano, S., Non-Heme Imine-Based Iron Complexes as Catalysts for Oxidative Processes. *Adv. Synth. Catal*. **2016,** *358* (6), 843-863.

26. Dantignana, V.; Milan, M.; Cussó, O.; Company, A.; Bietti, M.; Costas, M., Chemoselective Aliphatic C–H Bond Oxidation Enabled by Polarity Reversal. *ACS Cent. Sci*. **2017,** *3* (12), 1350-1358.

27. Ottenbacher, R. V.; Talsi, E. P.; Rybalova, T. V.; Bryliakov, K. P., Enantioselective Benzylic Hydroxylation of Arylalkanes with H_2O_2 in Fluorinated Alcohols in the Presence of Chiral Mn Aminopyridine Complexes. *ChemCatChem* **2018,** *10* (22), 5323-5330.

28. Wang, D.; Shuler, W. G.; Pierce, C. J.; Hilinski, M. K., An iminium salt organocatalyst for selective aliphatic C–H hydroxylation. *Org. Lett.* **2016,** *18* (15), 3826-3829.

29. Gaster, E.; Kozuch, S.; Pappo, D., Selective Aerobic Oxidation of Methylarenes to Benzaldehydes Catalyzed by N-Hydroxyphthalimide and Cobalt(II) Acetate in Hexafluoropropan-2-ol. *Angew. Chem. Int. Ed.* **2017,** *56* (21), 5912-5915.

30. Adams, A. M.; Du Bois, J., Organocatalytic C–H hydroxylation with Oxone® enabled by an aqueous fluoroalcohol solvent system. *Chem. Sci.* **2014,** *5* (2), 656-659.

31. Cussó, O.; Garcia-Bosch, I.; Ribas, X.; Lloret-Fillol, J.; Costas, M., Asymmetric epoxidation with H_2O_2 by manipulating the electronic properties of non-heme iron catalysts. *J. Am. Chem. Soc.* **2013,** *135* (39), 14871-14878.

32. Cussó, O.; Cianfanelli, M.; Ribas, X.; Klein Gebbink, R. J. M.; Costas, M., Iron catalyzed highly enantioselective epoxidation of cyclic aliphatic enones with aqueous H_2O_2. *J. Am. Chem. Soc.* **2016,** *138* (8), 2732-2738.

33. Cussó, O.; Garcia-Bosch, I.; Font, D.; Ribas, X.; Lloret-Fillol, J.; Costas, M., Highly stereoselective epoxidation with H_2O_2 catalyzed by electron-rich aminopyridine manganese catalysts. *Org. Lett.* **2013,** *15* (24), 6158-6161.

34. Milan, M.; Carboni, G.; Salamone, M.; Costas, M.; Bietti, M., Tuning Selectivity in Aliphatic C–H Bond Oxidation of N-Alkylamides and Phthalimides Catalyzed by Manganese Complexes. *ACS Catal.* **2017,** *7* (9), 5903-5911.

35. Mlondo, S. N.; O'Brien, P.; Thomas, P. J.; Helliwell, M.; Raftery, J.; Procter, D. J., Methanolysis of tetraphenylborate (BPh_4) as a reaction unit in halotris (2,4-pentadianato) complexes of Zr(IV) and Hf (IV). *Chem. Commun.* **2008,** (21), 2456-2458.

36. Grisdale, P. J.; Williams, J. L.; Glogowski, M.; Babb, B., Boron photochemistry. Possible role of bridged intermediates in the photolysis of borate complexes. *J. Org. Chem.* **1971,** *36* (4), 544-549.

37. Ross, S. D., The rate of oxidation of thiodiglycol and triethylamine by hydrogen peroxide. *J. Am. Chem. Soc.* **1946,** *68* (8), 1484-1485.

38. Gee, J.; Williamson, R., Kinetics of hydrogen peroxide oxidation of alkyl dimethyl amines. *J. Am. Oil Chem.' Soc.* **1997,** *74* (1), 65-67.

39. Chen, M. S.; White, M. C., A predictably selective aliphatic C–H oxidation reaction for complex molecule synthesis. *Science* **2007,** *318* (5851), 783-787.

40. Suzuki, K.; Oldenburg, P. D.; Que Jr, L., Iron-Catalyzed Asymmetric Olefin *cis*-Dihydroxylation with 97% Enantiomeric Excess. *Angew. Chem. Int. Ed.* **2008,** *47* (10), 1887-1889.

41. Morimoto, Y.; Takagi, Y.; Saito, T.; Ohta, T.; Ogura, T.; Tohnai, N.; Nakano, M.; Itoh, S., A Bis(μ-oxido)dinickel(III) Complex with a Triplet Ground State. *Angew. Chem. Int. Ed.* **2018,** *57* (26), 7640-7643.

42. Lide, D. R., *Handbook of Chemistry and Physics*. CRC Press, Boca Raton, FL: 2005.

43. Filler, R.; Schure, R. M., Highly acidic perhalogenated alcohols. A new synthesis of perfluoro-tert-butyl alcohol. *J. Org. Chem.* **1967,** *32* (4), 1217-1219.

44. Riddick, J.; Bunger, W.; Sakano, T., In Techniques of Chemistry 4th ed., Volume II. Organic Solvents. New York, NY: John Wiley and Sons, 1985; p 638.

45. Neimann, K.; Neumann, R., Electrophilic activation of hydrogen peroxide: selective oxidation reactions in perfluorinated alcohol solvents. *Org. Lett.* **2000,** *2* (18), 2861-2863.

46. Metelitsa, D. I., Mechanisms of the hydroxylation of aromatic compounds. *Russ. Chem. Rev.* **1971,** *40* (7), 563.

47. Walling, C.; Johnson, R. A., Fenton's reagent. V. Hydroxylation and side-chain cleavage of aromatics. *J. Am. Chem. Soc.* **1975,** *97* (2), 363-367.

48. Kunai, A.; Hata, S.; Ito, S.; Sasaki, K., The role of oxygen in the hydroxylation reaction of benzene with Fenton's reagent. Oxygen 18 tracer study. *J. Am. Chem. Soc.* **1986,** *108* (19), 6012-6016.

49. Kurata, T.; Watanabe, Y.; Katoh, M.; Sawaki, Y., Mechanism of aromatic hydroxylation in the Fenton and related reactions. One-electron oxidation and the NIH shift. *J. Am. Chem. Soc.* **1988,** *110* (22), 7472-7478.

50. Leaver, S. A.; Palaniandavar, M.; Kilner, C. A.; Halcrow, M. A., A new synthesis of bis(2-{pyrid-2-yl}ethyl)amine (L^{H}) from bis(2-{pyrid-2-yl}ethyl)hydroxylamine (L^{OH}), and the copper-dependent reduction of L^{OH} to L^{H}. *Dalton Trans.* **2003,** (22), 4224-4225.

51. Li, H.-Y.; Chen, C.-Y.; Cheng, H.-T.; Chu, Y.-H., Exploiting 1,2,3-triazolium ionic liquids for synthesis of tryptanthrin and chemoselective extraction of copper(II) ions and histidine-containing peptides. *Molecules* **2016,** *21* (10), 1355.

52. Wang, J.; Li, C.; Zhou, Q.; Wang, W.; Hou, Y.; Zhang, B.; Wang, X., Photocatalytic hydrogen evolution by Cu (II) complexes. *Dalton Trans.* **2016,** *45* (13), 5439-5443.

53. Alilou, E.; Hallaoui, A.; Ghadraoui, E.; Giorgi, M.; Pierrot, M.; Reglier, M., Two TEPA–Copper(II) Complexes {TEPA is Tris[2-(2-pyridyl)ethyl]amine}. *Acta Crystallogr. C* **1997,** *53* (5), 559-562.

54. Lonnon, D. G.; Craig, D. C.; Colbran, S. B., Rhodium, palladium and platinum complexes of tris(pyridylalkyl)amine and tris(benzimidazolylmethyl)amine N_4-tripodal ligands. *Dalton Trans.* **2006,** (31), 3785-3797.

55. Kisslinger, S.; Kelm, H.; Zheng, S.; Beitat, A.; Würtele, C.; Wortmann, R.; Bonnet, S.; Herres-Pawlis, S.; Krüger, H. J.; Schindler, S., Synthesis and Characterization of Iron(II) Thiocyanate Complexes with Derivatives of the Tris(pyridine-2-ylmethyl)amine (tmpa) Ligand. *Z. Anorg. Allg. Chem* **2012,** *638* (12-13), 2069-2077.

56. Nagataki, T.; Tachi, Y.; Itoh, S., Ni^{II}(TPA) as an efficient catalyst for alkane hydroxylation with *m*-CPBA. *Chem. Commun.* **2006,** (38), 4016-4018.

57. Nagataki, T.; Ishii, K.; Tachi, Y.; Itoh, S., Ligand effects on Ni^{II}-catalysed alkane-hydroxylation with *m*-CPBA. *Dalton Trans.* **2007,** (11), 1120-1128.

58. Schreurs, A. M.; Xian, X.; Kroon-Batenburg, L. M., EVAL15: a diffraction data integration method based on ab initio predicted profiles. *J. Appl. Cryst.* **2010,** *43* (1), 70-82.

59. Duisenberg, A. J., Diffractometry and reflection profiles of anisotropic mosaic and split crystals. *Acta Cryst.* **1983,** *A39* (2), 211-216.

60. Sheldrick, G. M., (2014). SADABS. Universität of Göttingen, Germany.

61. Sheldrick, G. M., SHELXT–Integrated space-group and crystal-structure determination. *Acta Cryst.* **2015,** *A71* (1), 3-8.

62. Sheldrick, G. M., Crystal structure refinement with SHELXL. *Acta Cryst*. **2015,** *C71* (1), 3-8.

63. Spek, A. L., Structure validation in chemical crystallography. *Acta Cryst*. **2009,** *D65* (2), 148-155.

64. Spek, A. L., PLATON SQUEEZE: a tool for the calculation of the disordered solvent contribution to the calculated structure factors. *Acta Cryst*. **2015,** *C71* (1), 9-18.

Chapter 3

Aromatic C–H Hydroxylation Reactions with Hydrogen Peroxide Catalyzed by Bulky Manganese Complexes

Abstract

The oxidation of aromatic substrates to phenols with H_2O_2 as a benign oxidant remains an ongoing challenge in synthetic chemistry. Herein, we successfully achieved to catalyze aromatic C–H bond oxidations using a series of biologically inspired manganese catalysts in fluorinated alcohol solvents. While introduction of bulky substituents into the ligand structure of the catalyst favors aromatic C–H oxidations in alkylbenzenes, oxidation occurs at the benzylic position with ligands bearing electron-rich substituents. Therefore, the nature of the ligand is key in controlling the chemoselectivity of these Mn-catalyzed C–H oxidations. We show that introduction of bulky groups into the ligand prevents catalyst inhibition through phenolate-binding, consequently providing higher catalytic turnover numbers for phenol formation. Furthermore, employing halogenated carboxylic acids in the presence of bulky catalysts provides enhanced catalytic activities, which can be attributed to their low pK_a's that reduces catalyst inhibition by phenolate protonation as well as to their electron-withdrawing character that makes the manganese oxo species a more electrophilic oxidant. Moreover, to the best of our knowledge, the new system can accomplish the oxidation of alkylbenzenes with the highest yields so far reported for homogeneous arene hydroxylation catalysts. Overall our data provide a proof-of-concept of how Mn(II)/H_2O_2/RCO_2H oxidation systems are easily tunable by means of the solvent, carboxylic acid additive, and steric demand of the ligand. The chemo- and site-selectivity patterns of the current system, a negligible KIE, the observation of an NIH-shift, and the effectiveness of using ^{t}BuOOH as oxidant overall suggest that hydroxylation of aromatic C–H bonds proceeds through a metal-based mechanism, with no significant involvement of hydroxyl radicals, and via an arene oxide intermediate.

This chapter is based on:

Masferrer-Rius, E.; Borrell, M.; Lutz, M.; Costas, M.; Klein Gebbink, R. J. M. *Adv. Synth. Catal.* **2021**, *363*, 3783-3795

3.1 Introduction

Oxidations of organic compounds are essential reactions widely studied in academia as well as in the chemical industry. The interest mainly arises by the fact that the oxygenated organic molecules can be further used to produce different classes of valuable chemicals, such as pharmaceuticals. Despite many research efforts, the selective oxidation of organic substrates still represents a critical challenge in synthetic chemistry. For instance, the direct one-step hydroxylation of aromatic molecules to the corresponding phenols could provide easy access to relevant building blocks for more complex molecules, thereby becoming a highly desired reaction.

To date, several bioinspired iron and manganese complexes have been shown to perform aliphatic C–H oxidations[1-21] as well as olefin oxidation reactions[22-35], whereas hydroxylation of aromatic compounds has remained an ongoing issue since recent years.[36-54] In earlier studies, an iron complex supported by the tpa ligand (tpa = tris(2-pyridylmethyl)amine) was found to be capable of stoichiometrically oxidizing ligated perbenzoic acids through the self-hydroxylation of the aromatic ring, forming iron(III)-salicylate complexes.[36] Also, an iron complex based on the bpmen ligand (bpmen = *N*,*N*'-dimethyl-*N*,*N*'-bis(2-picolyl)ethylenediamine) showed activity for the hydroxylation of aromatic compounds using H_2O_2, although strong coordination of phenolates to the iron(III) center prevented efficient catalysis.[37, 39] An iron complex supported by a N-heterocyclic carbene ligand has been shown to be cable of hydroxylating benzene and alkylbenzenes with H_2O_2 as well, albeit at low conversions and yields for phenol products, and with the formation of benzylic oxidized products from alkylbenzene substrates.[40, 43] Recent research progress indicates that iron complexes supported by bpbp-type ligands (bpbp = *N*,*N*'-bis(2-pyridylmethyl)-2,2'-bipyrrolidine) can hydroxylate aromatic substrates with H_2O_2.[44, 45, 50] However, overoxidation products and modest selectivities for oxidation of the aromatic ring were observed, resulting in mixtures of products in which oxidation has taken place on aromatic as well as aliphatic positions. A manganese complex supported by the Bn-TPEN ligand (Bn-TPEN = *N*-benzyl-*N*,*N*'*N*'-tris(2-pyridylmethyl)-1,2-diaminoethane) has been found to oxidize naphthalene, among other substrates, with iodosylbenzene as oxidant.[51] However, efficient catalytic turnover numbers (TON) were not achieved. Later, a manganese tpa complex incorporated into mesoporous silica-alumina was described to be active in the selective hydroxylation of benzene derivatives with H_2O_2.[52] Interestingly, incorporation of the complex into the mesoporous support was necessary to get useful catalytic activities. Very recently, intramolecular aromatic hydroxylation, as well as intermolecular hydroxylation of benzene to phenol, has been demonstrated with an iron complex based on the Bn-TPEN ligand through O–O bond heterolysis of an Fe(III)–OOH species to form an Fe(V)=O oxidant.[49]

Other transition-metal complexes have also been developed as homogeneous catalysts for aromatic C–H oxidations with H_2O_2 as the oxidant.[55-61] Itoh *et al*. demonstrated the catalytic ability of a nickel complex supported by a tripodal tetradentate aminopyridine ligand in the direct hydroxylation of aromatics using a significant excess of oxidant (Figure 1).[55] High TONs were only achieved using extremely low concentration of catalyst under long reaction times; yet, absolute yields of phenol products do not exceed 7.5%. Remarkably though, when the complex was used at 10 mol% loading with respect to the substrate, 21% phenol yield was formed (2 turnovers per nickel).[55, 62] Later, Kodera *et al*. described a dinuclear copper complex as catalyst for the hydroxylation of aromatics, showing good selectivities for phenol products (Figure 1).[56] Again, an elevated TON (12,550) was obtained under low catalyst concentration, with phenol yields up to 21% for benzene oxidation. Di Stefano *et al*. reported an iminopyridine iron complex capable of oxidizing aromatic substrates, as well as aromatic amino acids, under mild reaction conditions (Figure 1).[42, 63] However, for all these examples, aromatic oxidation of alkylbenzenes is effectively accompanied by benzylic hydroxylation. In addition, recently reported nickel, copper and cobalt complexes supported by aminopyridine ligands accomplished the oxidation of benzene to phenol in improved yields (29-41%) (Figure 1).[59-61]

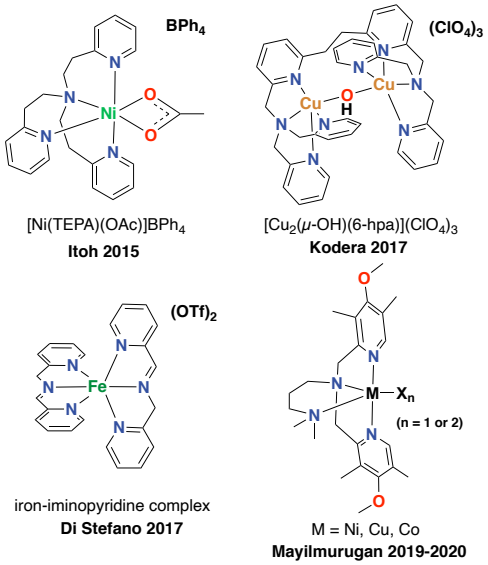

Figure 1. Examples of metal complexes previously employed in aromatic C–H hydroxylation reactions with H_2O_2.

Previously, we have shown that bulky iron complexes with *tris*-(isopropyl)silyl (tips) moieties catalyze the site-selective oxidation of alkyl C–H bonds with H_2O_2, affording high product yields and enhanced preferential oxidation of secondary over tertiary C–H bonds.[9] Likewise, manganese complexes supported by aminopyridine ligands catalyze chemo- and enantioselective aliphatic C–H oxidation with H_2O_2.[6, 10, 11, 15-18, 20, 64-67] Recently, White *et al*. reported that a bulky manganese complex with pendant *o*–CF_3-substituted aryl rings can oxidize

methylene groups in the presence of aromatic functionalities.[21] The authors also report non-productive aromatic substrate oxidation as a side-reaction. Finally, fluorinated alcohols have recently been shown to be suitable solvents for oxidation chemistry, preserving the first-formed alcohol products and, thus, reducing overoxidation reactions.[15, 64, 68-73]

Herein, we focus on the use of bioinspired manganese complexes for the oxidation of aromatic substrates. We demonstrate that the application of bulky Mn catalysts in the presence of fluorinated alcohol solvents favors the oxidation at the aromatic ring over the oxidation of benzylic positions, providing an improved route to produce phenols. On the basis of previous literature examples which propose that product inhibition through metal-phenolate binding prevents catalytic turnover in aromatic oxidation reactions, we rationalized that the presence of bulky tips groups in position 5 of the pyridine rings may help in preventing product inhibition. Our study also shows that the yields of the aromatic reactions are further improved by using halogenated carboxylic acids as additives, which in part can be attributed to their lower pK_a's which reduces product inhibition through a favorable acid-base equilibrium between the acetic acid and the (substituted) phenol products. Overall, our study has resulted in the development of a highly selective manganese-based catalyst system that performs arene hydroxylation reactions with H_2O_2 as a benign oxidant with improved yields of (substituted) phenol products with respect to the previously described homogeneous catalysts.

3.2 Results and Discussion

3.2.1 Aliphatic *vs* Aromatic C–H Oxidation

For our study we have investigated complexes of the type $[M(OTf)_2(L)]$ based on the bpmcn, bpbp, bpbi and bpmen ligand families (Scheme 1) (bpmcn = *N,N'*-dimethyl-*N,N'*-bis(2-picolyl)-cyclohexane-*trans*-1,2-diamine, bpbi = *N,N'*-bis(2-picolyl)-2,2'-bis-isoindoline). We have included manganese complexes containing electron-rich, as well as bulky pyridines.

Initially, we focused our attention on the hydroxylation of propylbenzene as substrate using 1 mol% of **Mn(^{tips}bpmcn)**, **Mn(^{dMM}bpmcn)**, or **Mn(bpmcn)** as catalyst (Table 1). Catalytic oxidation reactions were carried out by mixing the Mn(II) catalyst and AcOH (2 equiv.) into a solution of propylbenzene (1 equiv.) in TFE (TFE = 2,2,2-trifluoroethanol) at 0 °C. A sub-stoichiometric amount of aqueous H_2O_2 (0.5 equiv., 35% w/w solution) was added dropwise through a syringe pump over a period of 30 min. Interestingly, chemoselectivity was found to be largely dependent on the catalyst used. The bulky manganese complex **Mn(^{tips}bpmcn)** favors the oxidation at the aromatic ring, providing the *para*-phenol as the major product, together

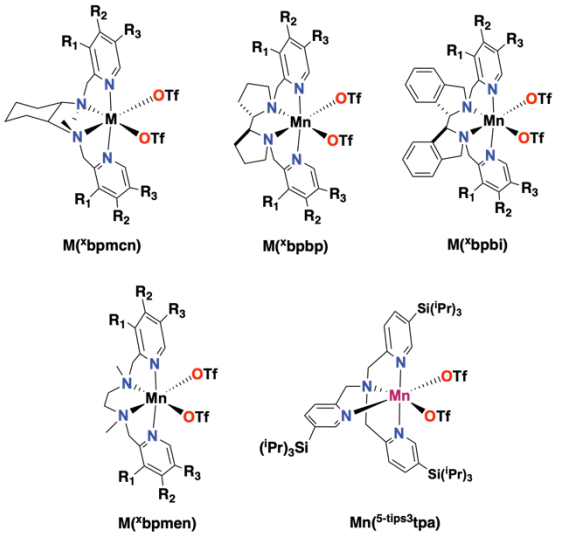

	R_1	R_2	R_3
Mn(bpmcn)	-H	-H	-H
Mn(^{dMM}bpmcn)	-Me	-OMe	-Me
Mn(^{tips}bpmcn)	-H	-H	-Si(^{i}Pr)$_3$
Fe(^{tips}bpmcn)	-H	-H	-Si(^{i}Pr)$_3$
Mn(bpbp)	-H	-H	-H
Mn(^{dMM}bpbp)	-Me	-OMe	-Me
Mn(^{tips}bpbp)	-H	-H	-Si(^{i}Pr)$_3$
Mn(bpbi)	-H	-H	-H
Mn(^{tips}bpbi)	-H	-H	-Si(^{i}Pr)$_3$
Mn(bpmen)	-H	-H	-H
Mn(^{tips}bpmen)	-H	-H	-Si(^{i}Pr)$_3$

Scheme 1. Manganese and iron complexes employed in this chapter.

with *ortho*-phenol and propyl-*p*-benzoquinone as minor products. Some 1-phenyl-1-propanol was also detected as minor product in this case, showing a ratio of aromatic:aliphatic oxidation of 7.3:1. In contrast, when the electron-rich catalyst **Mn(^{dMM}bpmcn)** was used the chemoselectivity changed completely, and preference for the oxidation at the benzylic position was observed with a ratio of aromatic:aliphatic oxidation products of 1:13.5. This observation is in agreement with previous reports on the use of electron-rich manganese complexes for asymmetric benzylic oxidations, where no aromatic oxidation products were detected.[15, 64, 73]

Table 1. Oxidation of propylbenzene in TFE with different manganese catalysts.

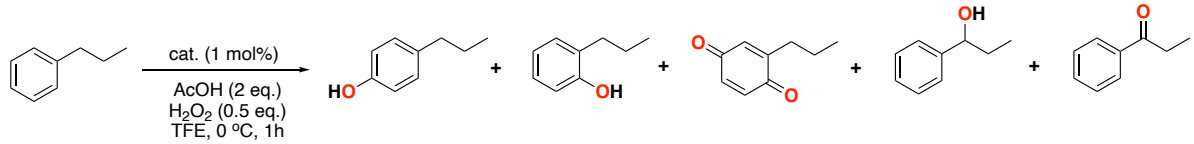

Catalyst	r.s.m[a]	*p*-Phenol[b]	*o*-Phenol[b]	Quinone[b]	Alcohol[b]	Ketone[b]	MB[c]	Ratio[d]
Mn(^{tips}bpmcn)	68	9 (18)	1 (3)	2 (8)	2 (4)	n.d.	88	7.3:1
Mn(^{dMM}bpmcn)	65	1 (2)	n.d.	n.d.	12 (23)	1 (4)	85	1:13.5
Mn(bpmcn)	72	3 (6)	1 (2)	3 (11)	4 (9)	n.d.	89	2.1:1

[a]Remaining starting material (r.s.m) in %. [b]Yields in % with respect to substrate determined by GC against an internal standard. In parenthesis yields in % with respect to H_2O_2. Yields are calculated considering that 2 equiv. of H_2O_2 are necessary for the formation of the ketone and quinone products. [c]Mass balance (MB) was calculated considering remaining starting material and all products formed, plus a percentage of substrate loss calculated with blank experiments (an average of 6% of substrate is lost): MB = (r.s.m %) + (Product Yields %) + (Substrate loss). [d]Ratio (aromatic:aliphatic) = n(*p*-phenol) + n(*o*-phenol) + n(quinone) / n(alcohol) + n(ketone). n.d. = non-detected.

With the parent **Mn(bpmcn)** complex, we observed both oxidation at the aromatic ring as well as at the benzylic position in a ratio of 2.1:1, respectively, showing a slight preference for aromatic oxidation.

Worthy of note are the blue colors that progressively form in the reaction mixtures after starting the addition of H_2O_2 to the reaction mixture containing the substrate and the catalyst (**Mn(**^{tips}**bpmcn)** or **Mn(bpmcn)**). We hypothesize that these colors are charge transfer bands arising from phenolate binding to the Mn center, which in turn inhibits the catalyst and prevents further catalytic turnover.[74-78] Consistent with this hypothesis, ESI-MS analysis of a mixture of **Mn(**^{tips}**bpmcn)** (1 mol%), *tert*-butylbenzene (1 equiv), AcOH (2 equiv) and H_2O_2 (1 equiv) at 0 °C in TFE showed a main peak at m/z = 493.8060, which corresponds to the formation of a complex ion composed of a **Mn(**^{tips}**bpmcn)** fragment and a coupled bis(phenolate) fragment ([Mn(^{tips}bpmcn)($C_6H_3OC(CH_3)_3)_2$]$^{2+}$, calcd m/z 493.8064). Importantly, the blue color was observed immediately after the start of H_2O_2 addition in the case of **Mn(bpmcn)**, whereas for the reaction with **Mn(**^{tips}**bpmcn)** the blue color appears later in the course of the reaction. These observations lead us to believe that the bulky tips groups help in preventing phenolate binding, and thus, allow for higher catalytic turnover numbers. A control experiment without an aromatic substrate did not show the appearance of the blue colors described above.

Comparing our result on arene hydroxylation catalyzed by **Mn(**^{tips}**bpmcn)** with previous literature examples, such as the systems described by Itoh[55] and Kodera[56], we can conclude that the current system performs the hydroxylation of an alkylbenzene with yields commensurate to state of the art homogeneous catalysts, at a relatively low catalyst loading. Furthermore, the nature of the ligand in the current system seems key for diverting the chemoselectivity of the catalyst from oxidation of the more activated benzylic position to the hydroxylation of the aromatic ring, showing a catalyst dependent selectivity. Yet, overall the reactions shown in Table 1 suffer from moderate conversions and yields, but do show reasonable mass balances. Noteworthy is that blank experiments without catalyst showed that a certain amount of substrate is lost during the reaction and analysis protocol (~6 %). This loss was taken into account to calculate the mass balances in Table 1.

3.2.2 Screening of Catalysts

Based on these results, we selected bulky manganese complexes with different amine backbones for further screening for the oxidation of aromatic C–H bonds (Scheme 1). A bulky iron complex, **Fe(**^{tips}**bpmcn)**, was also included in our study. The parent complexes without any substituents on the pyridines were considered as well. For all cases, the metal center adopts a C_2-symmetric *cis*-α topology, with the two pyridines *trans* to each other. A new manganese

complex supported by a bulky tripodal tetradentate ligand based on the tpa motif ($^{5\text{-tips}3}$tpa)[34] was also included.

Tert-butylbenzene was used as a model substrate since it lacks benzylic C–H bonds to selectively screen for activity in aromatic oxidation. Using stoichiometric amounts of H_2O_2, crude mixtures were analyzed by GC, detecting mainly 4-*tert*-butylphenol as the oxidized product, next to unreacted substrate. Interestingly, no *ortho*-hydroxylation product was observed, which is in contrast to, *e.g.*, the oxidation of *tert*-butylbenzene catalyzed by an iminopyridine Fe(II) complex.[42] In general, poor mass balances were observed for these reactions. We believe that a side reaction might happen, leading to overoxidized by-products, which we have not been able to identify yet. However, interest was focused here on the formation of the phenol product. First, a screening of different solvents was done (Scheme 2).

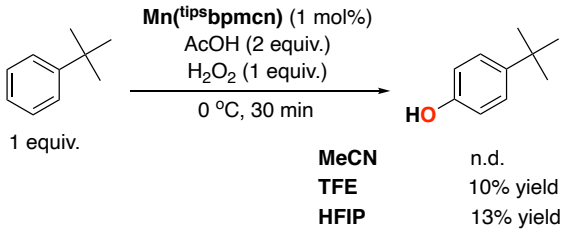

Scheme 2. Oxidation of tert-butylbenzene in different solvent.

Next to TFE, HFIP (HFIP = 1,1,1,3,3,3-hexafluoro-2-propanol) was found to be an appropriate solvent as well, allowing similar phenol formation as TFE. Interestingly, acetonitrile is not a suitable solvent, showing no formation of the desired phenol product. The positive effect of using fluorinated alcohol solvents may be attributed to their strong hydrogen donor ability, which decreases the nucleophilicity of the phenol, thereby allowing higher catalytic turnover numbers by hampering product inhibition. These findings inspired us to use manganese complexes in the presence of fluorinated alcohol solvents in further investigations.

Next, we proceeded to screen the different complexes shown in Scheme 1 using TFE (Table 2). Overall, complexes bearing bulky, tips-appended ligands exhibited a better catalytic activity, showing higher conversion and phenol production compared to their parent complexes. Maximum yields for the 4-*tert*-butyphenol product were obtained using **Mn($^{\text{tips}}$bpmcn)**, **Mn($^{\text{tips}}$bpbi),** and **Mn($^{\text{tips}}$bpmen)** (Table 2, entry 2, 7 and 9), whereas the other complexes show good conversions but lower yields. The current findings suggest the relevance of steric effects in aromatic hydroxylation reactions, whereas electronic effects may play a less important role. We believe that product inhibition in complexes with bulky ligands occurs to a lower extent in comparison to complexes with non-bulky ligands. Besides, iron complex **Fe($^{\text{tips}}$bpmcn)**, supported by a bulky bpmcn ligand, provided a poor yield (Table 2, entry 3). Iron complexes

Table 2. Oxidation of *tert*-butylbenzene with H_2O_2 catalyzed by different manganese and iron complexes as catalysts.[a]

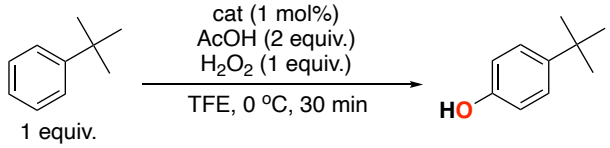

Entry	cat. (1.0 mol%)	4-*tert*-butylphenol yield (%)[b]	Conv. (%)[b]
1	**Mn(bpmcn)**	2	28
2	**Mn(^{tips}bpmcn)**	9	30
3	**Fe(^{tips}bpmcn)**	2	27
4	**Mn(bpbp)**	1	28
5	**Mn(^{tips}bpbp)**	4	38
6	**Mn(bpbi)**	2	35
7	**Mn(^{tips}bpbi)**	8	41
8	**Mn(bpmen)**	2	26
9	**Mn(^{tips}bpmen)**	9	43
10	**Mn(^{dMM}bpbp)**	1	30
11	**Mn($^{5\text{-}tips3}$tpa)**	1	25
12	**Mn(OTf)$_2$**	n.d.	6
13	-	n.d.	10

[a]Reaction conditions: Mn-cat. : H_2O_2 : substrate : HOAc = 1 : 100 : 100 : 200, in TFE at 0ºC. [b]Conversion and yields determined from crude reaction mixtures by GC. n.d. = non-detected.

with N4 ligands have been reported as catalysts for aromatic oxidation by Bryliakov and co-workers.[45, 46] Yet, we believe that product inhibition in these catalysts through phenolate-ironcoordination is more prominent than with our manganese complexes, which translates in much low catalytic efficiency for the iron catalysts. Accordingly, we focused our study exclusively on the use of manganese complexes as catalysts. Complex **Mn($^{5\text{-}tips3}$tpa)**, which bears a sterically encumbered tripodal tetradentate aminopyridine ligand based on the tpa scaffold, also provided a poor 4-*tert*-butylphenol yield (Table 2, entry 11); indicating that the use of linear tetradentate aminopyridine ligands with a *cis*-α topology seems preferred over the use of tripodal ligands. Manganese triflate was also tested as catalyst, showing no reaction.

Catalyst **Mn(^{tips}bpmcn)** was then chosen for further reaction optimization (Table 3) since it showed the better selectivity for phenol production. Different reaction temperatures, reaction times, catalyst loadings, equiv. of H_2O_2 and additives were tested. However, at this point yields for phenol product were still modest (up to 15 % yield).

Table 3. Optimization of reaction conditions for the oxidation of *tert*-butylbenzene using catalyst **Mn(tipsbpmcn)**.[a]

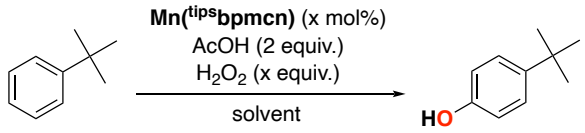

Entry	Catalyst loading (mol%)	Solvent	H_2O_2 (equiv)	Reaction time (min.)	temp. (°C)	Conversion (%)[b]	Yield Phenol (%)[b]
1	1	TFE	1	30	0	29.8	9.1
2	1	TFE	1	30	-30	55.2	12.8
3[c]	1	TFE	1	30	-30	52.8	10.9
4[d]	1	TFE	1	30	-30	0	n.d.
5	1	TFE	3	30	-30	58.7	2.9
6	1	TFE	5	30	-30	72.8	2.9
7[e]	1	TFE	1	30	-30	53.1	14.2
8[e]	1	TFE	1	30	-30	26.6	7.4
9[e]	0.5	TFE	1	30	-30	52.9	12.9
10[e]	2	TFE	1	30	-30	56.1	14.6
11[e]	1	TFE	1	60	-30	53.1	15.1

[a]Reaction conditions: Mn-cat. : H_2O_2 : substrate : HOAc = 1 : 100 : 100 : 200, 0°C, oxidant added by syringe pump over 30 minutes. Total reaction volume of 2 mL. [b]Conversion and yields determined from crude reaction mixtures by GC. [c]Triflic acid was used as additive (0.1 mol%). [d]$Sc(OTf)_3$ was used as additive (5 equiv). [e]Total reaction volume of 2 mL instead of 0.5 mL. n.d. = non-detected.

3.2.3 Carboxylic Acid Additives

Carboxylic acids have been investigated in detail as additives in H_2O_2-mediated oxidation catalysis. We found that very low phenol product formation was observed when the oxidation of *tert*-butylbenzene was run without the addition of any carboxylic acid, showing that this additive is crucial for reactivity (Table 4, entry 1). As previously discussed in the literature catalysis might proceed through a "carboxylic acid-assisted" pathway, in which the acid helps in the heterolytic cleavage of the O–O bond of a Mn(III) hydroperoxo intermediate to form a Mn(V) oxo species, responsible for the oxidation of the aromatic substrate.[13, 79-82] Alternatively, the acid could also help in C–H bond activation, as in acetate-assisted C–H activation with palladium.[83-85] Since introduction of bulky substituents in the ligand has been found to be a key feature in order to obtain catalytic turnover, several bulkier carboxylic acids were tested. Carboxylic acids with longer alkyl chains, *i.e.* propionic acid and butyric acid, showed low phenol formation compared to acetic acid (Table 4, entries 3 and 4). When bulkier carboxylic acids such as isobutyric acid, pivalic acid, and 2-ethylhexanoic acid were tested, yields for the

Table 4. Oxidation of *tert*-butylbenzene in HFIP using different carboxylic acids.[a]

Entry	Carboxylic acid	4-*tert*-butylphenol yield (%)[b]
1	-	4
2	Acetic acid	13
3	Propionic acid	6
4	Butyric acid	6
5	Isobutyric acid	3
6	Pivalic acid	1
7	2-ethylhexanoic acid	5
8	Chloroacetic acid	26
9	Dichloroacetic acid	29
10	Trichloroacetic acid	2
11	Fluoroacetic acid	26
12	Difluoroacetic acid	21
13	Trifluoroacetic acid	n.d.
14	Iodoacetic acid	6
15	*N*,*N*-dimethylglycine	2
16	2-nitrobenzoic acid	23
17	3-nitrobenzoic acid	25

[a]Reaction conditions: **Mn(**^{tips}**bpmcn)** : H_2O_2 : substrate : RCO_2H = 1 : 100 : 100 : 200, in HFIP at 0 °C.
[b]Conversion and yields determined from crude reaction mixtures by GC. n.d. = non-detected.

desired oxidized product also decreased (Table 4, entries 5, 6 and 7). Therefore, our findings show that the introduction of bulk into the carboxylic acid additive decreases product formation. Similar trends were observed when either HFIP or TFE were used as solvent (Table 5).

Next, we considered the use of halogenated carboxylic acids, which have been used previously in oxidation reactions.[21, 67, 86] Interestingly, we have found that chloroacetic acid, dichloroacetic acid, fluoroacetic acid, and difluoroacetic acid afford a significant increase in yield for the desired phenol product, with up to 29% 4-*tert*-butylphenol yield (Table 4, entry 9). The reason of this improvement could be related to the pK_a of the carboxylic acids, which varies significantly within the series of tested aliphatic carboxylic acids. The role of the lower pK_a of these carboxylic acids in arene hydroxylation reactions could be twofold. First, it keeps the phenol products protonated, which hampers catalyst deactivation by phenolate binding. Second, the electron-withdrawing character of these acids makes the proposed Mn(V) oxo species more electrophilic, which may result in a more reactive oxidant towards arenes. The use of nitrobenzoic acids also lead to increased phenol formation compared to the use of acetic

acid. However, in these cases side-product formation through arene hydroxylation of the nitrobenzoic acid was observed. In the presence of halogenated carboxylic acids higher catalytic activities were achieved in HFIP compared to TFE (Table 4 and 5).

Table 5. Oxidation of *tert*-butylbenzene in TFE using different carboxylic acids.[a]

Entry	Carboxylic acid	Conversion (%)[b]	Yield Phenol (%)[b]
1	-	6.8	n.d.
2	Formic acid	20.5	8.2
3	Acetic acid	53.1	14.2
4	Propionic acid	45.2	7.1
5	Butyric acid	52.5	6.1
6	2,2-Dimethylbutyric acid	46.2	2.8
7	3,3-Dimethylbutyric acid	37.5	3.6
8	2-Ethylhexanoic acid	41.8	4.0
9	Isobutyric acid	48.1	4.1
10	Pivalic acid	50.7	3.5
11	Chloroacetic acid	53.9	23.5
12	Dichloroacetic acid	52.1	24.7
13[c]	Trichloroacetic acid	5.2	n.d.
14[c]	Trifluoroacetic acid	8.8	0.8
15[d]	4-nitrobenzoic acid	34.0	7.5

[a]Reaction conditions: Mn-cat. : H_2O_2 : substrate : HOAc = 1 : 100 : 100 : 200, in TFE at –30 °C, oxidant added by syringe pump over 30 minutes. Total reaction volume of 2 mL. [b]Conversion and yields determined from crude reaction mixtures by GC. [c]Reaction mixture remained colorless. [d]4-nitrobenzoic acid was not completely soluble in the reaction mixture. n.d. = non-detected.

Increasing the acidity has a positive effect, going from acetic acid ($pK_a = 4.76$) to 3-nitrobenzoic acid ($pK_a = 3.46$), chloroacetic acid ($pK_a = 2.87$), fluoroacetic acid ($pK_a = 2.59$), 2-nitrobenzoic acid ($pK_a = 2.17$) and dichloroacetic acid ($pK_a = 1.35$) (Figure 2).[87] However, the use of trichloroacetic acid ($pK_a = 0.66$) or trifluoroacetic acid ($pK_a = 0.52$) lead to a dramatic decrease in catalytic activity, which might be due to protonation of the amine moieties of the ligand. Iodoacetic acid ($pK_a = 3.18$) provided good conversion but a poor phenol yield, which could be explained by the weaker C–halogen bond that may lead to side reactions (Table 4, entry 14). N,N-dimethylglycine was also not a suitable additive, showing poor yield for the desired phenol product, as well as low substrate conversion (Table 4, entry 15). Thus, we can conclude that sterics on the carboxylic acid additive are not good for the arene hydroxylation reaction, and that there is an optimum pK_a of the acid additive.

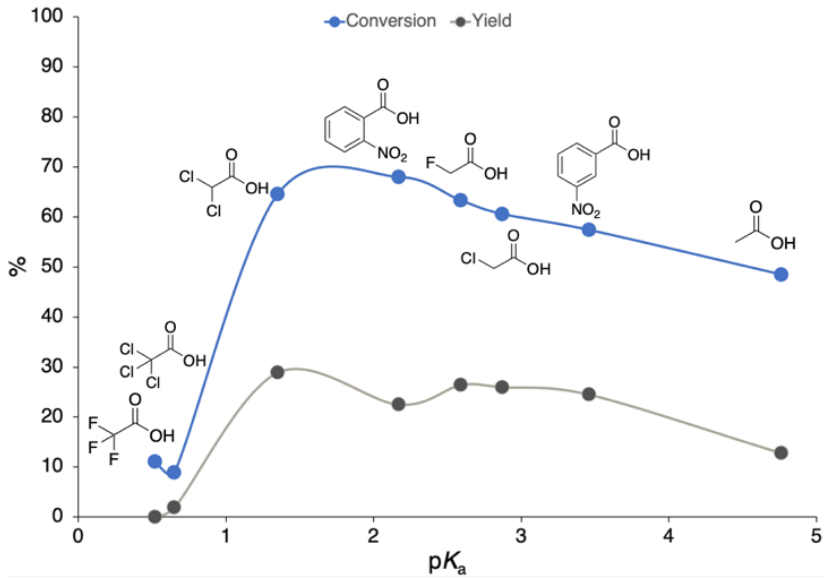

Figure 2. Effect of pK_a of the carboxylic acid additive on the hydroxylation of *tert*-butylbenzene. Reaction conditions: **Mn(**^{tips}**bpmcn)** : H_2O_2 : substrate :RCO_2H = 1 : 100 :100 : 200, in HFIP at 0 °C.

While it may be initially regarded as a modest value, the 29% yield obtained for 4-*tert*-butylphenol in a completely site selective manner is remarkable when compared with literature precedents; a recently reported iminopyridine Fe(II) catalyst has been shown to be capable of oxidizing *tert*-butylbenzene to 4-*tert*-butylphenol in 23% yield, together with the *ortho*-phenol and benzoquinone as minor products, which at that time were the highest numbers reported for *tert*-butylbenzene oxidation.[42]

Further investigations on the effect of halogenated carboxylic acids showed that the conversion and yield do not drastically change between 0.5 to 8 equiv. of acid when **Mn(**^{tips}**bpmcn)** is used as catalyst (Table 6). This allows catalysis to be performed at a much lower carboxylic acid loading.

Next, bulky manganese complexes with different amine backbones in the ligand structure were tested in the aromatic hydroxylation of *tert*-butylbenzene using optimized chloro- and dichloroacetic acid loadings (Figure 3). The use of chloroacetic acid afforded similar efficiencies for the four catalysts tested, **Mn(**^{tips}**bpmcn)** being the one that showed better conversion and yield. For dichloroacetic acid, we observed that **Mn(**^{tips}**bpmcn)** and **Mn(**^{tips}**bpbp)** performed best, with **Mn(**^{tips}**bpmcn)** showing significantly higher conversion and yield. In contrast, **Mn(**^{tips}**bpbi)** and **Mn(**^{tips}**bpmen)** showed very poor results when using dichloroacetic acid. A similar reactivity trend was observed when TFE was used as solvent (Figure 4). Therefore, we can conclude that the amine backbone in the ligand structure of the manganese complexes has a considerable impact on catalytic activity. Besides, we believe that

Table 6. Effect of different equivalents of dichloroacetic acid in aromatic C–H oxidation of *tert*-butylbenzene.[a]

Entry	Equiv. of Cl_2CHCO_2H	Conversion (%)[b]	Yield Phenol (%)[b]
1	0	19.1	3.9
2	0.5	68.0	29.2
3	1	69.0	29.7
4	2	64.6	28.9
5	4	66.1	30.3
6	6	69.2	30.0
7	8	66.9	29.4
8	10	36.7	19.1
9	15	39.4	20.1

[a]Reaction conditions: Mn-cat. : H_2O_2 : substrate = 1 : 100 : 100 , in HFIP at 0°C, oxidant added by syringe pump over 30 minutes. Total reaction volume of 2 mL. [b]Conversion and yields determined from crude reaction mixtures by GC.

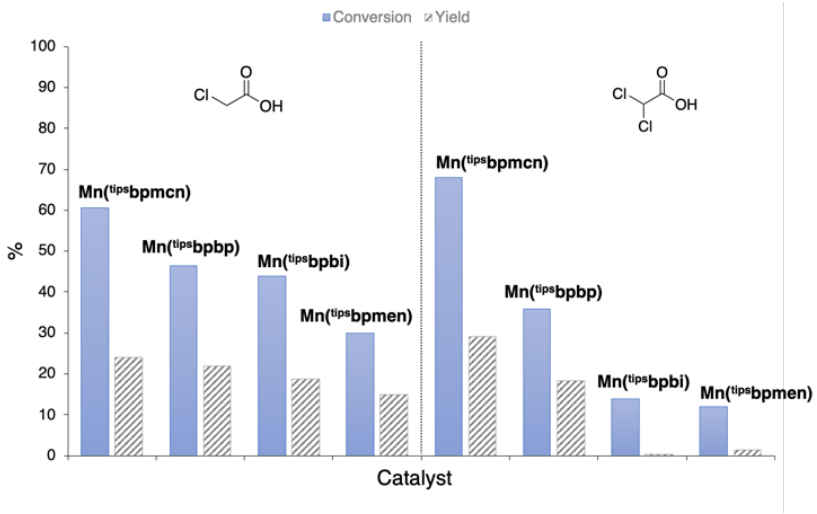

Figure 3. Effect of different amine ligand backbones on the Mn-catalyzed hydroxylation of tert-butylbenzene in HFIP. Reaction condiions: Mn-cat.: H_2O_2 : substrate : RCO_2H = 1 : 100 : 100 : 50, in HFIP at 0 °C.

the simpler ethylene diamine backbone is less stable under acidic conditions, since with dichloroacetic acid as additive a poor 4-*tert*-butylphenol yield is afforded. Consistent with this hypothesis, this complex is more efficient under low carboxylic acid loadings; hydroxylation of *tert*-butylbenzene with **Mn(tipsbpmen)** leads to only 6% 4-*tert*-butylphenol yield when 2 equivalents of chloroacetic acid are used, whereas 15% yield is obtained with 0.5 equiv. of the acid.

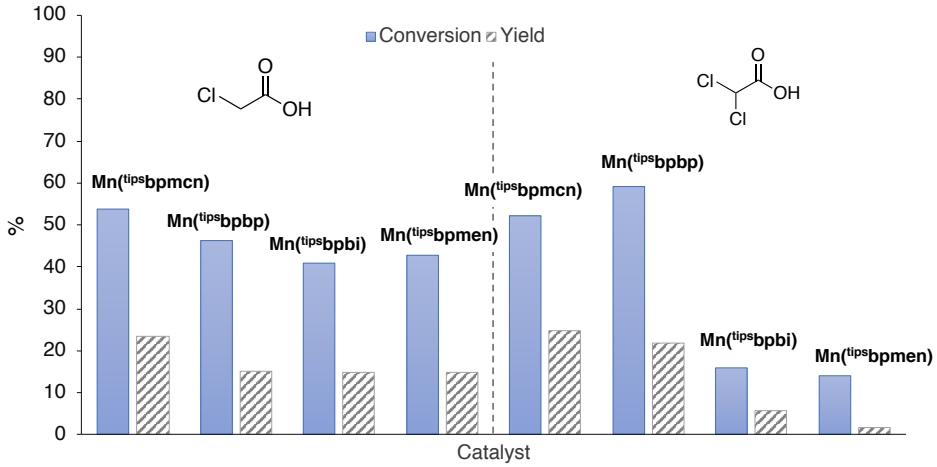

Figure 4. Effect of different amine ligand backbones on the Mn-catalyzed hydroxylation of tert-butylbenzene in TFE. Reaction condiions: Mn-cat.: H_2O_2 : substrate : RCO_2H = 1 : 100 : 100 : 50, in TFE at 0 °C.

Table 7. Investigation of dichloroacetic acid as additive with different manganese complexes.

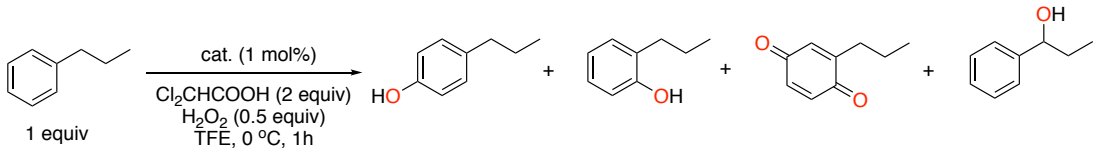

Entry	Catalyst	r.s.m (%)[a]	*p*-Phenol[b]	*o*-Phenol[b]	Quinone[b]	Alcohol[b]	MB[c]
1	**Mn(tipsbpmcn)**	68	14 (28)	4 (9)	1 (3)	Traces	92
2	**Mn(dMMbpmcn)**	90	3 (6)	2 (3)	Traces	Traces	>99
3	**Mn(bpmcn)**	85	5 (10)	2 (5)	Traces	Traces	97

[a]Remaining starting material. [b]Yields with respect to substrate determined by GC against an internal standard. In parenthesis yields respect to H_2O_2. Yields are calculated considering that 2 equiv of H_2O_2 are necessary for the formation of the quinone product. Yields for propyl-*p*-benzoquinone were calculated with the response factor of methyl-*p*-benzoquinone. [c]Mass balance was calculated considering remaining starting material and all products formed, plus a percentage of substrate loss calculated from blank experiments (an average of 5% of substrate is lost): MB = (r.s.m %) + (Product Yields %) + (Substrate loss).

Finally, we have further investigated the role of the halogenated carboxylic acid additives by examining the use of dichloroacetic acid with different manganese complexes for the hydroxylation of propylbenzene, this time at a low H_2O_2 loading (Table 7). Our earlier findings showed that for **Mn(tipsbpmcn)** the use of dichloroacetic acid provides an enhanced catalytic activity compared to the use of AcOH (compare Tables 1 and 7). On the other hand, for the electron-rich complex **Mn(dMMbpmcn)** a complete change in chemoselectivity from aliphatic to aromatic hydroxylation was observed when switching to dichloroacetic acid, albeit at low

yields (compare Tables 1 and 7). For the parent complex **Mn(bpmcn)** an increased activity for aromatic hydroxylation was observed when dichloroacetic acid was employed instead of AcOH. Remarkably, traces of 1-phenyl-1-propanol were detected for all these catalysts when dichloroacetic acid was employed, revealing that the use of a halogenated carboxylic acid increases the selectivity towards the oxidation of aromatic C–H bonds for these complexes in a general sense, avoiding the generation of products originating from oxidation at a more activated benzylic position.

3.2.4 Substrate Scope

Aromatic C–H hydroxylation of different substrates has been explored under the optimized experimental conditions using the manganese complex **Mn(**^{tips}**bpmcn)** (Table 8). In general, our current Mn(II)/H_2O_2/$Cl_2CHCOOH$ catalytic system affords higher yields and substantially improved selectivities for aromatic over aliphatic C–H oxidation.

At first, we considered benzene as substrate, which leads to phenol in a remarkable yield of 32%, along with *para*-benzoquinone in 7% yield (Table 8, entry 1). Interestingly, when phenol was used as the substrate, 13% yield of *para*-benzoquinone was observed; showing that the primary oxidation product in benzene hydroxylation can indeed engage in a second oxidation step (Table 8, entry 2). Next, we extended our study to the oxidation of alkylbenzenes. Oxidized products were obtained in remarkable total product yields ranging from 29 to 37%, with the *para*-phenol as the main product in all cases, which is reminiscent to reactions proceeding via an electrophilic aromatic substitution type of mechanism. Toluene was oxidized to *para*-cresol in 22% yield, together with *ortho*-cresol and methyl-*para*-benzoquinone in 8 and 1% yield, respectively (Table 8, entry 3). Recent studies on aromatic oxidations have shown other complexes to be capable of oxidizing the aromatic ring of toluene as well, however, showing significant amounts of aliphatic oxidation towards benzyl alcohol or benzaldehyde products.[42, 55, 56, 59, 60] Remarkably, **Mn(**^{tips}**bpmcn)** shows an excellent selectivity for oxidation of the aromatic ring over the aliphatic site chain. Oxidation of other alkylbenzene derivatives with more reactive benzylic C–H bonds was also explored. Ethylbenzene provided 4-ethylphenol as the major product in 26% yield, along with 2-ethylphenol and ethyl-*para*-benzoquinone in 8 and 2% yield, respectively (Table 8, entry 4). For the oxidation of propylbenzene, we observed 4-propylphenol, 2-propylphenol and propyl-*para*-benzoquinone in 24, 8, and 2% yield, respectively (Table 8, entry 5). Cumene was also considered, which bears a more encumbered isopropyl substituent with a weak 3^0 benzylic C–H bond. 4-Isopropylphenol and 2-isopropylphenol were obtained in 30 and 5% yield, respectively. Minor amounts of isopropyl-*para*-benzoquinone were also detected in 2% yield (Table 8, entry 6). To the best of our knowledge, hydroxylation of this group of alkylbenzene substrates catalyzed by the current

system provides the highest yields reported to date with homogeneous catalysts. Remarkably, only traces of benzylic oxidation products were detected in these reactions, suggesting that the current catalytic system is selective for aromatic hydroxylation reactions. A cautious note must be introduced at this point because some of these compounds show the lowest mass balance of all substrates tested in this study, which raises the possibility that benzylic oxidation products are also formed but overoxidized to non-detected products. Important to note is that no formation of ketone products was observed, *i.e.* secondary oxidation of initial benzylic alcohol products does not seem to take place. Blank experiments without catalyst were done to calculate the amount of substrate loss during the reactions, and were used to calculate the mass balances in Table 8.

We observed a correlation between the bulk of the lateral alkyl chain in the aromatic substrate and the product profile. Our results clearly show that increasing the bulk of the substituents on the substrate translates into a decreased formation of *ortho*-phenol product, which is likely due to steric effects of both the catalyst and the substrate. The amounts of *ortho*-phenol were similar for toluene, ethylbenzene, and propylbenzene. However, when a bulkier

Table 8. Product analysis in the oxidation of benzene and its derivatives catalyzed by **Mn(**^{tips}**bpmcn)**[a]

Entry	Substrate (r.s.m %)[b]	*p*-Phenol (%)[c]	*o*-Phenol (%)[c]	Quinone (%)[c]	Benzylic oxidation (%)[d]	Mass balance (%)[e]
1	 44	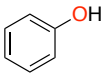 32	–	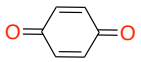 7	–	88
2	 70	–	–	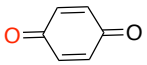 13	–	86
3	 49	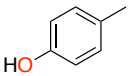 22	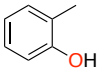 8	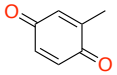 1	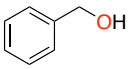 traces	80
4	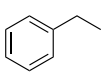 34	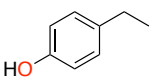 26	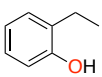 8	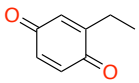 2	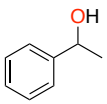 traces	71
5	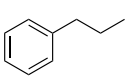 45	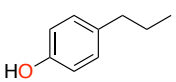 24	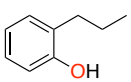 8	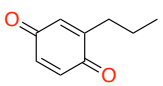 2	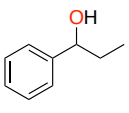 traces	81

Table 8 (continued)

6	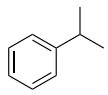 38	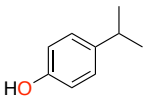 30	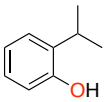 5	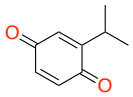 2	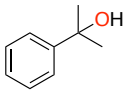 traces	75
7	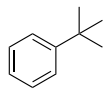 32	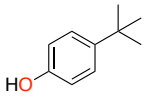 29	–	–	–	66
8	 45	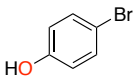 8	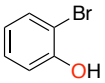 14	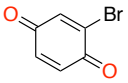 5	–	72
9	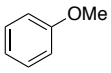 84	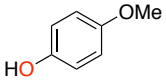 6	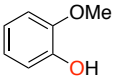 4	–	–	94[f]
10	 > 99	–	–	–	–	> 99[f]

[a]Reaction conditions: **Mn(**^{tips}**bpmcn)** : H_2O_2 : substrate : $Cl_2CHCOOH$ = 1 : 100 : 100 : 50, in HFIP at 0 °C for 30 min. [b]Remaining starting material (r.s.m.) determined from crude reaction mixtures by GC. [c]Product yields determined from crude reaction mixtures by GC. [d]Benzaldehyde or ketone products were not detected. [e]Mass balance was calculated considering remaining starting material and all products formed, plus a percentage of substrate loss calculated from blank experiments: MB = (r.s.m %) + (Product Yields %) + (Substrate loss %). [f]Percentage of substrate loss was not calculated.

substrate, such as in cumene, was used, the yield for the *ortho*-phenol decreased. More remarkably is the oxidation of *tert*-butylbenzene, where no *ortho*-phenol product was detected at all, *i.e*. 4-*tert*-butylphenol was detected as the only product in 29% yield (Table 8, entry 7). The current data contrasts with the oxidation of cumene catalyzed by a Ni(II) complex supported by an aminopyridine ligand, where mixtures of *ortho*-, *meta*- and *para*-phenols were obtained together with benzylic oxidized products; albeit in very low yields.[55] Thus, our data indicate the importance of steric catalyst effects to dictate the regioselectivity of the hydroxylation reaction.

Using bromobenzene as substrate, 2-bromophenol and 4-bromophenol were obtained in 14 and 8% yield, respectively. 2-Bromo-1,4-benzoquinone was also detected in 5% yield (Table 8, entry 8). The formation of *ortho* and *para* phenols is in agreement with classical aromatic substitution reactions, halogen and alkyl substituents being *ortho* and *para* directing groups. However, of importance is the different selectivity observed for bromobenzene compared to

the alkylbenzene substrates; where the *ortho*-phenol was obtained as the main oxidized product in the former case, the *para*-phenol was the major product in the latter case.

An electron-donating substituent was expected to enhance the reactivity of the arene substrate in our system. Nonetheless, anisole showed a poor reactivity, with 4-methoxyphenol and 2-methoxyphenol being produced in only 6 and 4% yield, respectively (Table 8, entry 9). No benzoquinone was detected in this case. For benzonitrile, bearing an electron-withdrawing cyano group, no oxidized products were detected (Table 8, entry 10). While the cyano group could deactivate the aromatic ring towards electrophiles, the coordinating ability of the methoxy and cyano groups in anisole and benzonitrile might also interfere with catalysis. We also believe that the poor catalytic activity for anisole may be due to strong binding of the first formed hydroxylated product to the metal center (indicated by a strong color change to purple). Indeed, competitive experiments using equimolar amounts of anisole and *tert*-butylbenzene show only 2 % 4-*tert*-butylphenol yield, demonstrating catalyst deactivation in the presence of anisole.

Amino acid substrates are particularly interesting because of their biological significance and their molecular complexity, containing different types of C–H bonds. We therefore examined the catalytic hydroxylation of phenylalanine. Our idea was to extrapolate the reactivity that we have observed using simple aromatic substrates to the oxidation of more complex molecules. Interestingly, we found that oxidation at the *para*-position of the aromatic ring of a protected phenylalanine yields the corresponding tyrosine as the main product in 7% yield, which represents 7 catalytic turn-overs per Mn (Scheme 3). The hydroxylation of phenylalanine might be further optimized by variation of reaction conditions and protecting groups.

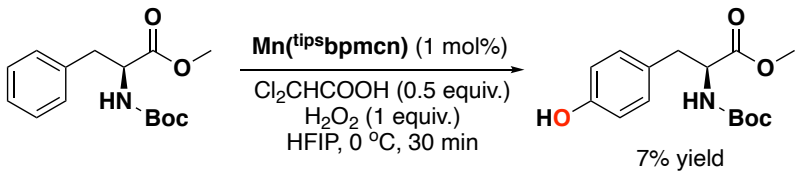

Scheme 3. Aromatic C–H hydroxylation of a natural product.

3.2.5 Mechanistic Considerations

Finally, our efforts have been devoted to the understanding of the mechanism of the aromatic hydroxylation reaction. Generally, activation of H_2O_2 by manganese or iron complexes supported by aminopyridine ligands leads to electrophilic oxidants.[8, 26, 28, 79, 80] It is proposed that the starting Mn(II) complex is first oxidized to a Mn(III) hydroperoxo species, which then converts to a Mn(V) oxo complex through O–O bond heterolysis,[13, 79, 80] this last step being assisted by the carboxylic acid additive (Scheme 4). We propose that the aromatic

hydroxylation reaction occurs via a similar oxidizing species, without the involvement of oxygen-centered radicals. It is well-known that free radicals, such as hydroxyl radicals generated via a Fenton process, can perform the oxidation of aromatic C–H bonds, but show low efficiencies and selectivities.[88-91] The involvement of such radicals would lead to side products through lateral site chain oxidation in alkylbenzene derivatives, because these oxygen-centered radicals are unable to differentiate between C–H bonds of different strengths.[42, 92] In addition, hydroxylation of alkylbenzenes via hydroxyl radicals give a specific distribution of *ortho*-, *meta*- and *para*-phenol isomers.[93] Several of our observations speak against the involvement of hydroxyl radicals in our aromatic hydroxylation reaction, and point towards a metal-based oxidation mechanism.

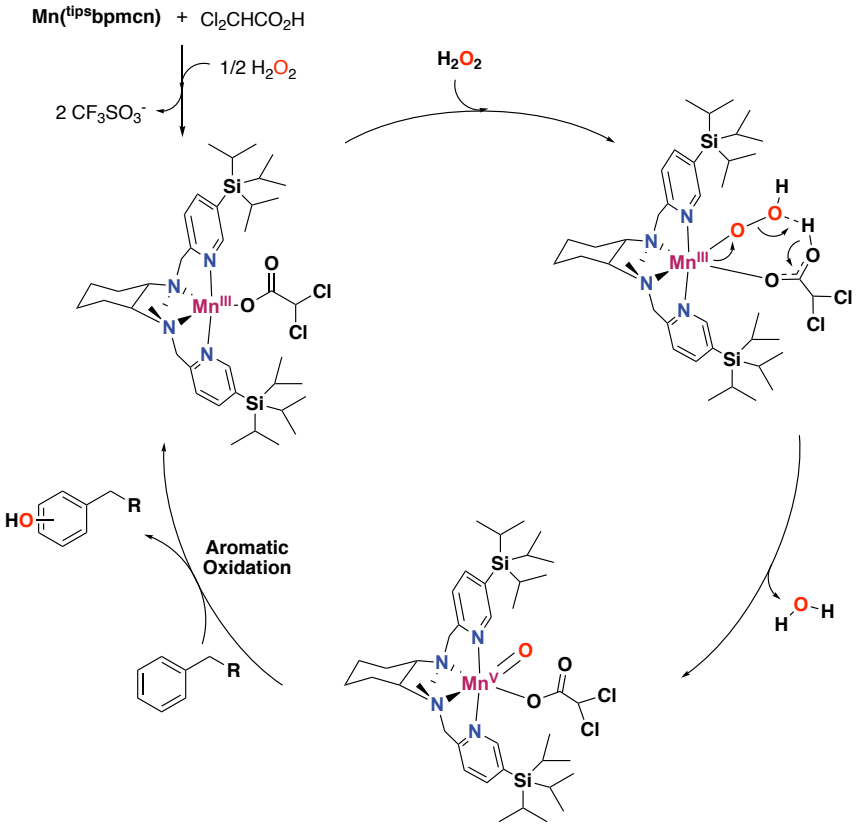

Scheme 4. Proposed mechanistic cycle based on the carboxylic acid assisted O–O cleavage of non-heme Fe and Mn complexes.[8, 13, 26, 94, 95]

Our catalysis experiments show that oxidation of electron-rich benzene derivatives leads to the formation of *para* and *ortho* phenol products, with no formation of the *meta* isomer. This clearly contrasts with other catalysts capable of performing arene hydroxylation, such as the systems reported by Itoh[55], Bryliakov[45] and Di Stefano[42], where mixtures of *ortho*-, *meta*- and *para*-phenols were observed; and thus, suggests that the current reaction undergoes through a more selective species. In contrast, when switching to electron-poor substrates, no aromatic hydroxylation reaction takes place with the current system. These observations agree with the

proposal of an electrophilic manganese-oxo species, with a reactivity sensitive to the electronic nature of the substrate.

Previous studies have shown that the oxidation of toluene with hydroxyl radicals afford cresols with a distribution of 71 : 9 : 20 for *ortho* : *meta* : *para* isomers.[93] The current Chapter has shown that the bulky **Mn(**^{tips}**bpmcn)** catalyst is capable of oxidizing toluene with high selectivity, affording a ratio of 27 : 0 : 73 for the *ortho*-, *meta*- and *para*-cresols, respectively. Therefore, our data clearly show a distinct distribution of isomers compared with the reaction involving hydroxyl radicals, and consequently point towards the involvement of a metal-based mechanism.

To get further insight in the mechanism, we considered performing the hydroxylation reaction with another oxidant than H_2O_2. Remarkably, we found that catalytic hydroxylation of *tert*-butylbenzene by **Mn(**^{tips}**bpmcn)** in fluorinated alcohol solvents can also be accomplished employing ^{t}BuOOH as oxidant, generating 4-*tert*-butylphenol as the oxidized product in 9% yield. It is known that oxidations with ^{t}BuOOH can proceed through a Fenton-type process, generating free-diffusing *tert*-butoxy and *tert*-butylperoxy radicals that can engage in hydrogen abstraction reactions with aliphatic C–H bonds.[26, 96, 97] However, ^{t}BuOOH activation does not produce hydroxyl radicals, and *tert*-butoxy radicals, unlike hydroxyl radicals, do not add to aromatic rings.[98] Another evidence against the involvement of hydroxyl radicals is that the aromatic hydroxylation reactions catalyzed by **Mn(**^{tips}**bpmcn)** are not affected by the presence, or absence, of air. Independent experiments carried out under air and under a nitrogen atmosphere showed similar efficiencies for the generation of 4-*tert*-butylphenol (Table 9). In contrast, a significant impact of air on product yields is observed when oxidations are mediated by oxygen-centered radicals.[42, 90, 91, 99]

Next, we carried out a kinetic isotope effect (KIE) experiment using a 1:1 mixture of benzene and perdeuterated benzene as substrate and **Mn(**^{tips}**bpmcn)** as catalyst. From the ratio of phenol to phenol-d_5, a KIE value of 0.97 ± 0.06 was determined for this reaction. This value rules out Fenton-type processes, for which a KIE of 1.7 has been reported.[100] Overall, our combined data suggest that aromatic hydroxylation reactions catalyzed by **Mn(**^{tips}**bpmcn)** occur through a metal-based mechanism, with no significant involvement of hydroxyl radicals. Besides, the high bond dissociation energy of aromatic C–H's discard a HAT initiated process. Instead, the data is consistent with an aromatic hydroxylation mechanism via electrophilic attack of the high valent metal oxo on the aromatic ring. As a first option, the KIE value found in this study is compatible with the formation of a Wheland type of intermediate found in an electrophilic aromatic substitution mechanism. Alternatively, an initial arene epoxidation reaction conducted by the high valent manganese-oxo species, followed by an acid catalyzed re-aromatization to

Table 9. Investigation on the presence or absence of atmospheric oxygen in the oxidation of *tert*-butylbenzene.[a]

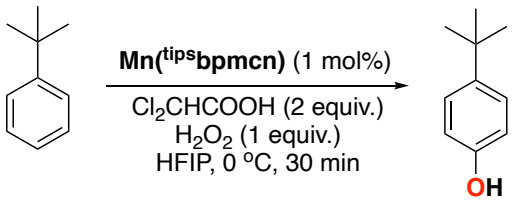

Entry	Conditions	Conversion (%)[b]	Yield Phenol (%)[b]
1	Under air	65	29
2	Under N_2	59	26

[a]Reaction conditions: Mn-cat. : H_2O_2 : substrate = 1 : 100 : 100 , in HFIP at 0 °C, oxidant added by syringe pump over 30 minutes. Total reaction volume of 2 mL. [b]Conversion and yields determined from crude reaction mixtures by GC.

form the corresponding phenol could also be a plausible mechanism.[101] Both proposed processes show a negligible KIE, which is consistent with a change in hybridization from sp^2 to sp^3 of the aromatic carbon where the oxidation takes place.[42, 102]

To get further insight into the arene hydroxylation mechanism, we performed a catalytic experiment using 1-*tert*-butyl-4-deuterobenzene to probe the occurrence of an NIH shift (Scheme 5). This characteristic feature of arene hydroxylation reactions based on the migration of a substituent from the formal hydroxylation site to an adjacent carbon position can indicate the involvement of an arene oxide as a reaction intermediate.[103-107] Based on our previous experiments, we know that hydroxylation of *tert*-butylbenzene only occurs at the *para*-position of the benzene ring.

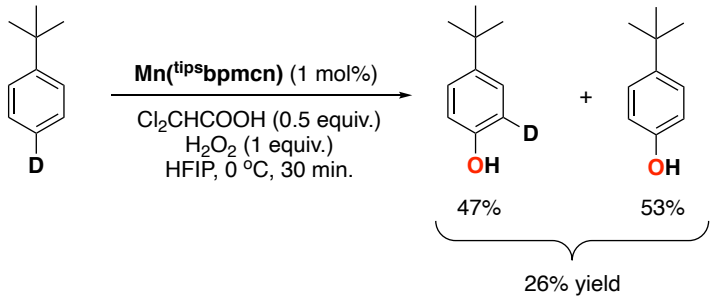

Scheme 5. Deuterium labeling study.

Combined GC and GC-MS analysis of the reaction with 1-*tert*-butyl-4-deuterobenzene indeed showed the exclusive formation of *para*-phenol products (26%), with a 4-*tert*-butyl-2-deuterophenol and 4-*tert*-butylphenol ratio of 47/53, indicating that an NIH-shift takes place during the reaction. On basis of this observation, we suggest that the aromatic hydroxylation

reaction most likely occurs through an arene epoxidation mechanism, involving the generation of a cyclohexadienone intermediate after arene oxide formation.

We propose that the use of an electron-deficient acid can make the metal oxo species more electrophilic, as well as reducing catalyst inhibition by phenolates protonation. These effects, together with a sterically demanding aminopyridine ligand, translate into an oxidizing agent reactive towards the *para*-position of the aromatic ring instead of the (benzylic) aliphatic C–H bonds. Overall, we believe that there is a synergy between the carboxylic acid and the manganese complex, as was recently also shown for methylene and tertiary C–H oxidation catalyzed by other manganese complexes with chloroacetic acid as additive.[21, 67, 108] Further investigations into the exact role of halogenated carboxylic acids are required to understand how chemoselectivity is governed in these aromatic hydroxylation reactions.

3.3 Conclusions

We have presented a new catalytic procedure for the direct one-step hydroxylation of aromatic C–H bonds to the corresponding phenol products using manganese complexes in combination with H_2O_2. Pivotal to our findings is the use of sterically encumbered tetradentate aminopyridine ligands in combination with a halogenated carboxylic acid additive and a fluorinated alcohol solvent. We have shown that complexes with bulky ligands perform better in arene oxidations by preventing coordination of the phenolate products to the manganese center. Remarkably, the use of bulky manganese complexes favors aromatic oxidation over (benzylic) aliphatic C–H bond oxidation, whereas electron-rich manganese complexes selectively oxidize the weaker benzylic C–H bonds, demonstrating a dependency of the chemoselectivity on the catalyst. A synthetically relevant property of the current Mn system is that oxidation of a broad range of aromatic substrates can be accomplished. Notable is the oxidation of monoalkylbenzenes using **Mn(^{tips}bpmcn)** as the catalyst, which to our knowledge provide the highest phenol product yields reported to date for homogeneous catalysts. The overall product profiles of this system, in combination with a negligible KIE effect and the effectiveness of using ^{t}BuOOH as oxidant, overall point towards a metal-based mechanism, with no significantly involvement of oxygen-centered radicals. Besides, the observation of a NIH shift indicates that aromatic oxidation with the current system is likely to occur via an arene epoxidation pathway.

Future efforts will be focused on the understanding of the factors that govern product selectivity, as well as of possible catalyst deactivation pathways that lead to the still moderate product yields observed in this study. Additional investigations of the current catalytic system will also focus on a further insight in the overall modest mass balances obtained. Overall, our

current findings represent a next step in the design of molecular catalysts for the selective oxidation of aromatic substrates, and provide a stepping stone for the further development of selective oxidation catalysts based on manganese.

3.4 Experimental Section

3.4.1 General Remarks

The synthesis of manganese and iron complexes and other air- and moisture-sensitive reactions was performed under an inert nitrogen atmosphere using standard Schlenk line and glovebox techniques. All catalytic oxidation reactions were run under air with no precautions taken to exclude moisture. The solvents diethyl ether and acetonitrile were purified using an MBraun MB SPS-800 solvent purification system. Tetrahydrofuran and methanol were dried with sodium and magnesium turnings, respectively, and distilled under nitrogen prior to use. Ligands *S,S*-bpmcn[109], *R,R*-^{tips}bpmcn[110], *S,S*-^{tips}bpmcn[110], *S,S*-bpbp[111], *S,S*-^{tips}bpbp[110], *S,S*-bpbi[112], *S,S*-^{tips}bpbi[112], bpmen[113], $^{5\text{-}tips3}$tpa[34], (*S,S*)-^{dMM}bpmcn[26] and (*S,S*)-^{dMM}bpbp[26] were synthesized according to literature procedures. $Mn(OTf)_2$ was bought from Sigma-Aldrich. Manganese complexes **Mn(bpmcn)**[114], **Mn(^{tips}bpmcn)**[11], **Fe(^{tips}bpmcn)**[110], **Mn(bpbp)**[65], **Mn(^{tips}bpbp)**[11], **Mn(bpbi)**[115], **Mn(bpmen)**[114], **Mn(^{dMM}bpmcn)**[116] and **Mn(^{dMM}bpbp)**[25] were synthesized according to literature procedures.

Tert-butylbenzene, benzene, ethylbenzene, propylbenzene, cumene, bromobenzene, anisole and benzonitrile were filtered through a plug of alumina before being used in catalysis. Toluene was taken from an MBraun MB SPS-800 solvent purification system. All other reagents and reaction products were obtained commercially and used without further purification. Column chromatography was performed using Merck silica gel (60-200 mesh). ^{1}H, ^{13}C, and ^{19}F NMR spectra were recorded with a 400 MHz Varian spectrometer at 25°C, chemical shifts (δ) are given in ppm referenced to the residual solvent peak. IR spectra were recorded with a Perkin-Elmer Spectrum One FTIR spectrometer. ESI-MS spectra were recorded with an Advion expression compact mass. High resolution mass spectrometry (HRMS) was performed on a Brucker MicrOTOF-Q^{II} (Q-TOF) instrument with a quadrupole analyzer. GC analyses were performed on a Perkin-Elmer Clarus 500 Gas Chromatograph equipped with a PE Elite-5 column ((30m x 0.32 mm x 0.25 μm), (5% phenyl)-(95% methyl)polysiloxane) and a flame-ionization detector. X-ray diffraction analysis was carried out using two different diffractometers: Bruker Kappa ApexII and Bruker D8 QUEST ECO.

Appendix B contains the supplementary information of this Chapter, which includes MS-data of the investigation on catalyst inhibition, ^{1}H-NMR spectra for the newly synthesized ligands and substrates, and representative GC chromatographs of the catalytic reactions.

3.4.2 Synthesis of Ligands, Manganese Complexes and Substrates

3.4.2.1 Synthesis of Ligands

^{tips}bpmen. NaOH (205.4 mg, 5.14 mmol) was added to a round-bottom flask charged with a stir bar and ^{tips}PyCH$_2$Cl (400 mg, 1.41 mmol) dissolved in CH_2Cl_2 (2 mL) and H_2O (2 mL). Subsequently, a solution containing *N,N*-dimethylethylenediamine (56.6 mg, 0.64 mmol) was added. The combined mixture was vigorously stirred overnight at room temperature. At this point, the organic phase was separated and the aqueous phase was extracted with CH_2Cl_2 (3 times). The combined organic extracts were dried over $MgSO_4$ and the solvent was eliminated under vacuum The obtained oil was purified by silica column

(petroleum ether:EtOAc 9:1 at first, then CH_2Cl_2:CH_3OH:NH_3 90:9:1) to provide the desired ligand as a light yellow-white solid (60% yield). ^{1}H NMR (400 MHz, $CDCl_3$) δ 8.60 (s, 2H), 7.73 (dd, *J* = 7.7, 1.8 Hz, 2H), 7.41 (d, *J* = 7.7 Hz, 2H), 3.68 (s, 4H), 2.68 (s, 4H), 2.29 (s, 6H), 1.45 – 1.34 (m, 6H), 1.07 (d, *J* = 7.4 Hz, 36H). ^{13}C NMR (100 MHz, $CDCl_3$) δ 159.06, 154.96, 143.61, 128.02, 122.68, 64.10, 55.60, 43.03, 18.57, 10.76.

3.4.2.2 Synthesis of Manganese Complexes

Mn(^{tips}bpmen): Under a nitrogen atmosphere in a glovebox, a solution of ^{tips}bpmen (128.5 mg, 0.22 mmol) in THF (2 mL) was added to a vigorously stirred solution of $Mn(OTf)_2$ (72.6 mg, 0.21 mmol) in THF (2 mL) at room temperature. The reaction mixture was stirred at rt overnight, providing a white precipitate. The precipitate was allowed to settle and the supernatant was removed. The remaining precipitate was washed with diethyl ether twice, then dissolved in CH_2Cl_2. The resulting solution contained some black impurities, which were removed *via* filtration through a filter paper. Subsequently, crystallization by slow vapor diffusion of diethyl ether into the CH_2Cl_2 solution afforded, in a few days, the desired complex as a white powder in 53% yield. ESI-MS calcd. *m/z* for $C_{34}H_{65}MnN_4O_2Si_2$ ($[Mn(L)(OH)_2+H]^+$): 672.4, found 671.9. FT-IR (ATR) ν, cm^{-1}: 2947-2868 $(C–H)_{sp3}$, 1591, 1460, 1312 1233, 1212, 1171, 1032, 982, 881, 697, 681, 636, 566, 512.

Mn(^{tips}bpbi): This complex was prepared in an analogous manner to the $[Mn(OTf)_2(^{tips}bpmen)]$ complex, starting from (*S,S*)-^{tips}bpbi ligand and $Mn(OTf)_2$. The desired complex was obtained as white crystals in 42% yield. ESI-MS calcd. *m/z* for $C_{46}H_{69}MnN_4O_2Si_2$ ($[Mn(L)(OH)_2+H]^+$): 820.4, found 819.9. FT-IR (ATR) ν, cm^{-1}: 2944-2866 $(C–H)_{sp3}$, 1594, 1456, 1312, 1215, 1160, 1037, 995, 960, 881, 865, 766, 726, 693, 637, 568, 514. Elemental Analysis (%) for $C_{48}H_{66}F_6MnN_4O_6S_2Si_2$ (MW = 1084.30 g/mol). Calculated C: 53.17, H: 6.14, N: 5.16; obtained C: 52.85, H: 5.61, N: 5.12. See section 3.4.3.1 for X-ray crystal structure.

Mn($^{5\text{-}tips3}$tpa): This complex was prepared in an analogous manner to the $[Mn(OTf)_2(^{tips}bpmen)]$ complex, starting with $^{5\text{-}tips3}$tpa ligand and $Mn(OTf)_2$. The desired complex was obtained as white crystals. HRMS (ESI-TOF): *m/z* calculated for $C_{46}H_{78}F_3MnN_4O_3SSi_3$, $[M\text{-}OTf]^+$ 962.4435, Found 962.4423. Elemental Analysis (%) for $C_{47}H_{78}F_6MnN_4O_6S_2Si_3$ (MW = 1112.47 g/mol). Calculated C: 50.74, H: 7.07, N: 5.04; obtained C: 50.53, H: 7.04, N: 5.28. See section 3.4.3.2 for X-ray crystal structure.

3.4.2.3 Synthesis of substrates

***tert*-butylbenzene-4-d$_1$.** 1-Bromo-4-*tert*-butylbenzene (5 mmol, 0.87 mL) was dissolved in 15 mL of anhydrous diethyl ether under inert atmosphere and cooled to –78 °C in an acetone/dry ice bath. Then 2.1 equiv of ^{t}*Bu*Li (1.9 M in pentane, 5.8 mL, 11 mmol) were added dropwise over 15 min, and the reaction mixture was let stir for 1 h. Then, the temperature was raised up to 0 °C and D_2O (1 mL) was added dropwise. The reaction mixture was let stir for 30 min. At this point, the reaction was quenched by addition of more water and extracted with diethyl ether (3 x 20 mL). The combined organic layers were dried over $MgSO_4$, concentrated on a rotatory evaporator and dried under reduced pressure to yield the desired compound (0.56 g, 4.13 mmol, 83% yield) as a colorless liquid. ^{1}H NMR (400 MHz, $CDCl_3$) δ 7.42 (d, *J* = 7.0 Hz, 2H), 7.32 (d, *J* = 7.0 Hz, 2H), 1.35 (s, 9H). Spectral properties of the products agree with the literature data.[117]

3.4.3 X-Ray Crystal Structure Determination of Mn(tipsbpbi)

$C_{48}H_{66}F_6MnN_4O_6S_2Si_2 \bullet C_4H_{10}O$, Fw = 1158.40, colourless plate, 0.38 × 0.19 × 0.08 mm^3, orthorhombic, $P2_12_12_1$ (no. 19), a = 13.6943(2), b = 14.3549(3), c = 30.9303(7) Å, V = 6080.3(2) Å^3, Z = 4, D_x = 1.265 g/cm^3, μ = 0.39 mm^{-1}. The diffraction experiment was performed on a Bruker Kappa ApexII diffractometer with sealed tube and Triumph monochromator (λ = 0.71073 Å) at a temperature of 150(2) K up to a resolution of $(\sin\theta/\lambda)_{max}$ = 0.65 Å^{-1}. The Eval15 software[118] was used for the intensity integration. A multiscan absorption correction and scaling was performed with SADABS[119] (correction range 0.68-0.75). A total of 108068 reflections was measured, 13972 reflections were unique (R_{int} = 0.058), 10924 reflections were observed [I>2σ(I)]. The structure was solved with Patterson superposition methods using SHELXT.[120] Structure refinement was performed with SHELXL-2018[121] on F^2 of all reflections. Non-hydrogen atoms were refined freely with anisotropic displacement parameters. All hydrogen atoms were introduced in calculated positions and refined with a riding model. One isopropyl group was refined with a disorder model. 702 Parameters were refined with 242 restraints (distances and angles of the isopropyl groups, displacement parameters of the disordered atoms). R1/wR2 [I > 2σ(I)]: 0.0413 / 0.0897. R1/wR2 [all refl.]: 0.0614 / 0.0971. S = 1.043. Flack parameter[122] x = 0.015(6). Residual electron density between -0.26 and 0.35 e/Å^3. Geometry calculations and checking for higher symmetry was performed with the PLATON program.[123]

3.4.4 Reaction Protocol for Catalytic Studies

3.4.4.1 General Procedure for Catalytic Hydroxylation Reaction

A 3 mL or 20 mL vial was charged with: substrate (1 equiv.) and the indicated loading of catalyst and corresponding solvent (0.5 mL or 2 mL). The carboxylic acid was added with indicated loading. The vial was cooled on an ice bath or acetonitrile/dry ice bath, depending on the desired temperature, with stirring. Subsequently, a solution of H_2O_2 in the corresponding solvent (indicated loading, diluted from a 35% H_2O_2 aqueous solution) was delivered by syringe pump over 30 min. After the oxidant addition, the resulting mixture was brought to room temperature, and at this point, a 0.8 M biphenyl solution in CH_3CN (0.5 equiv) was added as internal standard. The solution was filtered through a Celite©, silica and alumina plug, which was subsequently rinsed with 2 x 1 mL EtOAc. Then the sample was submitted to GC analysis to determine the mass balance, the conversion, and relative ratio of products by comparison with authentic samples. Yields for ethyl-*p*-benzoquinone, propyl-*p*-benzoquinone and isopropyl-*p*-benzoquinone were calculated with the response factor of methyl-*p*-benzoquinone.

3.4.4.2 Determination of Kinetic Deuterium Isotope Effect

Benzene (0.2 mmol), benzene-d_6 (0.2 mmol), and dichloroacetic acid (0.1 mmol) were added into a solution of **Mn(tipsbpmcn)** (2 μmol) in HFIP (2 mL). Subsequently, a solution of H_2O_2 (0.2 mmol, diluted from a 35% H_2O_2 aqueous solution) was added during a period of 30 min under constant stirring. The mixture was stirred for 30 minutes at 0 °C. After the oxidant addition, the resulting mixture was brought to room temperature, and the complex was removed by column chromatography with silica, which was subsequently rinsed with 2 x 1 mL EtOAc. Product distribution was determined by GC-MS. The kinetic isotope effect (KIE) was measured taking into account the abundances for ions with *m*/*z* = 94 and 99 for the phenol peak.

Author Contributions

E.M-R., M.C. and R.K.G. devised the project and designed experiments. E.M-R. performed the experiments and analyzed the data. M.B. analyzed data. M.L. performed X-ray analysis. E.M-R. wrote the Chapter and M.C. and R.K.G provided comments on the experiments and Chapter content.

3.5 References

1. Costas, M.; Chen, K.; Que Jr, L., Biomimetic nonheme iron catalysts for alkane hydroxylation. *Coord. Chem. Rev.* **2000,** *200*, 517-544.

2. Chen, M. S.; White, M. C., A predictably selective aliphatic C–H oxidation reaction for complex molecule synthesis. *Science* **2007,** *318* (5851), 783-787.

3. Nam, W., High-valent iron(IV)–oxo complexes of heme and non-heme ligands in oxygenation reactions. *Acc. Chem. Res.* **2007,** *40* (7), 522-531.

4. Gormisky, P. E.; White, M. C., Catalyst-controlled aliphatic C–H oxidations with a predictive model for site-selectivity. *J. Am. Chem. Soc.* **2013,** *135* (38), 14052-14055.

5. Ottenbacher, R. V.; Talsi, E. P.; Bryliakov, K. P., Mechanism of selective C–H hydroxylation mediated by manganese aminopyridine enzyme models. *ACS Catal.* **2014,** *5* (1), 39-44.

6. Shen, D.; Miao, C.; Wang, S.; Xia, C.; Sun, W., Efficient benzylic and aliphatic C–H oxidation with selectivity for methylenic sites catalyzed by a bioinspired manganese complex. *Org. Lett.* **2014,** *16* (4), 1108-1111.

7. Oloo, W. N.; Que Jr, L., Bioinspired Nonheme Iron Catalysts for C–H and C=C Bond Oxidation: Insights into the Nature of the Metal-Based Oxidants. *Acc. Chem. Res.* **2015,** *48* (9), 2612-2621.

8. Olivo, G.; Cussó, O.; Costas, M., Biologically Inspired C–H and C=C Oxidations with Hydrogen Peroxide Catalyzed by Iron Coordination Complexes. *Chem. Asian J.* **2016,** *11* (22), 3148-3158.

9. Font, D.; Canta, M.; Milan, M.; Cussó, O.; Ribas, X.; Klein Gebbink, R. J. M.; Costas, M., Readily accessible bulky iron catalysts exhibiting site selectivity in the oxidation of steroidal substrates. *Angew. Chem. Int. Ed.* **2016,** *55* (19), 5776-5779.

10. Milan, M.; Carboni, G.; Salamone, M.; Costas, M.; Bietti, M., Tuning Selectivity in Aliphatic C–H Bond Oxidation of N-Alkylamides and Phthalimides Catalyzed by Manganese Complexes. *ACS Catal.* **2017,** *7* (9), 5903-5911.

11. Milan, M.; Bietti, M.; Costas, M., Highly enantioselective oxidation of nonactivated aliphatic C–H bonds with hydrogen peroxide catalyzed by manganese complexes. *ACS Cent. Sci.* **2017,** *3* (3), 196-204.

12. Chen, J.; Lutz, M.; Milan, M.; Costas, M.; Otte, M.; Klein Gebbink, R. J. M., Non-Heme Iron Catalysts with a Rigid Bis-Isoindoline Backbone and Their Use in Selective Aliphatic C–H Oxidation. *Adv. Synth. Catal.* **2017,** *359*, 2590-2595.

13. Ottenbacher, R. V.; Talsi, E. P.; Bryliakov, K. P., Chiral Manganese Aminopyridine Complexes: the Versatile Catalysts of Chemo-and Stereoselective Oxidations with H_2O_2. *Chem. Rec.* **2018,** *18* (1), 78-90.

14. Milan, M.; Salamone, M.; Costas, M.; Bietti, M., The Quest for Selectivity in Hydrogen Atom Transfer Based Aliphatic C–H Bond Oxygenation. *Acc. Chem. Res.* **2018,** *51* (9), 1984-1995.

15. Ottenbacher, R. V.; Talsi, E. P.; Rybalova, T. V.; Bryliakov, K. P., Enantioselective Benzylic Hydroxylation of Arylalkanes with H_2O_2 in Fluorinated Alcohols in the Presence of Chiral Mn Aminopyridine Complexes. *ChemCatChem* **2018,** *10* (22), 5323-5330.

16. Milan, M.; Bietti, M.; Costas, M., Aliphatic C–H Bond Oxidation with Hydrogen Peroxide Catalyzed by Manganese Complexes: Directing Selectivity through Torsional Effects. *Org. Lett.* **2018,** *20* (9), 2720-2723.

17. Qiu, B.; Xu, D.; Sun, Q.; Miao, C.; Lee, Y.-M.; Li, X.-X.; Nam, W.; Sun, W., Highly Enantioselective Oxidation of Spirocyclic Hydrocarbons by Bioinspired Manganese Catalysts and Hydrogen Peroxide. *ACS Catal.* **2018,** *8* (3), 2479-2487.

18. Wang, W.; Xu, D.; Sun, Q.; Sun, W., Efficient Aliphatic C–H Bond Oxidation Catalyzed by Manganese Complexes with Hydrogen Peroxide. *Chem. Asian J.* **2018,** *13* (17), 2458-2464.

19. White, M. C.; Zhao, J., Aliphatic C–H Oxidations for Late-Stage Functionalization. *J. Am. Chem. Soc.* **2018,** *140* (43), 13988-14009.

20. Qiu, B.; Xu, D.; Sun, Q.; Lin, J.; Sun, W., Manganese-Catalyzed Asymmetric Oxidation of Methylene C–H of Spirocyclic Oxindoles and Dihydroquinolinones with Hydrogen Peroxide. *Org. Lett.* **2019,** *21* (3), 618-622.

21. Zhao, J.; Nanjo, T.; de Lucca Jr, E. C.; White, M. C., Chemoselective methylene oxidation in aromatic molecules. *Nature* **2019,** *11*, 213-221.

22. Wu, M.; Wang, B.; Wang, S.; Xia, C.; Sun, W., Asymmetric Epoxidation of Olefins with Chiral Bioinspired Manganese Complexes. *Org. Lett.* **2009,** *11* (16), 3622-3625.

23. Ottenbacher, R. V.; Bryliakov, K. P.; Talsi, E. P., Non-Heme Manganese Complexes Catalyzed Asymmetric Epoxidation of Olefins by Peracetic Acid and Hydrogen Peroxide. *Adv. Synth. Catal.* **2011,** *353* (6), 885-889.

24. Garcia-Bosch, I.; Gomez, L.; Polo, A.; Ribas, X.; Costas, M., Stereoselective Epoxidation of Alkenes with Hydrogen Peroxide using a Bipyrrolidine-Based Family of Manganese Complexes. *Adv. Synth. Catal.* **2012,** *354* (1), 65-70.

25. Cussó, O.; Garcia-Bosch, I.; Font, D.; Ribas, X.; Lloret-Fillol, J.; Costas, M., Highly stereoselective epoxidation with H_2O_2 catalyzed by electron-rich aminopyridine manganese catalysts. *Org. Lett.* **2013,** *15* (24), 6158-6161.

26. Cussó, O.; Garcia-Bosch, I.; Ribas, X.; Lloret-Fillol, J.; Costas, M., Asymmetric epoxidation with H_2O_2 by manipulating the electronic properties of non-heme iron catalysts. *J. Am. Chem. Soc.* **2013,** *135* (39), 14871-14878.

27. Ottenbacher, R. V.; Samsonenko, D. G.; Talsi, E. P.; Bryliakov, K. P., Highly Enantioselective Bioinspired Epoxidation of Electron-Deficient Olefins with H_2O_2 on Aminopyridine Mn Catalysts. *ACS Catal.* **2014,** *4* (5), 1599-1606.

28. Cussó, O.; Ribas, X.; Costas, M., Biologically inspired non-heme iron-catalysts for asymmetric epoxidation; design principles and perspectives. *Chem. Commun.* **2015,** *51* (76), 14285-14298.

29. Cussó, O.; Cianfanelli, M.; Ribas, X.; Klein Gebbink, R. J. M.; Costas, M., Iron catalyzed highly enantioselective epoxidation of cyclic aliphatic enones with aqueous H_2O_2. *J. Am. Chem. Soc.* **2016,** *138* (8), 2732-2738.

30. Shen, D.; Qiu, B.; Xu, D.; Miao, C.; Xia, C.; Sun, W., Enantioselective Epoxidation of Olefins with H_2O_2 Catalyzed by Bioinspired Aminopyridine Manganese Complexes. *Org. Lett.* **2016,** *18* (3), 372-375.

31. Du, J.; Miao, C.; Xia, C.; Lee, Y.-M.; Nam, W.; Sun, W., Mechanistic Insights into the Enantioselective Epoxidation of Olefins by Bioinspired Manganese Complexes: Role of Carboxylic Acid and Nature of Active Oxidant. *ACS Catal.* **2018,** *8* (5), 4528-4538.

32. Clarasó, C.; Vicens, L.; Polo, A.; Costas, M., Enantioselective Epoxidation of β,β-Disubstituted Enamides with a Manganese Catalyst and Aqueous Hydrogen Peroxide. *Org. Lett.* **2019,** *21*, 2430-2435.

33. Mitra, M.; Cussó, O.; Bhat, S. S.; Sun, M.; Cianfanelli, M.; Costas, M.; Nordlander, E., Highly enantioselective epoxidation of olefins by H_2O_2 catalyzed by a non-heme Fe(II) catalyst of a chiral tetradentate ligand. *Dalton Trans.* **2019,** *48* (18), 6123-6131.

34. Borrell, M.; Costas, M., Mechanistically driven development of an iron catalyst for selective *syn*-dihydroxylation of alkenes with aqueous hydrogen peroxide. *J. Am. Chem. Soc.* **2017,** *139* (36), 12821-12829.

35. Vicens, L.; Olivo, G.; Costas, M., Rational Design of Bioinspired Catalysts for Selective Oxidations. *ACS Catal.* **2020,** *10* (15), 8611-8631.

36. Oh, N. Y.; Seo, M. S.; Lim, M. H.; Consugar, M. B.; Park, M. J.; Rohde, J.-U.; Han, J.; Kim, K. M.; Kim, J.; Que Jr, L., Self-hydroxylation of perbenzoic acids at a nonheme iron(II) center. *Chem. Commun.* **2005,** (45), 5644-5646.

37. Taktak, S.; Flook, M.; Foxman, B. M.; Que Jr, L.; Rybak-Akimova, E. V., *ortho*-Hydroxylation of benzoic acids with hydrogen peroxide at a non-heme iron center. *Chem. Commun.* **2005,** (42), 5301-5303.

38. Thibon, A.; Bartoli, J.-F.; Guillot, R.; Sainton, J.; Martinho, M.; Mansuy, D.; Banse, F., Non-heme iron polyazadentate complexes as catalysts for aromatic hydroxylation by H_2O_2: Particular efficiency of tetrakis(2-pyridylmethyl)ethylenediamine–iron(II) complexes. *J. Mol. Catal. Chem.* **2008,** *287* (1-2), 115-120.

39. Makhlynets, O. V.; Rybak-Akimova, E. V., Aromatic Hydroxylation at a Non-Heme Iron Center: Observed Intermediates and Insights into the Nature of the Active Species. *Chem. Eur. J.* **2010,** *16* (47), 13995-14006.

40. Raba, A.; Cokoja, M.; Herrmann, W. A.; Kühn, F. E., Catalytic hydroxylation of benzene and toluene by an iron complex bearing a chelating di-pyridyl-di-NHC ligand. *Chem. Commun.* **2014,** *50* (78), 11454-11457.

41. Kejriwal, A.; Bandyopadhyay, P.; Biswas, A. N., Aromatic hydroxylation using an oxo-bridged diiron(III) complex: a bio-inspired functional model of toluene monooxygenases. *Dalton Trans.* **2015,** *44* (39), 17261-17267.

42. Capocasa, G.; Olivo, G.; Barbieri, A.; Lanzalunga, O.; Di Stefano, S., Direct hydroxylation of benzene and aromatics with H_2O_2 catalyzed by a self-assembled iron complex: evidence for a metal-based mechanism. *Catal. Sci. Technol.* **2017,** *7* (23), 5677-5686.

43. Lindhorst, A. C.; Schütz, J.; Netscher, T.; Bonrath, W.; Kühn, F. E., Catalytic oxidation of aromatic hydrocarbons by a molecular iron–NHC complex. *Catal. Sci. Technol.* **2017,** *7* (9), 1902-1911.

44. Lyakin, O. Y.; Zima, A. M.; Tkachenko, N. V.; Bryliakov, K. P.; Talsi, E. P., Direct Evaluation of the Reactivity of Nonheme Iron(V)-Oxo Intermediates Toward Arenes. *ACS Catal.* **2018**, *8* (6), 5255-5260.

45. Tkachenko, N. V.; Ottenbacher, R. V.; Lyakin, O. Y.; Zima, A. M.; Samsonenko, D. G.; Talsi, E. P.; Bryliakov, K. P., Highly Efficient Aromatic C–H Oxidation with H_2O_2 in the Presence of Iron Complexes of the PDP Family. *ChemCatChem* **2018,** *10* (18), 4052-4057.

46. Tkachenko, N. V.; Lyakin, O. Y.; Zima, A. M.; Talsi, E. P.; Bryliakov, K. P., Effect of different carboxylic acids on the aromatic hydroxylation with H_2O_2 in the presence of an iron aminopyridine complex. *J. Organomet. Chem.* **2018,** *871*, 130-134.

47. Kal, S.; Draksharapu, A.; Que Jr, L., Sc^{3+} (or $HClO_4$) Activation of a Nonheme Fe^{III}–OOH Intermediate for the Rapid Hydroxylation of Cyclohexane and Benzene. *J. Am. Chem. Soc.* **2018,** *140* (17), 5798-5804.

48. Kal, S.; Que Jr, L., Activation of a Non-Heme Fe^{III}-OOH by a Second Fe^{III} to Hydroxylate Strong C–H Bonds: Possible Implications for Soluble Methane Monooxygenase. *Angew. Chem.* **2019,** *58* (25), 8484-8488.

49. Xu, S.; Draksharapu, A.; Rasheed, W.; Que Jr, L., Acid pKa Dependence in O–O Bond Heterolysis of a Nonheme Fe^{III}–OOH Intermediate To Form a Potent Fe^{V}═ O Oxidant with Heme Compound I-Like Reactivity. *J. Am. Chem. Soc.* **2019,** *141* (40), 16093-16107.

50. Zima, A. M.; Lyakin, O. Y.; Lubov, D. P.; Bryliakov, K. P.; Talsi, E. P., Aromatic C–H oxidation by non-heme iron(V)-oxo intermediates bearing aminopyridine ligands. *Mol. Catal.* **2020,** *483*, 110708.

51. Wu, X.; Seo, M. S.; Davis, K. M.; Lee, Y.-M.; Chen, J.; Cho, K.-B.; Pushkar, Y. N.; Nam, W., A Highly Reactive Mononuclear Non-Heme Manganese(IV)−Oxo Complex That Can Activate the Strong C–H Bonds of Alkanes. *J. Am. Chem. Soc.* **2011,** *133* (50), 20088-20091.

52. Aratani, Y.; Yamada, Y.; Fukuzumi, S., Selective hydroxylation of benzene derivatives and alkanes with hydrogen peroxide catalysed by a manganese complex incorporated into mesoporous silica–alumina. *Chem. Commun.* **2015,** *51* (22), 4662-4665.

53. Ottenbacher, R. V.; Talsi, E. P.; Bryliakov, K. P., Recent progress in catalytic oxygenation of aromatic C–H groups with the environmentally benign oxidants H_2O_2 and O_2. *Appl Organomet Chem.* **2020**, *34*, e5900.

54. Fukuzumi, S.; Ohkubo, K., One-Step Selective Hydroxylation of Benzene to Phenol. *Asian J. Org. Chem.* **2015,** *4* (9), 836-845.

55. Morimoto, Y.; Bunno, S.; Fujieda, N.; Sugimoto, H.; Itoh, S., Direct hydroxylation of benzene to phenol using hydrogen peroxide catalyzed by nickel complexes supported by pyridylalkylamine ligands. *J. Am. Chem. Soc.* **2015,** *137* (18), 5867-5870.

56. Tsuji, T.; Zaoputra, A. A.; Hitomi, Y.; Mieda, K.; Ogura, T.; Shiota, Y.; Yoshizawa, K.; Sato, H.; Kodera, M., Specific Enhancement of Catalytic Activity by a Dicopper Core: Selective Hydroxylation of Benzene to Phenol with Hydrogen Peroxide. *Angew. Chem. Int. Ed.* **2017,** *129* (27), 7887-7890.

57. Vilella, L.; Conde, A.; Balcells, D.; Díaz-Requejo, M. M.; Lledós, A.; Pérez, P. J., A competing, dual mechanism for catalytic direct benzene hydroxylation from combined experimental-DFT studies. *Chem. Sci.* **2017,** *8* (12), 8373-8383.

58. Kwong, H. K.; Lo, P. K.; Yiu, S. M.; Hirao, H.; Lau, K. C.; Lau, T. C., Highly Selective and Efficient Ring Hydroxylation of Alkylbenzenes with Hydrogen Peroxide and an Osmium(VI) Nitrido Catalyst. *Angew. Chem. Int. Ed.* **2017,** *56* (40), 12260-12263.

59. Muthuramalingam, S.; Anandababu, K.; Velusamy, M.; Mayilmurugan, R., One step phenol synthesis from benzene catalysed by nickel(II) complexes. *Catal. Sci. Technol.* **2019,** *9* (21), 5991-6001.

60. Muthuramalingam, S.; Anandababu, K.; Velusamy, M.; Mayilmurugan, R., Benzene Hydroxylation by Bioinspired Copper (II) Complexes: Coordination Geometry versus Reactivity. *Inorg. Chem.* **2020,** *59*, 5918-5928.

61. Anandababu, K.; Muthuramalingam, S.; Velusamy, M.; Mayilmurugan, R., Single-step benzene hydroxylation by cobalt(II) catalysts via a cobalt(III)-hydroperoxo intermediate. *Catal. Sci. Technol.* **2020,** *10*, 2540-2548.

62. Masferrer-Rius, E.; Hopman, R. M.; van der Kleij, J.; Lutz, M.; Klein Gebbink, R. J. M., On the Ability of Nickel Complexes Derived from Tripodal Aminopyridine Ligands to Catalyze Arene Hydroxylations. *CHIMIA* **2020,** *74* (6), 489-494.

63. Ticconi, B.; Colcerasa, A.; Di Stefano, S.; Lanzalunga, O.; Lapi, A.; Mazzonna, M.; Olivo, G., Oxidative functionalization of aliphatic and aromatic amino acid derivatives with H_2O_2 catalyzed by a nonheme imine based iron complex. *RSC Adv.* **2018,** *8* (34), 19144-19151.

64. Dantignana, V.; Milan, M.; Cussó, O.; Company, A.; Bietti, M.; Costas, M., Chemoselective Aliphatic C–H Bond Oxidation Enabled by Polarity Reversal. *ACS Cent. Sci.* **2017,** *3* (12), 1350-1358.

65. Ottenbacher, R. V.; Samsonenko, D. G.; Talsi, E. P.; Bryliakov, K. P., Highly Efficient, Regioselective, and Stereospecific Oxidation of Aliphatic C–H Groups with H_2O_2, Catalyzed by Aminopyridine Manganese Complexes. *Org. Lett.* **2012,** *14* (17), 4310-4313.

66. Talsi, E. P.; Samsonenko, D. G.; Ottenbacher, R. V.; Bryliakov, K. P., Highly Enantioselective C–H Oxidation of Arylalkanes with H_2O2 in the Presence of Chiral Mn-Aminopyridine Complexes. *ChemCatChem* **2017,** *9* (24), 4580-4586.

67. Chambers, R. K.; Zhao, J.; Delaney, C. P.; White, M. C., Chemoselective Tertiary C–H Hydroxylation for Late-Stage Functionalization with Mn(PDP)/Chloroacetic Acid Catalysis. *Adv. Synth. Catal.* **2020,** *362* (2), 417-423.

68. Roberts, B. P., Polarity-reversal catalysis of hydrogen-atom abstraction reactions: concepts and applications in organic chemistry. *Chem. Soc. Rev.* **1999,** *28* (1), 25-35.

69. Wang, D.; Shuler, W. G.; Pierce, C. J.; Hilinski, M. K., An iminium salt organocatalyst for selective aliphatic C–H hydroxylation. *Org. Lett.* **2016,** *18* (15), 3826-3829.

70. Gaster, E.; Kozuch, S.; Pappo, D., Selective Aerobic Oxidation of Methylarenes to Benzaldehydes Catalyzed by N-Hydroxyphthalimide and Cobalt(II) Acetate in Hexafluoropropan-2-ol. *Angew. Chem. Int. Ed.* **2017,** *56* (21), 5912-5915.

71. Adams, A. M.; Du Bois, J., Organocatalytic C–H hydroxylation with Oxone® enabled by an aqueous fluoroalcohol solvent system. *Chem. Sci.* **2014,** *5* (2), 656-659.

72. Borrell, M.; Gil-Caballero, S.; Bietti, M.; Costas, M., Site-selective and product chemoselective aliphatic CH bond hydroxylation of polyhydroxylated substrates. *ACS Catal.* **2020,** *10* (8), 4702-4709.

73. Ottenbacher, R. V.; Talsi, E. P.; Bryliakov, K. P., Highly Enantioselective Undirected Catalytic Hydroxylation of Benzylic CH_2 Groups with H_2O_2. *J. Catal.* **2020,** *390*, 170-177.

74. Neves, A.; Erthal, S. M.; Vencato, I.; Ceccato, A. S.; Mascarenhas, Y. P.; Nascimento, O. R.; Horner, M.; Batista, A. A., Synthesis, crystal structure, electrochemical, and spectroelectrochemical properties of the new manganese(III) complex $[Mn^{III}(BBPEN)][PF_6]$[H_2BBPEN=N,N'-bis(2-hydroxybenzyl)-N,N'-bis(2-methylpyridyl)ethylenediamine]. *Inorg. Chem.* **1992,** *31* (23), 4749-4755.

75. Wada, S.; Mikuriya, M., Synthesis and structural characterization of dinuclear manganese(III) complexes with cyclam-based macrocyclic ligands having Schiff-base pendant arms as chelating agents. *Bull. Chem. Soc. Jpn.* **2008,** *81* (3), 348-357.

76. Mandal, D.; Chatterjee, P. B.; Bhattacharya, S.; Choi, K.-Y.; Clérac, R.; Chaudhury, M., Tetra-, tri-, and mononuclear manganese(II/III) complexes of a phenol-based N_2O_2 capping ligand: use of carboxylates as ancillary ligands in tuning the nuclearity of the complexes. *Inorg. Chem.* **2009,** *48* (5), 1826-1835.

77. Sankaralingam, M.; Palaniandavar, M., Tuning the olefin epoxidation by manganese(III) complexes of bisphenolate ligands: effect of Lewis basicity of ligands on reactivity. *Dalton Trans.* **2014,** *43* (2), 538-550.

78. Mikuriya, M.; Kurahashi, S.; Tomohara, S.; Koyama, Y.; Yoshioka, D.; Mitsuhashi, R.; Sakiyama, H., Synthesis, Crystal Structures, and Magnetic Properties of Mixed-Valent Tetranuclear Complexes with Y-Shaped $Mn^{II}_2Mn^{III}_2$ Core. *Magnetochemistry* **2019,** *5* (1), 8.

79. Talsi, E. P.; Bryliakov, K. P., Chemo-and stereoselective C–H oxidations and epoxidations/*cis*-dihydroxylations with H_2O_2, catalyzed by non-heme iron and manganese complexes. *Coord. Chem. Rev.* **2012,** *256* (13-14), 1418-1434.

80. Bryliakov, K. P.; Talsi, E. P., Active sites and mechanisms of bioinspired oxidation with H_2O_2, catalyzed by non-heme Fe and related Mn complexes. *Coord. Chem. Rev.* **2014,** *276*, 73-96.

81. Lyakin, O. Y.; Ottenbacher, R. V.; Bryliakov, K. P.; Talsi, E. P., Asymmetric epoxidations with H_2O_2 on Fe and Mn aminopyridine catalysts: probing the nature of active species by combined electron paramagnetic resonance and enantioselectivity study. *ACS Catal.* **2012,** *2* (6), 1196-1202.

82. Ottenbacher, R. V.; Talsi, E. P.; Bryliakov, K. P., Mechanism of selective C–H hydroxylation mediated by manganese aminopyridine enzyme models. *ACS Catal.* **2015,** *5* (1), 39-44.

83. Ryabov, A. D.; Sakodinskaya, I. K.; Yatsimirsky, A. K., Kinetics and mechanism of ortho-palladation of ring-substituted NN-dimethylbenzylamines. *J. Chem. Soc., Dalton Trans.* **1985,** (12), 2629-2638.

84. Lafrance, M.; Gorelsky, S. I.; Fagnou, K., High-yielding palladium-catalyzed intramolecular alkane arylation: reaction development and mechanistic studies. *J. Am. Chem. Soc.* **2007,** *129* (47), 14570-14571.

85. Maleckis, A.; Kampf, J. W.; Sanford, M. S., A Detailed Study of Acetate-Assisted C–H Activation at Palladium(IV) Centers. *J. Am. Chem. Soc.* **2013,** *135* (17), 6618-6625.

86. de Boer, J. W.; Brinksma, J.; Browne, W. R.; Meetsma, A.; Alsters, P. L.; Hage, R.; Feringa, B. L., *Cis*-dihydroxylation and epoxidation of alkenes by $[Mn_2O(RCO_2)_2(tmtacn)_2]$: tailoring the selectivity of a highly H_2O_2-efficient catalyst. *J. Am. Chem. Soc.* **2005,** *127* (22), 7990-7991.

87. pK_a values were taken from: Haynes, W. M., *Handbook of Chemistry and Physics*. 91st ed.; CRC Press (Taylor and Francis Group): Boca Raton, FL.

88. Metelitsa, D. I., Mechanisms of the hydroxylation of aromatic compounds. *Russ. Chem. Rev.* **1971,** *40* (7), 563.

89. Walling, C.; Johnson, R. A., Fenton's reagent. V. Hydroxylation and side-chain cleavage of aromatics. *J. Am. Chem. Soc.* **1975,** *97* (2), 363-367.

90. Kunai, A.; Hata, S.; Ito, S.; Sasaki, K., The role of oxygen in the hydroxylation reaction of benzene with Fenton's reagent. Oxygen 18 tracer study. *J. Am. Chem. Soc.* **1986,** *108* (19), 6012-6016.

91. Kurata, T.; Watanabe, Y.; Katoh, M.; Sawaki, Y., Mechanism of aromatic hydroxylation in the Fenton and related reactions. One-electron oxidation and the NIH shift. *J. Am. Chem. Soc.* **1988,** *110* (22), 7472-7478.

92. Olivo, G.; Lanzalunga, O.; Di Stefano, S., Non-Heme Imine-Based Iron Complexes as Catalysts for Oxidative Processes. *Adv. Synth. Catal.* **2016,** *358* (6), 843-863.

93. Marusawa, H.; Ichikawa, K.; Narita, N.; Murakami, H.; Ito, K.; Tezuka, T., Hydroxyl radical as a strong electrophilic species. *Bioorg. Med. Chem.* **2002,** *10* (7), 2283-2290.

94. Mas-Ballesté, R.; Que, L., Iron-catalyzed olefin epoxidation in the presence of acetic acid: insights into the nature of the metal-based oxidant. *J. Am. Chem. Soc.* **2007,** *129* (51), 15964-15972.

95. Ottenbacher, R. V.; Talsi, E. P.; Bryliakov, K. P., Direct selective oxidative functionalization of C–H bonds with H_2O_2: Mn-Aminopyridine complexes challenge the dominance of non-heme Fe catalysts. *Molecules* **2016,** *21* (11), 1454.

96. MacFaul, P. A.; Ingold, K.; Wayner, D.; Que, L., A Putative Monooxygenase Mimic Which Functions via Well-Disguised Free Radical Chemistry1. *J. Am. Chem. Soc.* **1997,** *119* (44), 10594-10598.

97. Ingold, K. U., MacFaul, P. A., *Biomimetic oxidations catalyzed by transition metal complexes*. Meunier, B., Ed.; Imperial College Press: London, 2000; p 45.

98. Hiatt, R.; Clipsham, J.; Visser, T., The induced decomposition of tert-butyl hydroperoxide. *Can. J. Chem.* **1964,** *42* (12), 2754-2757.

99. Ito, S.; Mitarai, A.; Hikino, K.; Hirama, M.; Sasaki, K., Deactivation reaction in the hydroxylation of benzene with Fenton's reagent. *J. Org. Chem.* **1992,** *57* (25), 6937-6941.

100. Augusti, R.; Dias, A. O.; Rocha, L. L.; Lago, R. M., Kinetics and mechanism of benzene derivative degradation with Fenton's reagent in aqueous medium studied by MIMS. *The Journal of Physical Chemistry A* **1998,** *102* (52), 10723-10727.

101. Siddiqi, Z.; Wertjes, W. C.; Sarlah, D., Chemical Equivalent of Arene Monooxygenases: Dearomative Synthesis of Arene Oxides and Oxepines. *J. Am. Chem. Soc.* **2020,** *142* (22), 10125-10131.

102. Lowry, T. H.; Richardson, K. S., *Mechanism and Theory in Organic Chemistry*. III edn, Harper & Row Publishers, New York, 1987; p 628.

103. Ortiz de Montellano, P. R., Cytochrome P450: Structure, Mechanism, and Biochemistry. *2nd ed.* ed.; Ortiz de Montellano, P. R., Ed. Plenum Press, New York: 1995; pp 245-303.

104. Meunier, B.; De Visser, S. P.; Shaik, S., Mechanism of oxidation reactions catalyzed by cytochrome P450 enzymes. *Chem. Rev.* **2004,** *104* (9), 3947-3980.

105. Korzekwa, K. R.; Swinney, D. C.; Trager, W. F., Isotopically labeled chlorobenzenes as probes for the mechanism of cytochrome P-450 catalyzed aromatic hydroxylation. *Biochemistry* **1989,** *28* (23), 9019-9027.

106. de Visser, S. P.; Shaik, S., A proton-shuttle mechanism mediated by the porphyrin in benzene hydroxylation by cytochrome P450 enzymes. *J. Am. Chem. Soc.* **2003,** *125* (24), 7413-7424.

107. Kudrik, E. V.; Sorokin, A. B., N-Bridged Diiron Phthalocyanine Catalyzes Oxidation of Benzene with H_2O_2 via Benzene Oxide with NIH Shift Evidenced by Using 1,3,5-[D_3]Benzene as a Probe. *Chem. Eur. J.* **2008,** *14* (24), 7123-7126.

108. Feng, K.; Quevedo, R. E.; Kohrt, J. T.; Oderinde, M. S.; Reilly, U.; White, M. C., Late-stage oxidative C(sp^3)–H methylation. *Nature* **2020,** *580* (7805), 621-627.

109. Esarey, S. L.; Holland, J. C.; Bartlett, B. M., Determining the Fate of a Non-Heme Iron Oxidation Catalyst Under Illumination, Oxygen, and Acid. *Inorg. Chem.* **2016,** *55*, 11040-11049.

110. Font, D.; Canta, M.; Milan, M.; Cussó, O.; Ribas, X.; Klein Gebbink, R. J. M.; Costas, M., Readily accessible bulky iron catalysts exhibiting site selectivity in the oxidation of steroidal substrates. *Angew. Chem. Int. Ed.* **2016,** *55* (19), 5776-5779.

111. S., C. M.; White, M. C., A Predictably Selective Aliphatic C–H Oxidation Reaction for Complex Molecule Synthesis. *Science* **2007,** *318*, 783-787.

112. Chen, J.; Lutz, M.; Milan, M.; Costas, M.; Otte, M.; Klein Gebbink, R. J. M., Non-Heme Iron Catalysts with a Rigid Bis-Isoindoline Backbone and Their Use in Selective Aliphatic C–H Oxidation. *Adv. Synth. Catal.* **2017,** *359*, 2590-2595.

113. Mautner, F. A.; Koikawa, M.; Mikuriya, M.; Harrelson, E. V.; Massoud, S. S., Copper(II)-azido complexes constructed from polypyridyl amine ligands. *Polyhedron* **2013,** *59*, 17-22.

114. Murphy, A.; Dubois, G.; Stack, T. D. P., Efficient Epoxidation of Electron-Deficient Olefins with a Cationic Manganese Complex. *J. Am. Chem. Soc.* **2003,** *125*, 5250-5251.

115. Chen, J.; de Liedekerke Beaufort, M.; Gyurik, L.; Dorresteijn, J.; Otte, M.; Klein Gebbink, R. J. M., Highly efficient epoxidation of vegetable oils catalyzed by a manganese complex with hydrogen peroxide and acetic acid. *Green Chem.* **2019,** *21* (9), 2436-2447.

116. Urbanová, K.; Ramírez-Macías, I.; Martín-Escolano, R.; Rosales, M. J.; Cussó, O.; Serrano, J.; Sánchez-Moreno, M.; Costas, M.; Ribas, X.; Marín, C., Effective Tetradentate Compound Complexes against Leishmania spp. that Act on Critical Enzymatic Pathways of These Parasites. *Molecules* **2019,** *24* (1), 134.

117. Patra, T.; Mukherjee, S.; Ma, J.; Strieth-Kalthoff, F.; Glorius, F., Visible-Light-Photosensitized Aryl and Alkyl Decarboxylative Functionalization Reactions. *Angew. Chem. Int. Ed.* **2019,** *58* (31), 10514-10520.

118. Schreurs, A. M.; Xian, X.; Kroon-Batenburg, L. M., EVAL15: a diffraction data integration method based on ab initio predicted profiles. *J. Appl. Crystallogr.* **2010,** *43* (1), 70-82.

119. Sheldrick, B. M., SADABS. **2014**, Universität Göttingen, Germany.

120. Sheldrick, G. M., SHELXT–Integrated space-group and crystal-structure determination. *Acta Cryst.* **2015,** *A71* (1), 3-8.

121. Sheldrick, G. M., Crystal structure refinement with SHELXL. *Acta Cryst.* **2015,** *C71* (1), 3-8.

122. Parsons, S.; Flack, H. D.; Wagner, T., Use of intensity quotients and differences in absolute structure refinement. *Acta Cryst.* **2013,** *B69* (3), 249-259.

123. Spek, A. L., Structure validation in chemical crystallography. *Acta Cryst.* **2009,** *D65* (2), 148-155.